PCT WORLD INTELLECTUAL PROPERTY ORGANIZATION
International Bureau

INTERNATIONAL APPLICATION PUBLISHED UNDER THE PATENT COOPERATION TREATY (PCT)

(51) International Patent Classification 6 : C30B 15/14, 29/06 — A1

(11) International Publication Number: **WO 00/00675**

(43) International Publication Date: 6 January 2000 (06.01.00)

(21) International Application Number: PCT/US99/13643

(22) International Filing Date: 18 June 1999 (18.06.99)

(30) Priority Data:
60/090,799 26 June 1998 (26.06.98) US

(71) Applicant: MEMC ELECTRONIC MATERIALS, INC. [US/US]; 501 Pearl Drive, P.O. Box 8, St. Peters, MO 63376 (US).

(72) Inventors: SCHRENKER, Richard, G.; 15566 Rose Gate Lane, Chesterfield, MO (US). LUTER, William, L.; 1037 Picardy Lane, St. Charles, MO (US).

(74) Agents: HEJLEK, Edward, J. et al.; Senniger, Powers, Leavitt & Roedel, 16th floor, One Metropolitan Square, St. Louis, MO 63102 (US).

(81) Designated States: CN, JP, KR, SG, European patent (AT, BE, CH, CY, DE, DK, ES, FI, FR, GB, GR, IE, IT, LU, MC, NL, PT, SE).

Published
With international search report.

(54) Title: CRYSTAL PULLER FOR GROWING LOW DEFECT DENSITY, SELF-INTERSTITIAL DOMINATED SILICON

(57) Abstract

A crystal puller for growing monocrystalline silicon ingots according to the Czochralski method which are devoid of agglomerated intrinsic point defects over a substantial portion of the radius of the ingot comprises a housing defining an interior having a lower growth chamber and an upper pull chamber. The pull chamber has a smaller transverse dimension than the growth chamber. A crucible is disposed in the growth chamber of the housing for containing molten silicon. A pulling mechanism is provided for pulling a growing ingot upward from the molten silicon through the growth chamber and pull chamber. An electrical resistance heater has a heating element sized and shaped for being disposed at least partially within the upper pull chamber of the housing in radially spaced relationship with the outer surface of the growing ingot for radiating heat to the ingot as it is pulled upward in the pull chamber relative to the molten silicon. The heating element has an upper end and a lower end. The lower end of the heating element is disposed substantially closer to the molten silicon than the upper end when the heating element is placed in the housing.

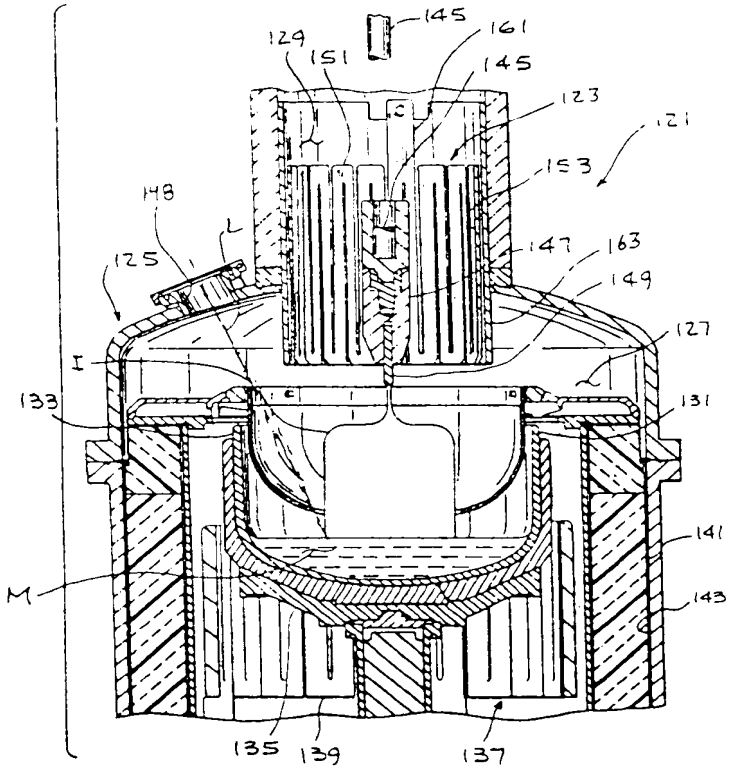

FOR THE PURPOSES OF INFORMATION ONLY

Codes used to identify States party to the PCT on the front pages of pamphlets publishing international applications under the PCT.

AL	Albania	**ES**	Spain	**LS**	Lesotho	**SI**	Slovenia
AM	Armenia	**FI**	Finland	**LT**	Lithuania	**SK**	Slovakia
AT	Austria	**FR**	France	**LU**	Luxembourg	**SN**	Senegal
AU	Australia	**GA**	Gabon	**LV**	Latvia	**SZ**	Swaziland
AZ	Azerbaijan	**GB**	United Kingdom	**MC**	Monaco	**TD**	Chad
BA	Bosnia and Herzegovina	**GE**	Georgia	**MD**	Republic of Moldova	**TG**	Togo
BB	Barbados	**GH**	Ghana	**MG**	Madagascar	**TJ**	Tajikistan
BE	Belgium	**GN**	Guinea	**MK**	The former Yugoslav Republic of Macedonia	**TM**	Turkmenistan
BF	Burkina Faso	**GR**	Greece			**TR**	Turkey
BG	Bulgaria	**HU**	Hungary	**ML**	Mali	**TT**	Trinidad and Tobago
BJ	Benin	**IE**	Ireland	**MN**	Mongolia	**UA**	Ukraine
BR	Brazil	**IL**	Israel	**MR**	Mauritania	**UG**	Uganda
BY	Belarus	**IS**	Iceland	**MW**	Malawi	**US**	United States of America
CA	Canada	**IT**	Italy	**MX**	Mexico	**UZ**	Uzbekistan
CF	Central African Republic	**JP**	Japan	**NE**	Niger	**VN**	Viet Nam
CG	Congo	**KE**	Kenya	**NL**	Netherlands	**YU**	Yugoslavia
CH	Switzerland	**KG**	Kyrgyzstan	**NO**	Norway	**ZW**	Zimbabwe
CI	Côte d'Ivoire	**KP**	Democratic People's Republic of Korea	**NZ**	New Zealand		
CM	Cameroon			**PL**	Poland		
CN	China	**KR**	Republic of Korea	**PT**	Portugal		
CU	Cuba	**KZ**	Kazakstan	**RO**	Romania		
CZ	Czech Republic	**LC**	Saint Lucia	**RU**	Russian Federation		
DE	Germany	**LI**	Liechtenstein	**SD**	Sudan		
DK	Denmark	**LK**	Sri Lanka	**SE**	Sweden		
EE	Estonia	**LR**	Liberia	**SG**	Singapore		

CRYSTAL PULLER FOR GROWING LOW DEFECT DENSITY, SELF-INTERSTITIAL DOMINATED SILICON

BACKGROUND OF THE INVENTION

The present invention generally relates to crystal pullers used in the preparation of semiconductor grade single crystal silicon which is used in the manufacture of electronic components. More particularly, the present invention relates to a crystal puller for producing single crystal silicon ingots and wafers which are self-interstitial dominated and devoid of agglomerated intrinsic point defects over a substantial portion of the ingot radius.

Single crystal silicon, which is the starting material for most semiconductor electronic component fabrication, is commonly prepared by the so-called Czochralski ("Cz") method. The growth of a crystal ingot is most commonly carried out in a crystal pulling furnace. In this method, polycrystalline silicon ("polysilicon") is charged to a crucible and melted by a heater surrounding the outer surface of the crucible side wall. A seed crystal is brought into contact with the molten silicon and a single crystal ingot is grown by slow extraction via a crystal puller. After formation of a neck is complete, the diameter of the crystal ingot is enlarged by decreasing the pulling rate and/or the melt temperature until the desired or target diameter is reached. The cylindrical main body of the crystal which has an approximately constant diameter is then grown by controlling the pull rate and the melt temperature while compensating for the decreasing melt level. Near the end of the growth process, the crystal diameter must be reduced gradually to form an end-cone. Typically, the end-cone is formed by increasing the pull rate and heat supplied to the crucible. When the diameter becomes small enough, the ingot is then separated from the melt.

Heaters used for melting silicon in the crucible are typically electrical resistance heaters in which an electrical current flows through a heating element constructed of a resistive heating material (e.g., graphite). The resistance to the flow of current generates heat that radiates from the heating element to the crucible and silicon contained therein. The heating element comprises vertically oriented heating segments of equal length and cross-section arranged in side-by-side relationship and connected to each other in a serpentine configuration. That is, adjacent segments are connected to each other at the tops or bottoms of the segments in an alternating manner to form a continuous electrical circuit throughout the heating element. The heating power generated by the heating element is generally a function of the cross-sectional area of the segments.

In recent years, it has been recognized that a number of defects in single crystal silicon form in the crystal growth chamber as the ingot cools after solidification. Such defects arise, in part, due to the presence of an excess (i.e. a concentration above the solubility limit) of intrinsic point defects in the crystal lattice, which are vacancies and self-interstitials. Silicon crystal ingots grown from a melt are typically grown with an excess of one or the other type of intrinsic point defect, either crystal lattice vacancies ("V") or silicon self-interstitials ("I"). It has been suggested that the type and initial concentration of these point defects in the silicon are determined at the time of solidification and, if these concentrations reach a level of critical supersaturation in the system and the mobility of the point defects is sufficiently high, a reaction, or an agglomeration event,

will likely occur. Agglomerated intrinsic point defects in silicon can severely impact the yield potential of the material in the production of complex and highly integrated circuits.

Vacancy-type defects are recognized to be the origin of such observable crystal defects as D-defects, Flow Pattern Defects (FPDs), Gate Oxide Integrity (GOI) Defects, Crystal Originated Particle (COP) Defects, crystal originated Light Point Defects (LPDs), as well as certain classes of bulk defects observed by infrared light scattering techniques such as Scanning Infrared Microscopy and Laser Scanning Tomography. Also present in regions of excess vacancies are defects which act as the nuclei for ring oxidation induced stacking faults (OISF). It is speculated that this particular defect is a high temperature nucleated oxygen agglomerate catalyzed by the presence of excess vacancies.

Defects relating to self-interstitials are less well studied. They are generally regarded as being low densities of interstitial-type dislocation loops or networks. Such defects are not responsible for gate oxide integrity failures, an important wafer performance criterion, but they are widely recognized to be the cause of other types of device failures usually associated with current leakage problems.

The density of such vacancy and self-interstitial agglomerated defects in Czochralski silicon is conventionally within the range of about $1*10^3/cm^3$ to about $1*10^7/cm^3$. While these values are relatively low, agglomerated intrinsic point defects are of rapidly increasing importance to device manufacturers and, in fact, are now seen as yield-limiting factors in device fabrication processes.

To date, there generally exists three main approaches to dealing with the problem of agglomerated intrinsic point defects. The first approach includes

methods which focus on crystal pulling techniques in order to reduce the number density of agglomerated intrinsic point defects in the ingot. This approach can be further subdivided into those methods having crystal pulling conditions which result in the formation of vacancy dominated material, and those methods having crystal pulling conditions which result in the formation of self-interstitial dominated material. For example, it has been suggested that the number density of agglomerated defects can be reduced by (i) controlling v/G_0 to grow an ingot in which crystal lattice vacancies are the dominant intrinsic point defect, and (ii) influencing the nucleation rate of the agglomerated defects by altering (generally, by slowing down) the cooling rate of the silicon ingot as it is pulled upward from the melt surface.

To this end, U.S. Patent No. 5,248,378 (Oda et al.) discloses an apparatus for producing single silicon crystal in which a passive heat insulator is disposed in the crystal puller above the crucible to reduce the rate of cooling of the growing ingot above 1150°C. However, heat insulators or heat shields such as that disclosed by Oda et al. generally cannot slow the cooling of the ingot to a rate sufficient to substantially reduce the number of defects in the ingot.

Oda et al. further disclose that the insulator may be replaced by a heater for heating the growing ingot. The heater is positioned in the growth chamber of the crystal puller between the top of the crucible and the transition portion of the crystal puller housing. The heater radiates heat to the ingot to slow the rate of cooling above 1150°C. However, while the apparatus disclosed in Oda et al. is capable of reducing the number density of agglomerated defects, it does not prevent their formation because the cooling rate is still too rapid to prevent such formation. As the requirements

imposed by device manufacturers become more and more stringent, the presence of these defects will continue to become more of a problem.

Moreover, because of the limited space in the growth chamber of conventional crystal pullers, it would be impractical to increase the length or size of the heater disclosed by Oda et al. to further reduce the cooling rate of the growing ingot. Increasing the length of the heater would shield the ingot against viewing by the diameter control apparatus via the view port in the puller housing. Granular feeder hardware, laser melt level apparatus and other devices typically found in the growth chamber of conventional crystal pullers would also interfere with the ability to increase the length of the heater.

Others have suggested reducing the pull rate, during the growth of the body of the crystal, to a value less than about 0.4 mm/minute. However, by itself, this suggestion is also not satisfactory because such pull rates lead to the formation of single crystal silicon having a high concentration of self-interstitials. This high concentration, in turn, leads to the formation of agglomerated self-interstitial defects and all the resulting problems associated with such defects.

A second approach to dealing with the problem of agglomerated intrinsic point defects includes methods which focus on the dissolution or annihilation of agglomerated intrinsic point defects subsequent to their formation. Generally, this is achieved by using high temperature heat treatments of the silicon in wafer form. For example, Fusegawa et al. propose, in European Patent Application 503,816 A1, growing the silicon ingot at a growth rate in excess of 0.8 mm/minute, and heat treating the wafers which are sliced from the ingot at a temperature in the range of 1150°C to 1280°C to reduce the defect density in a thin region near the wafer

surface. The specific treatment needed will vary depending upon the concentration and location of agglomerated intrinsic point defects in the wafer. Different wafers cut from a crystal which does not have a uniform axial concentration of such defects may require different post-growth processing conditions. Furthermore, such wafer heat treatments are relatively costly, have the potential for introducing metallic impurities into the silicon wafers, and are not universally effective for all types of crystal-related defects.

A third approach to dealing with the problem of agglomerated intrinsic point defects is the epitaxial deposition of a thin crystalline layer of silicon on the surface of a single crystal silicon wafer. This process provides a single crystal silicon wafer having a surface which is substantially free of agglomerated intrinsic point defects. Epitaxial deposition, however, substantially increases the cost of the wafer.

In view of these developments, a need continues to exist for a crystal puller designed to inhibit the formation of agglomerated intrinsic point defects by suppressing the agglomeration reactions which produce them. Rather than simply limiting the rate at which such defects form, or attempting to annihilate some of the defects after they have formed, a crystal puller which suppresses agglomeration reactions would yield a silicon substrate that is substantially free of agglomerated intrinsic point defects. Such a crystal puller would also produce single crystal silicon wafers having epi-like yield potential, in terms of the number of integrated circuits obtained per wafer, without having the high costs associated with an epitaxial process.

SUMMARY OF THE INVENTION

Among the several objects and features of the present invention may be noted the provision of a crystal puller for producing single crystal silicon ingots and wafers which are self-interstitial dominated and devoid of agglomerated intrinsic point defects over a substantial portion of the ingot radius; the provision of such a crystal puller which substantially reduces the cooling rate of an ingot being grown in the puller; the provision of such a crystal puller which substantially increases the time during which the temperature of the growing ingot is above 1050°C; and the provision of an electrical resistance heater for use in such a crystal puller which does not impede viewing of the growing ingot via the view port in the puller housing.

Generally, a crystal puller of the present invention for growing monocrystalline silicon ingots according to the Czochralski method which are devoid of agglomerated intrinsic point defects over a substantial portion of the radius of the ingot comprises a housing defining an interior having a lower growth chamber and an upper pull chamber. The pull chamber has a smaller transverse dimension than the growth chamber. A crucible is disposed in the growth chamber of the housing for containing molten silicon. A pulling mechanism is provided for pulling a growing ingot upward from the molten silicon through the growth chamber and pull chamber. An electrical resistance heater has a heating element sized and shaped for being disposed at least partially within the upper pull chamber of the housing in radially spaced relationship with the outer surface of the growing ingot for radiating heat to the ingot as it is pulled upward in the pull chamber relative to the

molten silicon. The heating element has an upper end and a lower end. The lower end of the heating element is disposed substantially closer to the molten silicon than the upper end when the heating element is placed in the housing.

Other objects and features of the present invention will be in part apparent and in part pointed out hereinafter.

BRIEF DESCRIPTION OF THE DRAWINGS

FIG. 1 is a graph which shows an example of how the initial concentration of self-interstitials, [I], and vacancies, [V], changes with an increase in the value of the ratio v/G_0, where v is the growth rate and G_0 is the average axial temperature gradient.

FIG. 2 is a graph which shows an example of how ΔG_I, the change in free energy required for the formation of agglomerated interstitial defects, increases as the temperature, T, decreases, for a given initial concentration of self-interstitials, [I].

FIG. 3 is a graph which shows an example of how ΔG_I, the change in free energy required for the formation of agglomerated interstitial defects, decreases (as the temperature, T, decreases) as a result of the suppression of the concentration of self-interstitials, [I], through the means of radial diffusion. The solid line depicts the case for no radial diffusion whereas the dotted line includes the effect of diffusion.

FIG. 4 is a graph which shows an example of how ΔG_I, the change in free energy required for the formation of agglomerated interstitial defects, is sufficiently decreased (as the temperature, T, decreases), as a result of the suppression of the concentration of self-interstitials, [I], through the means of radial

diffusion, such that an agglomeration reaction is prevented. The solid line depicts the case for no radial diffusion whereas the dotted line includes the effect of diffusion.

FIG. 5 is a graph which shows an example of how the initial concentration of self-interstitials, [I], and vacancies, [V], can change along the radius of an ingot or wafer, as the value of the ratio v/G_0 decreases, due to an increase in the value of G_0. Note that at the V/I boundary a transition occurs from vacancy dominated material to self-interstitial dominated material.

FIG. 6 is a top plan view of a single crystal silicon ingot or wafer showing regions of vacancy, V, and self-interstitial, I, dominated materials respectively, as well as the V/I boundary that exists between them.

FIG. 7a is a graph which shows an example of how the initial concentration of vacancies or self-interstitials changes as a function of radial position due to radial diffusion of self-interstitials. Also shown is how such diffusion causes the location of the V/I boundary to move closer to the center of the ingot (as a result of the recombination of vacancies and self-interstitials), as well as the concentration of self-interstitials, [I], to be suppressed.

FIG. 7b is a graph of ΔG_I as a function of radial position which shows an example of how the suppression of self-interstitial concentration, [I], (as depicted in FIG. 7a) is sufficient to maintain ΔG_I everywhere to a value which is less than the critical value at which the silicon self-interstitial reaction occurs.

FIG. 7c is a graph which shows another example of how the initial concentration of vacancies or self-interstitials changes as a function of radial position due to radial diffusion of self-interstitials. Note that, in comparison to FIG. 7a, such diffusion caused the location of the V/I boundary to be closer to the center

of the ingot (as a result of the recombination of vacancies and self-interstitials), resulting in an increase in the concentration of interstitials in the region outside of the V/I boundary.

FIG. 7d is a graph of ΔG_I as a function of radial position which shows an example of how the suppression of self-interstitial concentration, [I], (as depicted in FIG. 7c) is not sufficient to maintain ΔG_I everywhere to a value which is less than the critical value at which the silicon self-interstitial reaction occurs.

FIG. 7e is a graph which shows another example of how the initial concentration of vacancies or self-interstitials changes as a function of radial position due to radial diffusion of self-interstitials. Note that, in comparison to FIG. 7a, increased diffusion resulted in greater suppression the self-interstitial concentration.

FIG. 7f is a graph of ΔG_I as a function of radial position which shows an example of how greater suppression of the self-interstitial concentration, [I], (as depicted in FIG. 7e) results in a greater degree of suppression in ΔG_I, as compared to FIG. 7b.

FIG. 7g is a graph which shows another example of how the initial concentration of vacancies or self-interstitials changes as a function of radial position due to radial diffusion of self-interstitials. Note that, in comparison to FIG. 7c, increased diffusion resulted in greater suppression the self-interstitial concentration.

FIG. 7h is a graph of ΔG_I as a function of radial position which shows an example of how greater suppression of the self-interstitial concentration, [I], (as depicted in FIG. 7g) results in a greater degree of suppression in ΔG_I, as compared to FIG. 7d.

FIG. 7i is a graph which shows another example of how the initial concentration of vacancies or self-interstitials changes as a function of radial position due to radial diffusion of self-interstitials. Note that in this example a sufficient quantity of self-interstitials recombine with vacancies, such that there is no longer a vacancy-dominated region.

FIG. 7j is a graph of ΔG_I as a function of radial position which shows an example of how radial diffusion of self-interstitials (as depicted in FIG. 7i) is sufficient to maintain a suppression of agglomerated interstitial defects everywhere along the crystal radius.

FIG. 8 is a longitudinal, cross-sectional view of a single crystal silicon ingot showing, in detail, an axially symmetric region of a constant diameter portion of the ingot.

FIG. 9 is a longitudinal, cross-sectional view of a segment of a constant diameter portion of a single crystal silicon ingot, showing in detail axial variations in the width of an axially symmetric region.

FIG. 10 is a longitudinal, cross-sectional view of a segment of a constant diameter portion of a single crystal silicon ingot having axially symmetric region of a width which is less than the radius of the ingot, showing in detail that this region further contains a generally cylindrical region of vacancy dominated material.

FIG. 11 is a latitudinal, cross-sectional view of the axially symmetric region depicted in FIG. 10.

FIG. 12 is a longitudinal, cross-sectional view of a segment of a constant diameter portion of a single crystal silicon ingot having an axially symmetric region of a width which is equal to the radius of the ingot,

showing in detail that this region is a generally cylindrical region of self-interstitial dominated material which is substantially free of agglomerated intrinsic point defects.

FIG. 13 is an image produced by a scan of the minority carrier lifetime of an axial cut of the ingot following a series of oxygen precipitation heat treatments, showing in detail a generally cylindrical region of vacancy dominated material, a generally annular shaped axially symmetric region of self-interstitial dominated material, the V/I boundary present between them, and a region of agglomerated interstitial defects.

FIG. 14 is a graph of pull rate (i.e. seed lift) as a function of crystal length, showing how the pull rate is decreased linearly over a portion of the length of the crystal.

FIG. 15 is an image produced by a scan of the minority carrier lifetime of an axial cut of the ingot following a series of oxygen precipitation heat treatments, as described in Example 1.

FIG. 16 is a graph of pull rate as a function of crystal length for each of four single crystal silicon ingots, labeled 1-4 respectively, which are used to yield a curve, labeled $v^*(Z)$, as described in Example 1.

FIG. 17 is a graph of the average axial temperature gradient at the melt/solid interface, G_0, as a function of radial position, for two different cases as described in Example 2.

FIG. 18 is a graph of the initial concentration of vacancies, [V], or self-interstitials, [I], as a function of radial position, for two different cases as described Example 2.

FIG. 19 is a graph of temperature as a function of axial position, showing the axial temperature profile in ingots for two different cases as described in Example 3.

FIG. 20 is a graph of the self-interstitial concentrations resulting from the two cooling conditions illustrated in Fig. 19 and as more fully described in Example 3.

FIG. 21 is an image produced by a scan of the minority carrier lifetime of an axial cut of an entire ingot following a series of oxygen precipitation heat treatments, as described in Example 4.

FIG. 22 is a graph illustrating the position of the V/I boundary as a function of the length of the single crystal silicon ingot, as described in Example 5.

FIG. 23a is an image produced by a scan of the minority carrier lifetime of an axial cut of a segment of an ingot, ranging from about 100 mm to about 250 mm from the shoulder of the ingot, following a series of oxygen precipitation heat treatments, as described in Example 6.

FIG. 23b is an image produced by a scan of the minority carrier lifetime of an axial cut of a segment of an ingot, ranging from about 250 mm to about 400 mm from the shoulder of the ingot, following a series of oxygen precipitation heat treatments, as described in Example 6.

FIG. 24 is a graph illustrating the axial temperature profile for an ingot in four different hot zone configurations.

FIG. 25 is a graph of the axial temperature gradient, G_0, at various axial positions for an ingot, as described in Example 7.

FIG. 26 is a graph of the radial variations in the average axial temperature gradient, G_0, at various for an ingot, as described in Example 7.

FIG. 27 is a graph illustrating the relationship between the width of the axially symmetric region and the cooling rate, as described in Example 7.

FIG. 28 is a photograph of an axial cut of a segment of an ingot, ranging from about 235 mm to about 350 mm from the shoulder of the ingot, following copper decoration and a defect-delineating etch, described in Example 7.

FIG. 29 is a photograph of an axial cut of a segment of an ingot, ranging from about 305 mm to about 460 mm from the shoulder of the ingot, following copper decoration and a defect-delineating etch, described in Example 7.

FIG. 30 is a photograph of an axial cut of a segment of an ingot, ranging from about 140 mm to about 275 mm from the shoulder of the ingot, following copper decoration and a defect-delineating etch, described in Example 7.

FIG. 31 is a photograph of an axial cut of a segment of an ingot, ranging from about 600 mm to about 730 mm from the shoulder of the ingot, following copper decoration and a defect-delineating etch, described in Example 7.

FIG. 32 is a schematic, fragmentary vertical section of a crystal puller of the present invention showing an electrical resistance heater of a first embodiment as it is positioned during growth of a single crystal silicon ingot;

FIG. 33 is a perspective view of the electrical resistance heater of FIG. 1;

FIG. 34 is a perspective view of a second embodiment of an electrical resistance heater for use in the crystal puller of FIG. 1;

FIG. 35 is a perspective view of a third embodiment of an electrical resistance heater for use in the crystal puller of Fig. 1;

FIG. 36 is a schematic vertical section of a crystal puller without the electrical resistance heater of FIG. 1, showing temperature isotherms of a crystal ingot grown in the puller using a finite element analysis;

FIG. 37 is a schematic vertical section of a crystal puller of the present invention including the electrical resistance heater of FIG. 1, showing temperature isotherms of a crystal ingot grown in the puller using a finite element analysis;

FIG. 38 is a schematic vertical section of a crystal puller similar to that shown in FIG. 37, but including an electrical resistance heater having a longer length than the heater of FIG. 37, showing temperature isotherms of a crystal ingot grown in the puller using a finite element analysis; and

FIG. 39 is a plot of the ingot isotherm data from FIGS. 36, 37 and 38 comparing the ingot axial temperature versus the distance of the ingot from the molten source material.

Corresponding reference characters indicate corresponding parts throughout the several views of the drawings.

DETAILED DESCRIPTION OF THE PREFERRED EMBODIMENTS

Based upon experimental evidence to date, it appears that the type and initial concentration of intrinsic point defects is initially determined as the ingot cools from the temperature of solidification (i.e., about 1410°C) to a temperature greater than 1300°C (i.e., at least about 1325 °C, at least about 1350 °C or even at least about 1375 °C). That is, the type and initial concentration of these defects are controlled by the ratio v/G_0, where v is the growth velocity and G_0 is the average axial temperature gradient over this temperature range.

Referring to Fig. 1, for increasing values of v/G_0, a transition from decreasingly self-interstitial dominated growth to increasingly vacancy dominated growth occurs near a critical value of v/G_0 which, based upon currently available information, appears to be about 2.1×10^{-5} cm^2/sK, where G_0 is determined under conditions in which the axial temperature gradient is constant within the temperature range defined above. At this critical value, the concentrations of these intrinsic point defects are at equilibrium.

As the value of v/G_0 exceeds the critical value, the concentration of vacancies increases. Likewise, as the value of v/G_0 falls below the critical value, the concentration of self-interstitials increases. If these concentrations reach a level of critical supersaturation in the system, and if the mobility of the point defects is sufficiently high, a reaction, or an agglomeration event, will likely occur. Agglomerated intrinsic point defects in silicon can severely impact the yield potential of the material in the production of complex and highly integrated circuits.

It has been discovered that the reaction in which silicon self-interstitial atoms react to produce agglomerated interstitial defects can be suppressed. Without being bound to any particular theory, it is believed that the concentration of self-interstitials is controlled during the growth and cooling of the crystal ingot such that the change in free energy of the system never exceeds a critical value at which the agglomeration reaction spontaneously occurs to produce agglomerated interstitial defects.

In general, the change in system free energy available to drive the reaction in which agglomerated interstitial defects are formed from silicon self-interstitials in single crystal silicon is governed by Equation (I):

$$\Delta G_I = kT \ln\left(\frac{[I]}{[I]^{eq}}\right) \quad (I)$$

wherein

ΔG_I is the change in free energy,

k is the Boltzmann constant,

T is the temperature in K,

[I] is the concentration of self-interstitials at a point in space and time in the single crystal silicon, and

$[I]^{eq}$ is the equilibrium concentration of self interstitials at the same point in space and time at which [I] occurs and at the temperature, T.

According to this equation, for a given concentration of self-interstitials, [I], a decrease in the temperature, T, generally results in an increase in ΔG_I due to a sharp decrease in $[I]^{eq}$ with temperature.

Fig. 2 schematically illustrates the change in ΔG_I and the concentration of silicon self-interstitials for an ingot which is cooled from the temperature of solidification without simultaneously employing some means for suppression of the concentration of silicon self-interstitials. As the ingot cools, ΔG_I increases according to Equation (I), due to the increasing supersaturation of [I], and the energy barrier for the formation of agglomerated interstitial defects is approached. As cooling continues, this energy barrier is eventually exceeded, at which point a reaction occurs. This reaction results in the formation of agglomerated interstitial defects and the concomitant decrease in ΔG_I as the supersaturated system is relaxed, i.e., as the concentration of [I] decreases.

The agglomeration of self-interstitials can be avoided as the ingot cools from the temperature of solidification by maintaining the free energy of the silicon self-interstitial system at a value which is less than that at which an agglomeration reaction will occur. In other words, the system can be controlled so as to never become critically supersaturated. This can be achieved by establishing an initial concentration of self-interstitials (controlled by $v/G_0(r)$ as hereinafter defined) which is sufficiently low such that critical supersaturation is never achieved. However, in practice such concentrations are difficult to achieve across an entire crystal radius and, in general, therefore, critical supersaturation may be avoided by suppressing the initial silicon self-interstitial concentration subsequent to crystal solidification, i.e., subsequent to establishing the initial concentration determined by $v/G_0(r)$.

Figs. 3 and 4 schematically illustrate two possible effects of suppressing [I] upon the increase in ΔG_I as the ingot of Fig. 2 is cooled from the temperature of solidification. In Fig. 3, the suppression of [I] results in a decrease in the rate of increase of ΔG_I but, in this case, the suppression is insufficient to maintain ΔG_I everywhere at a value which is less than the critical value at which the reaction occurs; as a result, the suppression merely serves to reduce the temperature at which the reaction occurs. In Fig. 4, an increased suppression of [I] is sufficient to maintain ΔG_I everywhere to a value which is less than the critical value at which the reaction occurs; the suppression, therefore, inhibits the formation of defects.

Surprisingly, it has been found that due to the relatively large mobility of self-interstitials, which is generally about 10^{-4} cm^2/second, it is possible to effect the suppression over relatively large distances, i.e.

distances of about 5 cm to about 10 cm or more, by the radial diffusion of self-interstitials to sinks located at the crystal surface or to vacancy dominated regions located within the crystal. Radial diffusion can be effectively used to suppress the concentration of self-interstitials, provided sufficient time is allowed for the radial diffusion of the initial concentration of intrinsic point defects. In general, the diffusion time will depend upon the radial variation in the initial concentration of self-interstitials, with lesser radial variations requiring shorter diffusion times

Typically, the average axial temperature gradient, G_0, increases as a function of increasing radius for single crystal silicon, which is grown according to the Czochralski method. This means that the value of v/G_0 is typically not singular across the radius of an ingot. As a result of this variation, the type and initial concentration of intrinsic point defects is not constant. If the critical value of v/G_0, denoted in Figs. 5 and 6 as the V/I boundary 2, is reached at some point along the radius 4 of the ingot, the material will switch from being vacancy dominated to self-interstitial dominated. In addition, the ingot will contain an axially symmetric region of self-interstitial dominated material 6 (in which the initial concentration of silicon self-interstitial atoms increases as a function of increasing radius), surrounding a generally cylindrical region of vacancy dominated material 8 (in which the initial concentration of vacancies decreases as a function of increasing radius).

Figs. 7a and 7b schematically illustrate the effect of suppressing [I] upon the increase in ΔG_1 as an ingot is cooled from the temperature of solidification. When the ingot is pulled in accordance with the Czochralski method, the ingot contains an axially symmetric region of interstitial dominated material extending from the edge

of the ingot to the position along the radius at which the V/I boundary occurs and a generally cylindrical region of vacancy dominated material extending from the center of the ingot to the position along the radius at which the V/I boundary occurs. As the ingot is cooled from the temperature of solidification, radial diffusion of interstitial atoms causes a radially inward shift in the V/I boundary due to a recombination of self-interstitials with vacancies and a significant suppression of the self-interstitial concentration outside the V/I boundary. In addition, radial diffusion of self-interstitials to the surface of the crystal will occur as the crystal cools. The surface of the crystal is capable of maintaining near equilibrium point defect concentrations as the crystal cools. As a result, the suppression of [I] is sufficient to maintain ΔG_I everywhere to a value which is less than the critical value at which the silicon self-interstitial reaction occurs.

Referring now to Figs. 8 and 9, in a generally preferred process for suppressing the agglomeration of defects, a single crystal silicon ingot 10 is grown in accordance with the Czochralski method. The silicon ingot comprises a central axis 12, a seed-cone 14, an end-cone 16 and a constant diameter portion 18 between the seed-cone and the end-cone. The constant diameter portion has a circumferential edge 20 and a radius 4 extending from the central axis to the circumferential edge. The process comprises controlling the growth conditions, including growth velocity, v, the average axial temperature gradient, G_0, and the cooling rate, to cause the formation of an axially symmetric region 6 which, upon cooling of the ingot from the solidification temperature, is substantially free of agglomerated intrinsic point defects.

In one embodiment of the process, the growth conditions are controlled to maintain the V/I boundary 2 at a position which maximizes the volume of the axially symmetric region 6 relative to the volume of the constant diameter portion 18 of the ingot 10. In general, therefore, in this embodiment it is preferred that the axially symmetric region have a width 22 (as measured from the circumferential edge radially toward the central axis of the ingot) and a length 24 (as measured along the central axis of the ingot) which equals the radius 4 and length 26, respectively, of the constant diameter portion of the ingot. As a practical matter, however, operating conditions and crystal puller hardware constraints may dictate that the axially symmetric region occupy a lesser proportion of the constant diameter portion of the ingot. In general, therefore, the axially symmetric region in this embodiment preferably has a width of at least about 30%, more preferably at least about 40%, still more preferably at least about 60%, and most preferably at least about 80% of the radius of the constant diameter portion of the ingot. In addition, the axially symmetric region extends over a length of at least about 20%, preferably at least about 40%, more preferably at least about 60%, and still more preferably at least about 80% of the length of the constant diameter portion of the ingot.

Referring to Fig. 9, the width 22 of the axially symmetric region 6 may have some variation along the length of the central axis 12. For an axially symmetric region of a given length, therefore, the width is determined by measuring the distance from the circumferential edge 20 of the ingot 10 radially toward a point which is farthest from the central axis. In other words, the width 22 is measured such that the minimum distance within the given length 24 of the axially symmetric region 6 is determined.

Referring now to Figs. 10 and 11, when the axially symmetric region 6 of the constant diameter portion 18 of the ingot 10 has a width 22 which is less than the radius 4 of the constant diameter portion, the region is generally annular in shape. A generally cylindrical region of vacancy dominated material 8, which is centered about the central axis 12, is located radially inward of the generally annular shaped segment. Referring to Figure 12, it is to be understood that when the width 22 of the axially symmetric region 6 is equal to the radius 4 of the constant diameter portion 18, the region does not contain this vacancy dominated region; rather, the axially symmetric region itself is generally cylindrical and contains self-interstitial dominated material which is substantially free of agglomerated intrinsic point defects.

While it is generally preferred that the crystal growth conditions be controlled to maximize the width of the interstitial dominated region, there may be limits for a given crystal puller hot zone design. As the V/I boundary is moved closer to the central crystal axis, provided the cooling conditions and $G_0(r)$ do not change, where $G_0(r)$ is the radial variation of G_0, the minimum amount of radial diffusion required increases. In these circumstances, there may be a minimum radius of the vacancy dominated region which is required to suppress the formation of agglomerated interstitial defects by radial diffusion.

Figs. 7c and 7d schematically illustrate an example in which the minimum radius of the vacancy dominated region is exceeded. In this example, the cooling conditions and $G_0(r)$ are the same as those employed for the crystal of Figs. 7a and 7b in which there was sufficient outdiffusion to avoid agglomerated interstitial defects for the position of the V/I boundary illustrated. In Figs. 7c and 7d, the position of the V/I

boundary is moved closer to the central axis (relative to Figs. 7a and 7b) resulting in an increase in the concentration of interstitials in the region outside of the V/I boundary. As a result, more radial diffusion is required to sufficiently suppress the interstitial concentration. If sufficient outdiffusion is not achieved, the system ΔG_I will increase beyond the critical value and the reaction which produces agglomerated interstitial defects will occur, producing a region of these defects in an annular region between the V/I boundary and the edge of the crystal. The radius of the V/I boundary at which this occurs is the minimum radius for the given hot zone. This minimum radius is decreased if more radial diffusion of interstitials is allowed.

Figs. 7e, 7f, 7g and 7h illustrate the effect of an increased radial outdiffusion on interstitial concentration profiles and the rise of system ΔG_I for a crystal grown with the same initial vacancy and interstitial concentration profiles as the crystal exemplified in Figs. 7a, 7b, 7c and 7d. Increased radial diffusion of interstitials results in a greater suppression of interstitial concentration, thus suppressing the rise in the system ΔG_I to a greater degree than in Figs. 7a, 7b, 7c and 7d. In this case the system ΔG_I is not exceeded for the smaller radius of the V/I boundary.

Figs. 7i and 7j illustrate an example in which sufficient radial diffusion is allowed such that the minimum radius is reduced to zero by insuring sufficient radial diffusion to achieve a suppression of agglomerated interstitial defects everywhere along the crystal radius.

In one embodiment of the present process, the initial concentration of silicon self-interstitial atoms is controlled in the axially symmetric, self-interstitial dominated region of the ingot. Referring again to Fig. 1, in general, the initial concentration of silicon self-

interstitial atoms is controlled by controlling the crystal growth velocity, v, and the average axial temperature gradient, G_0, such that the value of the ratio v/G_0 is relatively near the critical value of this ratio, at which the V/I boundary occurs. In addition, the average axial temperature gradient, G_0, can be established such that the variation of G_0, i.e. $G_0(r)$, (and thus, $v/G_0(r)$) as a function of the ingot radius is also controlled.

The growth velocity, v, and the average axial temperature gradient, G_0, (as previously defined) are typically controlled such that the ratio v/G_0 ranges in value from about 0.5 to about 2.5 times the critical value of v/G_0 (i.e., about $1x10^{-5}$ cm^2/sK to about $5x10^{-5}$ cm^2/sK based upon currently available information for the critical value of v/G_0). Preferably, the ratio v/G_0 will range in value from about 0.6 to about 1.5 times the critical value of v/G_0 (i.e., about $1.3x10^{-5}$ cm^2/sK to about $3x10^{-5}$ cm^2/sK based upon currently available information for the critical value of v/G_0). Most preferably, the ratio v/G_0 will range in value from about 0.75 to about 1 times the critical value of v/G_0 (i.e., about $1.6x10^{-5}$ cm^2/sK to about $2.1x10^{-5}$ cm^2/sK based upon currently available information for the critical value of v/G_0). These ratios are achieved by independent control of the growth velocity, v, and the average axial temperature gradient, G_0.

In general, control of the average axial temperature gradient, G_0, may be achieved primarily through the design of the "hot zone" of the crystal puller, i.e. the graphite (or other materials) that makes up the heater, insulation, heat and radiation shields, among other things. Although the design particulars may vary depending upon the make and model of the crystal puller, in general, G_0 may be controlled using any of the means currently known in the art for controlling heat transfer

at the melt/solid interface, including reflectors, radiation shields, purge tubes, light pipes, and heaters. In general, radial variations in G_0 are minimized by positioning such an apparatus within about one crystal diameter above the melt/solid interface. G_0 can be controlled further by adjusting the position of the apparatus relative to the melt and crystal. This is accomplished either by adjusting the position of the apparatus in the hot zone, or by adjusting the position of the melt surface in the hot zone. In addition, when a heater is employed, G_0 may be further controlled by adjusting the power supplied to the heater. Any, or all, of these methods can be used during a batch Czochralski process in which melt volume is depleted during the process.

It is generally preferred for some embodiments of the present process that the average axial temperature gradient, G_0, be relatively constant as a function of diameter of the ingot. However, it should be noted that as improvements in hot zone design allow for variations in G_0 to be minimized, mechanical issues associated with maintaining a constant growth rate become an increasingly important factor. This is because the growth process becomes much more sensitive to any variation in the pull rate, which in turn directly effects the growth rate, v. In terms of process control, this means that it is favorable to have values for G_0 which differ over the radius of the ingot. Significant differences in the value of G_0, however, can result in a large concentration of self-interstitials generally increasing toward the wafer edge and, thereby, increase the difficultly in avoiding the formation of agglomerated intrinsic point defects.

In view of the foregoing, the control of G_0 involves a balance between minimizing radial variations in G_0 and maintaining favorable process control conditions.

Typically, therefore, the pull rate after about one diameter of the crystal length will range from about 0.2 mm/minute to about 0.8 mm/minute. Preferably, the pull rate will range from about 0.25 mm/minute to about 0.6 mm/minute and, more preferably, from about 0.3 mm/minute to about 0.5 mm/minute. It is to be noted that the pull rate is dependent upon both the crystal diameter and crystal puller design. The stated ranges are typical for 200 mm diameter crystals. In general, the pull rate will decrease as the crystal diameter increases. However, the crystal puller may be designed to allow pull rates in excess of those stated here. As a result, most preferably the crystal puller will be designed to enable the pull rate to be as fast as possible while still allowing for the formation of an axially symmetric region in accordance with the present process.

In a second and preferred embodiment, the amount of self-interstitial diffusion is controlled by controlling the cooling rate as the ingot is cooled from the solidification temperature (about 1410°C) to the temperature at which silicon self-interstitials become immobile, for commercially practical purposes. Silicon self-interstitials appear to be extremely mobile at temperatures near the solidification temperature of silicon, i.e. about 1410°C. This mobility, however, decreases as the temperature of the single crystal silicon ingot decreases. Generally, the diffusion rate of self-interstitials slows such a considerable degree that they are essentially immobile for commercially practical time periods at temperatures less than about 700°C, and perhaps at temperatures as great as 800°C, 900°C, 1000°C, or even 1050°C.

It is to be noted in this regard that, although the temperature at which a self-interstitial agglomeration reaction occurs may in theory vary over a wide range of temperatures, as a practical matter this range appears to

be relatively narrow for conventional, Czochralski grown silicon. This is a consequence of the relatively narrow range of initial self-interstitial concentrations which are typically obtained in silicon grown according to the Czochralski method. In general, therefore, a self-interstitial agglomeration reaction may occur, if at all, at temperatures within the range of about 1100°C to about 800°C, and typically at a temperature of about 1050°C.

Within the range of temperatures at which self-interstitials appear to be mobile, and depending upon the temperature in the hot zone, the cooling rate will typically range from about 0.1 °C/minute to about 3 °C/minute. Preferably, the cooling rate will range from about 0.1 °C/minute to about 1.5 °C/minute, more preferably from about 0.1 °C/minute to about 1 °C/minute, and still more preferably from about 0.1 °C/minute to about 0.5 °C/minute. Stated another way, to maximize the width of the axially symmetric region it is generally preferred that the silicon reside at a temperature in excess of about 1050 °C for a period of (i) at least about 5 hours, preferably at least about 10 hours, and more preferably at least about 15 hours for 150 mm nominal diameter silicon crystals, (ii) at least about 5 hours, preferably at least about 10 hours, more preferably at least about 20 hours, still more preferably at least about 25 hours, and most preferably at least about 30 hours for 200 mm nominal diameter silicon crystals, and (iii) at least about 20 hours, preferably at least about 40 hours, more preferably at least about 60 hours, and most preferably at least about 75 hours for silicon crystals having a nominal diameter greater than 200 mm. Referring to Fig. 24, axial temperature profiles may vary for different hot zone configurations designed to control the cooling rate of the ingot.

By controlling the cooling rate of the ingot within a range of temperatures in which self-interstitials

appear to be mobile, the self-interstitials may be given more time to diffuse to sinks located at the crystal surface, or to vacancy dominated regions, where they may be annihilated. The concentration of such interstitials may therefore be suppressed, which act to prevent an agglomeration event from occurring. Utilizing the diffusivity of interstitials by controlling the cooling rate acts to relax the otherwise stringent v/G_0 requirements that may be required in order to obtain an axially symmetric region free of agglomerated defects. Stated another way, as a result of the fact that the cooling rate may be controlled in order to allow interstitials more time to diffuse, a large range of v/G_0 values, relative to the critical value, are acceptable for purposes of obtaining an axially symmetric region free of agglomerated defects.

To achieve such cooling rates over appreciable lengths of the constant diameter portion of the crystal, consideration must also be given to the growth process of the end-cone of the ingot, as well as the treatment of the ingot once end-cone growth is complete. Typically, upon completion of the growth of the constant diameter portion of the ingot, the pull rate will be increased in order to begin the tapering necessary to form the end-cone. However, such an increase in pull rate will result in the lower segment of the constant diameter portion cooling more quickly within the temperature range in which interstitials are sufficiently mobile, as discussed above. As a result, these interstitials may not have sufficient time to diffuse to sinks to be annihilated; that is, the concentration in this lower segment may not be suppressed to a sufficient degree and agglomeration of interstitial defects may result.

In order to prevent the formation of such defects from occurring in this lower segment of the ingot, it is therefore preferred that constant diameter portion of the

ingot have a uniform thermal history in accordance with the Czochralski method. A uniform thermal history may be achieved by pulling the ingot from the silicon melt at a relatively constant rate during the growth of not only the constant diameter portion, but also during the growth of the end-cone of the crystal and possibly subsequent to growth of the end-cone. The relatively constant rate may be achieved, for example, by (i) reducing the rates of rotation of the crucible and crystal during the growth of the end-cone relative to the crucible and crystal rotation rates during the growth of the constant diameter portion of the crystal, and/or (ii) increasing the power supplied to the heater used to heat the silicon melt during the growth of the end-cone relative to the power conventionally supplied during end-cone growth. These additional adjustments of the process variables may occur either individually or in combination.

When the growth of the end-cone is initiated, a pull rate for the end-cone is established such that, any segment of the constant diameter portion of the ingot which remains at a temperature in excess of about 1050 °C experiences the same thermal history as other segment(s) of the constant diameter portion of the ingot which contain an axially symmetric region free of agglomerated intrinsic point defects which have already cooled to a temperature of less than about 1050 °C.

As previously noted, a minimum radius of the vacancy dominated region exists for which the suppression of agglomerated interstitial defects may be achieved. The value of the minimum radius depends on $v/G_0(r)$ and the cooling rate. As crystal puller and hot zone designs will vary, the ranges presented above for $v/G_0(r)$, pull rate, and cooling rate will also vary. Likewise these conditions may vary along the length of a growing crystal. Also as noted above, the width of the interstitial dominated region free of agglomerated

interstitial defects is preferably maximized. Thus, it is desirable to maintain the width of this region to a value which is as close as possible to, without exceeding, the difference between the crystal radius and the minimum radius of the vacancy dominated region along the length of the growing crystal in a given crystal puller.

The optimum width of the axially symmetric region and the required optimal crystal pulling rate profile for a given crystal puller hot zone design may be determined empirically. Generally speaking, this empirical approach involves first obtaining readily available data on the axial temperature profile for an ingot grown in a particular crystal puller, as well as the radial variations in the average axial temperature gradient for an ingot grown in the same puller. Collectively, this data is used to pull one or more single crystal silicon ingots, which are then analyzed for the presence of agglomerated interstitial defects. In this way, an optimum pull rate profile can be determined.

Fig. 13 is an image produced by a scan of the minority carrier lifetime of an axial cut of a section of a 200 mm diameter ingot following a series of oxygen precipitation heat-treatments which reveal defect distribution patterns. It depicts an example in which a near-optimum pull rate profile is employed for a given crystal puller hot zone design. In this example, a transition occurs from a $v/G_0(r)$ at which the maximum width of the interstitial dominated region is exceeded (resulting in the generation of regions of agglomerated interstitial defects 28) to an optimum $v/G_0(r)$ at which the axially symmetric region has the maximum width.

In addition to the radial variations in v/G_0 resulting from an increase in G_0 over the radius of the ingot, v/G_0 may also vary axially as a result of a change in v, or as a result of natural variations in G_0 due to

the Czochralski process. For a standard Czochralski process, v is altered as the pull rate is adjusted throughout the growth cycle, in order to maintain the ingot at a constant diameter. These adjustments, or changes, in the pull rate in turn cause v/G_0 to vary over the length of the constant diameter portion of the ingot. In accordance with the preferred process, the pull rate is therefore controlled in order to maximize the width of the axially symmetric region of the ingot. As a result, however, variations in the radius of the ingot may occur. In order to ensure that the resulting ingot has a constant diameter, the ingot is therefore preferably grown to a diameter larger than that which is desired. The ingot is then subjected to processes standard in the art to remove excess material from the surface, thus ensuring that an ingot having a constant diameter portion is obtained.

For an ingot prepared in accordance with the above described process and having a V/I boundary, i.e. an ingot containing material which is vacancy dominated, experience has shown that low oxygen content material, i.e., less than about 13 PPMA (parts per million atomic, ASTM standard F-121-83), is preferred. More preferably, the single crystal silicon contains less than about 12 PPMA oxygen, still more preferably less than about 11 PPMA oxygen, and most preferably less than about 10 PPMA oxygen. This is because, in medium to high oxygen contents wafers, i.e., 14 PPMA to 18 PPMA, the formation of oxygen-induced stacking faults and bands of enhanced oxygen clustering just inside the V/I boundary becomes more pronounced. Each of these are a potential source for problems in a given integrated circuit fabrication process. However, it is to be noted that, when the axially symmetric region has a width about equal to the

radius of the ingot, the oxygen content restriction is removed; this is because, given that no vacancy type material is present, the formation of such faults and clusters will not occur.

The effects of enhanced oxygen clustering may be further reduced by a number of methods, used singularly or in combination. For example, oxygen precipitate nucleation centers typically form in silicon which is annealed at a temperature in the range of about 350°C to about 750°C. For some applications, therefore, it may be preferred that the crystal be a "short" crystal, that is, a crystal which has been grown in a Czochralski process until the seed end has cooled from the melting point of silicon (about 1410° C) to about 750°C after which the ingot is rapidly cooled. In this way, the time spent in the temperature range critical for nucleation center formation is kept to a minimum and the oxygen precipitate nucleation centers have inadequate time to form in the crystal puller.

Preferably, however, oxygen precipitate nucleation centers formed during the growth of the single crystal are dissolved by annealing the single crystal silicon. Provided they have not been subjected to a stabilizing heat-treatment, oxygen precipitate nucleation centers can be annealed out of silicon by rapidly heating the silicon to a temperature of at least about 875° C, and preferably continuing to increase the temperature to at least 1000° C, at least 1100°C, or more. By the time the silicon reaches 1000° C, substantially all (e.g., >99%) of such defects have annealed out. It is important that the wafers be rapidly heated to these temperatures, i.e., that the rate of temperature increase be at least about 10° C per minute and more preferably at least about 50° C per minute. Otherwise, some or all of the oxygen precipitate nucleation centers may be stabilized by the heat-treatment. Equilibrium appears to be reached in

relatively short periods of time, i.e., on the order of about 60 seconds or less. Accordingly, oxygen precipitate nucleation centers in the single crystal silicon may be dissolved by annealing it at a temperature of at least about 875° C, preferably at least about 950°C, and more preferably at least about 1100°C, for a period of at least about 5 seconds, and preferably at least about 10 minutes.

The dissolution may be carried out in a conventional furnace or in a rapid thermal annealing (RTA) system. The rapid thermal anneal of silicon may be carried out in any of a number of commercially available rapid thermal annealing ("RTA") furnaces in which wafers are individually heated by banks of high power lamps. RTA furnaces are capable of rapidly heating a silicon wafer, e.g., they are capable of heating a wafer from room temperature to 1200 °C in a few seconds. One such commercially available RTA furnace is the model 610 furnace available from AG Associates (Mountain View, CA). In addition, the dissolution may be carried out on silicon ingots or on silicon wafers, preferably wafers.

It is to be noted that wafers prepared in accordance with the above process are suitable for use as substrates upon which an epitaxial layer may be deposited. Epitaxial deposition may be performed by means common in the art.

Furthermore, it is also to be noted that such wafers are suitable for use in combination with hydrogen or argon annealing treatments, such as the treatments described in European Patent Application No. 503,816 A1.

Detection of Agglomerated Defects

Agglomerated defects may be detected by a number of different techniques. For example, flow pattern defects, or D-defects, are typically detected by preferentially etching the single crystal silicon sample in a Secco etch

solution for about 30 minutes, and then subjecting the sample to microscopic inspection. (see, e.g., H. Yamagishi et al., Semicond. Sci. Technol. 7, A135 (1992)). Although standard for the detection of agglomerated vacancy defects, this process may also be used to detect agglomerated interstitial defects. When this technique is used, such defects appear as large pits on the surface of the sample when present.

Agglomerated defects may also be detected using laser scattering techniques, such as laser scattering tomography, which typically have a lower defect density detection limit that other etching techniques.

Additionally, agglomerated intrinsic point defects may be visually detect by decorating these defects with a metal capable of diffusing into the single crystal silicon matrix upon the application of heat. Specifically, single crystal silicon samples, such as wafers, slugs or slabs, may be visually inspected for the presence of such defects by first coating a surface of the sample with a composition containing a metal capable of decorating these defects, such as a concentrated solution of copper nitrate. The coated sample is then heated to a temperature between about 900°C and about 1000°C for about 5 minutes to about 15 minutes in order to diffuse the metal into the sample. The heat treated sample is then cooled to room temperature, thus causing the metal to become critically supersaturated and precipitate at sites within the sample matrix at which defects are present.

After cooling, the sample is first subjected to a non-defect delineating etch, in order to remove surface residue and precipitants, by treating the sample with a bright etch solution for about 8 to about 12 minutes. A

typical bright etch solution comprises about 55 percent nitric acid (70% solution by weight), about 20 percent hydrofluoric acid (49% solution by weight), and about 25 percent hydrochloric acid (concentrated solution).

The sample is then rinsed with deionized water and subjected to a second etching step by immersing the sample in, or treating it with, a Secco or Wright etch solution for about 35 to about 55 minutes. Typically, the sample will be etched using a Secco etch solution comprising about a 1:2 ratio of 0.15 M potassium dichromate and hydrofluoric acid (49% solution by weight). This etching step acts to reveal, or delineate, agglomerated defects which may be present.

Definitions

As used herein, the following phrases or terms shall have the given meanings: "agglomerated intrinsic point defects" mean defects caused (i) by the reaction in which vacancies agglomerate to produce D-defects, flow pattern defects, gate oxide integrity defects, crystal originated particle defects, crystal originated light point defects, and other such vacancy related defects, or (ii) by the reaction in which self-interstitials agglomerate to produce dislocation loops and networks, and other such self-interstitial related defects; "agglomerated interstitial defects" shall mean agglomerated intrinsic point defects caused by the reaction in which silicon self-interstitial atoms agglomerate; "agglomerated vacancy defects" shall mean agglomerated vacancy point defects caused by the reaction in which crystal lattice vacancies agglomerate; "radius" means the distance measured from a central axis to a circumferential edge of a wafer or ingot; "substantially free of agglomerated intrinsic point defects" shall mean a concentration of agglomerated defects which is less than the detection limit of these defects, which is currently about 10^3

defects/cm^3; "V/I boundary" means the position along the radius of an ingot or wafer at which the material changes from vacancy dominated to self-interstitial dominated; and "vacancy dominated" and "self-interstitial dominated" mean material in which the intrinsic point defects are predominantly vacancies or self-interstitials, respectively.

Examples

The following examples illustrate the above process for preparing a single crystal silicon ingot in which, as the ingot cools from the solidification temperature in accordance with the Czochralski method, the agglomeration of intrinsic point defects is prevented within an axially symmetric region of the constant diameter portion of the ingot, from which wafers may be sliced.

The following examples set forth one set of conditions that may be used to achieve the desired result. Alternative approaches exist for determining an optimum pull rate profile for a given crystal puller. For example, rather than growing a series of ingots at various pull rates, a single crystal could be grown at pull rates which increase and decrease along the length of the crystal; in this approach, agglomerated self-interstitial defects would be caused to appear and disappear multiple times during growth of a single crystal. Optimal pull rates could then be determined for a number of different crystal positions. Accordingly, the following examples should not be interpreted in a limiting sense.

Example 1

Optimization Procedure For A Crystal Puller Having A Pre-existing Hot Zone Design

A first 200 mm single crystal silicon ingot was grown under conditions in which the pull rate was ramped linearly from about 0.75 mm/min. to about 0.35 mm/min. over the length of the crystal. Fig. 14 shows the pull rate as a function of crystal length. Taking into account the pre-established axial temperature profile of a growing 200 mm ingot in the crystal puller and the pre-established radial variations in the average axial temperature gradient, G_0, i.e., the axial temperature gradient at the melt/solid interface, these pull rates were selected to insure that ingot would be vacancy dominated material from the center to the edge at one end of the ingot and interstitial dominated material from the center to the edge of the other end of the ingot. The grown ingot was sliced longitudinally and analyzed to determine where the formation of agglomerated interstitial defects begins.

Fig. 15 is an image produced by a scan of the minority carrier lifetime of an axial cut of the ingot over a section ranging from about 635 mm to about 760 mm from the shoulder of the ingot following a series of oxygen precipitation heat-treatments which reveal defect distribution patterns. At a crystal position of about 680 mm, a band of agglomerated interstitial defects 28 can be seen. This position corresponds to a critical pull rate of $v^*(680\ mm) = 0.33$ mm/min. At this point, the width of the axially symmetric region 6 (a region which is interstitial dominated material but which lacks agglomerated interstitial defects) is at its maximum; the width of the vacancy dominated region 8, $R_V^*(680)$ is about 35 mm and the width of the axially symmetric region, $R_I^*(680)$ is about 65 mm.

A series of four single crystal silicon ingots were then grown at steady state pull rates which were somewhat greater than and somewhat less than the pull rate at which the maximum width of the axially symmetric region of the first 200 mm ingot was obtained. Fig. 16 shows the pull rate as a function of crystal length for each of the four crystals, labeled, respectively, as 1-4. These four crystals were then analyzed to determine the axial position (and corresponding pull rate) at which agglomerated interstitial defects first appear or disappear. These four empirically determined points (marked "*") are shown in Fig. 16. Interpolation between and extrapolation from these points yielded a curve, labeled $v^*(Z)$ in Fig. 16. This curve represents, to a first approximation, the pull rate for 200 mm crystals as a function of length in the crystal puller at which the axially symmetric region is at its maximum width.

Growth of additional crystals at other pull rates and further analysis of these crystals would further refine the empirical definition of $v^*(Z)$.

Example 2

Reduction of Radial Variation in $G_0(r)$

Figs. 17 and 18 illustrate the improvement in quality that can be achieved by reduction of the radial variation in the axial temperature gradient at the melt/solid interface, $G_0(r)$. The initial concentration (about 1 cm from the melt/solid interface) of vacancies and interstitials are calculated for two cases with different $G_0(r)$: (1) $G_0(r) = 2.65 + 5\times10^{-4}r^2$ (K/mm) and (2) $G_0(r) = 2.65 + 5\times10^{-5}r^2$ (K/mm). For each case the pull rate was adjusted such that the boundary between vacancy-rich silicon and interstitial-rich silicon is at a radius of 3 cm. The pull rate used for case 1 and 2 were 0.4 and 0.35 mm/min, respectively. From Fig. 18 it is clear that the initial concentration of interstitials in the

interstitial-rich portion of the crystal is dramatically reduced as the radial variation in the initial axial temperature gradient is reduced. This leads to an improvement in the quality of the material since it becomes easier to avoid the formation of interstitial defect clusters due to supersaturation of interstitials.

Example 3

Increased Out-diffusion Time for Interstitials

Figs. 19 and 20 illustrate the improvement in quality that can be achieved by increasing the time for out-diffusion of interstitials. The concentration of interstitials is calculated for two cases with differing axial temperature profiles in the crystal, dT/dz. The axial temperature gradient at the melt/solid interface is the same for both cases, so that the initial concentration (about 1 cm from the melt/solid interface) of interstitials is the same for both cases. In this example, the pull rate was adjusted such that the entire crystal is interstitial-rich. The pull rate was the same for both cases, 0.32 mm/min. The longer time for interstitial out-diffusion in case 2 results in an overall reduction of the interstitial concentration. This leads to an improvement in the quality of the material since it becomes easier to avoid the formation of interstitial defect clusters due to supersaturation of interstitials.

Example 4

A 700 mm long, 150 mm diameter crystal was grown with a varying pull rate. The pull rate varied nearly linearly from about 1.2 mm/min at the shoulder to about 0.4 mm/min at 430 mm from the shoulder, and then nearly linearly back to about 0.65 mm/min at 700 mm from the shoulder. Under these conditions in this particular crystal puller, the entire radius is grown under

interstitial-rich conditions over the length of crystal ranging from about 320 mm to about 525 mm from the shoulder of the crystal. Referring now to Fig. 21, at an axial position of about 525 mm and a pull rate of about 0.47 mm/min, the crystal is free of agglomerated intrinsic point defects clusters across the entire diameter. Stated another way, there is one small section of the crystal in which the width of the axially symmetric region, i.e., the region which is substantially free of agglomerated defects, is equal to the radius of the ingot.

EXAMPLE 5

As described in Example 1, a series of single crystal silicon ingots were grown at varying pull rates and then analyzed to determine the axial position (and corresponding pull rate) at which agglomerated interstitial defects first appeared or disappeared. Interpolation between and extrapolation from these points, plotted on a graph of pull rate v. axial position, yielded a curve which represents, to a first approximation, the pull rate for a 200 mm crystal as a function of length in the crystal puller at which the axially symmetric region is at its maximum width. Additional crystals were then grown at other pull rates and further analysis of these crystals was used to refine this empirically determined optimum pull rate profile.

Using this data and following this optimum pull rate profile, a crystal of about 1000 mm in length and about 200 mm in diameter was grown. Slices of the grown crystal, obtained from various axial position, were then analyzed using oxygen precipitation methods standard in the art in order to (i) determine if agglomerated interstitial defects were formed, and (ii) determine, as

a function of the radius of the slice, the position of the V/I boundary. In this way the presence of an axially symmetric region was determined, as well as the width of this region a function of crystal length or position.

The results obtained for axial positions ranging from about 200 mm to about 950 mm from the shoulder of the ingot are present in the graph of Fig. 22. These results show that a pull rate profile may be determined for the growth of a single crystal silicon ingot such that the constant diameter portion of the ingot may contain an axially symmetric region having a width, as measured from the circumferential edge radially toward the central axis of the ingot, which is at least about 40% the length of the radius of the constant diameter portion. In addition, these results show that this axially symmetric region may have a length, as measured along the central axis of the ingot, which is about 75% of the length of the constant diameter portion of the ingot.

Example 6

A single crystal silicon ingot having a length of about 1100 mm and a diameter of about 150 mm was grown with a decreasing pull rate. The pull rate at the shoulder of the constant diameter portion of the ingot was about 1 mm/min.. The pull rate decreased exponentially to about 0.4 mm/min., which corresponded to an axial position of about 200 mm from the shoulder. The pull rate then decreased linearly until a rate of about 0.3 mm/min. was reached near the end of the constant diameter portion of the ingot.

Under these process conditions in this particular hot zone configuration, the resulting ingot contains a region wherein the axially symmetric region has a width which about equal to the radius of the ingot. Referring now to Figs. 23a and 23b, which are images produced by a

scan of the minority carrier lifetime of an axial cut of a portion of the ingot following a series of oxygen precipitation heat treatments, consecutive segments of the ingot, ranging in axial position from about 100 mm to about 250 mm and about 250 mm to about 400 mm are present. It can be seen from these figures that a region exists within the ingot, ranging in axial position from about 170 mm to about 290 mm from the shoulder, which is free of agglomerated intrinsic point defects across the entire diameter. Stated another way, a region is present within the ingot wherein the width of the axially symmetric region, i.e., the region which is substantially free of agglomerated interstitial defects, is about equal to the radius of the ingot.

In addition, in a region ranging from an axially position from about 125 mm to about 170 mm and from about 290 mm to greater than 400 mm there are axially symmetric regions of interstitial dominated material free of agglomerated intrinsic point defects surrounding a generally cylindrical core of vacancy dominated material which is also free of agglomerated intrinsic point defects.

Finally, in a region ranging axially from about 100 mm to about 125 mm there is an axially symmetric region of interstitial dominated material free of agglomerated defects surrounding a generally cylindrical core of vacancy dominated material. Within the vacancy dominated material, there is an axially symmetric region which is free of agglomerated defects surrounding a core containing agglomerated vacancy defects.

Example 7

Cooling Rate and Position of V/I Boundary

A series of single crystal silicon ingots (150 mm and 200 mm nominal diameter), were grown in accordance with the Czochralski method using different hot zone configurations which affected the residence time of the silicon at temperatures in excess of about 1050°C. The pull rate profile for each ingot was varied along the length of the ingot in an attempt to create a transition from a region of agglomerated vacancy point defects to a region of agglomerated interstitial point defects.

Once grown, the ingots were cut longitudinally along the central axis running parallel to the direction of growth, and then further divided into sections which were each about 2 mm in thickness. Using the copper decoration technique previously described, one set of such longitudinal sections was then heated and intentionally contaminated with copper, the heating conditions being appropriate for the dissolution of a high concentration of copper interstitials. Following this heat treatment, the samples were then rapidly cooled, during which time the copper impurities either outdiffused or precipitated at sites where oxide clusters or agglomerated interstitial defects where present. After a standard defect delineating etch, the samples were visually inspected for the presence of precipitated impurities; those regions which were free of such precipitated impurities corresponded to regions which were free of agglomerated interstitial defects.

Another set of the longitudinal sections was subjected to a series of oxygen precipitation heat treatments in order to cause the nucleation and growth of new oxide clusters prior to carrier lifetime mapping. Contrast bands in lifetime mapping were utilized in order to determine and measure the shape of the instantaneous melt/solid interface at various axial positions in each

ingot. Information on the shape of the melt/solid interface was then used, as discussed further below, to estimate the absolute value of, and the radial variation in, the average axial temperature gradient, G_0. This information was also used, in conjunction with the pull rate, to estimate the radial variation in v/G_0.

To more closely examine the effect growth conditions have on the resulting quality of a single crystal silicon ingot, several assumptions were made which, based on experimental evidence available to-date, are believed to be justified. First, in order to simplify the treatment of thermal history in terms of the time taken to cool to a temperature at which the agglomeration of interstitial defects occurs, it was assumed that about 1050°C is a reasonable approximation for the temperature at which the agglomeration of silicon self-interstitials occurs. This temperature appears to coincide with changes in agglomerated interstitial defect density observed during experiments in which different cooling rates were employed. Although, as noted above, whether agglomeration occurs is also a factor of the concentration of interstitials, it is believed that agglomeration will not occur at temperatures above about 1050°C because, given the range of interstitial concentrations typical for Czochralski-type growth processes, it is reasonable to assume that the system will not become critically supersaturated with interstitials above this temperature. Stated another way, for concentrations of interstitials which are typical for Czochralski-type growth processes, it is reasonable to assume that the system will not become critically supersaturated, and therefore an agglomeration event will not occur, above a temperature of about 1050°C.

The second assumption that was made to parameterize the effect of growth conditions on the quality of single crystal silicon is that the temperature dependence of silicon self-interstitial diffusivity is negligible. Stated another way, it is assumed that self-interstitials diffuse at the same rate at all temperatures between about 1400°C and about 1050°C. Understanding that about 1050°C is considered a reasonable approximation for the temperature of agglomeration, the essential point of this assumption is that the details of the cooling curve from the melting point does not matter. The diffusion distance depends only on the total time spent cooling from the melting point to about 1050°C.

Using the axial temperature profile data for each hot zone design and the actual pull rate profile for a particular ingot, the total cooling time from about 1400°C to about 1050°C may be calculated. It should be noted that the rate at which the temperature changes for each of the hot zones was reasonably uniform. This uniformity means that any error in the selection of a temperature of nucleation for agglomerated interstitial defects, i.e. about 1050°C, will arguably lead only to scaled errors in the calculated cooling time.

In order to determine the radial extent of the vacancy dominated region of the ingot ($R_{vacancy}$), or alternatively the width of the axially symmetric region, it was further assumed that the radius of the vacancy dominated core, as determined by the lifetime map, is equivalent to the point at solidification where $v/G_0=v/G_0$ critical. Stated another way, the width of the axially symmetric region was generally assumed to be based on the position of the V/I boundary after cooling to room temperature. This is pointed out because, as mentioned above, as the ingot cools recombination of vacancies and

silicon self-interstitials may occur. When recombination does occur, the actual position of the V/I boundary shifts inwardly toward the central axis of the ingot. It is this final position which is being referred to here.

To simplify the calculation of G_0, the average axial temperature gradient in the crystal at the time of solidification, the melt/solid interface shape was assumed to be the melting point isotherm. The crystal surface temperatures were calculated using finite element modeling (FEA) techniques and the details of the hot zone design. The entire temperature field within the crystal, and therefore G_0, was deduced by solving Laplace's equation with the proper boundary conditions, namely, the melting point along the melt/solid interface and the FEA results for the surface temperature along the axis of the crystal. The results obtained at various axial positions from one of the ingots prepared and evaluated are presented in Fig. 25.

To estimate the effect that radial variations in G_0 have on the initial interstitial concentration, a radial position R', that is, a position halfway between the V/I boundary and the crystal surface, was assumed to be the furthest point a silicon self-interstitial can be from a sink in the ingot, whether that sink be in the vacancy dominated region or on the crystal surface. By using the growth rate and the G_0 data for the above ingot, the difference between the calculated v/G_0 at the position R' and v/G_0 at the V/I boundary (i.e., the critical v/G_0 value) provides an indication of the radial variation in the initial interstitial concentration, as well as the effect this has on the ability for excess interstitials to reach a sink on the crystal surface or in the vacancy dominated region.

For this particular data set, it appears there is no systematic dependence of the quality of the crystal on the radial variation in v/G_0. As can be seen in Fig. 26, the axial dependence in the ingot is minimal in this sample. The growth conditions involved in this series of experiments represent a fairly narrow range in the radial variation of G_0. As a result, this data set is too narrow to resolve a discernable dependence of the quality (i.e., the presence of absence of a band of agglomerated intrinsic point defects) on the radial variation of G_0.

As noted, samples of each ingot prepared were evaluated at various axial positions for the present or absence of agglomerated interstitial defects. For each axial position examined, a correlation may be made between the quality of the sample and the width of the axially symmetric region. Referring now to Fig. 27, a graph may be prepared which compares the quality of the given sample to the time the sample, at that particular axial position, was allowed to cool from solidification to about 1050°C. As expected, this graph shows the width of the axially symmetric region (i.e., $R_{crystal} - R_{vacancy}$) has a strong dependence on the cooling history of the sample within this particular temperature range. In order of the width of the axially symmetric region to increase, the trend suggests that longer diffusion times, or slower cooling rates, are needed.

Based on the data present in this graph, a best fit line may be calculated which generally represents a transition in the quality of the silicon from "good" (i.e., defect-free) to "bad" (i.e., containing defects), as a function of the cooling time allowed for a given ingot diameter within this particular temperature range. This general relationship between the width of the

axially symmetric region and the cooling rate may be expressed in terms of the following equation:

$$(R_{crystal} - R_{transition})^2 = D_{eff} * t_{1050°C}$$

wherein

$R_{crystal}$ is the radius of the ingot,

$R_{transition}$ is the radius of the axially symmetric region at an axial position in the sample were a transition occurs in the interstitial dominated material from being defect-free to containing defects, or vice versa,

D_{eff} is a constant, about $9.3*10^{-4}$ cm^2sec^{-1}, which represents the average time and temperature of interstitial diffusivity, and

$t_{1050°C}$ is the time required for the given axial position of the sample to cool from solidification to about 1050°C.

Referring again to Fig. 27, it can be seen that, for a given ingot diameter, a cooling time may be estimated in order to obtain an axially symmetric region of a desired diameter. For example, for an ingot having a diameter of about 150 mm, an axially symmetric region having a width about equal to the radius of the ingot may be obtained if, between the temperature range of about 1410°C and about 1050°C, this particular portion of the ingot is allowed to cool for about 10 to about 15 hours. Similarly, for an ingot having a diameter of about 200 mm, an axially symmetric region having a width about equal to the radius of the ingot may be obtained if between this temperature range this particular portion of the ingot is allowed to cool for about 25 to about 35 hours. If this line is further extrapolated, cooling times of about 65 to about 75 hours may be needed in order to obtain an axially symmetric region having a width about equal to the radius of an ingot having a diameter of about 300 mm. It is to be noted in this regard that, as the diameter of the ingot increases,

additional cooling time is required due to the increase in distance that interstitials must diffuse in order to reach sinks at the ingot surface or the vacancy core.

Referring now to Figs. 28, 29, 30 and 31, the effects of increased cooling time for various ingots may be observed. Each of these figures depicts a portion of a ingot having a nominal diameter of 200 mm, with the cooling time from the temperature of solidification to 1050 °C progressively increasing from Fig. 28 to Fig. 31.

Referring to Fig. 28, a portion of an ingot, ranging in axial position from about 235 mm to about 350 mm from the shoulder, is shown. At an axial position of about 255 mm, the width of the axially symmetric region free of agglomerated interstitial defects is at a maximum, which is about 45% of the radius of the ingot. Beyond this position, a transition occurs from a region which is free of such defects, to a region in which such defects are present.

Referring now to Fig. 29, a portion of an ingot, ranging in axial position from about 305 mm to about 460 mm from the shoulder, is shown. At an axial position of about 360 mm, the width of the axially symmetric region free of agglomerated interstitial defects is at a maximum, which is about 65% of the radius of the ingot. Beyond this position, defect formation begins.

Referring now to Fig. 30, a portion of an ingot, ranging in axial position from about 140 mm to about 275 mm from the shoulder, is shown. At an axial position of about 210 mm, the width of the axially symmetric region is about equal to the radius of the ingot; that is, a small portion of the ingot within this range is free of agglomerated intrinsic point defects.

Referring now to Fig. 31, a portion of an ingot, ranging in axial position from about 600 mm to about 730 mm from the shoulder, is shown. Over an axial position ranging from about 640 mm to about 665 mm, the width of

the axially symmetric region is about equal to the radius of the ingot. In addition, the length of the ingot segment in which the width of the axially symmetric region is about equal to the radius of the ingot is greater than what is observed in connection with the ingot of Fig. 30.

When viewed in combination, therefore, Figs. 28, 29, 30, and 31 demonstrate the effect of cooling time to 1050 °C upon the width and the length of the defect-free, axially symmetric region. In general, the regions containing agglomerated interstitial defects occurred as a result of a continued decrease of the crystal pull rate leading to an initial interstitial concentration which was too large to reduce for the cooling time of that portion of the crystal. A greater length of the axially symmetric region means a larger range of pull rates (i.e., initial interstitial concentration) are available for the growth of such defect-free material. Increasing the cooling time allows for initially higher concentration of interstitials, as sufficient time for radial diffusion may be achieved to suppress the concentration below the critical concentration required for agglomeration of interstitial defects. Stated in other words, for longer cooling times, somewhat lower pull rates (and, therefore, higher initial interstitial concentrations) will still lead to maximum axially symmetric region 6. Therefore, longer cooling times lead to an increase in the allowable pull rate variation about the condition required for maximum axially symmetric region diameter and ease the restrictions on process control. As a result, the process for an axially symmetric region over large lengths of the ingot becomes easier.

Referring again to Fig. 31, over an axial position ranging from about 665 mm to greater than 730 mm from the shoulder of crystal, a region of vacancy dominated material free of agglomerated defects is present in which the width of the region is equal to the radius of the ingot.

Crystal Puller of the Present Invention

Referring now to Fig. 32, a crystal puller of the present invention for producing single crystal silicon ingots and wafers according to the above-described process which are devoid of agglomerated intrinsic point defects over a substantial portion of the ingot radius is generally indicated at 121. The crystal puller 121 is preferably of the type used to grow monocrystalline silicon ingots (e.g., ingot I of Fig. 32) according to the Czochralski method. The crystal puller 121 includes a housing (generally indicated at 125) comprising a generally cylindrical growth chamber 127, a generally cylindrical pull chamber 129 above the growth chamber wall, and a dome-shaped transition portion 132 interconnecting the growth chamber and pull chamber. The pull chamber 129 has a smaller transverse dimension than the growth chamber 127. A quartz crucible 131 disposed in the growth chamber 127 contains molten semiconductor source material M (e.g., silicon) from which the monocrystalline silicon ingot I is grown. The crucible 131 includes a cylindrical side wall 133 and is mounted on a turntable 135 for rotation about a vertical axis. The crucible 131 is also capable of being raised within the growth chamber 127 to maintain the surface of the molten source material M at the same level as the ingot I is grown and source material is removed from the melt.

A crucible heater, generally indicated at 137, for melting the source material M in the crucible 131 includes a generally vertically oriented heating element 139 surrounding the crucible in radially spaced relationship with the crucible side wall 33. The heating element 139 heats the crucible 131 to temperatures above the melting point of the source material M. Insulation 141 is positioned to confine the heat to the interior of the housing 125. In addition, there are passages in the housing 125, including at the upper pull chamber 129, for allowing circulation of cooling water. Some of these passages are designated by the reference numeral 143 in Fig. 32.

A pulling mechanism includes a pull shaft 145 extending down from a mechanism (not shown) above the pull chamber 129 capable of raising, lowering and rotating the pull shaft. The crystal puller 121 may have a pull wire (not shown) rather than a shaft 145, depending upon the type of puller. The pull shaft 145 terminates in a seed crystal chuck 147 which holds a seed crystal 149 used to grow the monocrystalline ingot I. The pull shaft 145 has been partially broken away in Fig. 32 for clarity in illustration of a raised position of the seed chuck 147 and ingot I. A view port 148 in the domed transition portion 132 of the housing 125 provides for viewing of the liquid/solid interface between the ingot I and the melt surface of the molten source material M by a conventional ingot diameter control device, such as a camera control device (not shown). A line of sight L from the view port 148 to the liquid/solid interface of the ingot I is indicated in dashed line in Fig. 32. The general construction and operation of the crystal puller 121, including the ingot

diameter control device is well known to those of ordinary skill in the art and will not be further described except to the extent explained more fully below.

An electrical resistance heater 123 for use in the crystal puller 121 of the present invention comprises a generally tubular heating element 151 mounted in the upper pull chamber 129 of the housing 125. A central opening 153 of the heating element 151 allows the growing ingot I to pass centrally through the heating element as it is pulled upward through the housing 125 of the puller 121. In the illustrated embodiment, the heating element 151 preferably extends downward a small distance into the crystal growth chamber 127, terminating substantially above the crucible 131 containing the molten source material M. More particularly, the bottom of the heating element 151 is spaced sufficiently above the melt surface so that the heating element does not obstruct the line of sight L of the ingot diameter control device via the view port 148. As an example, in a crystal puller used for growing ingots I having a diameter of 200mm, the heating element 151 of the heater preferably terminates approximately 300mm above the melt surface. It is understood that the heating element 151 need not extend down into growth chamber 127 at all, so that the entire heating element is disposed within the pull chamber 129, without departing from the scope of this invention.

The length of the heating element 151 is such that it extends upward within the pull chamber 129 to a predetermined height based on the desired amount of heat to be radiated to the growing ingot I and the axial portion of the ingot to which the heat is to be radiated. In general, as the length of the heating element 151 increases, the residence time of the ingot above 1050°C also increases. As an example, the heating element has a length preferably greater than about 300 mm. However, it

is contemplated that the heating element 151 may be sized to extend substantially the entire height of the pull chamber 129 so that the entire length of a fully grown ingot I extending within the pull chamber could be retained in the pull chamber at a temperature above 1050°C throughout its full growth period.

As shown in Fig. 2, the heating element 151 comprises vertically oriented heating segments 155 arranged in side-by-side relationship and connected to each other to form an electrical circuit. More particularly, upper and lower ends, designated 157 and 159, respectively, of adjacent heating segments 155 are alternatingly connected to each other in a continuous serpentine configuration forming a closed geometric shape; in the illustrated embodiment, a cylinder. Opposing mounting brackets 161 are connected to the top of the heating element 151 in electrical connection with the heating segments 155 and extend upward from the heating element for mounting the heater 123 on the housing 125 in the pull chamber 129. Openings (not shown) in the housing 125 allow the mounting brackets 161 to be electrically connected to a source of electrical current (not shown) by conventional electrodes (not shown) extending through the openings for connection with the mounting brackets to conduct current through the heating element 151. A tubular heat shield 163, preferably constructed of graphite, is disposed generally between the heating element 151 and the wall of the upper pull chamber 129 to inhibit cooling of the heating element by the housing 125.

The heating element 151 is constructed of a non-contaminating resistive heating material which provides resistance to the flow of electrical current therethrough; the power output generated by the heating element increasing with the electrical resistance of the material. A particularly preferred resistive heating

material is highly purified extruded graphite. However, the heating element 151 may be constructed of silicon carbide coated graphite, isomolded graphite, carbon fiber composite, tungsten, metal or other suitable materials without departing from the scope of this invention. It is also contemplated that the heating element 151 may be constructed of wire, such as tungsten or molybdenum wire, wrapped on a quartz tube to form a heating coil (not shown). The spacing between the coils may be varied to shape the power output profile of the heating element 151. The heating element 151 is preferably capable of radiating heat at a temperature in the range of 1000°C - 1100°C. It is understood, however, that heating elements capable of generating higher temperatures may be used and remain within the scope of this invention.

Figs. 34 and 35 illustrate alternative embodiments of the heater 123 in which the heating segments 155 of the heating element 151 are of varying lengths, with upper ends 157 of the segments being co-planar about the circumference of the heating element at the top of the heating element and lower ends 159 of the segments being staggered vertically with respect to each other because of the varying lengths of the segments. The lower ends 159 of the longest segments 165 define the bottom of the heating element 151. Varying the length of the heating segments in this manner provides a profiled heating power output along the height of the heating element 151; the heating power output increasing from the bottom to the top of the heating element for better profiling the cooling rate of the growing ingot I.

In a preferred method of construction of the heating element 151, vertically extending slots are cut into a tube (not shown) constructed of the resistive heating material to define the serpentine configuration. More particularly, downward extending slots 169 extend down from the top of the heating element 151 and terminate

short of the lower ends 159 of the segments 155, leaving adjacent segments connected to each other at the lower ends. Upward extending slots 171 extend up from the lower ends 159 of the segments 155 and terminate short of the top of the heating element 151, leaving adjacent segments connected to each other at the upper ends 157 of these segments. Alternating the downward and upward extending slots 169, 171 about the circumference of the heating element 151 creates the serpentine configuration of the heating element. Where the lengths of the heating segments 155 are non-uniform, such as in the embodiments of Figs. 34 and 35, portions of the tube (not shown) are cut away to generally define the stepped configuration of the lower ends 159 of the heating segments 155 prior to cutting the vertically extending slots 169, 171 in the tube.

In operation, polycrystalline silicon ("polysilicon") is deposited in the crucible 131 and melted by heat radiated from the crucible heater 137. The seed crystal 149 is brought into contact with the molten silicon M and a single crystal ingot I is grown by slow extraction via the pulling mechanism. The growing ingot I begins cooling immediately as it is pulled upward from the melt and continues to cool as it is pulled upward through the lower crystal growth chamber 127. As portions of the ingot I come into radial registration with the bottom of the heating element 151, heat is radiated by the heating element to these portions of the ingot to reduce the rate of further cooling.

By radiating heat to the ingot I at a temperature of at least 1000°C - 1100°C, the rate of cooling of the ingot between the solidification temperature (e.g., above 1400°C) and 1050°C is substantially reduced, thereby increasing the time during which the ingot resides at a temperature exceeding 1050°C. As portions of the ingot remain at temperatures above 1050°C for relatively long

time durations, radial diffusion of self-interstitials occurs to suppress the concentration below the critical concentration required for agglomeration of interstitial defects. As such, an ingot is produced in which a substantial radial portion of the ingot is self-interstitial dominated and devoid of agglomerated intrinsic point defects. As discussed above, the longer the ingot temperature resides above 1050°C, the radial portion of the ingot devoid of agglomerated intrinsic point defects increases.

As an example, a finite element model analysis was conducted to simulate the growth of three monocrystalline silicon ingots I, each having a diameter of 200mm, according to the Czochralski method in a crystal puller 121 of the type described above. Each of the ingots was grown at a pull rate of 0.3 mm/minute. Growth of the first ingot I was simulated without the heater 123 in the upper pull chamber 129 of the puller housing 125. An electrical resistance heater 123 such as that described above was modeled to simulate the growth of the second ingot I. The heater 123 had a length of about 350mm, extending down into the growth chamber 127 to a height of 493mm above the melt surface. The third ingot I was grown in a crystal puller 121 including a substantially longer heater 123; having a length of about 500mm and extending down into the growth chamber 127 to a height of 493mm above the melt surface.

With reference to Figs. 36, 37 and 38, the temperature of the ingot and various structure in the housing was recorded and isotherms were plotted to indicate the cooling pattern of the ingots. In each of the Figures, the temperatures given are in °K. None of the isotherms translate directly to 1050°C. However, for

comparison purposes, the approximate position of the 1050°C isotherm would be located between the isotherms indicated as legend numbers 10 and 11 as indicated by the dashed line in each of the Figures.

In Fig. 36 (corresponding to the ingot grown without the additional heater in the upper pull chamber) the isotherm representing 1050°C is spaced about 250 mm above the melt surface, indicating rapid cooling of the ingot. For the pull rate of 0.3 mm/min, this represents a residence time above 1050°C of approximately 14 hours.

When the heater 121 is used in the second growth simulation, as shown in Fig. 37, the isotherm representing 1050°C is spaced above the melt surface more than 600 mm. At a pull rate of 0.3 mm/min., the temperature of the growing ingot would reside above 1050° for a time period of more than 33 hours. As discussed above with respect to Example 7, this time period is within the range desired for producing an ingot in which the ingot is devoid of agglomerated intrinsic point defects substantially along the entire radius of the ingot. As seen in Fig. 38, increasing the length of the heater further increases the height of the 1050°C isotherm above the melt surface to about 900 mm, resulting in an ingot residence time above 1050°C of about 50 hours. Fig. 39 is a plot comparing the axial temperature profile of the three ingots produced in the finite element analyses.

It will be observed from the foregoing that the crystal puller described herein satisfies the various objectives of the present invention and attains other advantageous results. The heater 123 having a heating element 151 mounted and extending within the upper pull chamber is adequately sized to radiate heat along a sufficient axial portion of the growing ingot to substantially reduce the cooling rate of the ingot and increase the time during which the ingot temperature

resides above 1050°C. More particularly, the heating element 151 may be sized such that the time during which the ingot I resides above 1050°C is sufficiently long whereby the ingot is devoid of agglomerated intrinsic point defects along substantially the entire radius of the ingot. Increasing the length of the heating element 151 may also allow for the pull rate of the crystal to be increased (but remain within the range of rates in which interstitial dominated silicon is grown) to improve production capacity.

Importantly, by mounting and extending the heater 123 within the upper pull chamber 129 of the housing 125, the heating element 151 can be sized to its desired length without taking up substantial space in the lower growth chamber 127. This allows the heater 123 to be mounted in conventional crystal pullers without requiring additional space within the growth chamber 127 and without obstructing the line of sight from the view port 148 to the liquid/solid interface. The size limitations associated with the lack of space in the growth chamber of the housing are thus overcome.

As various changes could be made in the above constructions without departing from the scope of the invention, it is intended that all matter contained in the above description or shown in the accompanying drawings shall be interpreted as illustrative and not in a limiting sense.

WHAT IS CLAIMED IS:

1. A crystal puller for growing monocrystalline silicon ingots according to the Czochralski method which are devoid of agglomerated intrinsic point defects over a substantial portion of the radius of the ingot, the crystal puller comprising:

a housing defining an interior having a lower growth chamber and an upper pull chamber, the pull chamber having a smaller transverse dimension than the growth chamber;

a crucible in the growth chamber of the housing for containing molten silicon;

a pulling mechanism for pulling a growing ingot upward from the molten silicon through the growth chamber and pull chamber; and

an electrical resistance heater comprising a heating element sized and shaped for being disposed at least partially within the upper pull chamber of the housing in radially spaced relationship with the outer surface of the growing ingot for radiating heat to the ingot as it is pulled upward in the pull chamber relative to the molten silicon, the heating element having an upper end and a lower end, the lower end of the heating element being disposed substantially closer to the molten silicon than the upper end when the heating element is placed in the housing.

2. A crystal puller as set forth in claim 1 wherein the heating element extends down into the lower growth chamber of the housing.

3. A crystal puller as set forth in claim 2 further comprising a port in the housing for viewing the growing ingot from outside the housing while the ingot is being pulled upward from the molten silicon, the lower end of the heating element being at a height above the molten silicon such that viewing of the growing ingot in the interior of the growth chamber via the port in the housing is substantially unobstructed by the heating element.

4. A crystal puller as set forth in claim 1 wherein the housing comprises a pull chamber side wall defining the upper pull chamber, the heating element being mounted on the upper pull chamber wall within the upper pull chamber of the housing.

5. A crystal puller as set forth in claim 4 wherein the heating element includes first and second vertically oriented heating segments arranged in a generally side-by-side relationship and being electrically connected together, and first and second mounting brackets electrically connected to the respective heating segments, said mounting brackets being adapted for mounting the heating element on the housing within the upper pull chamber of the housing in electrical connection with a source of electrical current.

6. A crystal puller as set forth in claim 5 wherein the heating element is constructed such that the heating power output generated by the heating element gradually increases from the lower end to the upper end of the heating element.

7. A crystal puller as set forth in claim 6 wherein the first and second segments each have an upper end and a lower end, the second segment having a length substantially greater than the first segment and being arranged relative to the first segment so that when the heating element is placed in the housing the lower end of the second segment is disposed closer to the molten silicon in the crucible than the lower end of the first segment.

8. A crystal puller as set forth in claim 1 adapted for growing silicon ingots having a diameter of about 200mm, the heating element being sized to radiate sufficient heat to the growing ingot whereby the temperature of the ingot resides above 1050°C for a time period exceeding 25 hours.

9. A crystal puller as set forth in claim 8 in which the heating element is sized to radiate sufficient heat to the growing ingot whereby the temperature of the ingot resides above 1050°C for a time period exceeding 35 hours.

10. A crystal puller as set forth in claim 9 in which the heating element is sized to radiate sufficient heat to the growing ingot whereby the temperature of the ingot resides above 1050°C for a time period equal to or greater than about 50 hours.

FIG. 1

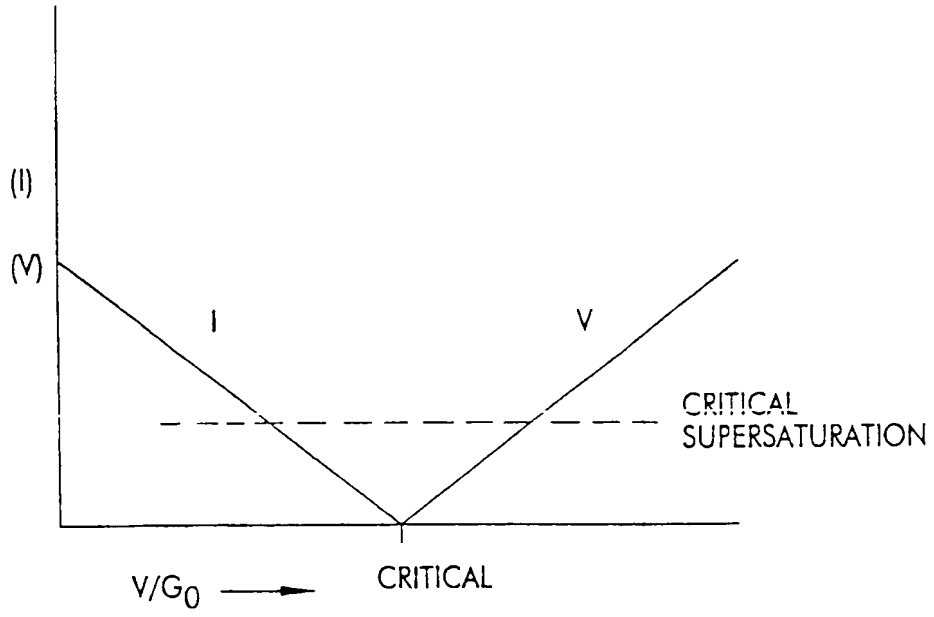

FIG. 2

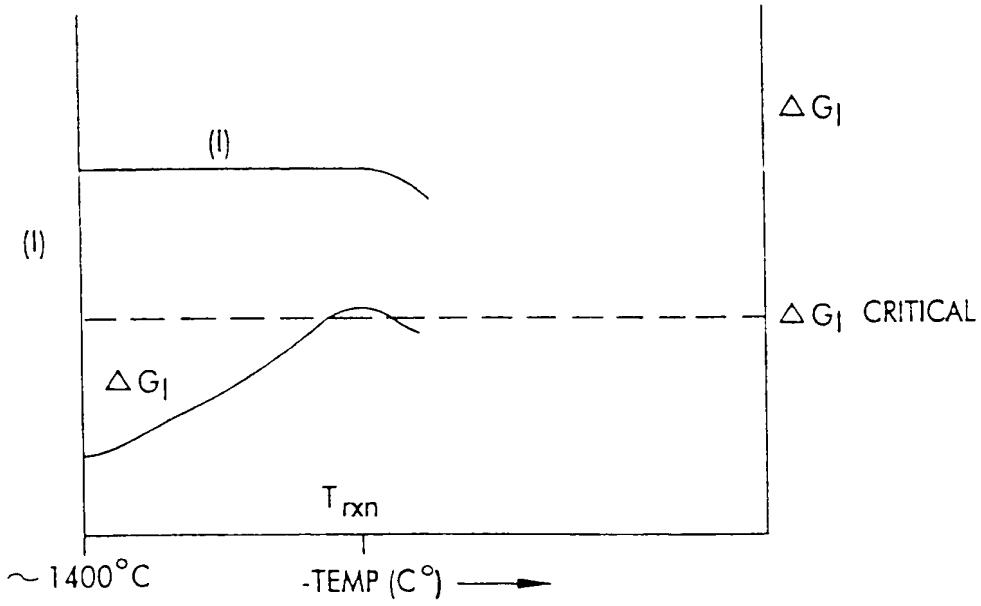

FIG. 3

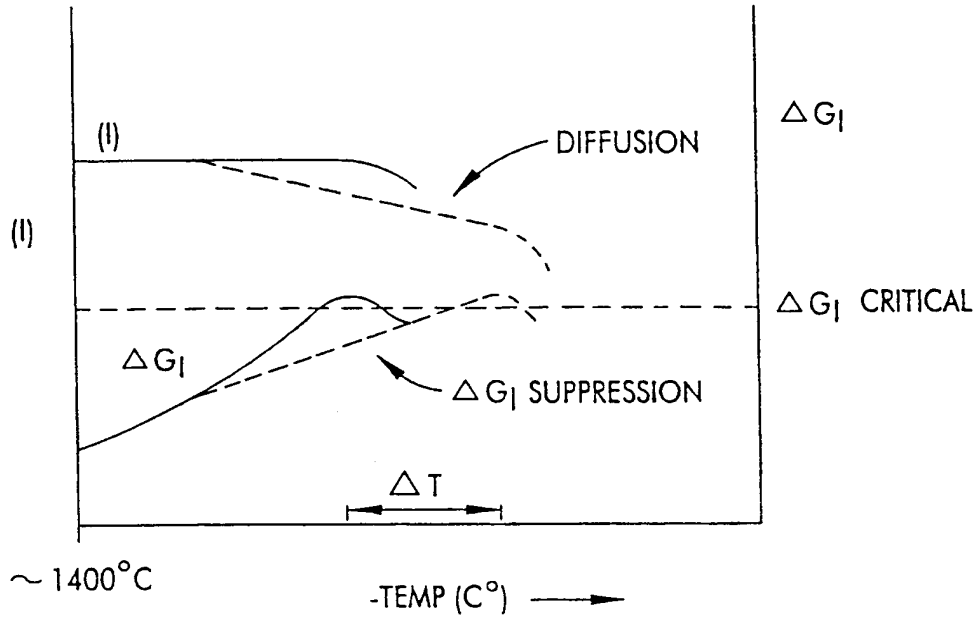

FIG. 4

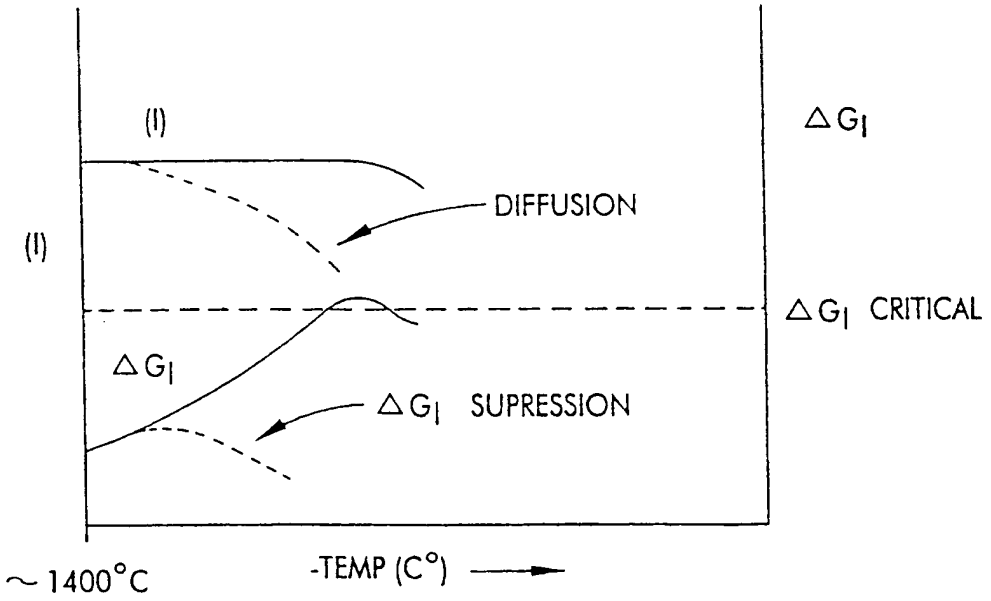

FIG. 5

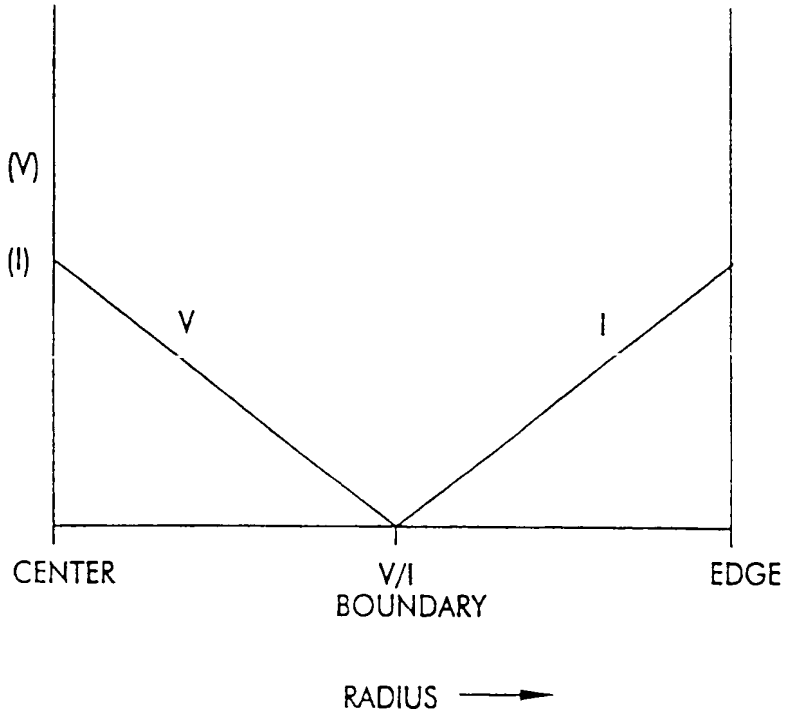

FIG. 6

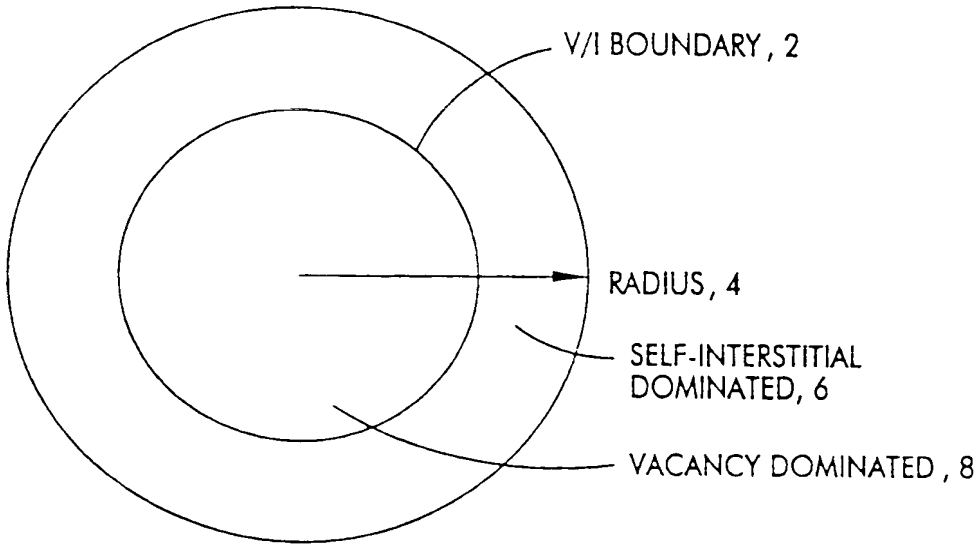

FIG.7A

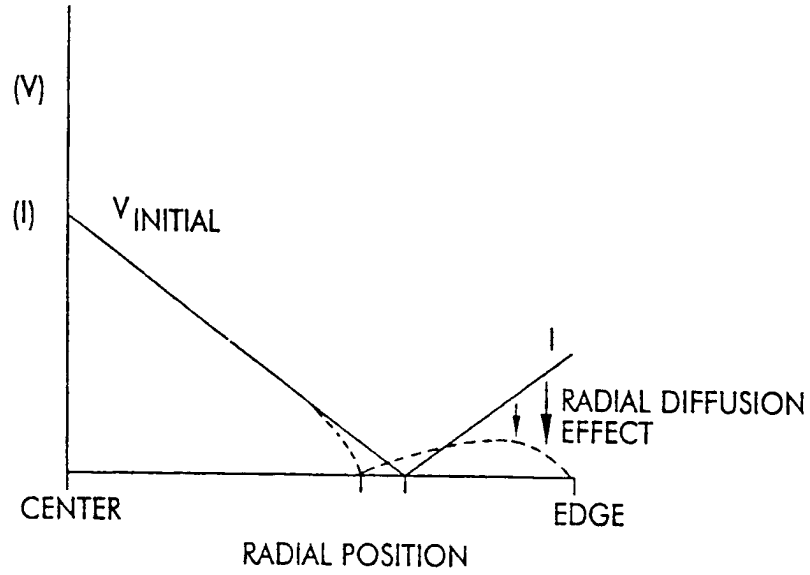

FIG.7B

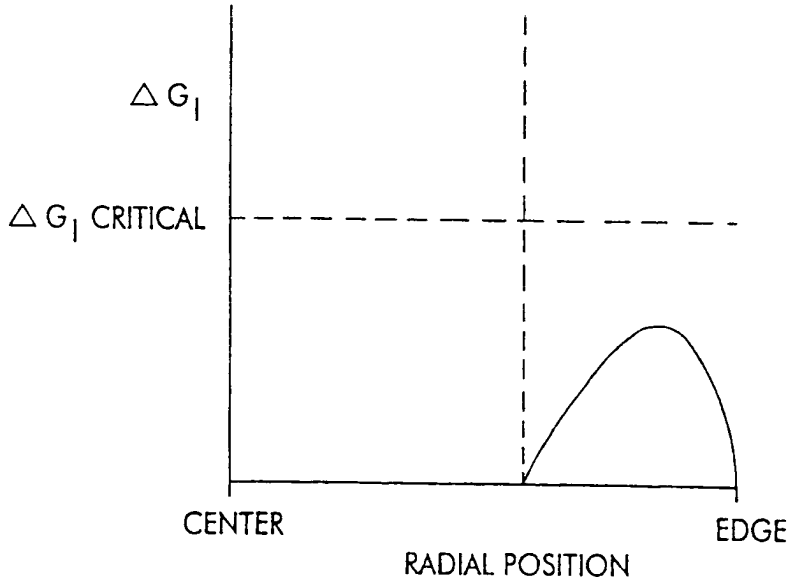

FIG.7C

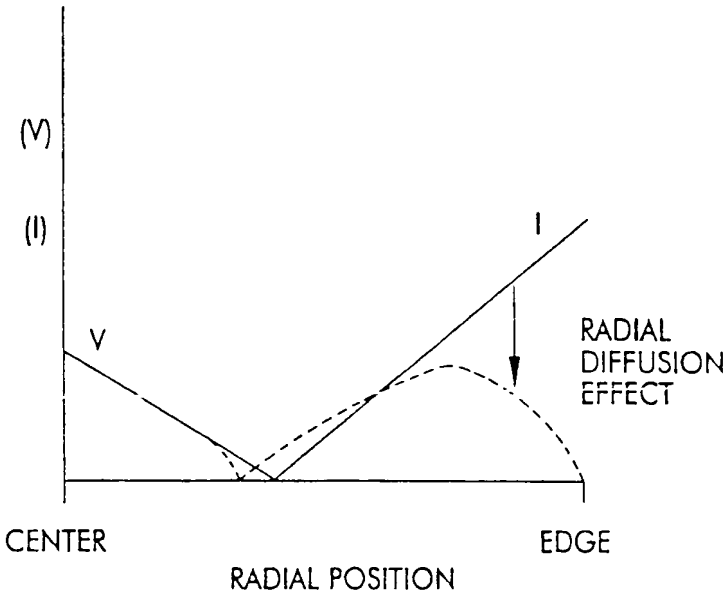

FIG.7D

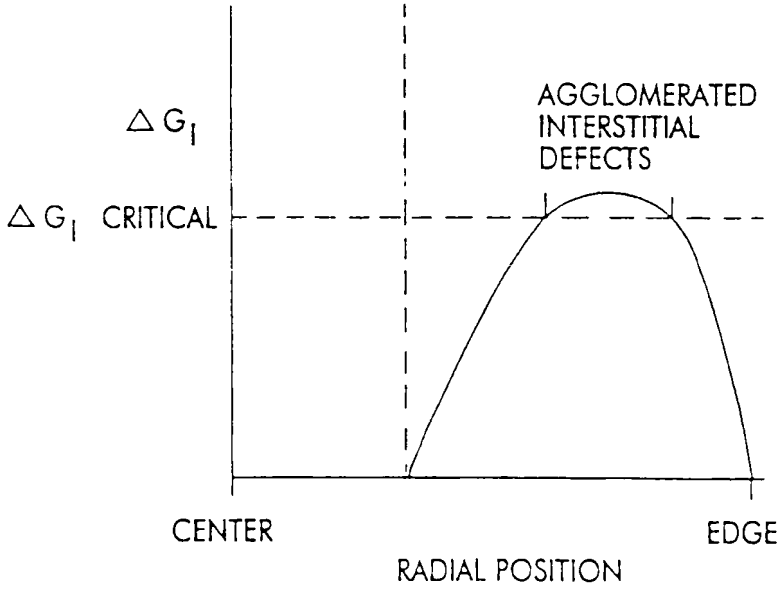

FIG.7E

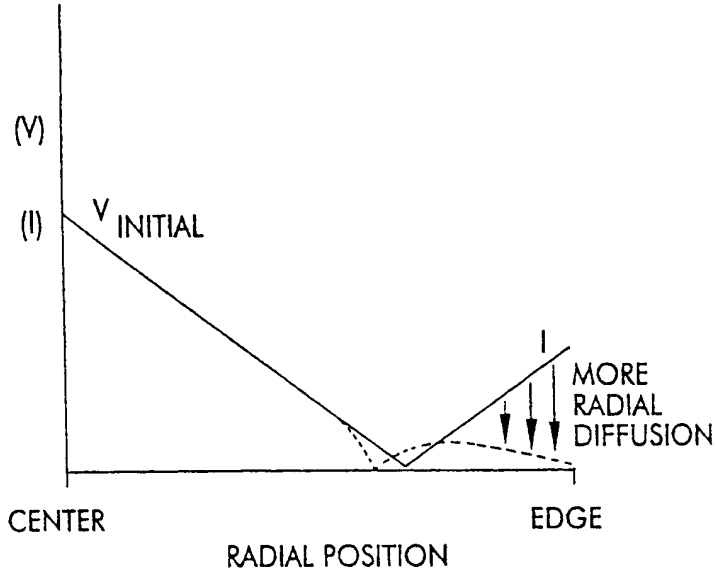

FIG.7F

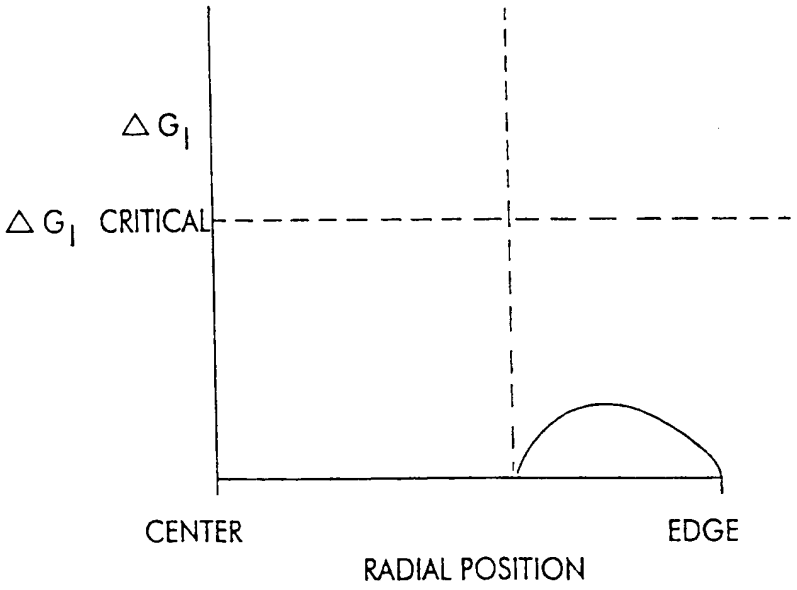

FIG.7G

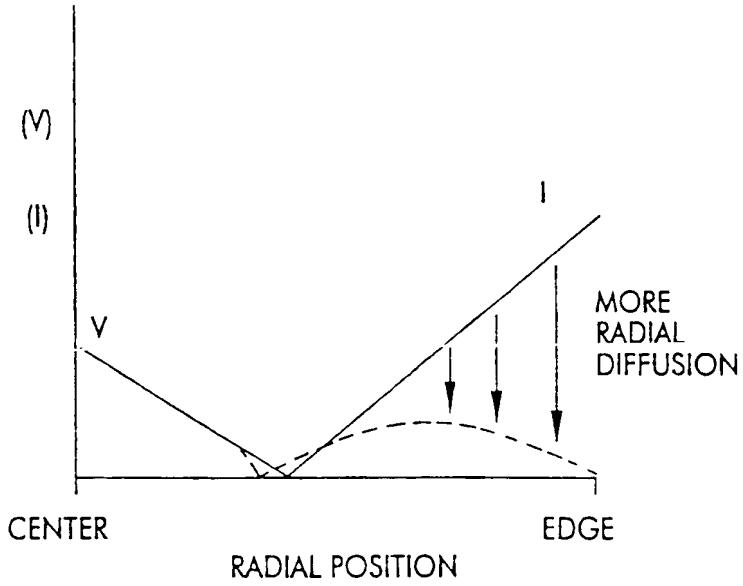

FIG.7H

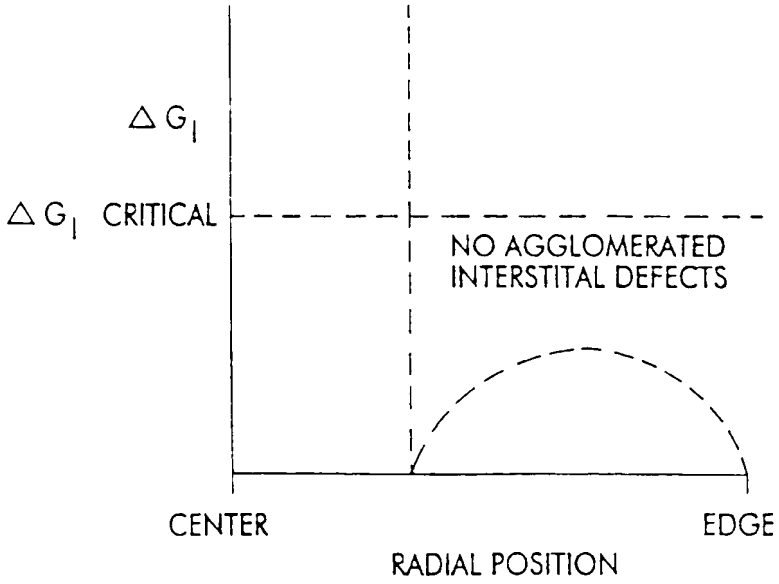

FIG.7I

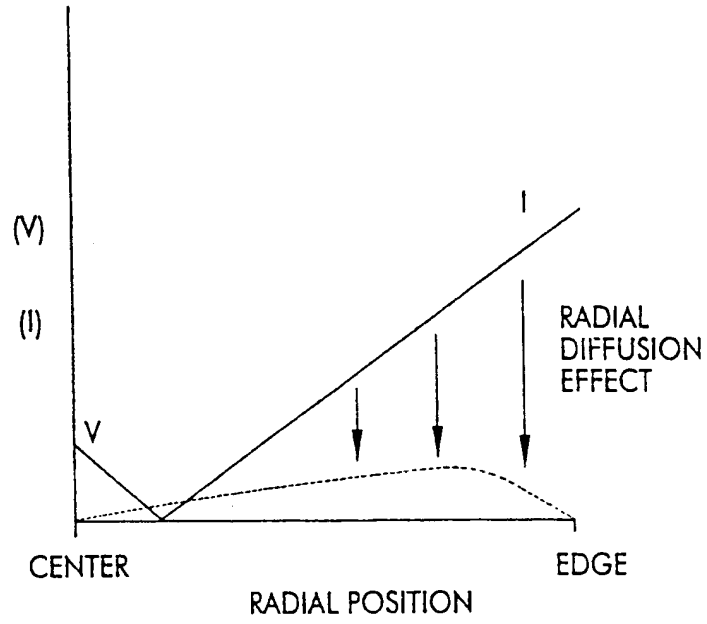

FIG.7J

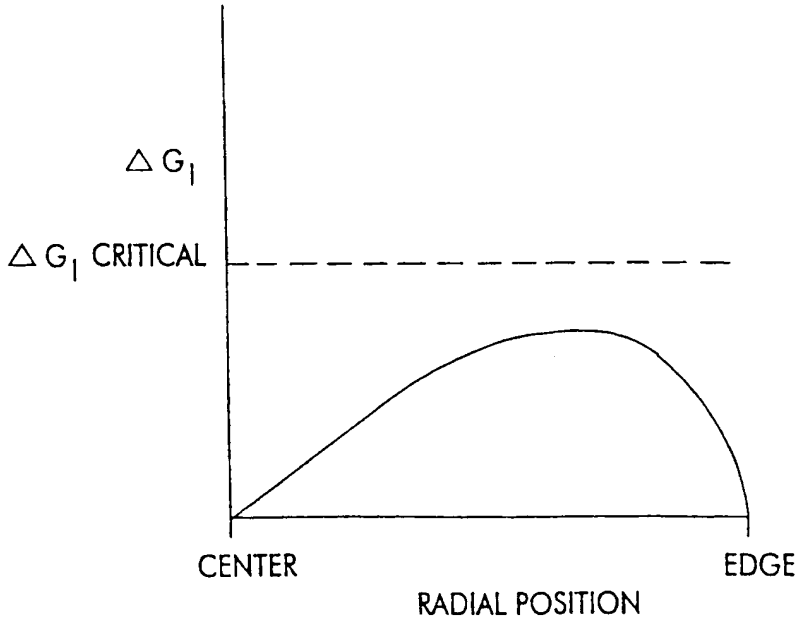

FIG. 8

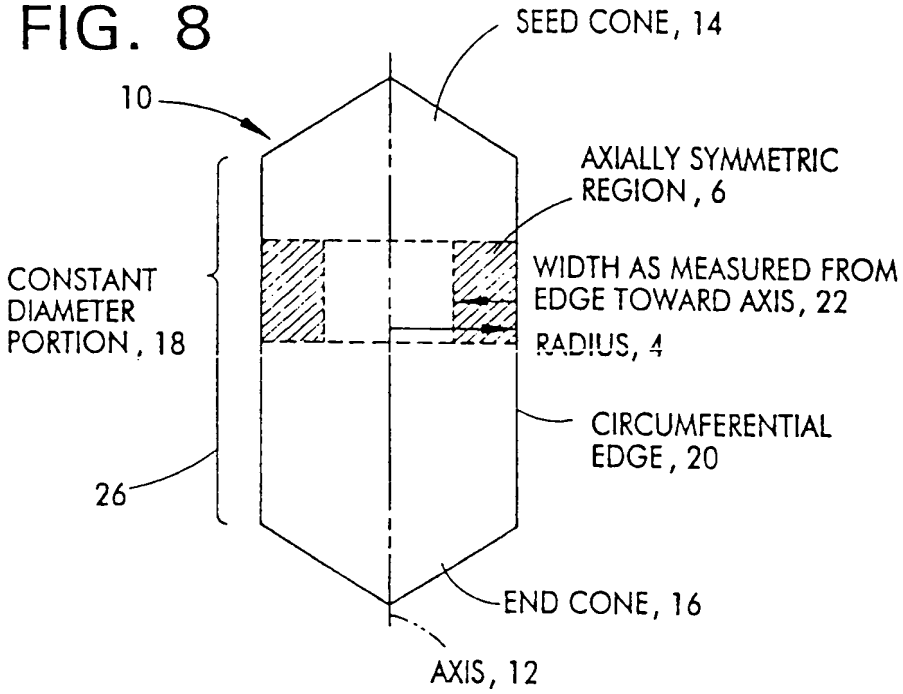

FIG. 9

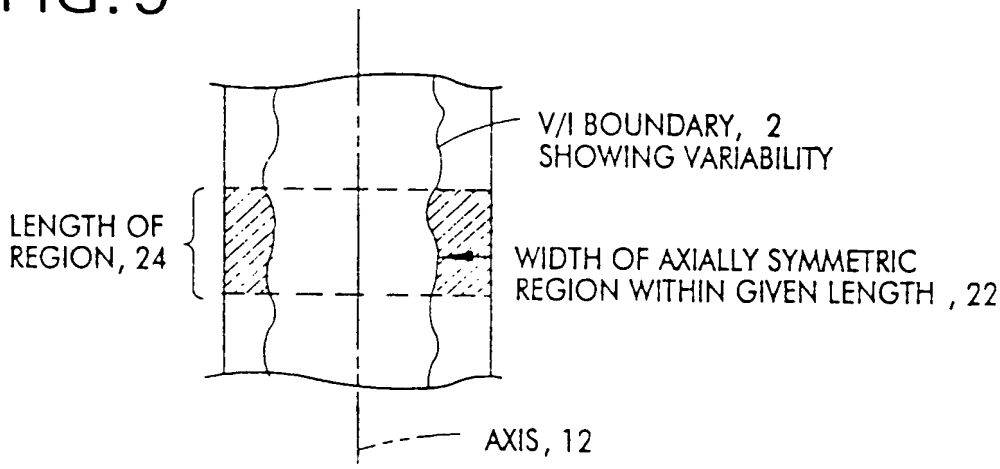

FIG.10

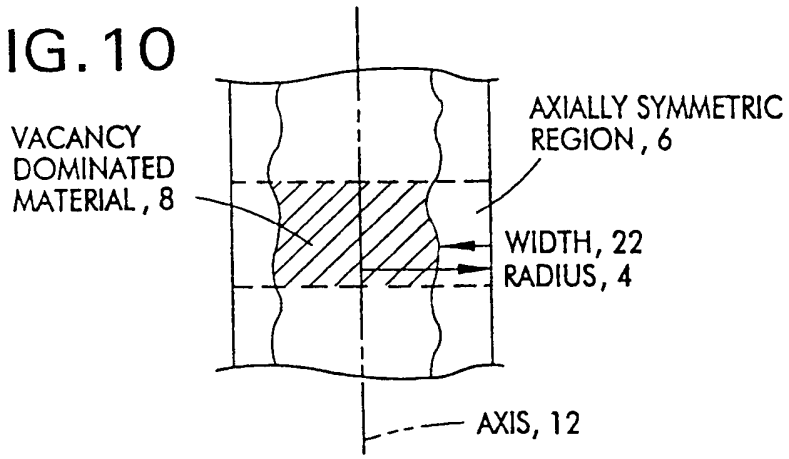

FIG.11

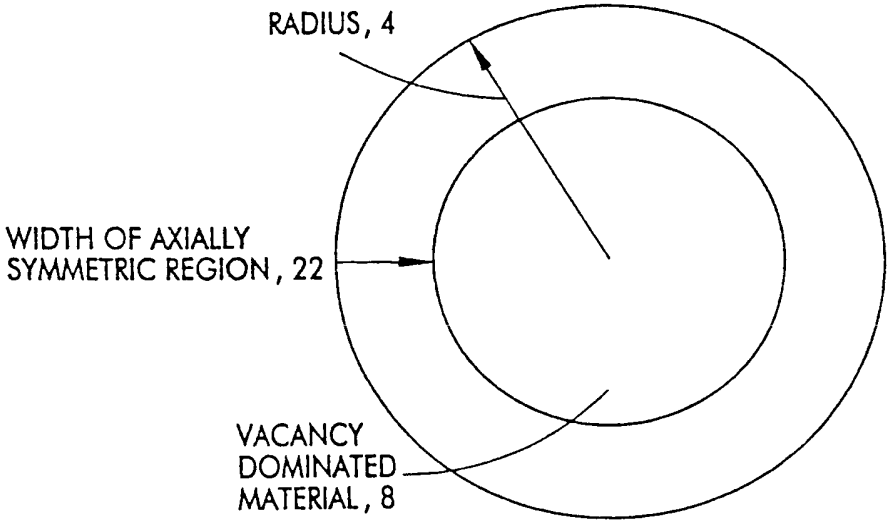

FIG.12

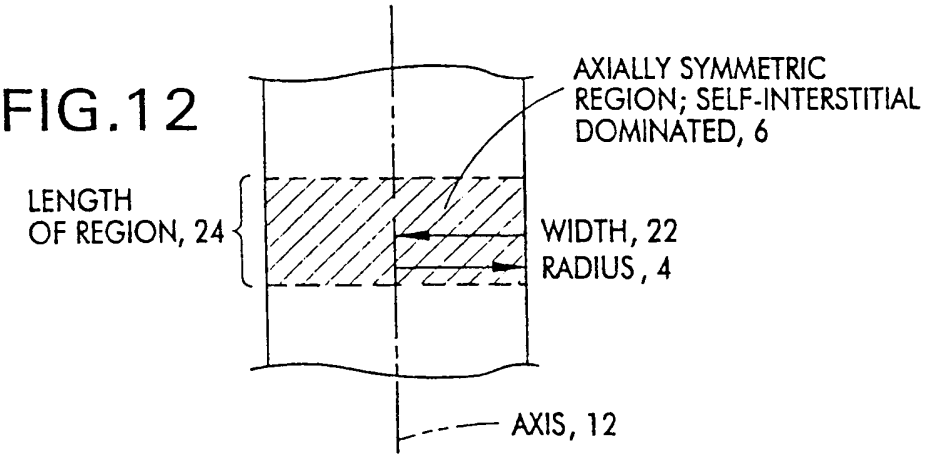

FIG.13

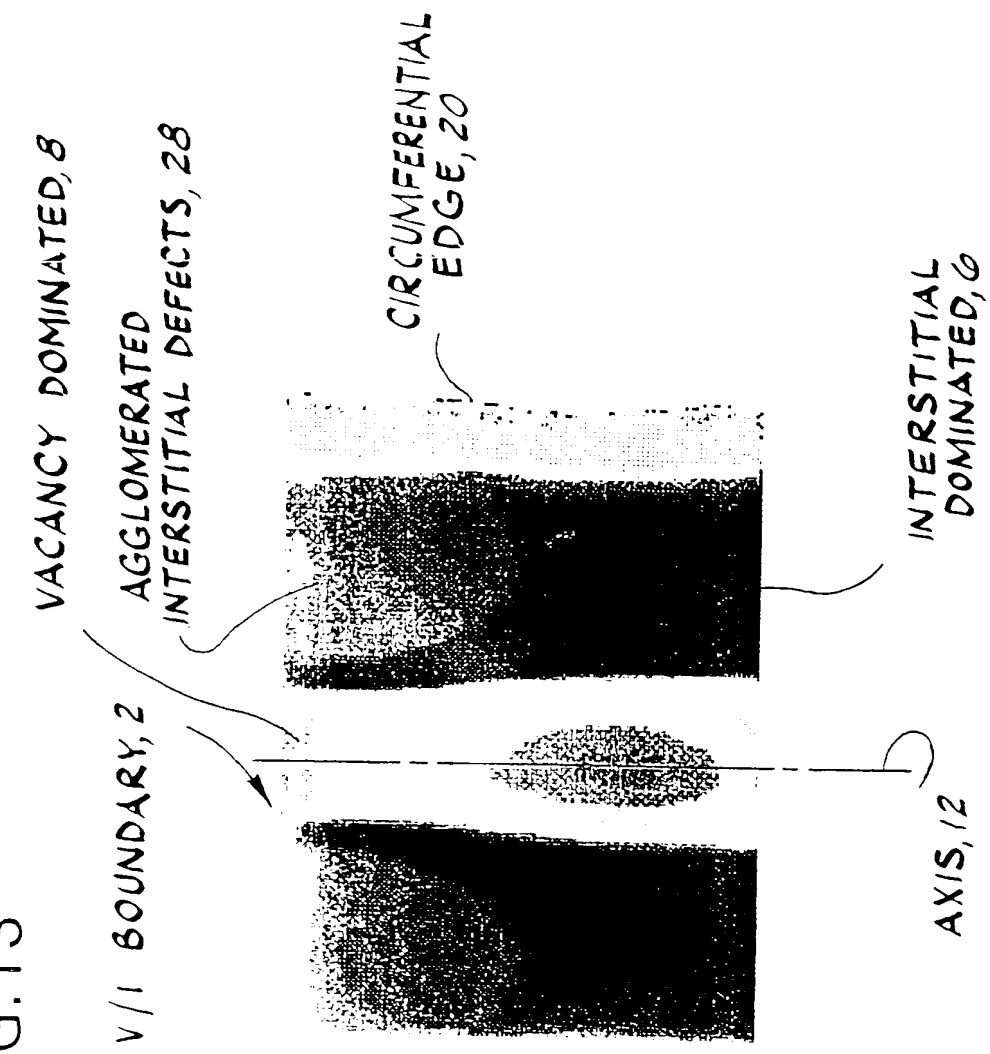

FIG.14

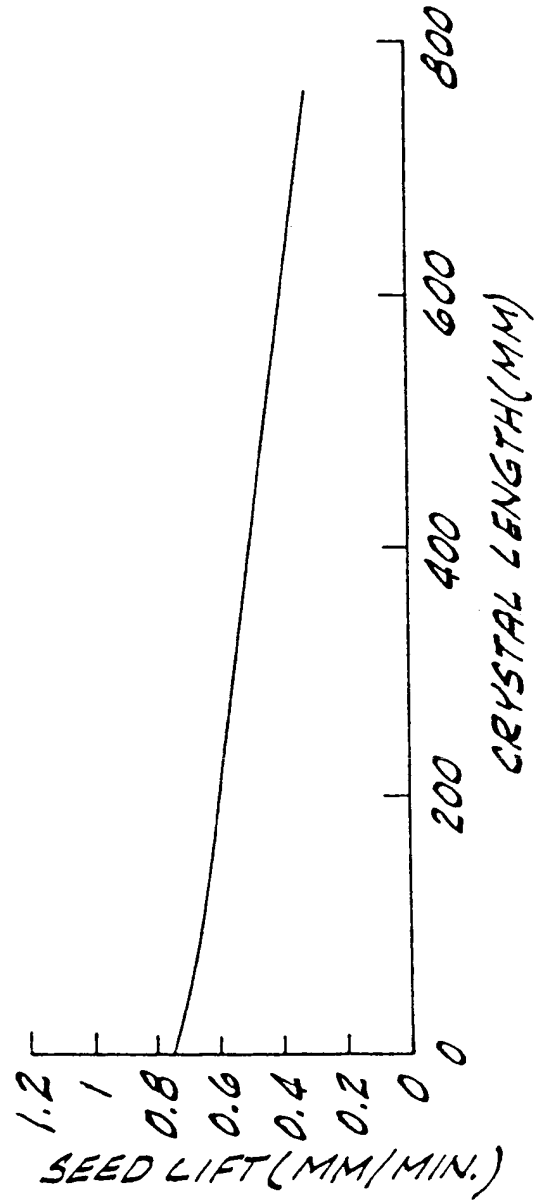

FIG. 15

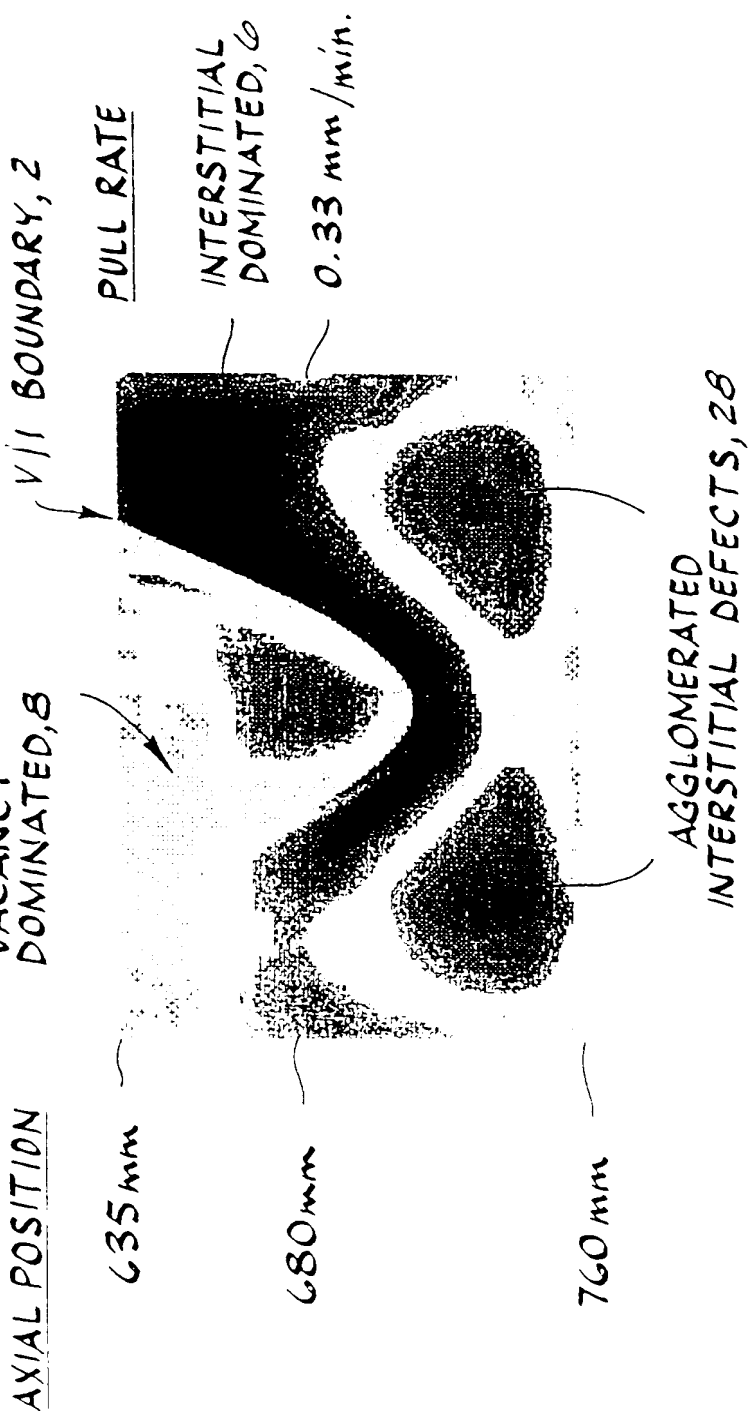

FIG.16

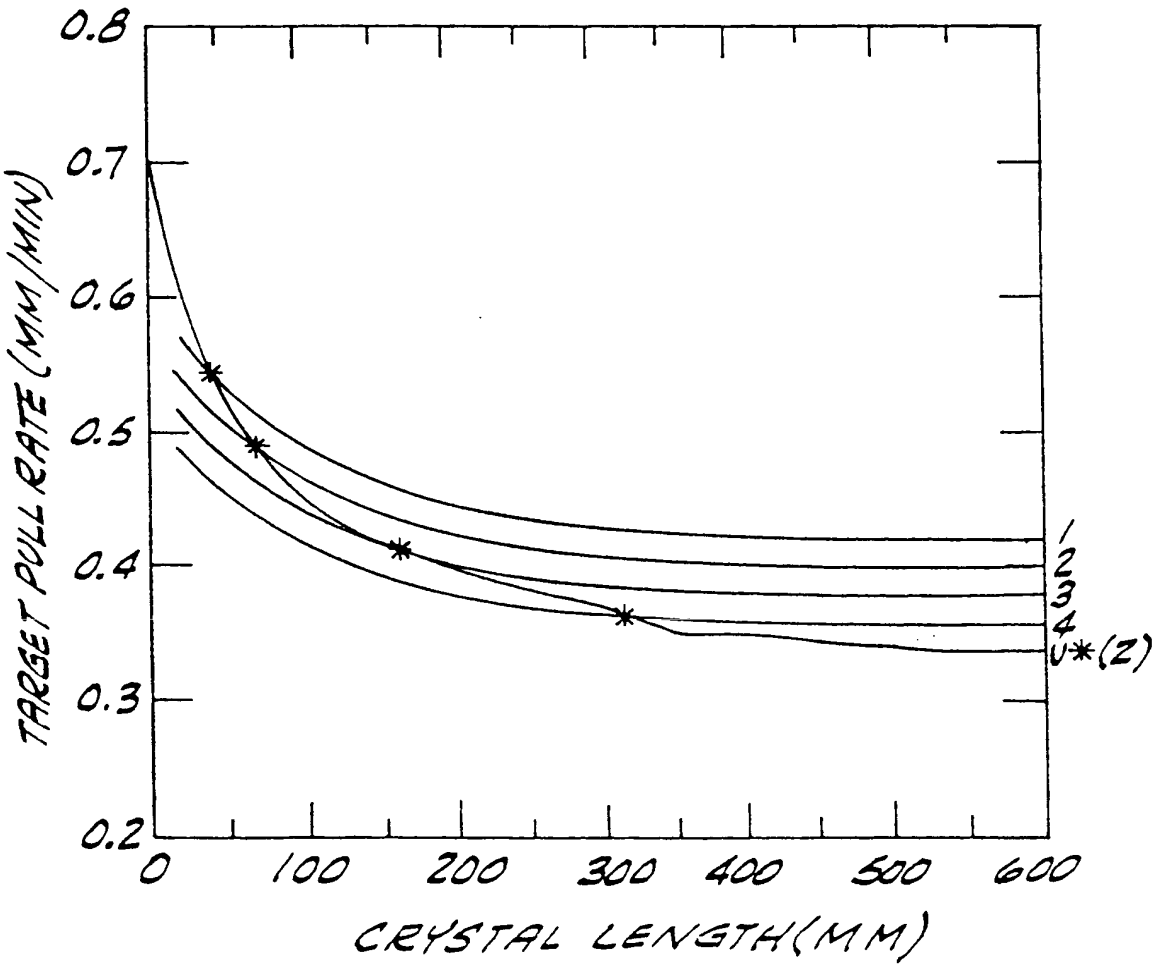

FIG. 17

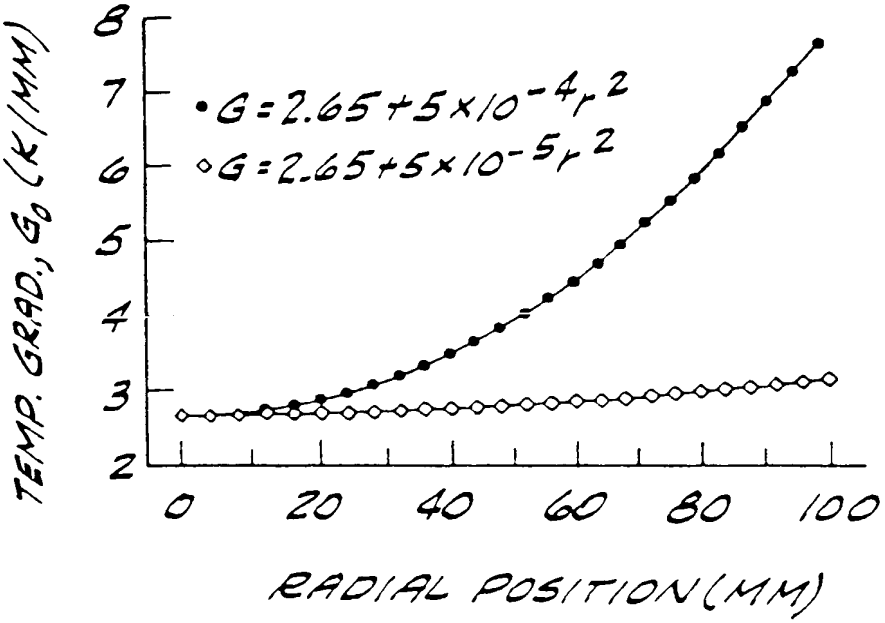

FIG. 18

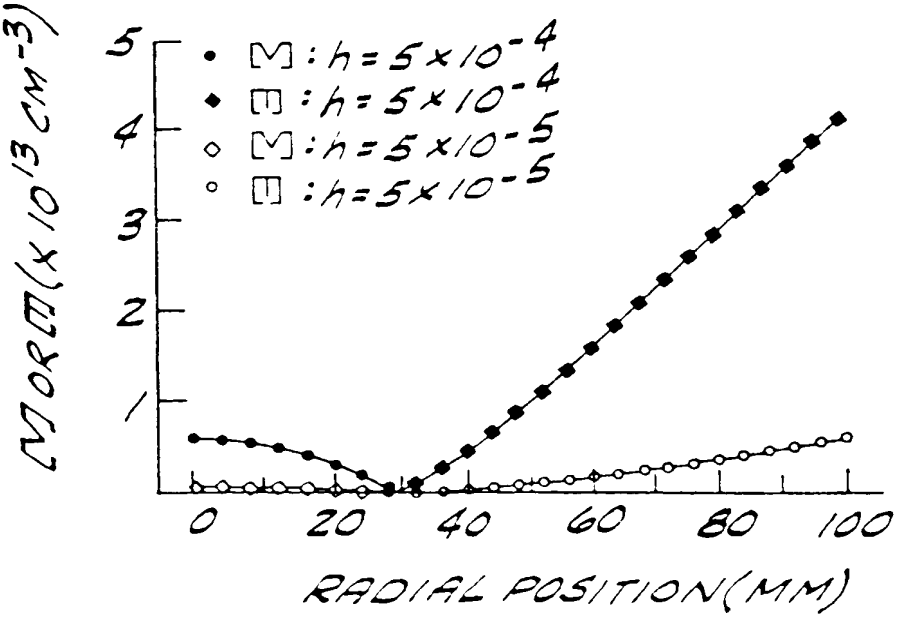

FIG.19

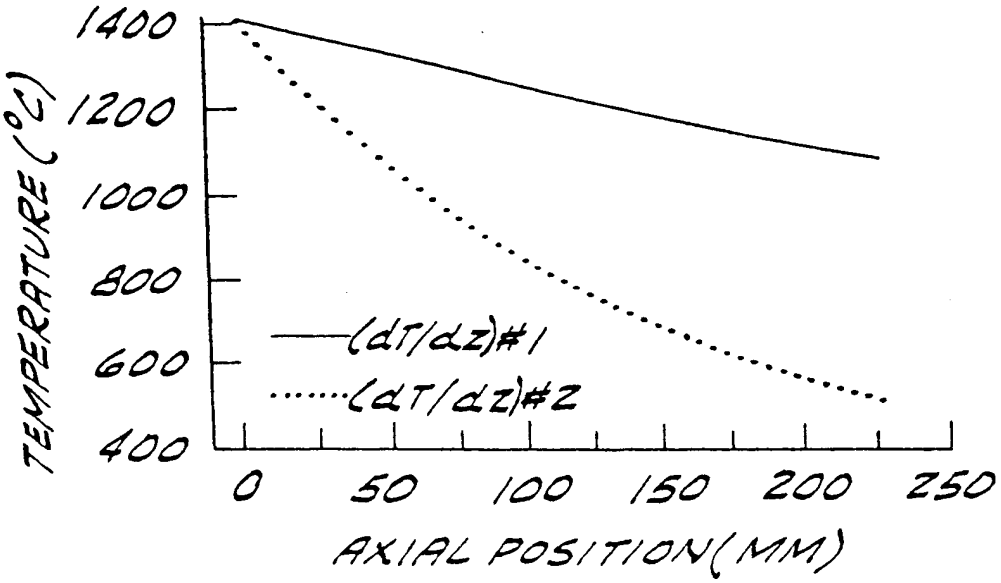

FIG.20

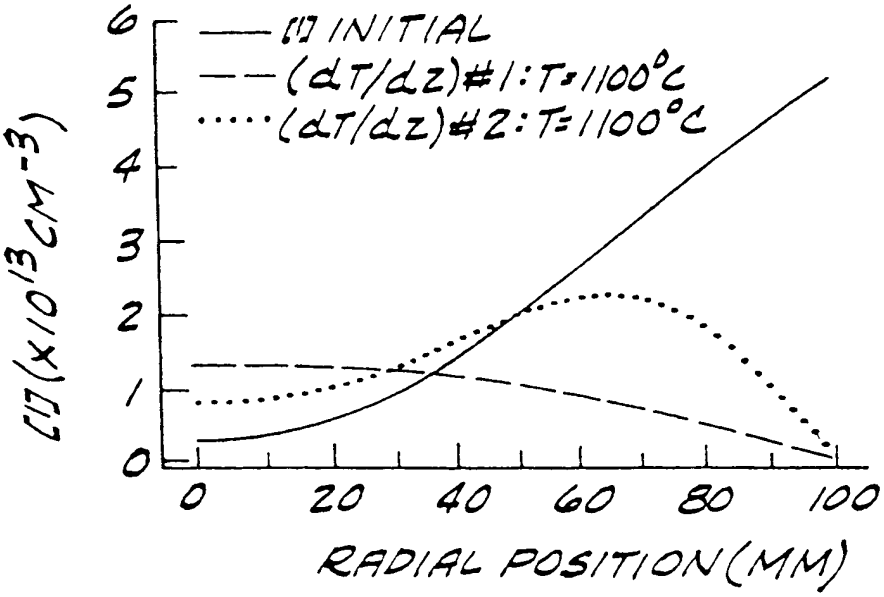

FIG.21

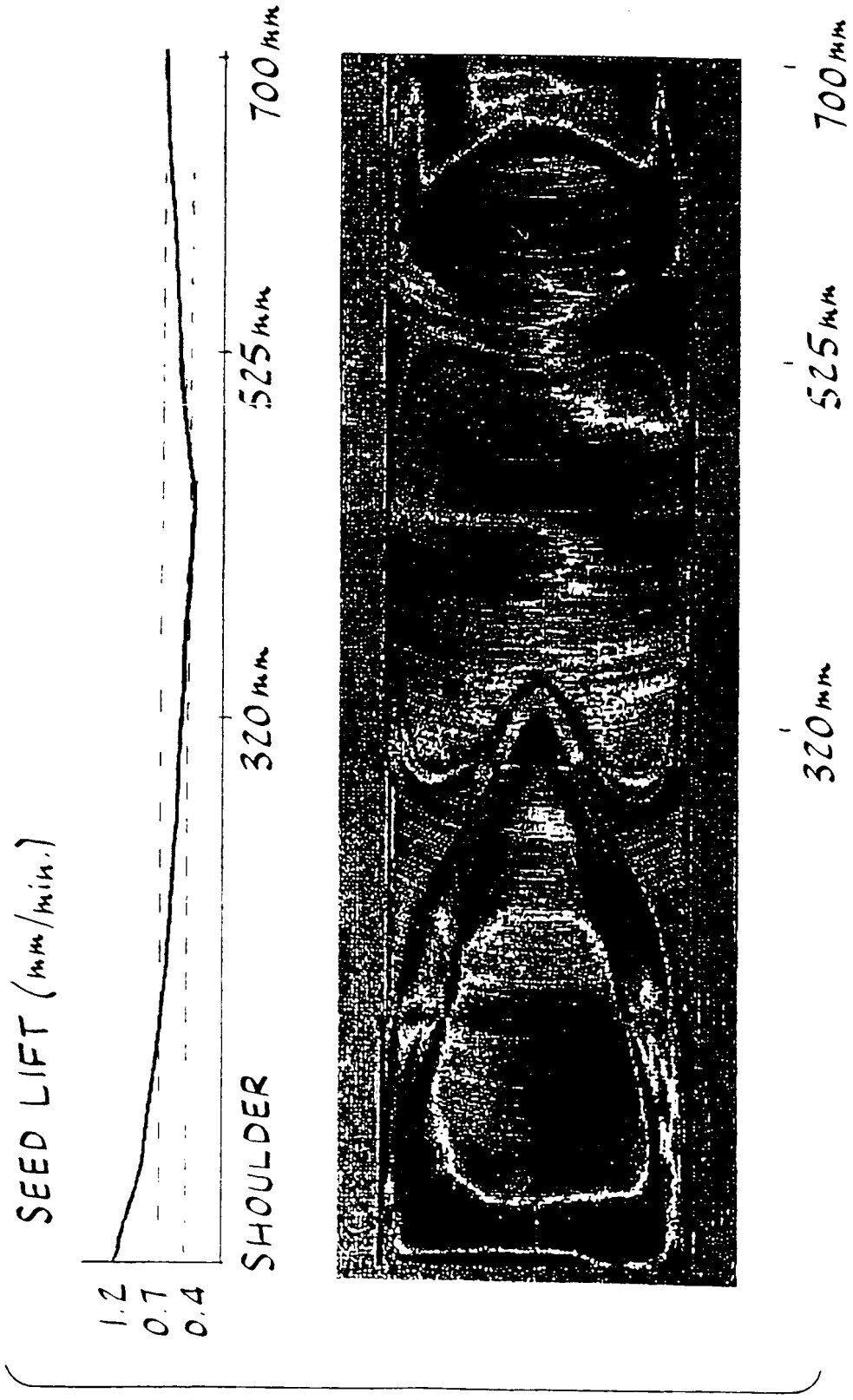

FIG.22

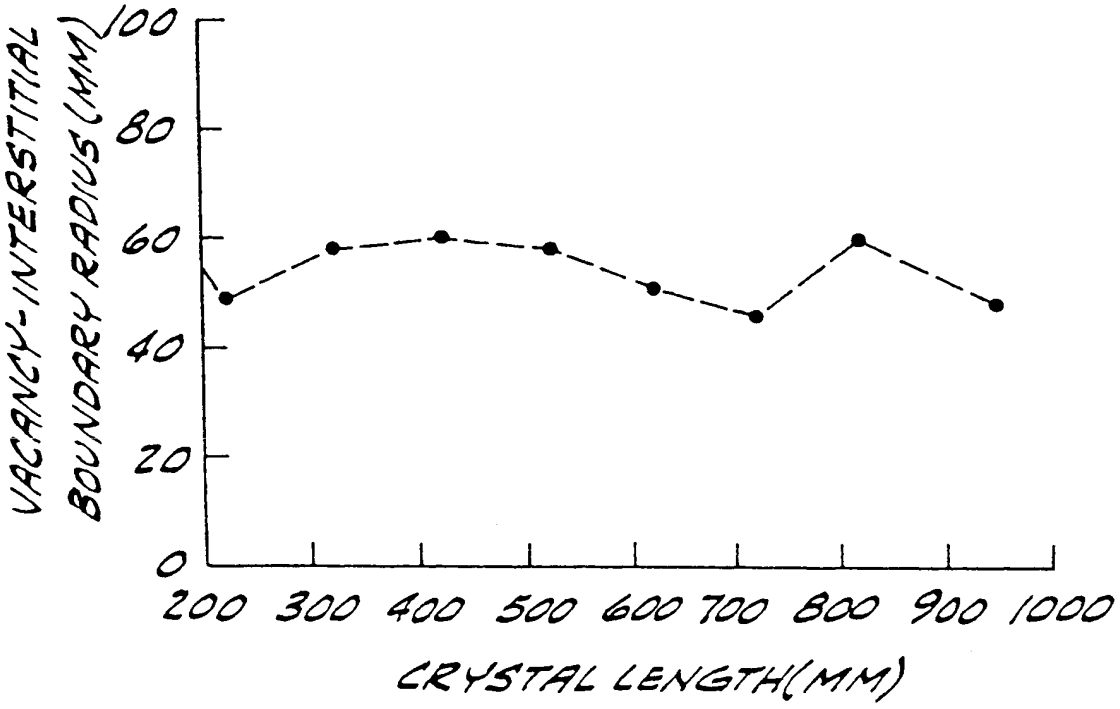

FIG.23A

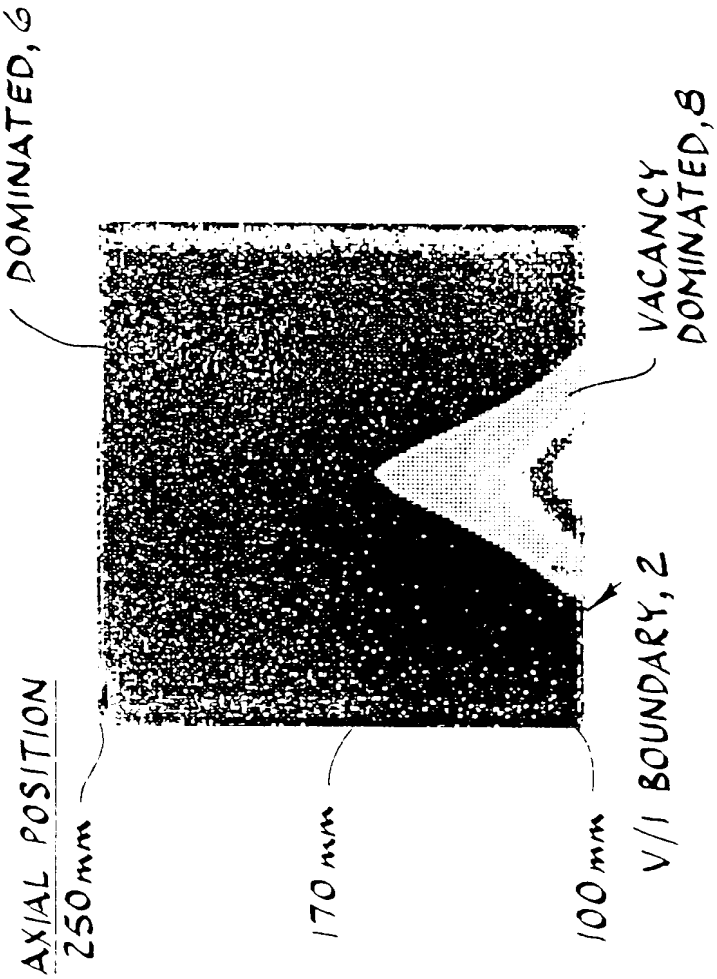

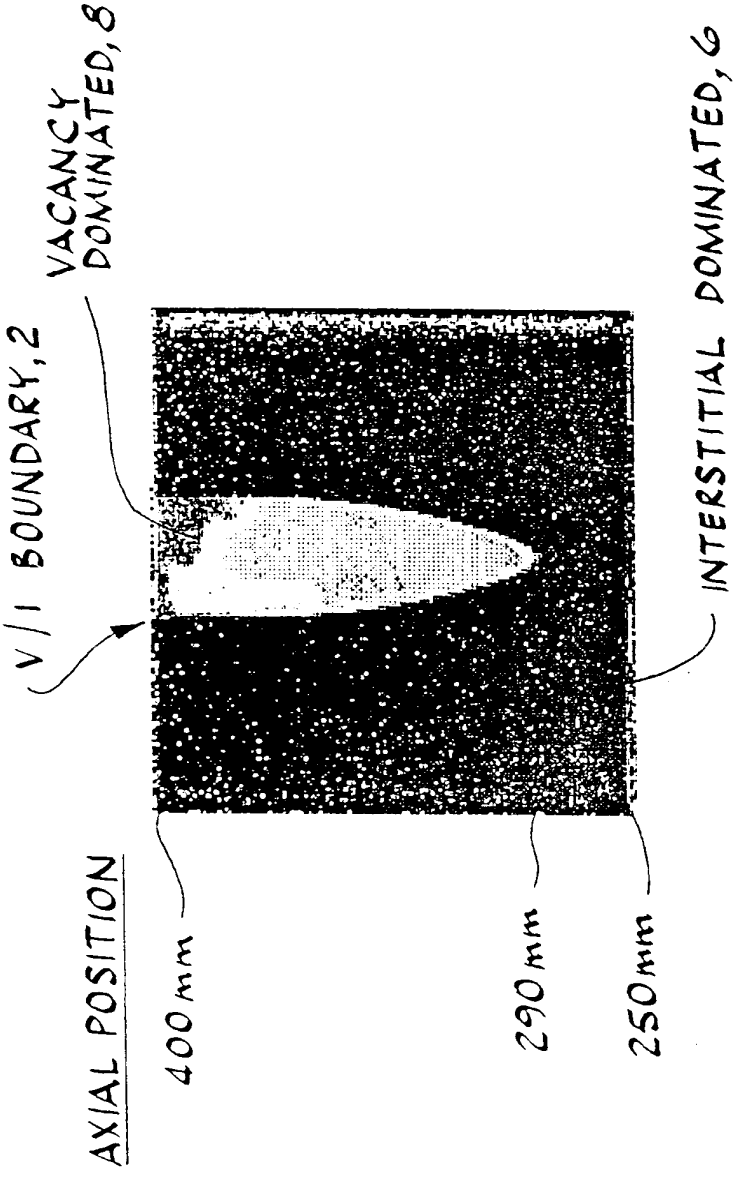

FIG.23B

FIG.24

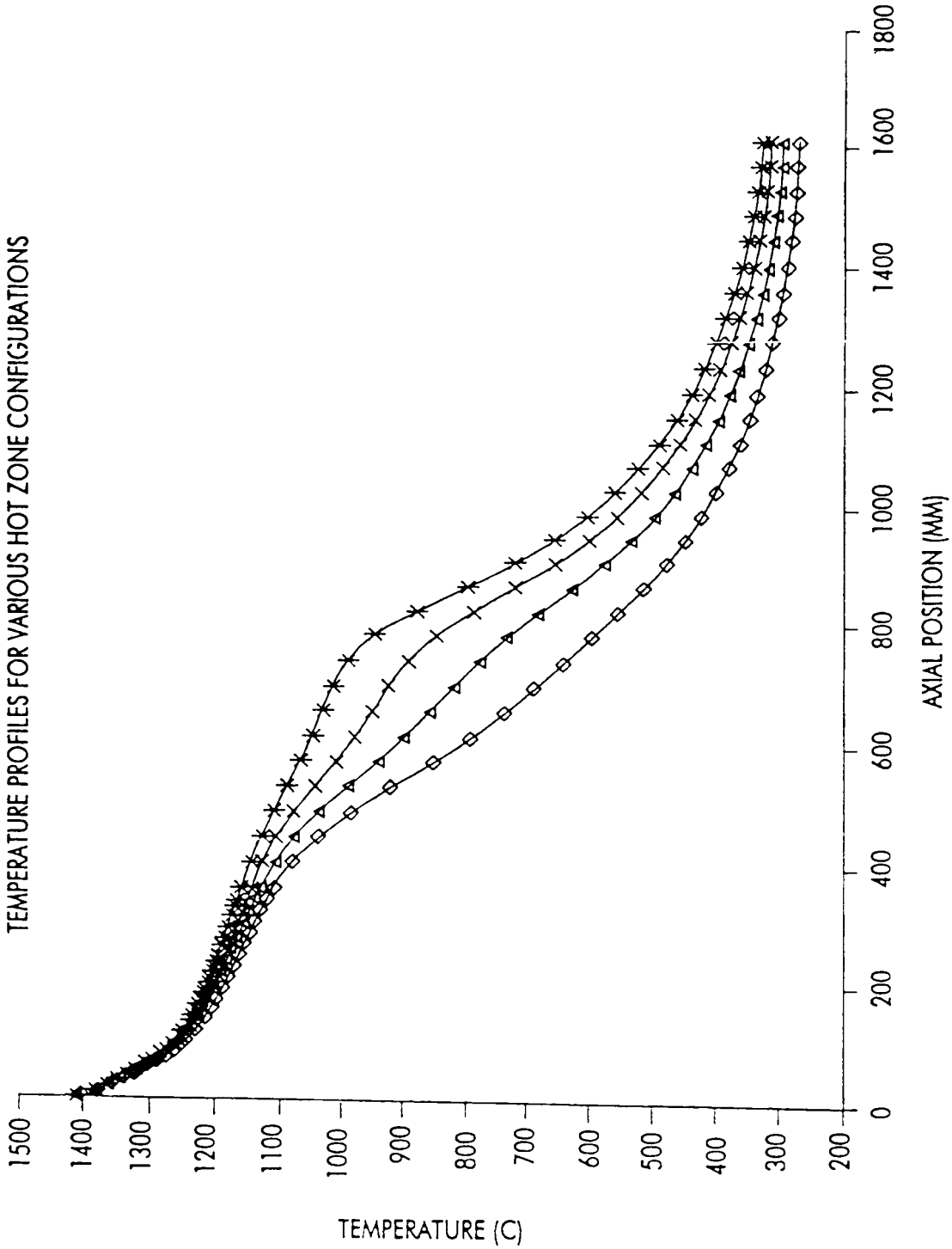

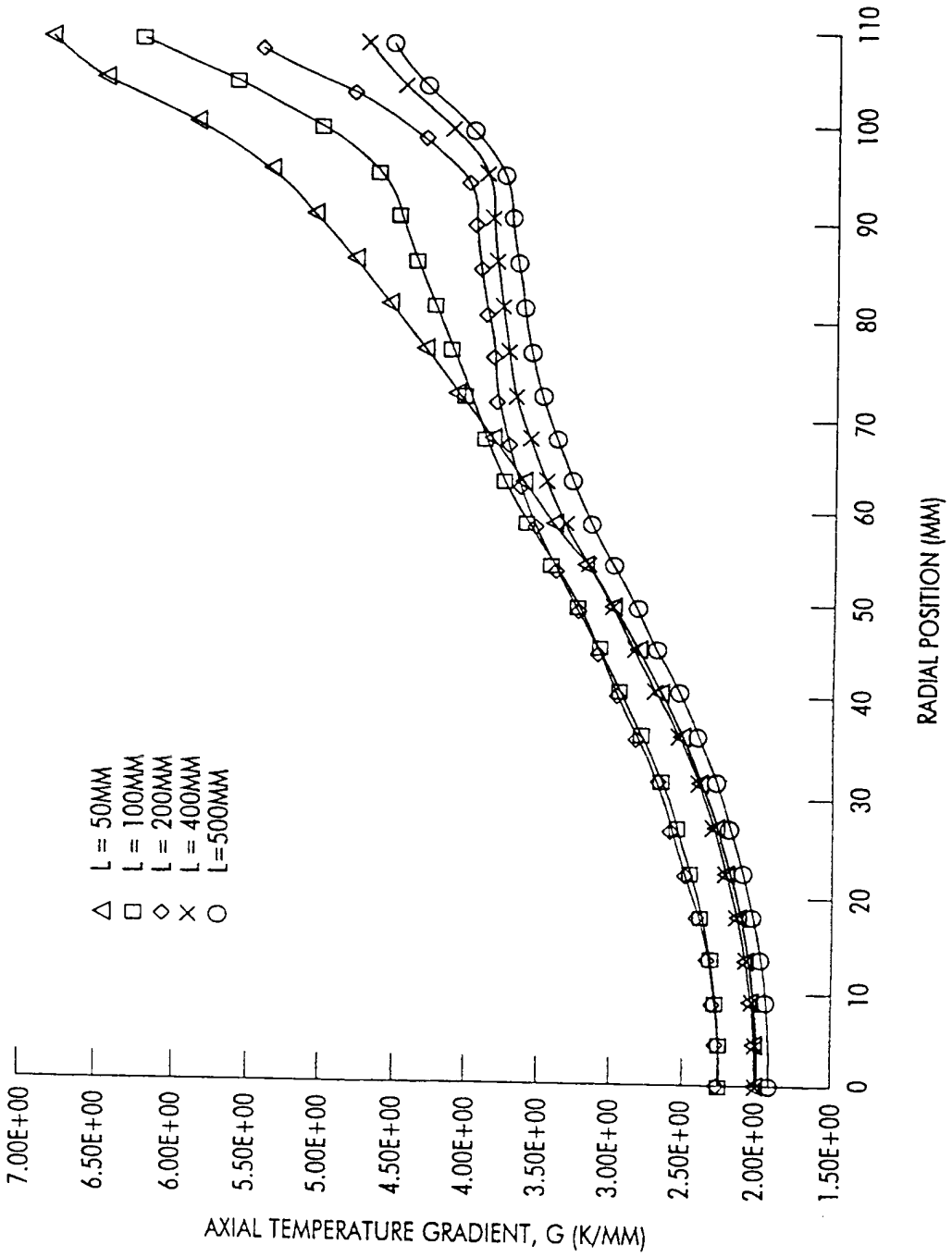

FIG.25

FIG.26

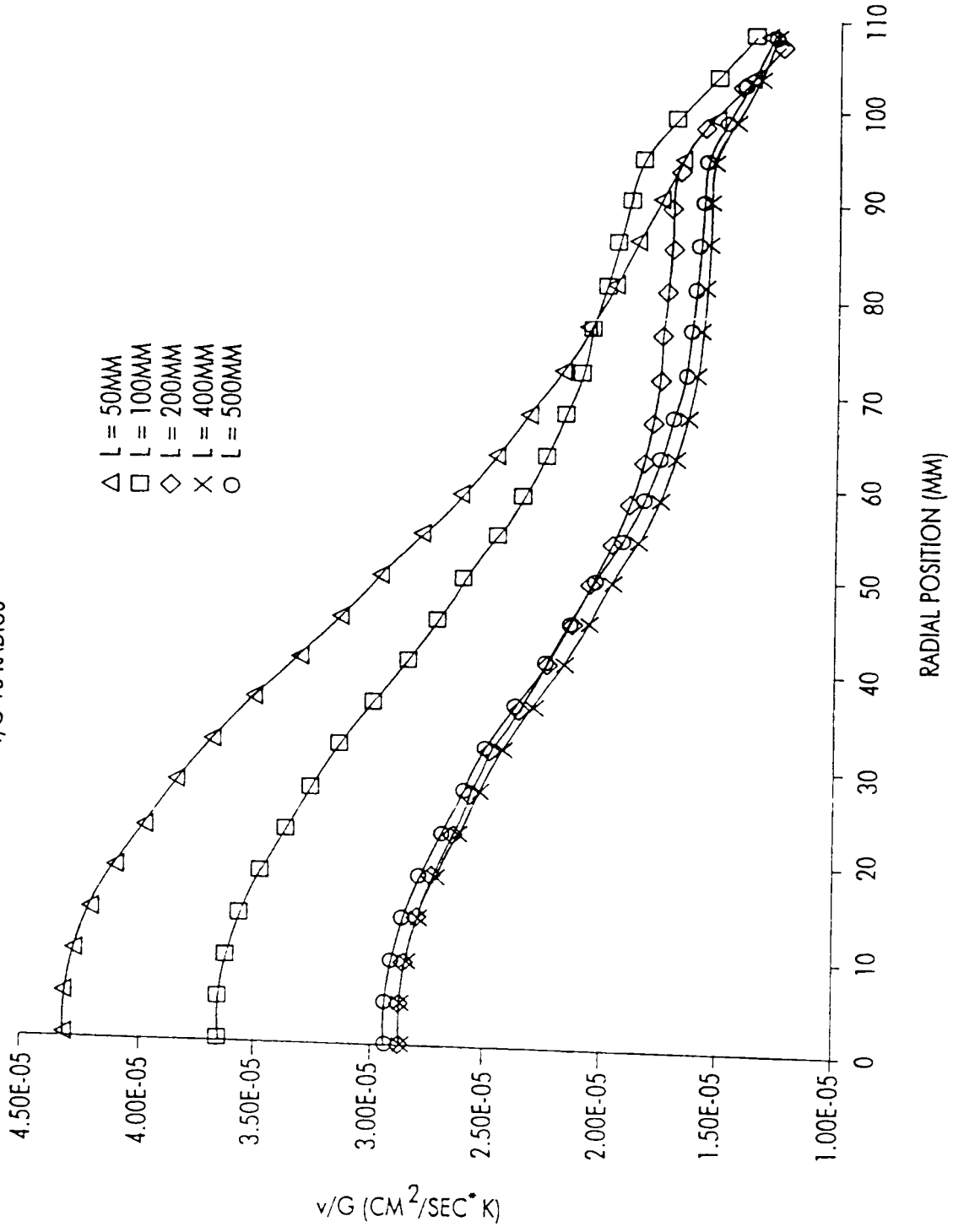

FIG.29

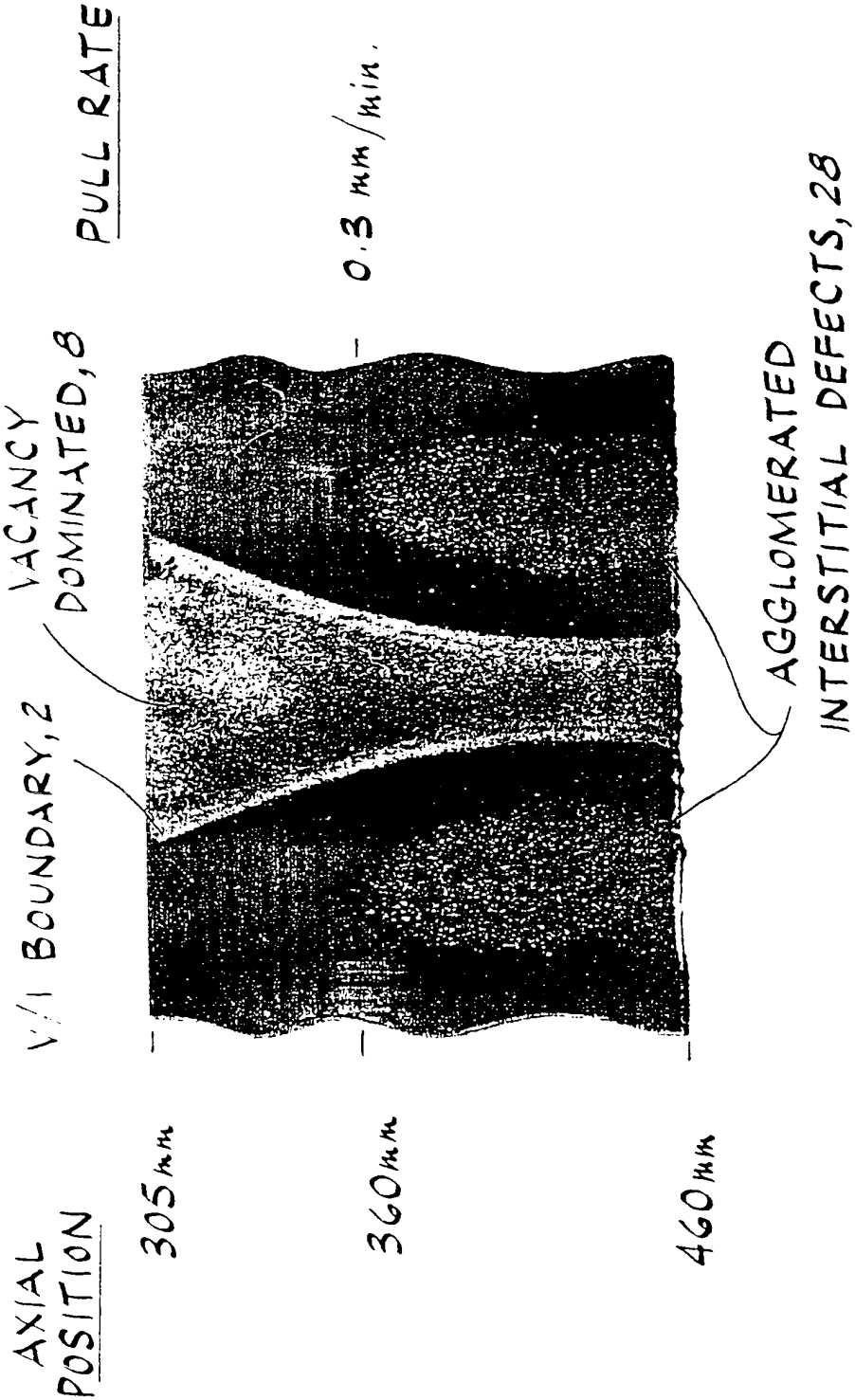

FIG.30

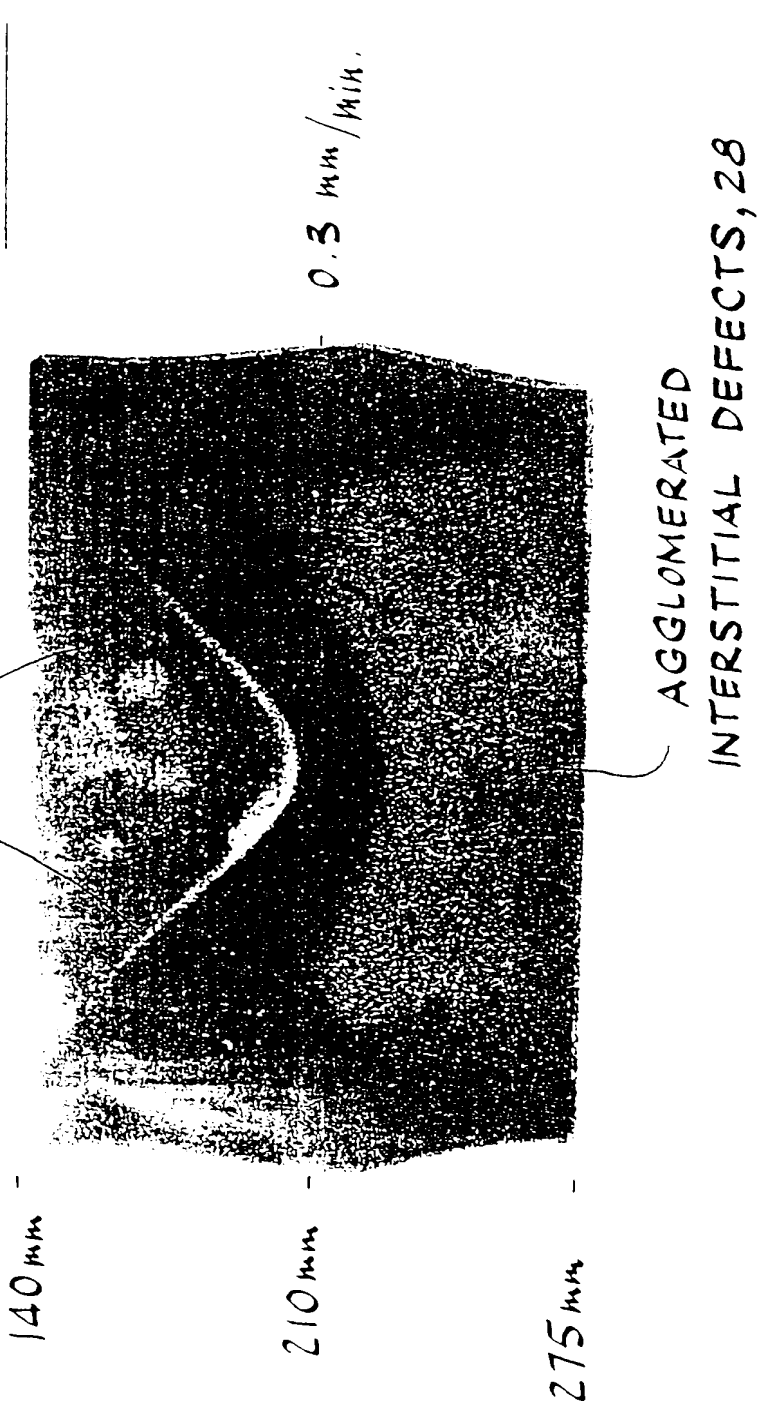

FIG.31

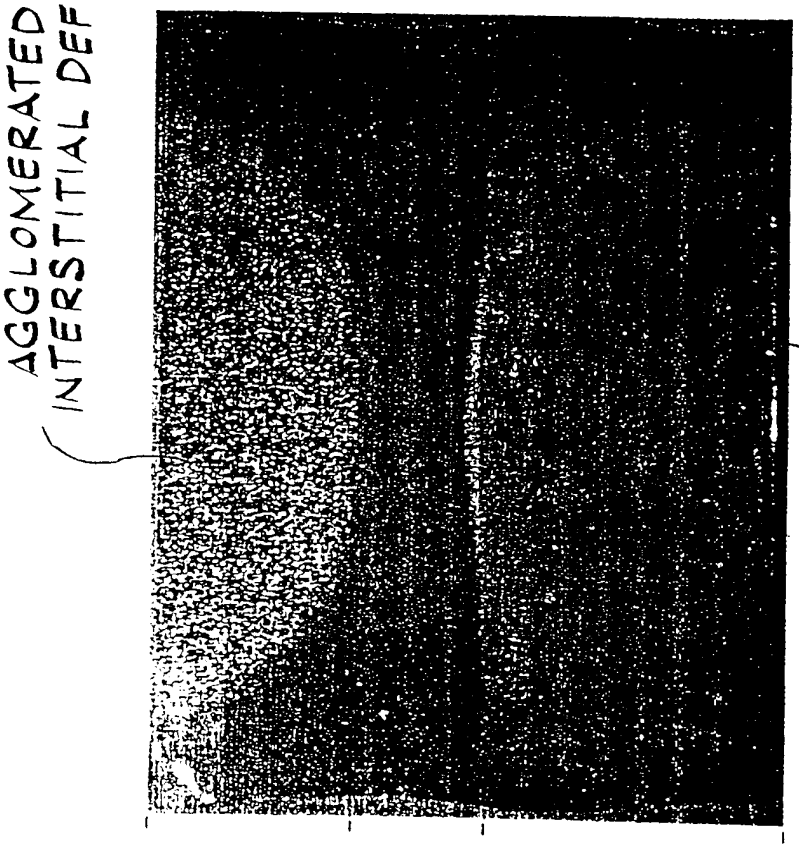

FIG.27

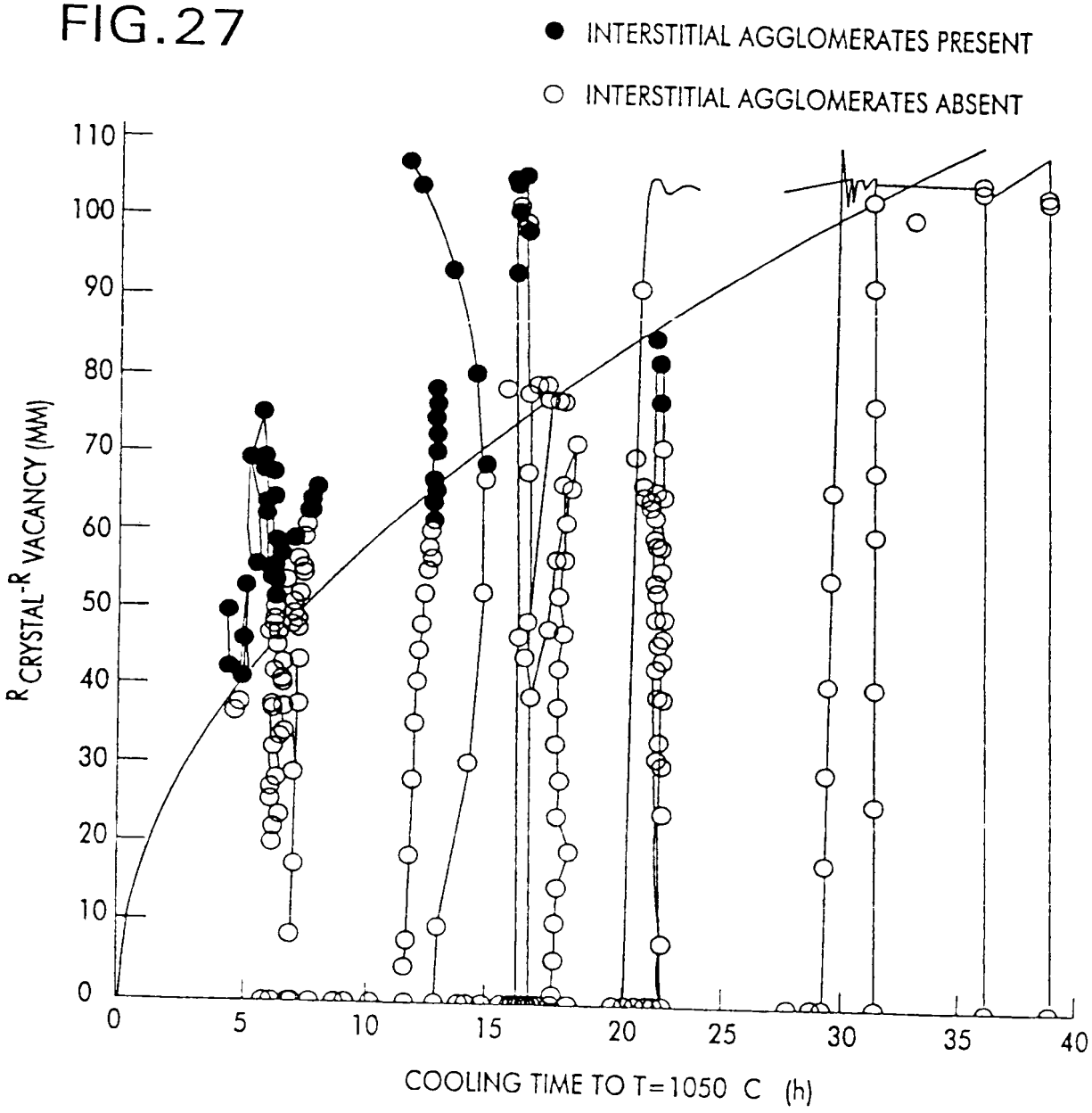

FIG.28

FIG. 32

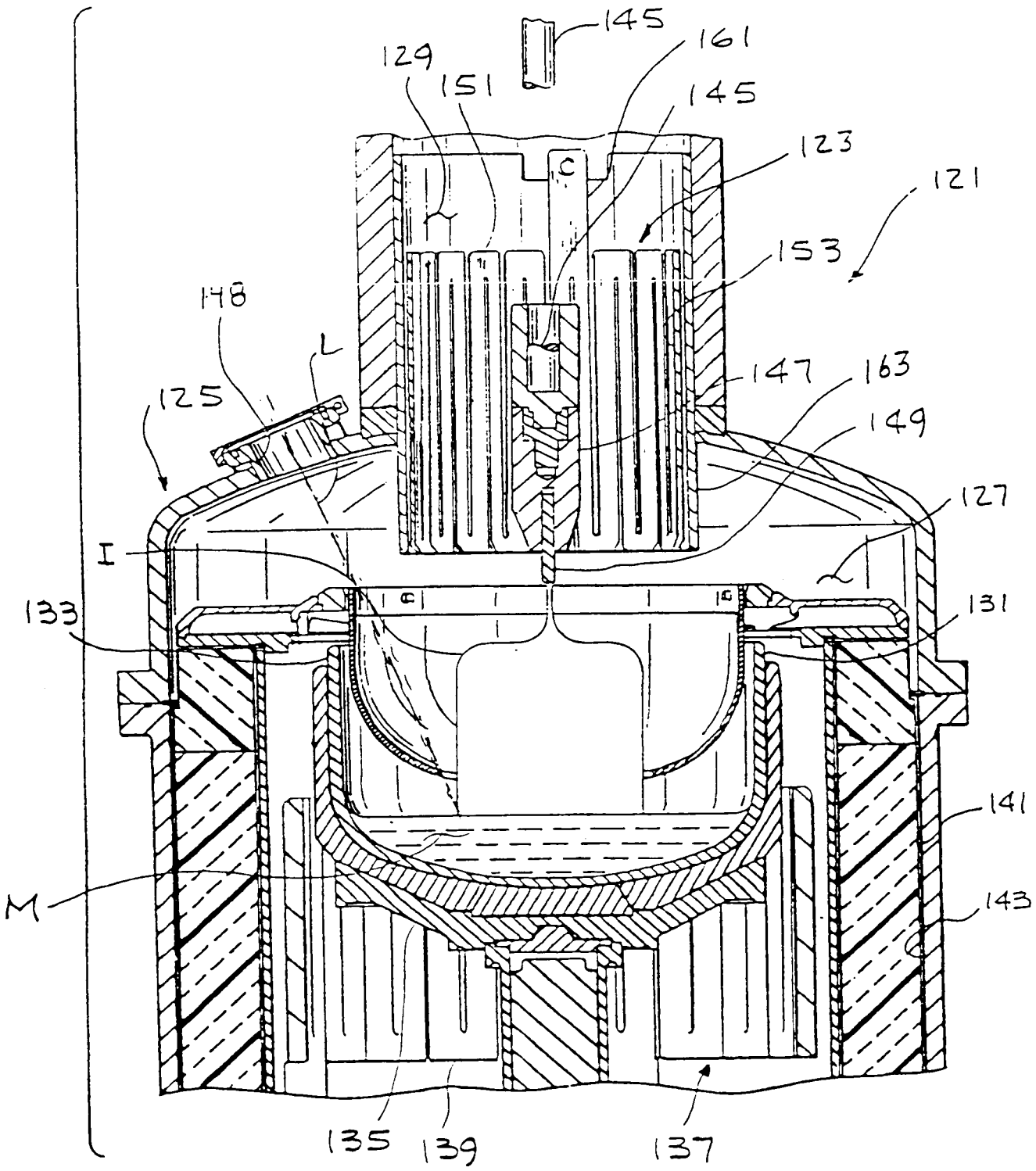

FIG. 33

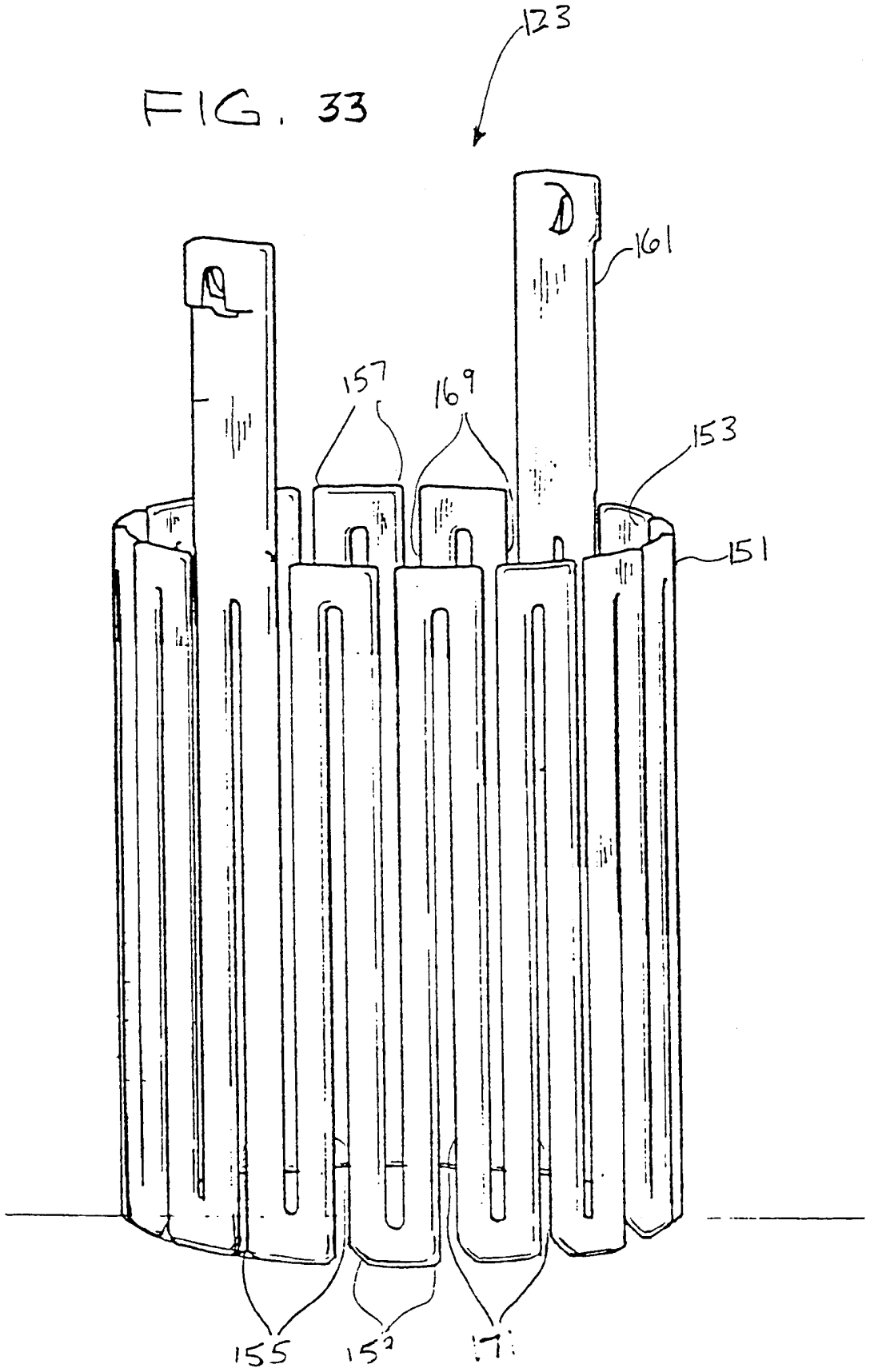

FIG. 34

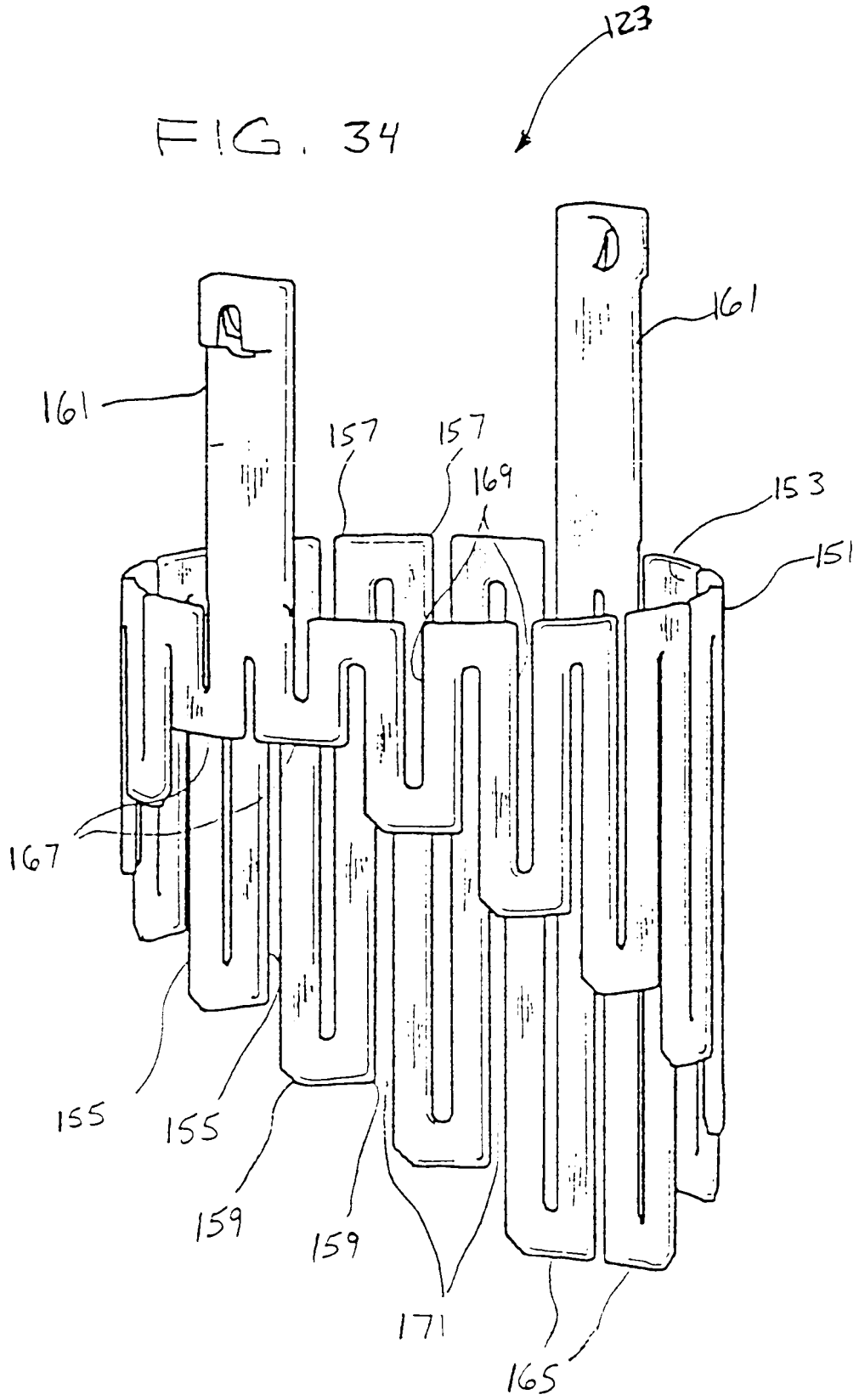

FIG. 35

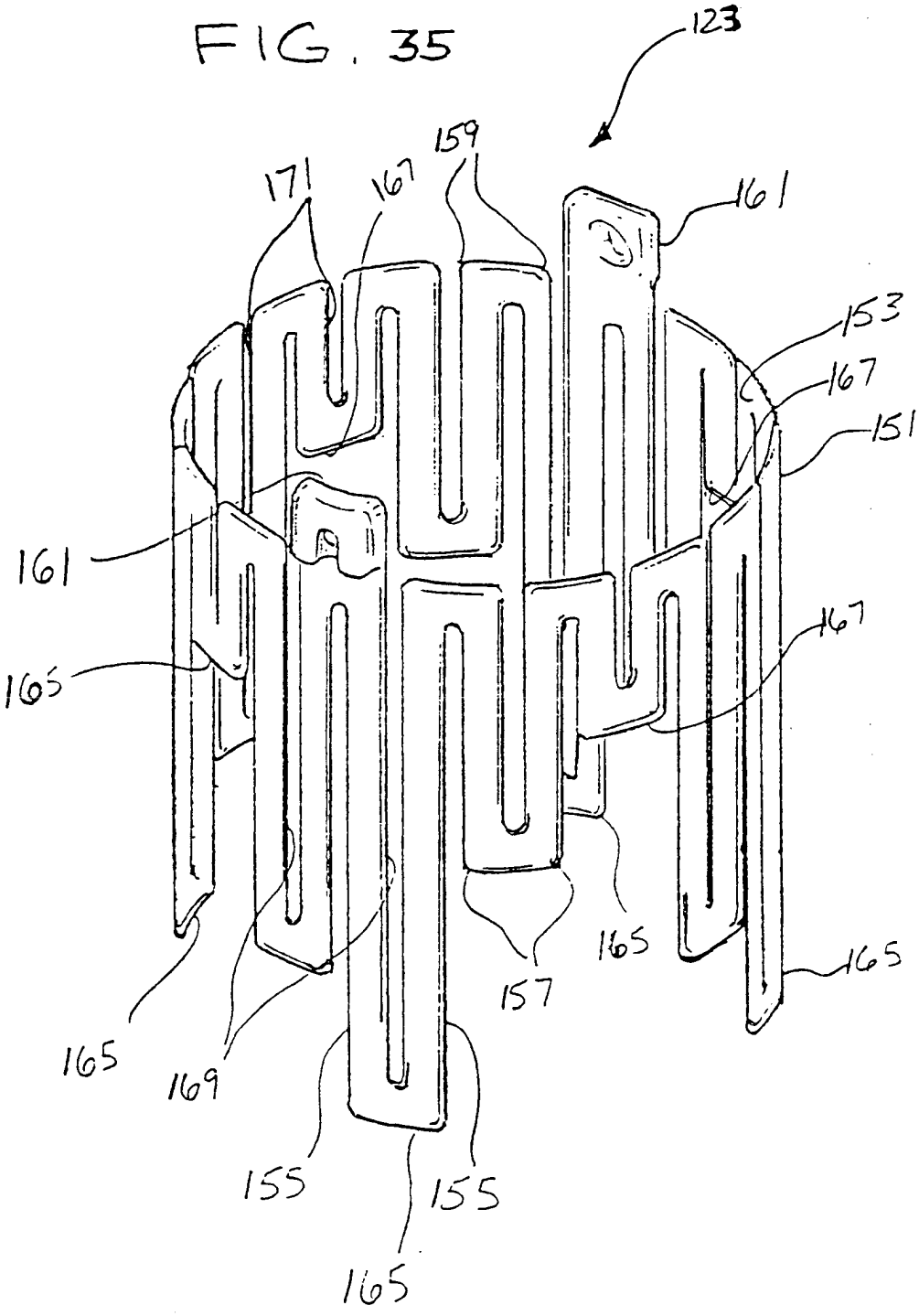

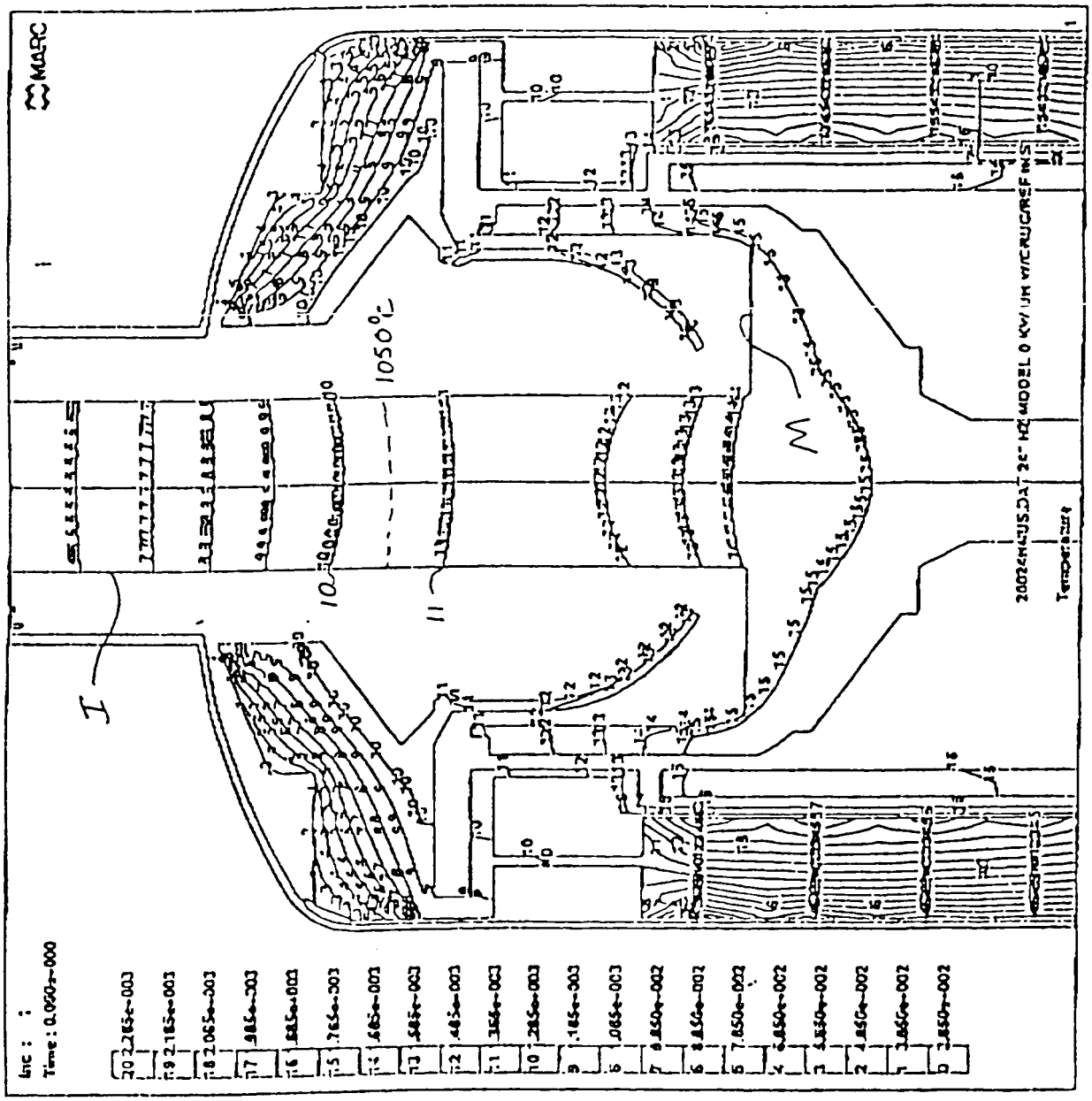

FIG. 36

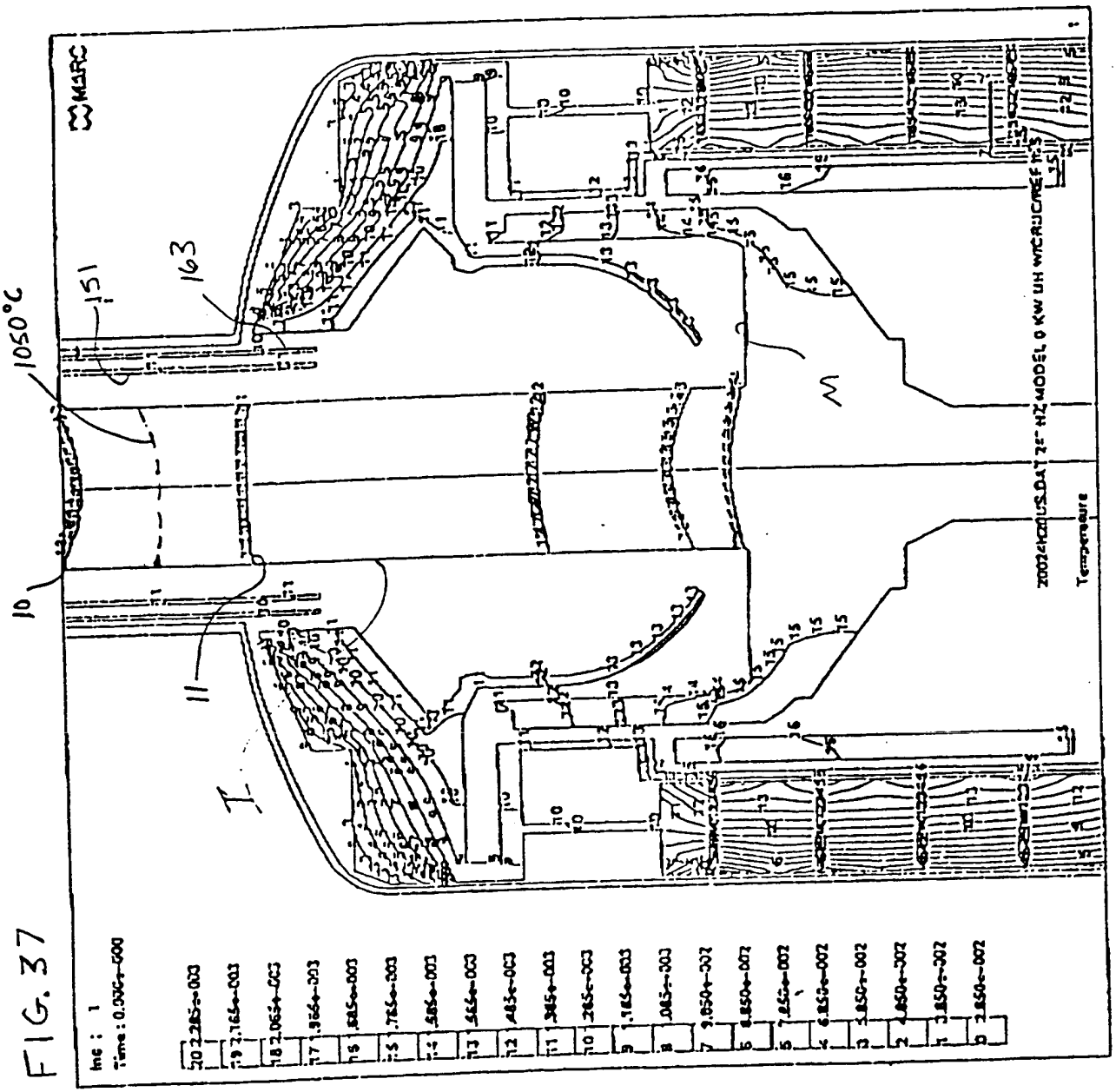

FIG. 37

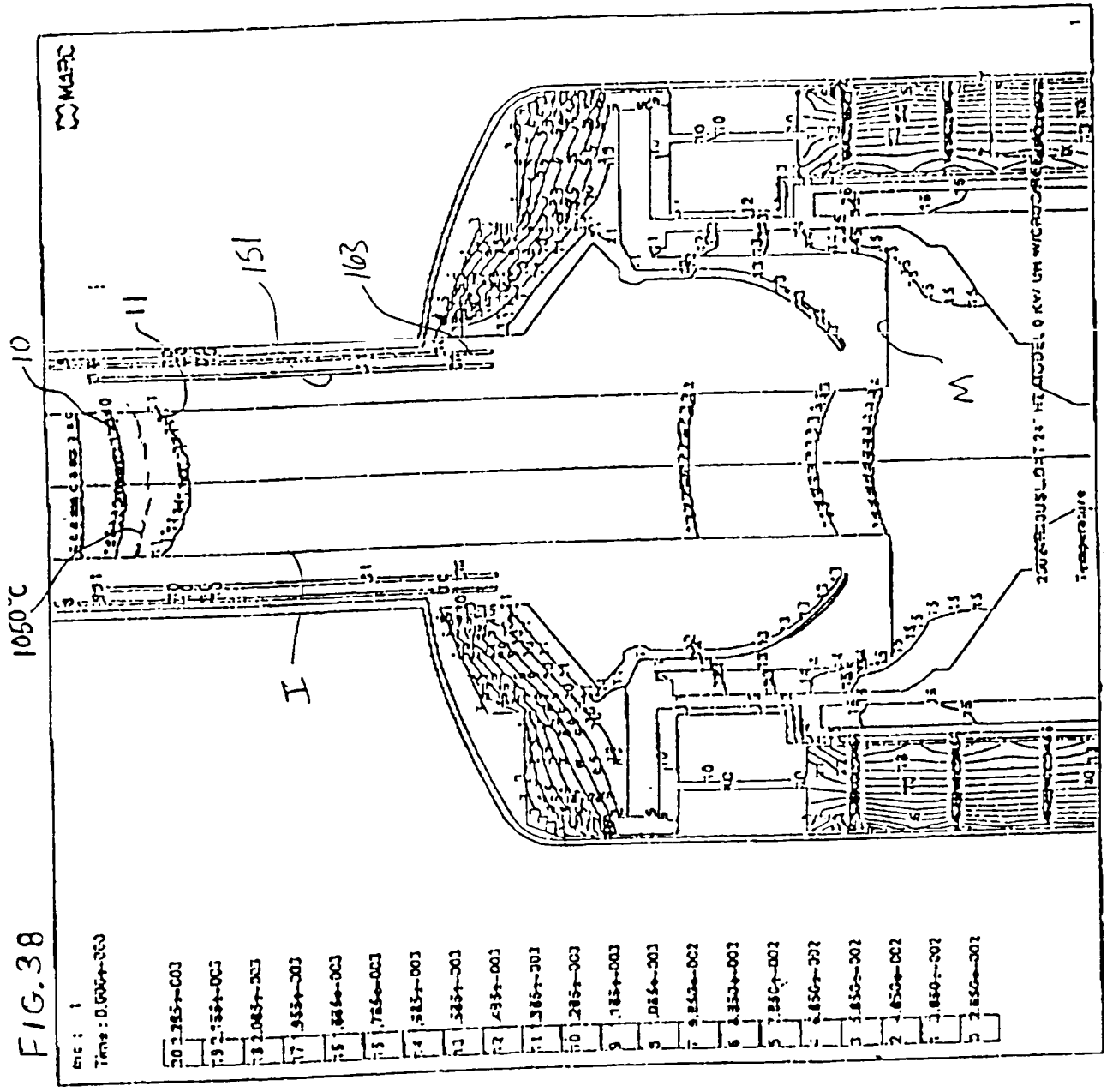

FIG. 38

FIG. 39
Effect of Upper Heater on Crystal Axial Temperature Profile

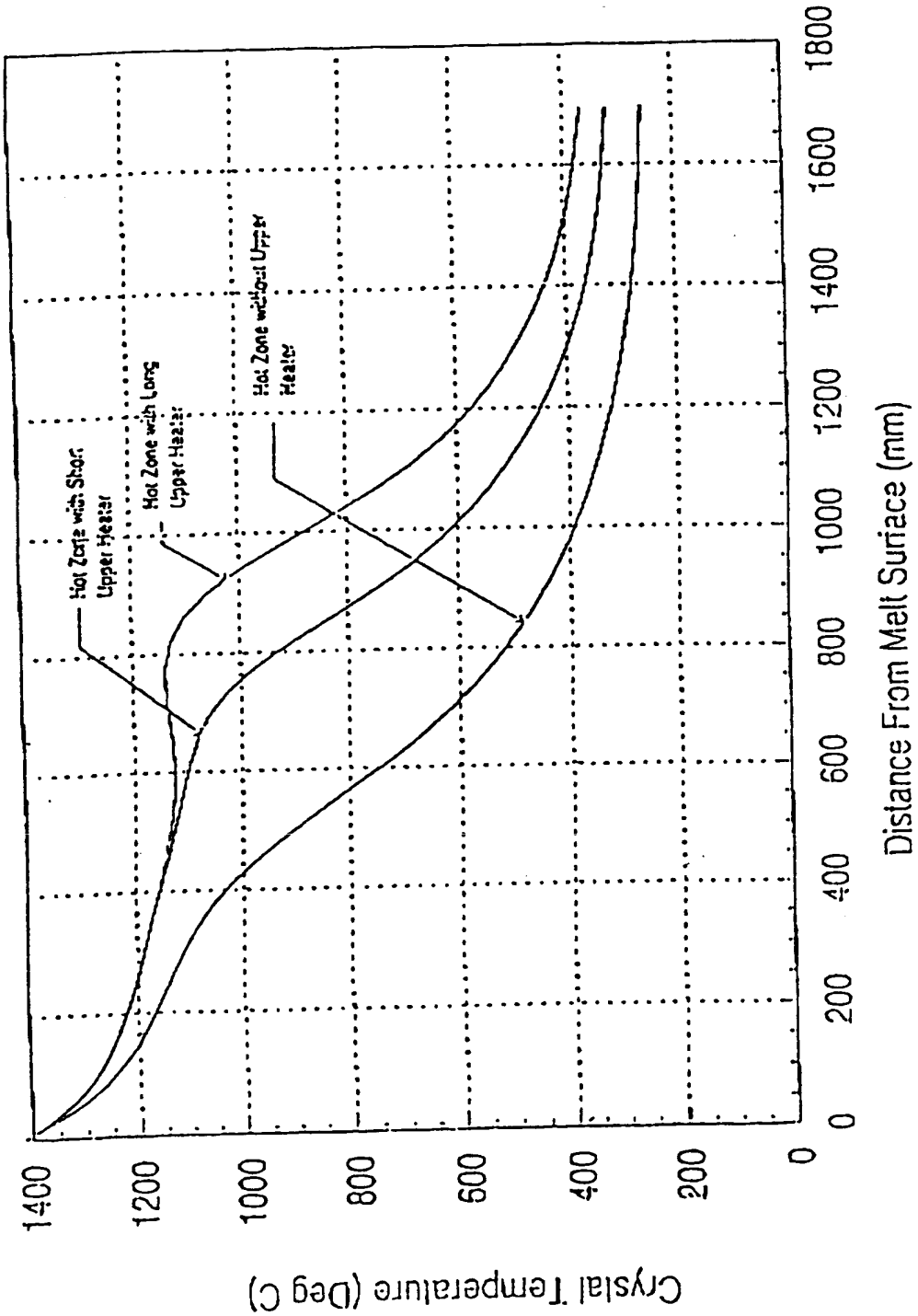

INTERNATIONAL SEARCH REPORT

Inte onal Application No
PC1/US 99/13643

A. CLASSIFICATION OF SUBJECT MATTER
IPC 6 C30B15/14 C30B29/06

According to International Patent Classification (IPC) or to both national classification and IPC

B. FIELDS SEARCHED

Minimum documentation searched (classification system followed by classification symbols)
IPC 6 C30B

Documentation searched other than minimum documentation to the extent that such documents are included in the fields searched

Electronic data base consulted during the international search (name of data base and, where practical, search terms used)

C. DOCUMENTS CONSIDERED TO BE RELEVANT

Category °	Citation of document, with indication, where appropriate, of the relevant passages	Relevant to claim No.
P,X	US 5 840 120 A (MEMC ELECTRONIC MATERIALS INC) 24 November 1998 (1998-11-24) column 5, line 54 - column 6, line 3; figure 3	1
X	PATENT ABSTRACTS OF JAPAN vol. 18, no. 357 (C-1221), 6 July 1994 (1994-07-06) & JP 06 092780 A (TOSHIBA CORP.), 5 April 1994 (1994-04-05) abstract	1
X	PATENT ABSTRACTS OF JAPAN vol. 98, no. 10, 31 August 1998 (1998-08-31) & JP 10 139600 A (SUMITOMO SITIX CORP), 26 May 1998 (1998-05-26)	1,4
Y	abstract	2

-/--

[X] Further documents are listed in the continuation of box C.

[X] Patent family members are listed in annex.

° Special categories of cited documents

"A" document defining the general state of the art which is not considered to be of particular relevance

"E" earlier document but published on or after the international filing date

"L" document which may throw doubts on priority claim(s) or which is cited to establish the publication date of another citation or other special reason (as specified)

"O" document referring to an oral disclosure, use, exhibition or other means

"P" document published prior to the international filing date but later than the priority date claimed

"T" later document published after the international filing date or priority date and not in conflict with the application but cited to understand the principle or theory underlying the invention

"X" document of particular relevance; the claimed invention cannot be considered novel or cannot be considered to involve an inventive step when the document is taken alone

"Y" document of particular relevance; the claimed invention cannot be considered to involve an inventive step when the document is combined with one or more other such documents, such combination being obvious to a person skilled in the art.

"&" document member of the same patent family

Date of the actual completion of the international search	Date of mailing of the international search report
9 September 1999	17/09/1999

Name and mailing address of the ISA	Authorized officer
European Patent Office, P.B. 5818 Patentlaan 2 NL - 2280 HV Rijswijk Tel. (+31-70) 340-2040, Tx. 31 651 epo nl, Fax: (+31-70) 340-3016	Cook, S

Form PCT/ISA/210 (second sheet) (July 1992)

INTERNATIONAL SEARCH REPORT

Inte onal Application No
PC./US 99/13643

C.(Continuation) DOCUMENTS CONSIDERED TO BE RELEVANT

Category °	Citation of document, with indication,where appropriate, of the relevant passages	Relevant to claim No.
Y	PATENT ABSTRACTS OF JAPAN vol. 18, no. 347 (C-1219), 30 June 1994 (1994-06-30) & JP 06 087686 A (MITSUBISHI MATERIALS CORP.), 29 March 1994 (1994-03-29) abstract	2
A	PATENT ABSTRACTS OF JAPAN vol. 11, no. 30 (C-400), 29 January 1987 (1987-01-29) & JP 61 201692 A (MITSUBISHI METAL CORP) abstract	1,8-10
X	PATENT ABSTRACTS OF JAPAN vol. 7, no. 225 (C-189) '1370!, 6 October 1983 (1983-10-06) & JP 58 120591 A (OKI DENKI KOGYO KK), 18 July 1983 (1983-07-18) abstract	1-3
A	EP 0 823 497 A (MEMC ELECTRONIC MATERIALS INC) 11 February 1998 (1998-02-11) example 3	1,8-10
A	EP 0 504 837 A (SHIN ETSU LTD) 23 September 1992 (1992-09-23)	

1

Form PCT/ISA/210 (continuation of second sheet) (July 1992)

INTERNATIONAL SEARCH REPORT

formation on patent family members

Inte ional Application No
PC /US 99/13643

Patent document cited in search report	Publication date	Patent family member(s)	Publication date
US 5840120 A	24-11-1998	NONE	
JP 06092780 A	05-04-1994	NONE	
JP 10139600 A	26-05-1998	NONE	
JP 06087686 A	29-03-1994	NONE	
JP 61201692 A	06-09-1986	JP 1742752 C	15-03-1993
		JP 3067994 B	24-10-1991
JP 58120591 A	18-07-1983	NONE	
EP 823497 A	11-02-1998	US 5779791 A	14-07-1998
		JP 10095698 A	14-04-1998
		SG 54540 A	16-11-1998
EP 504837 A	23-09-1992	JP 5070283 A	23-03-1993
		DE 69207454 D	22-02-1996
		DE 69207454 T	23-05-1996
		US 5248378 A	28-09-1993

Form PCT/ISA/210 (patent family annex) (July 1992)

CORRECTED VERSION*

PCT

WORLD INTELLECTUAL PROPERTY ORGANIZATION
International Bureau

INTERNATIONAL APPLICATION PUBLISHED UNDER THE PATENT COOPERATION TREATY (PCT)

(51) International Patent Classification 6 :
C30B 15/14, 29/06

A1

(11) International Publication Number: WO 00/00675

(43) International Publication Date: 6 January 2000 (06.01.00)

(21) International Application Number: PCT/US99/13643

(22) International Filing Date: 18 June 1999 (18.06.99)

(30) Priority Data:
60/090,799 26 June 1998 (26.06.98) US

(71) Applicant: MEMC ELECTRONIC MATERIALS, INC. [US/US]; 501 Pearl Drive, P.O. Box 8, St. Peters, MO 63376 (US).

(72) Inventors: SCHRENKER, Richard, G.; 15566 Rose Gate Lane, Chesterfield, MO (US). LUTER, William, L.; 1037 Picardy Lane, St. Charles, MO (US).

(74) Agents: HEJLEK, Edward, J. et al.; Senniger, Powers, Leavitt & Roedel, 16th floor, One Metropolitan Square, St. Louis, MO 63102 (US).

(81) Designated States: CN, JP, KR, SG, European patent (AT, BE, CH, CY, DE, DK, ES, FI, FR, GB, GR, IE, IT, LU, MC, NL, PT, SE).

Published
With international search report.

(54) Title: CRYSTAL PULLER FOR GROWING LOW DEFECT DENSITY, SELF-INTERSTITIAL DOMINATED SILICON

(57) Abstract

A crystal puller for growing monocrystalline silicon ingots according to the Czochralski method which are devoid of agglomerated intrinsic point defects over a substantial portion of the radius of the ingot comprises a housing defining an interior having a lower growth chamber and an upper pull chamber. The pull chamber has a smaller transverse dimension than the growth chamber. A crucible is disposed in the growth chamber of the housing for containing molten silicon. A pulling mechanism is provided for pulling a growing ingot upward from the molten silicon through the growth chamber and pull chamber. An electrical resistance heater has a heating element sized and shaped for being disposed at least partially within the upper pull chamber of the housing in radially spaced relationship with the outer surface of the growing ingot for radiating heat to the ingot as it is pulled upward in the pull chamber relative to the molten silicon. The heating element has an upper end and a lower end. The lower end of the heating element is disposed substantially closer to the molten silicon than the upper end when the heating element is placed in the housing.

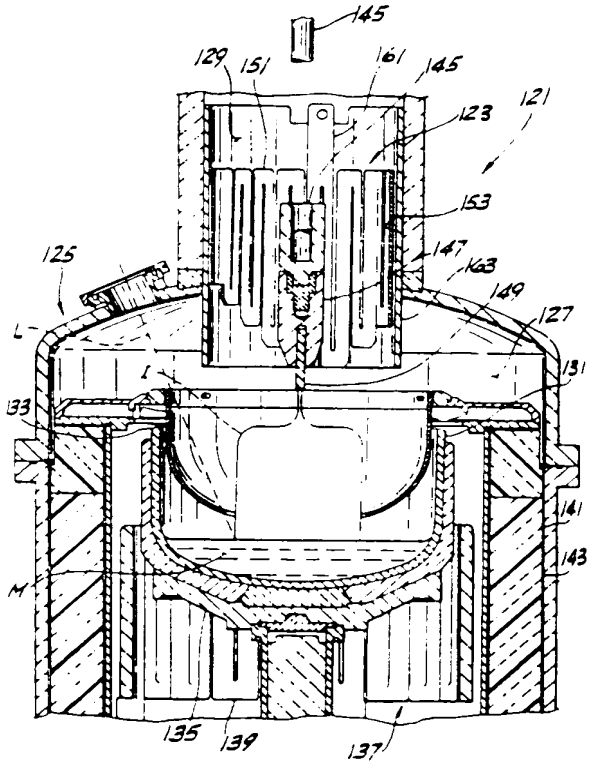

*(Referred to in PCT Gazette No. 13/2000, Section II)

FOR THE PURPOSES OF INFORMATION ONLY

Codes used to identify States party to the PCT on the front pages of pamphlets publishing international applications under the PCT.

AL	Albania	**ES**	Spain	**LS**	Lesotho	**SI**	Slovenia
AM	Armenia	**FI**	Finland	**LT**	Lithuania	**SK**	Slovakia
AT	Austria	**FR**	France	**LU**	Luxembourg	**SN**	Senegal
AU	Australia	**GA**	Gabon	**LV**	Latvia	**SZ**	Swaziland
AZ	Azerbaijan	**GB**	United Kingdom	**MC**	Monaco	**TD**	Chad
BA	Bosnia and Herzegovina	**GE**	Georgia	**MD**	Republic of Moldova	**TG**	Togo
BB	Barbados	**GH**	Ghana	**MG**	Madagascar	**TJ**	Tajikistan
BE	Belgium	**GN**	Guinea	**MK**	The former Yugoslav Republic of Macedonia	**TM**	Turkmenistan
BF	Burkina Faso	**GR**	Greece			**TR**	Turkey
BG	Bulgaria	**HU**	Hungary	**ML**	Mali	**TT**	Trinidad and Tobago
BJ	Benin	**IE**	Ireland	**MN**	Mongolia	**UA**	Ukraine
BR	Brazil	**IL**	Israel	**MR**	Mauritania	**UG**	Uganda
BY	Belarus	**IS**	Iceland	**MW**	Malawi	**US**	United States of America
CA	Canada	**IT**	Italy	**MX**	Mexico	**UZ**	Uzbekistan
CF	Central African Republic	**JP**	Japan	**NE**	Niger	**VN**	Viet Nam
CG	Congo	**KE**	Kenya	**NL**	Netherlands	**YU**	Yugoslavia
CH	Switzerland	**KG**	Kyrgyzstan	**NO**	Norway	**ZW**	Zimbabwe
CI	Côte d'Ivoire	**KP**	Democratic People's Republic of Korea	**NZ**	New Zealand		
CM	Cameroon			**PL**	Poland		
CN	China	**KR**	Republic of Korea	**PT**	Portugal		
CU	Cuba	**KZ**	Kazakstan	**RO**	Romania		
CZ	Czech Republic	**LC**	Saint Lucia	**RU**	Russian Federation		
DE	Germany	**LI**	Liechtenstein	**SD**	Sudan		
DK	Denmark	**LK**	Sri Lanka	**SE**	Sweden		
EE	Estonia	**LR**	Liberia	**SG**	Singapore		

CRYSTAL PULLER FOR GROWING LOW DEFECT DENSITY, SELF-INTERSTITIAL DOMINATED SILICON

BACKGROUND OF THE INVENTION

The present invention generally relates to crystal pullers used in the preparation of semiconductor grade single crystal silicon which is used in the manufacture of electronic components. More particularly, the present invention relates to a crystal puller for producing single crystal silicon ingots and wafers which are self-interstitial dominated and devoid of agglomerated intrinsic point defects over a substantial portion of the ingot radius.

Single crystal silicon, which is the starting material for most semiconductor electronic component fabrication, is commonly prepared by the so-called Czochralski ("Cz") method. The growth of a crystal ingot is most commonly carried out in a crystal pulling furnace. In this method, polycrystalline silicon ("polysilicon") is charged to a crucible and melted by a heater surrounding the outer surface of the crucible side wall. A seed crystal is brought into contact with the molten silicon and a single crystal ingot is grown by slow extraction via a crystal puller. After formation of a neck is complete, the diameter of the crystal ingot is enlarged by decreasing the pulling rate and/or the melt temperature until the desired or target diameter is reached. The cylindrical main body of the crystal which has an approximately constant diameter is then grown by controlling the pull rate and the melt temperature while compensating for the decreasing melt level. Near the end of the growth process, the crystal diameter must be reduced gradually to form an end-cone. Typically, the end-cone is formed by increasing the pull rate and heat supplied to the crucible. When the diameter becomes small enough, the ingot is then separated from the melt.

Heaters used for melting silicon in the crucible are typically electrical resistance heaters in which an electrical current flows through a heating element constructed of a resistive heating material (e.g., graphite). The resistance to the flow of current generates heat that radiates from the heating element to the crucible and silicon contained therein. The heating element comprises vertically oriented heating segments of equal length and cross-section arranged in side-by-side relationship and connected to each other in a serpentine configuration. That is, adjacent segments are connected to each other at the tops or bottoms of the segments in an alternating manner to form a continuous electrical circuit throughout the heating element. The heating power generated by the heating element is generally a function of the cross-sectional area of the segments.

In recent years, it has been recognized that a number of defects in single crystal silicon form in the crystal growth chamber as the ingot cools after solidification. Such defects arise, in part, due to the presence of an excess (i.e. a concentration above the solubility limit) of intrinsic point defects in the crystal lattice, which are vacancies and self-interstitials. Silicon crystal ingots grown from a melt are typically grown with an excess of one or the other type of intrinsic point defect, either crystal lattice vacancies ("V") or silicon self-interstitials ("I"). It has been suggested that the type and initial concentration of these point defects in the silicon are determined at the time of solidification and, if these concentrations reach a level of critical supersaturation in the system and the mobility of the point defects is sufficiently high, a reaction, or an agglomeration event,

will likely occur. Agglomerated intrinsic point defects in silicon can severely impact the yield potential of the material in the production of complex and highly integrated circuits.

Vacancy-type defects are recognized to be the origin of such observable crystal defects as D-defects, Flow Pattern Defects (FPDs), Gate Oxide Integrity (GOI) Defects, Crystal Originated Particle (COP) Defects, crystal originated Light Point Defects (LPDs), as well as certain classes of bulk defects observed by infrared light scattering techniques such as Scanning Infrared Microscopy and Laser Scanning Tomography. Also present in regions of excess vacancies are defects which act as the nuclei for ring oxidation induced stacking faults (OISF). It is speculated that this particular defect is a high temperature nucleated oxygen agglomerate catalyzed by the presence of excess vacancies.

Defects relating to self-interstitials are less well studied. They are generally regarded as being low densities of interstitial-type dislocation loops or networks. Such defects are not responsible for gate oxide integrity failures, an important wafer performance criterion, but they are widely recognized to be the cause of other types of device failures usually associated with current leakage problems.

The density of such vacancy and self-interstitial agglomerated defects in Czochralski silicon is conventionally within the range of about $1*10^3/cm^3$ to about $1*10^7/cm^3$. While these values are relatively low, agglomerated intrinsic point defects are of rapidly increasing importance to device manufacturers and, in fact, are now seen as yield-limiting factors in device fabrication processes.

To date, there generally exists three main approaches to dealing with the problem of agglomerated intrinsic point defects. The first approach includes

methods which focus on crystal pulling techniques in order to reduce the number density of agglomerated intrinsic point defects in the ingot. This approach can be further subdivided into those methods having crystal pulling conditions which result in the formation of vacancy dominated material, and those methods having crystal pulling conditions which result in the formation of self-interstitial dominated material. For example, it has been suggested that the number density of agglomerated defects can be reduced by (i) controlling v/G_0 to grow an ingot in which crystal lattice vacancies are the dominant intrinsic point defect, and (ii) influencing the nucleation rate of the agglomerated defects by altering (generally, by slowing down) the cooling rate of the silicon ingot as it is pulled upward from the melt surface.

To this end, U.S. Patent No. 5,248,378 (Oda et al.) discloses an apparatus for producing single silicon crystal in which a passive heat insulator is disposed in the crystal puller above the crucible to reduce the rate of cooling of the growing ingot above 1150°C. However, heat insulators or heat shields such as that disclosed by Oda et al. generally cannot slow the cooling of the ingot to a rate sufficient to substantially reduce the number of defects in the ingot.

Oda et al. further disclose that the insulator may be replaced by a heater for heating the growing ingot. The heater is positioned in the growth chamber of the crystal puller between the top of the crucible and the transition portion of the crystal puller housing. The heater radiates heat to the ingot to slow the rate of cooling above 1150°C. However, while the apparatus disclosed in Oda et al. is capable of reducing the number density of agglomerated defects, it does not prevent their formation because the cooling rate is still too rapid to prevent such formation. As the requirements

imposed by device manufacturers become more and more stringent, the presence of these defects will continue to become more of a problem.

Moreover, because of the limited space in the growth chamber of conventional crystal pullers, it would be impractical to increase the length or size of the heater disclosed by Oda et al. to further reduce the cooling rate of the growing ingot. Increasing the length of the heater would shield the ingot against viewing by the diameter control apparatus via the view port in the puller housing. Granular feeder hardware, laser melt level apparatus and other devices typically found in the growth chamber of conventional crystal pullers would also interfere with the ability to increase the length of the heater.

Others have suggested reducing the pull rate, during the growth of the body of the crystal, to a value less than about 0.4 mm/minute. However, by itself, this suggestion is also not satisfactory because such pull rates lead to the formation of single crystal silicon having a high concentration of self-interstitials. This high concentration, in turn, leads to the formation of agglomerated self-interstitial defects and all the resulting problems associated with such defects.

A second approach to dealing with the problem of agglomerated intrinsic point defects includes methods which focus on the dissolution or annihilation of agglomerated intrinsic point defects subsequent to their formation. Generally, this is achieved by using high temperature heat treatments of the silicon in wafer form. For example, Fusegawa et al. propose, in European Patent Application 503,816 A1, growing the silicon ingot at a growth rate in excess of 0.8 mm/minute, and heat treating the wafers which are sliced from the ingot at a temperature in the range of 1150°C to 1280°C to reduce the defect density in a thin region near the wafer

surface. The specific treatment needed will vary depending upon the concentration and location of agglomerated intrinsic point defects in the wafer. Different wafers cut from a crystal which does not have a uniform axial concentration of such defects may require different post-growth processing conditions. Furthermore, such wafer heat treatments are relatively costly, have the potential for introducing metallic impurities into the silicon wafers, and are not universally effective for all types of crystal-related defects.

A third approach to dealing with the problem of agglomerated intrinsic point defects is the epitaxial deposition of a thin crystalline layer of silicon on the surface of a single crystal silicon wafer. This process provides a single crystal silicon wafer having a surface which is substantially free of agglomerated intrinsic point defects. Epitaxial deposition, however, substantially increases the cost of the wafer.

In view of these developments, a need continues to exist for a crystal puller designed to inhibit the formation of agglomerated intrinsic point defects by suppressing the agglomeration reactions which produce them. Rather than simply limiting the rate at which such defects form, or attempting to annihilate some of the defects after they have formed, a crystal puller which suppresses agglomeration reactions would yield a silicon substrate that is substantially free of agglomerated intrinsic point defects. Such a crystal puller would also produce single crystal silicon wafers having epi-like yield potential, in terms of the number of integrated circuits obtained per wafer, without having the high costs associated with an epitaxial process.

SUMMARY OF THE INVENTION

Among the several objects and features of the present invention may be noted the provision of a crystal puller for producing single crystal silicon ingots and wafers which are self-interstitial dominated and devoid of agglomerated intrinsic point defects over a substantial portion of the ingot radius; the provision of such a crystal puller which substantially reduces the cooling rate of an ingot being grown in the puller; the provision of such a crystal puller which substantially increases the time during which the temperature of the growing ingot is above 1050°C; and the provision of an electrical resistance heater for use in such a crystal puller which does not impede viewing of the growing ingot via the view port in the puller housing.

Generally, a crystal puller of the present invention for growing monocrystalline silicon ingots according to the Czochralski method which are devoid of agglomerated intrinsic point defects over a substantial portion of the radius of the ingot comprises a housing defining an interior having a lower growth chamber and an upper pull chamber. The pull chamber has a smaller transverse dimension than the growth chamber. A crucible is disposed in the growth chamber of the housing for containing molten silicon. A pulling mechanism is provided for pulling a growing ingot upward from the molten silicon through the growth chamber and pull chamber. An electrical resistance heater has a heating element sized and shaped for being disposed at least partially within the upper pull chamber of the housing in radially spaced relationship with the outer surface of the growing ingot for radiating heat to the ingot as it is pulled upward in the pull chamber relative to the

molten silicon. The heating element has an upper end and a lower end. The lower end of the heating element is disposed substantially closer to the molten silicon than the upper end when the heating element is placed in the housing.

Other objects and features of the present invention will be in part apparent and in part pointed out hereinafter.

BRIEF DESCRIPTION OF THE DRAWINGS

FIG. 1 is a graph which shows an example of how the initial concentration of self-interstitials, [I], and vacancies, [V], changes with an increase in the value of the ratio v/G_0, where v is the growth rate and G_0 is the average axial temperature gradient.

FIG. 2 is a graph which shows an example of how ΔG_I, the change in free energy required for the formation of agglomerated interstitial defects, increases as the temperature, T, decreases, for a given initial concentration of self-interstitials, [I].

FIG. 3 is a graph which shows an example of how ΔG_I, the change in free energy required for the formation of agglomerated interstitial defects, decreases (as the temperature, T, decreases) as a result of the suppression of the concentration of self-interstitials, [I], through the means of radial diffusion. The solid line depicts the case for no radial diffusion whereas the dotted line includes the effect of diffusion.

FIG. 4 is a graph which shows an example of how ΔG_I, the change in free energy required for the formation of agglomerated interstitial defects, is sufficiently decreased (as the temperature, T, decreases), as a result of the suppression of the concentration of self-interstitials, [I], through the means of radial

diffusion, such that an agglomeration reaction is prevented. The solid line depicts the case for no radial diffusion whereas the dotted line includes the effect of diffusion.

FIG. 5 is a graph which shows an example of how the initial concentration of self-interstitials, [I], and vacancies, [V], can change along the radius of an ingot or wafer, as the value of the ratio v/G_0 decreases, due to an increase in the value of G_0. Note that at the V/I boundary a transition occurs from vacancy dominated material to self-interstitial dominated material.

FIG. 6 is a top plan view of a single crystal silicon ingot or wafer showing regions of vacancy, V, and self-interstitial, I, dominated materials respectively, as well as the V/I boundary that exists between them.

FIG. 7a is a graph which shows an example of how the initial concentration of vacancies or self-interstitials changes as a function of radial position due to radial diffusion of self-interstitials. Also shown is how such diffusion causes the location of the V/I boundary to move closer to the center of the ingot (as a result of the recombination of vacancies and self-interstitials), as well as the concentration of self-interstitials, [I], to be suppressed.

FIG. 7b is a graph of ΔG_I as a function of radial position which shows an example of how the suppression of self-interstitial concentration, [I], (as depicted in FIG. 7a) is sufficient to maintain ΔG_I everywhere to a value which is less than the critical value at which the silicon self-interstitial reaction occurs.

FIG. 7c is a graph which shows another example of how the initial concentration of vacancies or self-interstitials changes as a function of radial position due to radial diffusion of self-interstitials. Note that, in comparison to FIG. 7a, such diffusion caused the location of the V/I boundary to be closer to the center

of the ingot (as a result of the recombination of vacancies and self-interstitials), resulting in an increase in the concentration of interstitials in the region outside of the V/I boundary.

FIG. 7d is a graph of ΔG_I as a function of radial position which shows an example of how the suppression of self-interstitial concentration, [I], (as depicted in FIG. 7c) is not sufficient to maintain ΔG_I everywhere to a value which is less than the critical value at which the silicon self-interstitial reaction occurs.

FIG. 7e is a graph which shows another example of how the initial concentration of vacancies or self-interstitials changes as a function of radial position due to radial diffusion of self-interstitials. Note that, in comparison to FIG. 7a, increased diffusion resulted in greater suppression the self-interstitial concentration.

FIG. 7f is a graph of ΔG_I as a function of radial position which shows an example of how greater suppression of the self-interstitial concentration, [I], (as depicted in FIG. 7e) results in a greater degree of suppression in ΔG_I, as compared to FIG. 7b.

FIG. 7g is a graph which shows another example of how the initial concentration of vacancies or self-interstitials changes as a function of radial position due to radial diffusion of self-interstitials. Note that, in comparison to FIG. 7c, increased diffusion resulted in greater suppression the self-interstitial concentration.

FIG. 7h is a graph of ΔG_I as a function of radial position which shows an example of how greater suppression of the self-interstitial concentration, [I], (as depicted in FIG. 7g) results in a greater degree of suppression in ΔG_I, as compared to FIG. 7d.

FIG. 7i is a graph which shows another example of how the initial concentration of vacancies or self-interstitials changes as a function of radial position due to radial diffusion of self-interstitials. Note that in this example a sufficient quantity of self-interstitials recombine with vacancies, such that there is no longer a vacancy-dominated region.

FIG. 7j is a graph of ΔG_I as a function of radial position which shows an example of how radial diffusion of self-interstitials (as depicted in FIG. 7i) is sufficient to maintain a suppression of agglomerated interstitial defects everywhere along the crystal radius.

FIG. 8 is a longitudinal, cross-sectional view of a single crystal silicon ingot showing, in detail, an axially symmetric region of a constant diameter portion of the ingot.

FIG. 9 is a longitudinal, cross-sectional view of a segment of a constant diameter portion of a single crystal silicon ingot, showing in detail axial variations in the width of an axially symmetric region.

FIG. 10 is a longitudinal, cross-sectional view of a segment of a constant diameter portion of a single crystal silicon ingot having axially symmetric region of a width which is less than the radius of the ingot, showing in detail that this region further contains a generally cylindrical region of vacancy dominated material.

FIG. 11 is a latitudinal, cross-sectional view of the axially symmetric region depicted in FIG. 10.

FIG. 12 is a longitudinal, cross-sectional view of a segment of a constant diameter portion of a single crystal silicon ingot having an axially symmetric region of a width which is equal to the radius of the ingot,

showing in detail that this region is a generally cylindrical region of self-interstitial dominated material which is substantially free of agglomerated intrinsic point defects.

FIG. 13 is an image produced by a scan of the minority carrier lifetime of an axial cut of the ingot following a series of oxygen precipitation heat treatments, showing in detail a generally cylindrical region of vacancy dominated material, a generally annular shaped axially symmetric region of self-interstitial dominated material, the V/I boundary present between them, and a region of agglomerated interstitial defects.

FIG. 14 is a graph of pull rate (i.e. seed lift) as a function of crystal length, showing how the pull rate is decreased linearly over a portion of the length of the crystal.

FIG. 15 is an image produced by a scan of the minority carrier lifetime of an axial cut of the ingot following a series of oxygen precipitation heat treatments, as described in Example 1.

FIG. 16 is a graph of pull rate as a function of crystal length for each of four single crystal silicon ingots, labeled 1-4 respectively, which are used to yield a curve, labeled $v^*(Z)$, as described in Example 1.

FIG. 17 is a graph of the average axial temperature gradient at the melt/solid interface, G_0, as a function of radial position, for two different cases as described in Example 2.

FIG. 18 is a graph of the initial concentration of vacancies, [V], or self-interstitials, [I], as a function of radial position, for two different cases as described Example 2.

FIG. 19 is a graph of temperature as a function of axial position, showing the axial temperature profile in ingots for two different cases as described in Example 3.

FIG. 20 is a graph of the self-interstitial concentrations resulting from the two cooling conditions illustrated in Fig. 19 and as more fully described in Example 3.

FIG. 21 is an image produced by a scan of the minority carrier lifetime of an axial cut of an entire ingot following a series of oxygen precipitation heat treatments, as described in Example 4.

FIG. 22 is a graph illustrating the position of the V/I boundary as a function of the length of the single crystal silicon ingot, as described in Example 5.

FIG. 23a is an image produced by a scan of the minority carrier lifetime of an axial cut of a segment of an ingot, ranging from about 100 mm to about 250 mm from the shoulder of the ingot, following a series of oxygen precipitation heat treatments, as described in Example 6.

FIG. 23b is an image produced by a scan of the minority carrier lifetime of an axial cut of a segment of an ingot, ranging from about 250 mm to about 400 mm from the shoulder of the ingot, following a series of oxygen precipitation heat treatments, as described in Example 6.

FIG. 24 is a graph illustrating the axial temperature profile for an ingot in four different hot zone configurations.

FIG. 25 is a graph of the axial temperature gradient, G_0, at various axial positions for an ingot, as described in Example 7.

FIG. 26 is a graph of the radial variations in the average axial temperature gradient, G_0, at various for an ingot, as described in Example 7.

FIG. 27 is a graph illustrating the relationship between the width of the axially symmetric region and the cooling rate, as described in Example 7.

FIG. 28 is a photograph of an axial cut of a segment of an ingot, ranging from about 235 mm to about 350 mm from the shoulder of the ingot, following copper decoration and a defect-delineating etch, described in Example 7.

FIG. 29 is a photograph of an axial cut of a segment of an ingot, ranging from about 305 mm to about 460 mm from the shoulder of the ingot, following copper decoration and a defect-delineating etch, described in Example 7.

FIG. 30 is a photograph of an axial cut of a segment of an ingot, ranging from about 140 mm to about 275 mm from the shoulder of the ingot, following copper decoration and a defect-delineating etch, described in Example 7.

FIG. 31 is a photograph of an axial cut of a segment of an ingot, ranging from about 600 mm to about 730 mm from the shoulder of the ingot, following copper decoration and a defect-delineating etch, described in Example 7.

FIG. 32 is a schematic, fragmentary vertical section of a crystal puller of the present invention showing an electrical resistance heater of a first embodiment as it is positioned during growth of a single crystal silicon ingot;

FIG. 33 is a perspective view of the electrical resistance heater of FIG. 1;

FIG. 34 is a perspective view of a second embodiment of an electrical resistance heater for use in the crystal puller of FIG. 1;

FIG. 35 is a perspective view of a third embodiment of an electrical resistance heater for use in the crystal puller of Fig. 1;

FIG. 36 is a schematic vertical section of a crystal puller without the electrical resistance heater of FIG. 1, showing temperature isotherms of a crystal ingot grown in the puller using a finite element analysis;

FIG. 37 is a schematic vertical section of a crystal puller of the present invention including the electrical resistance heater of FIG. 1, showing temperature isotherms of a crystal ingot grown in the puller using a finite element analysis;

FIG. 38 is a schematic vertical section of a crystal puller similar to that shown in FIG. 37, but including an electrical resistance heater having a longer length than the heater of FIG. 37, showing temperature isotherms of a crystal ingot grown in the puller using a finite element analysis; and

FIG. 39 is a plot of the ingot isotherm data from FIGS. 36, 37 and 38 comparing the ingot axial temperature versus the distance of the ingot from the molten source material.

Corresponding reference characters indicate corresponding parts throughout the several views of the drawings.

DETAILED DESCRIPTION OF THE PREFERRED EMBODIMENTS

Based upon experimental evidence to date, it appears that the type and initial concentration of intrinsic point defects is initially determined as the ingot cools from the temperature of solidification (i.e., about 1410°C) to a temperature greater than 1300°C (i.e., at least about 1325 °C, at least about 1350 °C or even at least about 1375 °C). That is, the type and initial concentration of these defects are controlled by the ratio v/G_0, where v is the growth velocity and G_0 is the average axial temperature gradient over this temperature range.

Referring to Fig. 1, for increasing values of v/G_0, a transition from decreasingly self-interstitial dominated growth to increasingly vacancy dominated growth occurs near a critical value of v/G_0 which, based upon currently available information, appears to be about 2.1×10^{-5} cm^2/sK, where G_0 is determined under conditions in which the axial temperature gradient is constant within the temperature range defined above. At this critical value, the concentrations of these intrinsic point defects are at equilibrium.

As the value of v/G_0 exceeds the critical value, the concentration of vacancies increases. Likewise, as the value of v/G_0 falls below the critical value, the concentration of self-interstitials increases. If these concentrations reach a level of critical supersaturation in the system, and if the mobility of the point defects is sufficiently high, a reaction, or an agglomeration event, will likely occur. Agglomerated intrinsic point defects in silicon can severely impact the yield potential of the material in the production of complex and highly integrated circuits.

It has been discovered that the reaction in which silicon self-interstitial atoms react to produce agglomerated interstitial defects can be suppressed. Without being bound to any particular theory, it is believed that the concentration of self-interstitials is controlled during the growth and cooling of the crystal ingot such that the change in free energy of the system never exceeds a critical value at which the agglomeration reaction spontaneously occurs to produce agglomerated interstitial defects.

In general, the change in system free energy available to drive the reaction in which agglomerated interstitial defects are formed from silicon self-interstitials in single crystal silicon is governed by Equation (I):

$$\Delta G_I = kT \ln\left(\frac{[I]}{[I]^{eq}}\right) \quad (I)$$

wherein

ΔG_I is the change in free energy,

k is the Boltzmann constant,

T is the temperature in K,

[I] is the concentration of self-interstitials at a point in space and time in the single crystal silicon, and

$[I]^{eq}$ is the equilibrium concentration of self-interstitials at the same point in space and time at which [I] occurs and at the temperature, T.

According to this equation, for a given concentration of self-interstitials, [I], a decrease in the temperature, T, generally results in an increase in ΔG_I due to a sharp decrease in $[I]^{eq}$ with temperature.

Fig. 2 schematically illustrates the change in ΔG_I and the concentration of silicon self-interstitials for an ingot which is cooled from the temperature of solidification without simultaneously employing some means for suppression of the concentration of silicon self-interstitials. As the ingot cools, ΔG_I increases according to Equation (I), due to the increasing supersaturation of [I], and the energy barrier for the formation of agglomerated interstitial defects is approached. As cooling continues, this energy barrier is eventually exceeded, at which point a reaction occurs. This reaction results in the formation of agglomerated interstitial defects and the concomitant decrease in ΔG_I as the supersaturated system is relaxed, i.e., as the concentration of [I] decreases.

The agglomeration of self-interstitials can be avoided as the ingot cools from the temperature of solidification by maintaining the free energy of the silicon self-interstitial system at a value which is less than that at which an agglomeration reaction will occur. In other words, the system can be controlled so as to never become critically supersaturated. This can be achieved by establishing an initial concentration of self-interstitials (controlled by $v/G_0(r)$ as hereinafter defined) which is sufficiently low such that critical supersaturation is never achieved. However, in practice such concentrations are difficult to achieve across an entire crystal radius and, in general, therefore, critical supersaturation may be avoided by suppressing the initial silicon self-interstitial concentration subsequent to crystal solidification, i.e., subsequent to establishing the initial concentration determined by $v/G_0(r)$.

Figs. 3 and 4 schematically illustrate two possible effects of suppressing [I] upon the increase in ΔG_I as the ingot of Fig. 2 is cooled from the temperature of solidification. In Fig. 3, the suppression of [I] results in a decrease in the rate of increase of ΔG_I but, in this case, the suppression is insufficient to maintain ΔG_I everywhere at a value which is less than the critical value at which the reaction occurs; as a result, the suppression merely serves to reduce the temperature at which the reaction occurs. In Fig. 4, an increased suppression of [I] is sufficient to maintain ΔG_I everywhere to a value which is less than the critical value at which the reaction occurs; the suppression, therefore, inhibits the formation of defects.

Surprisingly, it has been found that due to the relatively large mobility of self-interstitials, which is generally about 10^{-4} cm^2/second, it is possible to effect the suppression over relatively large distances, i.e.

distances of about 5 cm to about 10 cm or more, by the radial diffusion of self-interstitials to sinks located at the crystal surface or to vacancy dominated regions located within the crystal. Radial diffusion can be effectively used to suppress the concentration of self-interstitials, provided sufficient time is allowed for the radial diffusion of the initial concentration of intrinsic point defects. In general, the diffusion time will depend upon the radial variation in the initial concentration of self-interstitials, with lesser radial variations requiring shorter diffusion times.

Typically, the average axial temperature gradient, G_0, increases as a function of increasing radius for single crystal silicon, which is grown according to the Czochralski method. This means that the value of v/G_0 is typically not singular across the radius of an ingot. As a result of this variation, the type and initial concentration of intrinsic point defects is not constant. If the critical value of v/G_0, denoted in Figs. 5 and 6 as the V/I boundary 2, is reached at some point along the radius 4 of the ingot, the material will switch from being vacancy dominated to self-interstitial dominated. In addition, the ingot will contain an axially symmetric region of self-interstitial dominated material 6 (in which the initial concentration of silicon self-interstitial atoms increases as a function of increasing radius), surrounding a generally cylindrical region of vacancy dominated material 8 (in which the initial concentration of vacancies decreases as a function of increasing radius).

Figs. 7a and 7b schematically illustrate the effect of suppressing [I] upon the increase in ΔG_I as an ingot is cooled from the temperature of solidification. When the ingot is pulled in accordance with the Czochralski method, the ingot contains an axially symmetric region of interstitial dominated material extending from the edge

of the ingot to the position along the radius at which the V/I boundary occurs and a generally cylindrical region of vacancy dominated material extending from the center of the ingot to the position along the radius at which the V/I boundary occurs. As the ingot is cooled from the temperature of solidification, radial diffusion of interstitial atoms causes a radially inward shift in the V/I boundary due to a recombination of self-interstitials with vacancies and a significant suppression of the self-interstitial concentration outside the V/I boundary. In addition, radial diffusion of self-interstitials to the surface of the crystal will occur as the crystal cools. The surface of the crystal is capable of maintaining near equilibrium point defect concentrations as the crystal cools. As a result, the suppression of [I] is sufficient to maintain ΔG_I everywhere to a value which is less than the critical value at which the silicon self-interstitial reaction occurs.

Referring now to Figs. 8 and 9, in a generally preferred process for suppressing the agglomeration of defects, a single crystal silicon ingot 10 is grown in accordance with the Czochralski method. The silicon ingot comprises a central axis 12, a seed-cone 14, an end-cone 16 and a constant diameter portion 18 between the seed-cone and the end-cone. The constant diameter portion has a circumferential edge 20 and a radius 4 extending from the central axis to the circumferential edge. The process comprises controlling the growth conditions, including growth velocity, v, the average axial temperature gradient, G_0, and the cooling rate, to cause the formation of an axially symmetric region 6 which, upon cooling of the ingot from the solidification temperature, is substantially free of agglomerated intrinsic point defects.

In one embodiment of the process, the growth conditions are controlled to maintain the V/I boundary 2 at a position which maximizes the volume of the axially symmetric region 6 relative to the volume of the constant diameter portion 18 of the ingot 10. In general, therefore, in this embodiment it is preferred that the axially symmetric region have a width 22 (as measured from the circumferential edge radially toward the central axis of the ingot) and a length 24 (as measured along the central axis of the ingot) which equals the radius 4 and length 26, respectively, of the constant diameter portion of the ingot. As a practical matter, however, operating conditions and crystal puller hardware constraints may dictate that the axially symmetric region occupy a lesser proportion of the constant diameter portion of the ingot. In general, therefore, the axially symmetric region in this embodiment preferably has a width of at least about 30%, more preferably at least about 40%, still more preferably at least about 60%, and most preferably at least about 80% of the radius of the constant diameter portion of the ingot. In addition, the axially symmetric region extends over a length of at least about 20%, preferably at least about 40%, more preferably at least about 60%, and still more preferably at least about 80% of the length of the constant diameter portion of the ingot.

Referring to Fig. 9, the width 22 of the axially symmetric region 6 may have some variation along the length of the central axis 12. For an axially symmetric region of a given length, therefore, the width is determined by measuring the distance from the circumferential edge 20 of the ingot 10 radially toward a point which is farthest from the central axis. In other words, the width 22 is measured such that the minimum distance within the given length 24 of the axially symmetric region 6 is determined.

Referring now to Figs. 10 and 11, when the axially symmetric region 6 of the constant diameter portion 18 of the ingot 10 has a width 22 which is less than the radius 4 of the constant diameter portion, the region is generally annular in shape. A generally cylindrical region of vacancy dominated material 8, which is centered about the central axis 12, is located radially inward of the generally annular shaped segment. Referring to Figure 12, it is to be understood that when the width 22 of the axially symmetric region 6 is equal to the radius 4 of the constant diameter portion 18, the region does not contain this vacancy dominated region; rather, the axially symmetric region itself is generally cylindrical and contains self-interstitial dominated material which is substantially free of agglomerated intrinsic point defects.

While it is generally preferred that the crystal growth conditions be controlled to maximize the width of the interstitial dominated region, there may be limits for a given crystal puller hot zone design. As the V/I boundary is moved closer to the central crystal axis, provided the cooling conditions and $G_0(r)$ do not change, where $G_0(r)$ is the radial variation of G_0, the minimum amount of radial diffusion required increases. In these circumstances, there may be a minimum radius of the vacancy dominated region which is required to suppress the formation of agglomerated interstitial defects by radial diffusion.

Figs. 7c and 7d schematically illustrate an example in which the minimum radius of the vacancy dominated region is exceeded. In this example, the cooling conditions and $G_0(r)$ are the same as those employed for the crystal of Figs. 7a and 7b in which there was sufficient outdiffusion to avoid agglomerated interstitial defects for the position of the V/I boundary illustrated. In Figs. 7c and 7d, the position of the V/I

boundary is moved closer to the central axis (relative to Figs. 7a and 7b) resulting in an increase in the concentration of interstitials in the region outside of the V/I boundary. As a result, more radial diffusion is required to sufficiently suppress the interstitial concentration. If sufficient outdiffusion is not achieved, the system ΔG_I will increase beyond the critical value and the reaction which produces agglomerated interstitial defects will occur, producing a region of these defects in an annular region between the V/I boundary and the edge of the crystal. The radius of the V/I boundary at which this occurs is the minimum radius for the given hot zone. This minimum radius is decreased if more radial diffusion of interstitials is allowed.

Figs. 7e, 7f, 7g and 7h illustrate the effect of an increased radial outdiffusion on interstitial concentration profiles and the rise of system ΔG_I for a crystal grown with the same initial vacancy and interstitial concentration profiles as the crystal exemplified in Figs. 7a, 7b, 7c and 7d. Increased radial diffusion of interstitials results in a greater suppression of interstitial concentration, thus suppressing the rise in the system ΔG_I to a greater degree than in Figs. 7a, 7b, 7c and 7d. In this case the system ΔG_I is not exceeded for the smaller radius of the V/I boundary.

Figs. 7i and 7j illustrate an example in which sufficient radial diffusion is allowed such that the minimum radius is reduced to zero by insuring sufficient radial diffusion to achieve a suppression of agglomerated interstitial defects everywhere along the crystal radius.

In one embodiment of the present process, the initial concentration of silicon self-interstitial atoms is controlled in the axially symmetric, self-interstitial dominated region of the ingot. Referring again to Fig. 1, in general, the initial concentration of silicon self-

interstitial atoms is controlled by controlling the crystal growth velocity, v, and the average axial temperature gradient, G_0, such that the value of the ratio v/G_0 is relatively near the critical value of this ratio, at which the V/I boundary occurs. In addition, the average axial temperature gradient, G_0, can be established such that the variation of G_0, i.e. $G_0(r)$, (and thus, $v/G_0(r)$) as a function of the ingot radius is also controlled.

The growth velocity, v, and the average axial temperature gradient, G_0, (as previously defined) are typically controlled such that the ratio v/G_0 ranges in value from about 0.5 to about 2.5 times the critical value of v/G_0 (i.e., about $1x10^{-5}$ cm^2/sK to about $5x10^{-5}$ cm^2/sK based upon currently available information for the critical value of v/G_0). Preferably, the ratio v/G_0 will range in value from about 0.6 to about 1.5 times the critical value of v/G_0 (i.e., about $1.3x10^{-5}$ cm^2/sK to about $3x10^{-5}$ cm^2/sK based upon currently available information for the critical value of v/G_0). Most preferably, the ratio v/G_0 will range in value from about 0.75 to about 1 times the critical value of v/G_0 (i.e., about $1.6x10^{-5}$ cm^2/sK to about $2.1x10^{-5}$ cm^2/sK based upon currently available information for the critical value of v/G_0). These ratios are achieved by independent control of the growth velocity, v, and the average axial temperature gradient, G_0.

In general, control of the average axial temperature gradient, G_0, may be achieved primarily through the design of the "hot zone" of the crystal puller, i.e. the graphite (or other materials) that makes up the heater, insulation, heat and radiation shields, among other things. Although the design particulars may vary depending upon the make and model of the crystal puller, in general, G_0 may be controlled using any of the means currently known in the art for controlling heat transfer

at the melt/solid interface, including reflectors, radiation shields, purge tubes, light pipes, and heaters. In general, radial variations in G_0 are minimized by positioning such an apparatus within about one crystal diameter above the melt/solid interface. G_0 can be controlled further by adjusting the position of the apparatus relative to the melt and crystal. This is accomplished either by adjusting the position of the apparatus in the hot zone, or by adjusting the position of the melt surface in the hot zone. In addition, when a heater is employed, G_0 may be further controlled by adjusting the power supplied to the heater. Any, or all, of these methods can be used during a batch Czochralski process in which melt volume is depleted during the process.

It is generally preferred for some embodiments of the present process that the average axial temperature gradient, G_0, be relatively constant as a function of diameter of the ingot. However, it should be noted that as improvements in hot zone design allow for variations in G_0 to be minimized, mechanical issues associated with maintaining a constant growth rate become an increasingly important factor. This is because the growth process becomes much more sensitive to any variation in the pull rate, which in turn directly effects the growth rate, v. In terms of process control, this means that it is favorable to have values for G_0 which differ over the radius of the ingot. Significant differences in the value of G_0, however, can result in a large concentration of self-interstitials generally increasing toward the wafer edge and, thereby, increase the difficultly in avoiding the formation of agglomerated intrinsic point defects.

In view of the foregoing, the control of G_0 involves a balance between minimizing radial variations in G_0 and maintaining favorable process control conditions.

Typically, therefore, the pull rate after about one diameter of the crystal length will range from about 0.2 mm/minute to about 0.8 mm/minute. Preferably, the pull rate will range from about 0.25 mm/minute to about 0.6 mm/minute and, more preferably, from about 0.3 mm/minute to about 0.5 mm/minute. It is to be noted that the pull rate is dependent upon both the crystal diameter and crystal puller design. The stated ranges are typical for 200 mm diameter crystals. In general, the pull rate will decrease as the crystal diameter increases. However, the crystal puller may be designed to allow pull rates in excess of those stated here. As a result, most preferably the crystal puller will be designed to enable the pull rate to be as fast as possible while still allowing for the formation of an axially symmetric region in accordance with the present process.

In a second and preferred embodiment, the amount of self-interstitial diffusion is controlled by controlling the cooling rate as the ingot is cooled from the solidification temperature (about 1410°C) to the temperature at which silicon self-interstitials become immobile, for commercially practical purposes. Silicon self-interstitials appear to be extremely mobile at temperatures near the solidification temperature of silicon, i.e. about 1410°C. This mobility, however, decreases as the temperature of the single crystal silicon ingot decreases. Generally, the diffusion rate of self-interstitials slows such a considerable degree that they are essentially immobile for commercially practical time periods at temperatures less than about 700°C, and perhaps at temperatures as great as 800°C, 900°C, 1000°C, or even 1050°C.

It is to be noted in this regard that, although the temperature at which a self-interstitial agglomeration reaction occurs may in theory vary over a wide range of temperatures, as a practical matter this range appears to

be relatively narrow for conventional, Czochralski grown silicon. This is a consequence of the relatively narrow range of initial self-interstitial concentrations which are typically obtained in silicon grown according to the Czochralski method. In general, therefore, a self-interstitial agglomeration reaction may occur, if at all, at temperatures within the range of about 1100°C to about 800°C, and typically at a temperature of about 1050°C.

Within the range of temperatures at which self-interstitials appear to be mobile, and depending upon the temperature in the hot zone, the cooling rate will typically range from about 0.1 °C/minute to about 3 °C/minute. Preferably, the cooling rate will range from about 0.1 °C/minute to about 1.5 °C/minute, more preferably from about 0.1 °C/minute to about 1 °C/minute, and still more preferably from about 0.1 °C/minute to about 0.5 °C/minute. Stated another way, to maximize the width of the axially symmetric region it is generally preferred that the silicon reside at a temperature in excess of about 1050 °C for a period of (i) at least about 5 hours, preferably at least about 10 hours, and more preferably at least about 15 hours for 150 mm nominal diameter silicon crystals, (ii) at least about 5 hours, preferably at least about 10 hours, more preferably at least about 20 hours, still more preferably at least about 25 hours, and most preferably at least about 30 hours for 200 mm nominal diameter silicon crystals, and (iii) at least about 20 hours, preferably at least about 40 hours, more preferably at least about 60 hours, and most preferably at least about 75 hours for silicon crystals having a nominal diameter greater than 200 mm. Referring to Fig. 24, axial temperature profiles may vary for different hot zone configurations designed to control the cooling rate of the ingot.

By controlling the cooling rate of the ingot within a range of temperatures in which self-interstitials

appear to be mobile, the self-interstitials may be given more time to diffuse to sinks located at the crystal surface, or to vacancy dominated regions, where they may be annihilated. The concentration of such interstitials may therefore be suppressed, which act to prevent an agglomeration event from occurring. Utilizing the diffusivity of interstitials by controlling the cooling rate acts to relax the otherwise stringent v/G_0 requirements that may be required in order to obtain an axially symmetric region free of agglomerated defects. Stated another way, as a result of the fact that the cooling rate may be controlled in order to allow interstitials more time to diffuse, a large range of v/G_0 values, relative to the critical value, are acceptable for purposes of obtaining an axially symmetric region free of agglomerated defects.

To achieve such cooling rates over appreciable lengths of the constant diameter portion of the crystal, consideration must also be given to the growth process of the end-cone of the ingot, as well as the treatment of the ingot once end-cone growth is complete. Typically, upon completion of the growth of the constant diameter portion of the ingot, the pull rate will be increased in order to begin the tapering necessary to form the end-cone. However, such an increase in pull rate will result in the lower segment of the constant diameter portion cooling more quickly within the temperature range in which interstitials are sufficiently mobile, as discussed above. As a result, these interstitials may not have sufficient time to diffuse to sinks to be annihilated; that is, the concentration in this lower segment may not be suppressed to a sufficient degree and agglomeration of interstitial defects may result.

In order to prevent the formation of such defects from occurring in this lower segment of the ingot, it is therefore preferred that constant diameter portion of the

ingot have a uniform thermal history in accordance with the Czochralski method. A uniform thermal history may be achieved by pulling the ingot from the silicon melt at a relatively constant rate during the growth of not only the constant diameter portion, but also during the growth of the end-cone of the crystal and possibly subsequent to growth of the end-cone. The relatively constant rate may be achieved, for example, by (i) reducing the rates of rotation of the crucible and crystal during the growth of the end-cone relative to the crucible and crystal rotation rates during the growth of the constant diameter portion of the crystal, and/or (ii) increasing the power supplied to the heater used to heat the silicon melt during the growth of the end-cone relative to the power conventionally supplied during end-cone growth. These additional adjustments of the process variables may occur either individually or in combination.

When the growth of the end-cone is initiated, a pull rate for the end-cone is established such that, any segment of the constant diameter portion of the ingot which remains at a temperature in excess of about 1050 °C experiences the same thermal history as other segment(s) of the constant diameter portion of the ingot which contain an axially symmetric region free of agglomerated intrinsic point defects which have already cooled to a temperature of less than about 1050 °C.

As previously noted, a minimum radius of the vacancy dominated region exists for which the suppression of agglomerated interstitial defects may be achieved. The value of the minimum radius depends on $v/G_0(r)$ and the cooling rate. As crystal puller and hot zone designs will vary, the ranges presented above for $v/G_0(r)$, pull rate, and cooling rate will also vary. Likewise these conditions may vary along the length of a growing crystal. Also as noted above, the width of the interstitial dominated region free of agglomerated

interstitial defects is preferably maximized. Thus, it is desirable to maintain the width of this region to a value which is as close as possible to, without exceeding, the difference between the crystal radius and the minimum radius of the vacancy dominated region along the length of the growing crystal in a given crystal puller.

The optimum width of the axially symmetric region and the required optimal crystal pulling rate profile for a given crystal puller hot zone design may be determined empirically. Generally speaking, this empirical approach involves first obtaining readily available data on the axial temperature profile for an ingot grown in a particular crystal puller, as well as the radial variations in the average axial temperature gradient for an ingot grown in the same puller. Collectively, this data is used to pull one or more single crystal silicon ingots, which are then analyzed for the presence of agglomerated interstitial defects. In this way, an optimum pull rate profile can be determined.

Fig. 13 is an image produced by a scan of the minority carrier lifetime of an axial cut of a section of a 200 mm diameter ingot following a series of oxygen precipitation heat-treatments which reveal defect distribution patterns. It depicts an example in which a near-optimum pull rate profile is employed for a given crystal puller hot zone design. In this example, a transition occurs from a $v/G_0(r)$ at which the maximum width of the interstitial dominated region is exceeded (resulting in the generation of regions of agglomerated interstitial defects 28) to an optimum $v/G_0(r)$ at which the axially symmetric region has the maximum width.

In addition to the radial variations in v/G_0 resulting from an increase in G_0 over the radius of the ingot, v/G_0 may also vary axially as a result of a change in v, or as a result of natural variations in G_0 due to

the Czochralski process. For a standard Czochralski process, v is altered as the pull rate is adjusted throughout the growth cycle, in order to maintain the ingot at a constant diameter. These adjustments, or changes, in the pull rate in turn cause v/G_0 to vary over the length of the constant diameter portion of the ingot. In accordance with the preferred process, the pull rate is therefore controlled in order to maximize the width of the axially symmetric region of the ingot. As a result, however, variations in the radius of the ingot may occur. In order to ensure that the resulting ingot has a constant diameter, the ingot is therefore preferably grown to a diameter larger than that which is desired. The ingot is then subjected to processes standard in the art to remove excess material from the surface, thus ensuring that an ingot having a constant diameter portion is obtained.

For an ingot prepared in accordance with the above described process and having a V/I boundary, i.e. an ingot containing material which is vacancy dominated, experience has shown that low oxygen content material, i.e., less than about 13 PPMA (parts per million atomic, ASTM standard F-121-83), is preferred. More preferably, the single crystal silicon contains less than about 12 PPMA oxygen, still more preferably less than about 11 PPMA oxygen, and most preferably less than about 10 PPMA oxygen. This is because, in medium to high oxygen contents wafers, i.e., 14 PPMA to 18 PPMA, the formation of oxygen-induced stacking faults and bands of enhanced oxygen clustering just inside the V/I boundary becomes more pronounced. Each of these are a potential source for problems in a given integrated circuit fabrication process. However, it is to be noted that, when the axially symmetric region has a width about equal to the

radius of the ingot, the oxygen content restriction is removed; this is because, given that no vacancy type material is present, the formation of such faults and clusters will not occur.

The effects of enhanced oxygen clustering may be further reduced by a number of methods, used singularly or in combination. For example, oxygen precipitate nucleation centers typically form in silicon which is annealed at a temperature in the range of about 350°C to about 750°C. For some applications, therefore, it may be preferred that the crystal be a "short" crystal, that is, a crystal which has been grown in a Czochralski process until the seed end has cooled from the melting point of silicon (about 1410° C) to about 750°C after which the ingot is rapidly cooled. In this way, the time spent in the temperature range critical for nucleation center formation is kept to a minimum and the oxygen precipitate nucleation centers have inadequate time to form in the crystal puller.

Preferably, however, oxygen precipitate nucleation centers formed during the growth of the single crystal are dissolved by annealing the single crystal silicon. Provided they have not been subjected to a stabilizing heat-treatment, oxygen precipitate nucleation centers can be annealed out of silicon by rapidly heating the silicon to a temperature of at least about 875° C, and preferably continuing to increase the temperature to at least 1000° C, at least 1100°C, or more. By the time the silicon reaches 1000° C, substantially all (e.g., >99%) of such defects have annealed out. It is important that the wafers be rapidly heated to these temperatures, i.e., that the rate of temperature increase be at least about 10° C per minute and more preferably at least about 50° C per minute. Otherwise, some or all of the oxygen precipitate nucleation centers may be stabilized by the heat-treatment. Equilibrium appears to be reached in

relatively short periods of time, i.e., on the order of about 60 seconds or less. Accordingly, oxygen precipitate nucleation centers in the single crystal silicon may be dissolved by annealing it at a temperature of at least about 875° C, preferably at least about 950°C, and more preferably at least about 1100°C, for a period of at least about 5 seconds, and preferably at least about 10 minutes.

The dissolution may be carried out in a conventional furnace or in a rapid thermal annealing (RTA) system. The rapid thermal anneal of silicon may be carried out in any of a number of commercially available rapid thermal annealing ("RTA") furnaces in which wafers are individually heated by banks of high power lamps. RTA furnaces are capable of rapidly heating a silicon wafer, e.g., they are capable of heating a wafer from room temperature to 1200 °C in a few seconds. One such commercially available RTA furnace is the model 610 furnace available from AG Associates (Mountain View, CA). In addition, the dissolution may be carried out on silicon ingots or on silicon wafers, preferably wafers.

It is to be noted that wafers prepared in accordance with the above process are suitable for use as substrates upon which an epitaxial layer may be deposited. Epitaxial deposition may be performed by means common in the art.

Furthermore, it is also to be noted that such wafers are suitable for use in combination with hydrogen or argon annealing treatments, such as the treatments described in European Patent Application No. 503,816 A1.

Detection of Agglomerated Defects

Agglomerated defects may be detected by a number of different techniques. For example, flow pattern defects, or D-defects, are typically detected by preferentially etching the single crystal silicon sample in a Secco etch

solution for about 30 minutes, and then subjecting the sample to microscopic inspection. (see, e.g., H. Yamagishi et al., Semicond. Sci. Technol. 7, A135 (1992)). Although standard for the detection of agglomerated vacancy defects, this process may also be used to detect agglomerated interstitial defects. When this technique is used, such defects appear as large pits on the surface of the sample when present.

Agglomerated defects may also be detected using laser scattering techniques, such as laser scattering tomography, which typically have a lower defect density detection limit that other etching techniques.

Additionally, agglomerated intrinsic point defects may be visually detect by decorating these defects with a metal capable of diffusing into the single crystal silicon matrix upon the application of heat. Specifically, single crystal silicon samples, such as wafers, slugs or slabs, may be visually inspected for the presence of such defects by first coating a surface of the sample with a composition containing a metal capable of decorating these defects, such as a concentrated solution of copper nitrate. The coated sample is then heated to a temperature between about 900°C and about 1000°C for about 5 minutes to about 15 minutes in order to diffuse the metal into the sample. The heat treated sample is then cooled to room temperature, thus causing the metal to become critically supersaturated and precipitate at sites within the sample matrix at which defects are present.

After cooling, the sample is first subjected to a non-defect delineating etch, in order to remove surface residue and precipitants, by treating the sample with a bright etch solution for about 8 to about 12 minutes. A

typical bright etch solution comprises about 55 percent nitric acid (70% solution by weight), about 20 percent hydrofluoric acid (49% solution by weight), and about 25 percent hydrochloric acid (concentrated solution).

The sample is then rinsed with deionized water and subjected to a second etching step by immersing the sample in, or treating it with, a Secco or Wright etch solution for about 35 to about 55 minutes. Typically, the sample will be etched using a Secco etch solution comprising about a 1:2 ratio of 0.15 M potassium dichromate and hydrofluoric acid (49% solution by weight). This etching step acts to reveal, or delineate, agglomerated defects which may be present.

Definitions

As used herein, the following phrases or terms shall have the given meanings: "agglomerated intrinsic point defects" mean defects caused (i) by the reaction in which vacancies agglomerate to produce D-defects, flow pattern defects, gate oxide integrity defects, crystal originated particle defects, crystal originated light point defects, and other such vacancy related defects, or (ii) by the reaction in which self-interstitials agglomerate to produce dislocation loops and networks, and other such self-interstitial related defects; "agglomerated interstitial defects" shall mean agglomerated intrinsic point defects caused by the reaction in which silicon self-interstitial atoms agglomerate; "agglomerated vacancy defects" shall mean agglomerated vacancy point defects caused by the reaction in which crystal lattice vacancies agglomerate; "radius" means the distance measured from a central axis to a circumferential edge of a wafer or ingot; "substantially free of agglomerated intrinsic point defects" shall mean a concentration of agglomerated defects which is less than the detection limit of these defects, which is currently about 10^3

defects/cm^3; "V/I boundary" means the position along the radius of an ingot or wafer at which the material changes from vacancy dominated to self-interstitial dominated; and "vacancy dominated" and "self-interstitial dominated" mean material in which the intrinsic point defects are predominantly vacancies or self-interstitials, respectively.

Examples

The following examples illustrate the above process for preparing a single crystal silicon ingot in which, as the ingot cools from the solidification temperature in accordance with the Czochralski method, the agglomeration of intrinsic point defects is prevented within an axially symmetric region of the constant diameter portion of the ingot, from which wafers may be sliced.

The following examples set forth one set of conditions that may be used to achieve the desired result. Alternative approaches exist for determining an optimum pull rate profile for a given crystal puller. For example, rather than growing a series of ingots at various pull rates, a single crystal could be grown at pull rates which increase and decrease along the length of the crystal; in this approach, agglomerated self-interstitial defects would be caused to appear and disappear multiple times during growth of a single crystal. Optimal pull rates could then be determined for a number of different crystal positions. Accordingly, the following examples should not be interpreted in a limiting sense.

Example 1

Optimization Procedure For A Crystal Puller Having A Pre-existing Hot Zone Design

A first 200 mm single crystal silicon ingot was grown under conditions in which the pull rate was ramped linearly from about 0.75 mm/min. to about 0.35 mm/min. over the length of the crystal. Fig. 14 shows the pull rate as a function of crystal length. Taking into account the pre-established axial temperature profile of a growing 200 mm ingot in the crystal puller and the pre-established radial variations in the average axial temperature gradient, G_0, i.e., the axial temperature gradient at the melt/solid interface, these pull rates were selected to insure that ingot would be vacancy dominated material from the center to the edge at one end of the ingot and interstitial dominated material from the center to the edge of the other end of the ingot. The grown ingot was sliced longitudinally and analyzed to determine where the formation of agglomerated interstitial defects begins.

Fig. 15 is an image produced by a scan of the minority carrier lifetime of an axial cut of the ingot over a section ranging from about 635 mm to about 760 mm from the shoulder of the ingot following a series of oxygen precipitation heat-treatments which reveal defect distribution patterns. At a crystal position of about 680 mm, a band of agglomerated interstitial defects 28 can be seen. This position corresponds to a critical pull rate of $v^*(680\ mm) = 0.33$ mm/min. At this point, the width of the axially symmetric region 6 (a region which is interstitial dominated material but which lacks agglomerated interstitial defects) is at its maximum; the width of the vacancy dominated region 8, $R_v^*(680)$ is about 35 mm and the width of the axially symmetric region, $R_i^*(680)$ is about 65 mm.

A series of four single crystal silicon ingots were then grown at steady state pull rates which were somewhat greater than and somewhat less than the pull rate at which the maximum width of the axially symmetric region of the first 200 mm ingot was obtained. Fig. 16 shows the pull rate as a function of crystal length for each of the four crystals, labeled, respectively, as 1-4. These four crystals were then analyzed to determine the axial position (and corresponding pull rate) at which agglomerated interstitial defects first appear or disappear. These four empirically determined points (marked "*") are shown in Fig. 16. Interpolation between and extrapolation from these points yielded a curve, labeled $v^*(Z)$ in Fig. 16. This curve represents, to a first approximation, the pull rate for 200 mm crystals as a function of length in the crystal puller at which the axially symmetric region is at its maximum width.

Growth of additional crystals at other pull rates and further analysis of these crystals would further refine the empirical definition of $v^*(Z)$.

Example 2

Reduction of Radial Variation in $G_0(r)$

Figs. 17 and 18 illustrate the improvement in quality that can be achieved by reduction of the radial variation in the axial temperature gradient at the melt/solid interface, $G_0(r)$. The initial concentration (about 1 cm from the melt/solid interface) of vacancies and interstitials are calculated for two cases with different $G_0(r)$: (1) $G_0(r) = 2.65 + 5\times10^{-4}r^2$ (K/mm) and (2) $G_0(r) = 2.65 + 5\times10^{-5}r^2$ (K/mm). For each case the pull rate was adjusted such that the boundary between vacancy-rich silicon and interstitial-rich silicon is at a radius of 3 cm. The pull rate used for case 1 and 2 were 0.4 and 0.35 mm/min, respectively. From Fig. 18 it is clear that the initial concentration of interstitials in the

interstitial-rich portion of the crystal is dramatically reduced as the radial variation in the initial axial temperature gradient is reduced. This leads to an improvement in the quality of the material since it becomes easier to avoid the formation of interstitial defect clusters due to supersaturation of interstitials.

Example 3

Increased Out-diffusion Time for Interstitials

Figs. 19 and 20 illustrate the improvement in quality that can be achieved by increasing the time for out-diffusion of interstitials. The concentration of interstitials is calculated for two cases with differing axial temperature profiles in the crystal, dT/dz. The axial temperature gradient at the melt/solid interface is the same for both cases, so that the initial concentration (about 1 cm from the melt/solid interface) of interstitials is the same for both cases. In this example, the pull rate was adjusted such that the entire crystal is interstitial-rich. The pull rate was the same for both cases, 0.32 mm/min. The longer time for interstitial out-diffusion in case 2 results in an overall reduction of the interstitial concentration. This leads to an improvement in the quality of the material since it becomes easier to avoid the formation of interstitial defect clusters due to supersaturation of interstitials.

Example 4

A 700 mm long, 150 mm diameter crystal was grown with a varying pull rate. The pull rate varied nearly linearly from about 1.2 mm/min at the shoulder to about 0.4 mm/min at 430 mm from the shoulder, and then nearly linearly back to about 0.65 mm/min at 700 mm from the shoulder. Under these conditions in this particular crystal puller, the entire radius is grown under

interstitial-rich conditions over the length of crystal ranging from about 320 mm to about 525 mm from the shoulder of the crystal. Referring now to Fig. 21, at an axial position of about 525 mm and a pull rate of about 0.47 mm/min, the crystal is free of agglomerated intrinsic point defects clusters across the entire diameter. Stated another way, there is one small section of the crystal in which the width of the axially symmetric region, i.e., the region which is substantially free of agglomerated defects, is equal to the radius of the ingot.

EXAMPLE 5

As described in Example 1, a series of single crystal silicon ingots were grown at varying pull rates and then analyzed to determine the axial position (and corresponding pull rate) at which agglomerated interstitial defects first appeared or disappeared. Interpolation between and extrapolation from these points, plotted on a graph of pull rate v. axial position, yielded a curve which represents, to a first approximation, the pull rate for a 200 mm crystal as a function of length in the crystal puller at which the axially symmetric region is at its maximum width. Additional crystals were then grown at other pull rates and further analysis of these crystals was used to refine this empirically determined optimum pull rate profile.

Using this data and following this optimum pull rate profile, a crystal of about 1000 mm in length and about 200 mm in diameter was grown. Slices of the grown crystal, obtained from various axial position, were then analyzed using oxygen precipitation methods standard in the art in order to (i) determine if agglomerated interstitial defects were formed, and (ii) determine, as

a function of the radius of the slice, the position of the V/I boundary. In this way the presence of an axially symmetric region was determined, as well as the width of this region a function of crystal length or position.

The results obtained for axial positions ranging from about 200 mm to about 950 mm from the shoulder of the ingot are present in the graph of Fig. 22. These results show that a pull rate profile may be determined for the growth of a single crystal silicon ingot such that the constant diameter portion of the ingot may contain an axially symmetric region having a width, as measured from the circumferential edge radially toward the central axis of the ingot, which is at least about 40% the length of the radius of the constant diameter portion. In addition, these results show that this axially symmetric region may have a length, as measured along the central axis of the ingot, which is about 75% of the length of the constant diameter portion of the ingot.

Example 6

A single crystal silicon ingot having a length of about 1100 mm and a diameter of about 150 mm was grown with a decreasing pull rate. The pull rate at the shoulder of the constant diameter portion of the ingot was about 1 mm/min.. The pull rate decreased exponentially to about 0.4 mm/min., which corresponded to an axial position of about 200 mm from the shoulder. The pull rate then decreased linearly until a rate of about 0.3 mm/min. was reached near the end of the constant diameter portion of the ingot.

Under these process conditions in this particular hot zone configuration, the resulting ingot contains a region wherein the axially symmetric region has a width which about equal to the radius of the ingot. Referring now to Figs. 23a and 23b, which are images produced by a

scan of the minority carrier lifetime of an axial cut of a portion of the ingot following a series of oxygen precipitation heat treatments, consecutive segments of the ingot, ranging in axial position from about 100 mm to about 250 mm and about 250 mm to about 400 mm are present. It can be seen from these figures that a region exists within the ingot, ranging in axial position from about 170 mm to about 290 mm from the shoulder, which is free of agglomerated intrinsic point defects across the entire diameter. Stated another way, a region is present within the ingot wherein the width of the axially symmetric region, i.e., the region which is substantially free of agglomerated interstitial defects, is about equal to the radius of the ingot.

In addition, in a region ranging from an axially position from about 125 mm to about 170 mm and from about 290 mm to greater than 400 mm there are axially symmetric regions of interstitial dominated material free of agglomerated intrinsic point defects surrounding a generally cylindrical core of vacancy dominated material which is also free of agglomerated intrinsic point defects.

Finally, in a region ranging axially from about 100 mm to about 125 mm there is an axially symmetric region of interstitial dominated material free of agglomerated defects surrounding a generally cylindrical core of vacancy dominated material. Within the vacancy dominated material, there is an axially symmetric region which is free of agglomerated defects surrounding a core containing agglomerated vacancy defects.

Example 7

Cooling Rate and Position of V/I Boundary

A series of single crystal silicon ingots (150 mm and 200 mm nominal diameter), were grown in accordance with the Czochralski method using different hot zone configurations which affected the residence time of the silicon at temperatures in excess of about 1050°C. The pull rate profile for each ingot was varied along the length of the ingot in an attempt to create a transition from a region of agglomerated vacancy point defects to a region of agglomerated interstitial point defects.

Once grown, the ingots were cut longitudinally along the central axis running parallel to the direction of growth, and then further divided into sections which were each about 2 mm in thickness. Using the copper decoration technique previously described, one set of such longitudinal sections was then heated and intentionally contaminated with copper, the heating conditions being appropriate for the dissolution of a high concentration of copper interstitials. Following this heat treatment, the samples were then rapidly cooled, during which time the copper impurities either outdiffused or precipitated at sites where oxide clusters or agglomerated interstitial defects where present. After a standard defect delineating etch, the samples were visually inspected for the presence of precipitated impurities; those regions which were free of such precipitated impurities corresponded to regions which were free of agglomerated interstitial defects.

Another set of the longitudinal sections was subjected to a series of oxygen precipitation heat treatments in order to cause the nucleation and growth of new oxide clusters prior to carrier lifetime mapping. Contrast bands in lifetime mapping were utilized in order to determine and measure the shape of the instantaneous melt/solid interface at various axial positions in each

ingot. Information on the shape of the melt/solid interface was then used, as discussed further below, to estimate the absolute value of, and the radial variation in, the average axial temperature gradient, G_0. This information was also used, in conjunction with the pull rate, to estimate the radial variation in v/G_0.

To more closely examine the effect growth conditions have on the resulting quality of a single crystal silicon ingot, several assumptions were made which, based on experimental evidence available to-date, are believed to be justified. First, in order to simplify the treatment of thermal history in terms of the time taken to cool to a temperature at which the agglomeration of interstitial defects occurs, it was assumed that about 1050°C is a reasonable approximation for the temperature at which the agglomeration of silicon self-interstitials occurs. This temperature appears to coincide with changes in agglomerated interstitial defect density observed during experiments in which different cooling rates were employed. Although, as noted above, whether agglomeration occurs is also a factor of the concentration of interstitials, it is believed that agglomeration will not occur at temperatures above about 1050°C because, given the range of interstitial concentrations typical for Czochralski-type growth processes, it is reasonable to assume that the system will not become critically supersaturated with interstitials above this temperature. Stated another way, for concentrations of interstitials which are typical for Czochralski-type growth processes, it is reasonable to assume that the system will not become critically supersaturated, and therefore an agglomeration event will not occur, above a temperature of about 1050°C.

The second assumption that was made to parameterize the effect of growth conditions on the quality of single crystal silicon is that the temperature dependence of silicon self-interstitial diffusivity is negligible. Stated another way, it is assumed that self-interstitials diffuse at the same rate at all temperatures between about 1400°C and about 1050°C. Understanding that about 1050°C is considered a reasonable approximation for the temperature of agglomeration, the essential point of this assumption is that the details of the cooling curve from the melting point does not matter. The diffusion distance depends only on the total time spent cooling from the melting point to about 1050°C.

Using the axial temperature profile data for each hot zone design and the actual pull rate profile for a particular ingot, the total cooling time from about 1400°C to about 1050°C may be calculated. It should be noted that the rate at which the temperature changes for each of the hot zones was reasonably uniform. This uniformity means that any error in the selection of a temperature of nucleation for agglomerated interstitial defects, i.e. about 1050°C, will arguably lead only to scaled errors in the calculated cooling time.

In order to determine the radial extent of the vacancy dominated region of the ingot ($R_{vacancy}$), or alternatively the width of the axially symmetric region, it was further assumed that the radius of the vacancy dominated core, as determined by the lifetime map, is equivalent to the point at solidification where $v/G_0=v/G_0$ critical. Stated another way, the width of the axially symmetric region was generally assumed to be based on the position of the V/I boundary after cooling to room temperature. This is pointed out because, as mentioned above, as the ingot cools recombination of vacancies and

silicon self-interstitials may occur. When recombination does occur, the actual position of the V/I boundary shifts inwardly toward the central axis of the ingot. It is this final position which is being referred to here.

To simplify the calculation of G_0, the average axial temperature gradient in the crystal at the time of solidification, the melt/solid interface shape was assumed to be the melting point isotherm. The crystal surface temperatures were calculated using finite element modeling (FEA) techniques and the details of the hot zone design. The entire temperature field within the crystal, and therefore G_0, was deduced by solving Laplace's equation with the proper boundary conditions, namely, the melting point along the melt/solid interface and the FEA results for the surface temperature along the axis of the crystal. The results obtained at various axial positions from one of the ingots prepared and evaluated are presented in Fig. 25.

To estimate the effect that radial variations in G_0 have on the initial interstitial concentration, a radial position R', that is, a position halfway between the V/I boundary and the crystal surface, was assumed to be the furthest point a silicon self-interstitial can be from a sink in the ingot, whether that sink be in the vacancy dominated region or on the crystal surface. By using the growth rate and the G_0 data for the above ingot, the difference between the calculated v/G_0 at the position R' and v/G_0 at the V/I boundary (i.e., the critical v/G_0 value) provides an indication of the radial variation in the initial interstitial concentration, as well as the effect this has on the ability for excess interstitials to reach a sink on the crystal surface or in the vacancy dominated region.

For this particular data set, it appears there is no systematic dependence of the quality of the crystal on the radial variation in v/G_0. As can be seen in Fig. 26, the axial dependence in the ingot is minimal in this sample. The growth conditions involved in this series of experiments represent a fairly narrow range in the radial variation of G_0. As a result, this data set is too narrow to resolve a discernable dependence of the quality (i.e., the presence of absence of a band of agglomerated intrinsic point defects) on the radial variation of G_0.

As noted, samples of each ingot prepared were evaluated at various axial positions for the present or absence of agglomerated interstitial defects. For each axial position examined, a correlation may be made between the quality of the sample and the width of the axially symmetric region. Referring now to Fig. 27, a graph may be prepared which compares the quality of the given sample to the time the sample, at that particular axial position, was allowed to cool from solidification to about 1050°C. As expected, this graph shows the width of the axially symmetric region (i.e., $R_{crystal} - R_{vacancy}$) has a strong dependence on the cooling history of the sample within this particular temperature range. In order of the width of the axially symmetric region to increase, the trend suggests that longer diffusion times, or slower cooling rates, are needed.

Based on the data present in this graph, a best fit line may be calculated which generally represents a transition in the quality of the silicon from "good" (i.e., defect-free) to "bad" (i.e., containing defects), as a function of the cooling time allowed for a given ingot diameter within this particular temperature range. This general relationship between the width of the

axially symmetric region and the cooling rate may be expressed in terms of the following equation:

$$(R_{crystal} - R_{transition})^2 = D_{eff} * t_{1050°C}$$

wherein

$R_{crystal}$ is the radius of the ingot,

$R_{transition}$ is the radius of the axially symmetric region at an axial position in the sample were a transition occurs in the interstitial dominated material from being defect-free to containing defects, or vice versa,

D_{eff} is a constant, about $9.3*10^{-4}$ cm^2sec^{-1}, which represents the average time and temperature of interstitial diffusivity, and

$t_{1050°C}$ is the time required for the given axial position of the sample to cool from solidification to about 1050°C.

Referring again to Fig. 27, it can be seen that, for a given ingot diameter, a cooling time may be estimated in order to obtain an axially symmetric region of a desired diameter. For example, for an ingot having a diameter of about 150 mm, an axially symmetric region having a width about equal to the radius of the ingot may be obtained if, between the temperature range of about 1410°C and about 1050°C, this particular portion of the ingot is allowed to cool for about 10 to about 15 hours. Similarly, for an ingot having a diameter of about 200 mm, an axially symmetric region having a width about equal to the radius of the ingot may be obtained if between this temperature range this particular portion of the ingot is allowed to cool for about 25 to about 35 hours. If this line is further extrapolated, cooling times of about 65 to about 75 hours may be needed in order to obtain an axially symmetric region having a width about equal to the radius of an ingot having a diameter of about 300 mm. It is to be noted in this regard that, as the diameter of the ingot increases,

additional cooling time is required due to the increase in distance that interstitials must diffuse in order to reach sinks at the ingot surface or the vacancy core.

Referring now to Figs. 28, 29, 30 and 31, the effects of increased cooling time for various ingots may be observed. Each of these figures depicts a portion of a ingot having a nominal diameter of 200 mm, with the cooling time from the temperature of solidification to 1050 °C progressively increasing from Fig. 28 to Fig. 31.

Referring to Fig. 28, a portion of an ingot, ranging in axial position from about 235 mm to about 350 mm from the shoulder, is shown. At an axial position of about 255 mm, the width of the axially symmetric region free of agglomerated interstitial defects is at a maximum, which is about 45% of the radius of the ingot. Beyond this position, a transition occurs from a region which is free of such defects, to a region in which such defects are present.

Referring now to Fig. 29, a portion of an ingot, ranging in axial position from about 305 mm to about 460 mm from the shoulder, is shown. At an axial position of about 360 mm, the width of the axially symmetric region free of agglomerated interstitial defects is at a maximum, which is about 65% of the radius of the ingot. Beyond this position, defect formation begins.

Referring now to Fig. 30, a portion of an ingot, ranging in axial position from about 140 mm to about 275 mm from the shoulder, is shown. At an axial position of about 210 mm, the width of the axially symmetric region is about equal to the radius of the ingot; that is, a small portion of the ingot within this range is free of agglomerated intrinsic point defects.

Referring now to Fig. 31, a portion of an ingot, ranging in axial position from about 600 mm to about 730 mm from the shoulder, is shown. Over an axial position ranging from about 640 mm to about 665 mm, the width of

the axially symmetric region is about equal to the radius of the ingot. In addition, the length of the ingot segment in which the width of the axially symmetric region is about equal to the radius of the ingot is greater than what is observed in connection with the ingot of Fig. 30.

When viewed in combination, therefore, Figs. 28, 29, 30, and 31 demonstrate the effect of cooling time to 1050 °C upon the width and the length of the defect-free, axially symmetric region. In general, the regions containing agglomerated interstitial defects occurred as a result of a continued decrease of the crystal pull rate leading to an initial interstitial concentration which was too large to reduce for the cooling time of that portion of the crystal. A greater length of the axially symmetric region means a larger range of pull rates (i.e., initial interstitial concentration) are available for the growth of such defect-free material. Increasing the cooling time allows for initially higher concentration of interstitials, as sufficient time for radial diffusion may be achieved to suppress the concentration below the critical concentration required for agglomeration of interstitial defects. Stated in other words, for longer cooling times, somewhat lower pull rates (and, therefore, higher initial interstitial concentrations) will still lead to maximum axially symmetric region 6. Therefore, longer cooling times lead to an increase in the allowable pull rate variation about the condition required for maximum axially symmetric region diameter and ease the restrictions on process control. As a result, the process for an axially symmetric region over large lengths of the ingot becomes easier.

Referring again to Fig. 31, over an axial position ranging from about 665 mm to greater than 730 mm from the shoulder of crystal, a region of vacancy dominated material free of agglomerated defects is present in which the width of the region is equal to the radius of the ingot.

Crystal Puller of the Present Invention

Referring now to Fig. 32, a crystal puller of the present invention for producing single crystal silicon ingots and wafers according to the above-described process which are devoid of agglomerated intrinsic point defects over a substantial portion of the ingot radius is generally indicated at 121. The crystal puller 121 is preferably of the type used to grow monocrystalline silicon ingots (e.g., ingot I of Fig. 32) according to the Czochralski method. The crystal puller 121 includes a housing (generally indicated at 125) comprising a generally cylindrical growth chamber 127, a generally cylindrical pull chamber 129 above the growth chamber wall, and a dome-shaped transition portion 132 interconnecting the growth chamber and pull chamber. The pull chamber 129 has a smaller transverse dimension than the growth chamber 127. A quartz crucible 131 disposed in the growth chamber 127 contains molten semiconductor source material M (e.g., silicon) from which the monocrystalline silicon ingot I is grown. The crucible 131 includes a cylindrical side wall 133 and is mounted on a turntable 135 for rotation about a vertical axis. The crucible 131 is also capable of being raised within the growth chamber 127 to maintain the surface of the molten source material M at the same level as the ingot I is grown and source material is removed from the melt.

A crucible heater, generally indicated at 137, for melting the source material M in the crucible 131 includes a generally vertically oriented heating element 139 surrounding the crucible in radially spaced relationship with the crucible side wall 33. The heating element 139 heats the crucible 131 to temperatures above the melting point of the source material M. Insulation 141 is positioned to confine the heat to the interior of the housing 125. In addition, there are passages in the housing 125, including at the upper pull chamber 129, for allowing circulation of cooling water. Some of these passages are designated by the reference numeral 143 in Fig. 32.

A pulling mechanism includes a pull shaft 145 extending down from a mechanism (not shown) above the pull chamber 129 capable of raising, lowering and rotating the pull shaft. The crystal puller 121 may have a pull wire (not shown) rather than a shaft 145, depending upon the type of puller. The pull shaft 145 terminates in a seed crystal chuck 147 which holds a seed crystal 149 used to grow the monocrystalline ingot I. The pull shaft 145 has been partially broken away in Fig. 32 for clarity in illustration of a raised position of the seed chuck 147 and ingot I. A view port 148 in the domed transition portion 132 of the housing 125 provides for viewing of the liquid/solid interface between the ingot I and the melt surface of the molten source material M by a conventional ingot diameter control device, such as a camera control device (not shown). A line of sight L from the view port 148 to the liquid/solid interface of the ingot I is indicated in dashed line in Fig. 32. The general construction and operation of the crystal puller 121, including the ingot

diameter control device is well known to those of ordinary skill in the art and will not be further described except to the extent explained more fully below.

An electrical resistance heater 123 for use in the crystal puller 121 of the present invention comprises a generally tubular heating element 151 mounted in the upper pull chamber 129 of the housing 125. A central opening 153 of the heating element 151 allows the growing ingot I to pass centrally through the heating element as it is pulled upward through the housing 125 of the puller 121. In the illustrated embodiment, the heating element 151 preferably extends downward a small distance into the crystal growth chamber 127, terminating substantially above the crucible 131 containing the molten source material M. More particularly, the bottom of the heating element 151 is spaced sufficiently above the melt surface so that the heating element does not obstruct the line of sight L of the ingot diameter control device via the view port 148. As an example, in a crystal puller used for growing ingots I having a diameter of 200mm, the heating element 151 of the heater preferably terminates approximately 300mm above the melt surface. It is understood that the heating element 151 need not extend down into growth chamber 127 at all, so that the entire heating element is disposed within the pull chamber 129, without departing from the scope of this invention.

The length of the heating element 151 is such that it extends upward within the pull chamber 129 to a predetermined height based on the desired amount of heat to be radiated to the growing ingot I and the axial portion of the ingot to which the heat is to be radiated. In general, as the length of the heating element 151 increases, the residence time of the ingot above 1050°C also increases. As an example, the heating element has a length preferably greater than about 300 mm. However, it

is contemplated that the heating element 151 may be sized to extend substantially the entire height of the pull chamber 129 so that the entire length of a fully grown ingot I extending within the pull chamber could be retained in the pull chamber at a temperature above 1050°C throughout its full growth period.

As shown in Fig. 2, the heating element 151 comprises vertically oriented heating segments 155 arranged in side-by-side relationship and connected to each other to form an electrical circuit. More particularly, upper and lower ends, designated 157 and 159, respectively, of adjacent heating segments 155 are alternatingly connected to each other in a continuous serpentine configuration forming a closed geometric shape; in the illustrated embodiment, a cylinder. Opposing mounting brackets 161 are connected to the top of the heating element 151 in electrical connection with the heating segments 155 and extend upward from the heating element for mounting the heater 123 on the housing 125 in the pull chamber 129. Openings (not shown) in the housing 125 allow the mounting brackets 161 to be electrically connected to a source of electrical current (not shown) by conventional electrodes (not shown) extending through the openings for connection with the mounting brackets to conduct current through the heating element 151. A tubular heat shield 163, preferably constructed of graphite, is disposed generally between the heating element 151 and the wall of the upper pull chamber 129 to inhibit cooling of the heating element by the housing 125.

The heating element 151 is constructed of a non-contaminating resistive heating material which provides resistance to the flow of electrical current therethrough; the power output generated by the heating element increasing with the electrical resistance of the material. A particularly preferred resistive heating

material is highly purified extruded graphite. However, the heating element 151 may be constructed of silicon carbide coated graphite, isomolded graphite, carbon fiber composite, tungsten, metal or other suitable materials without departing from the scope of this invention. It is also contemplated that the heating element 151 may be constructed of wire, such as tungsten or molybdenum wire, wrapped on a quartz tube to form a heating coil (not shown). The spacing between the coils may be varied to shape the power output profile of the heating element 151. The heating element 151 is preferably capable of radiating heat at a temperature in the range of 1000°C - 1100°C. It is understood, however, that heating elements capable of generating higher temperatures may be used and remain within the scope of this invention.

Figs. 34 and 35 illustrate alternative embodiments of the heater 123 in which the heating segments 155 of the heating element 151 are of varying lengths, with upper ends 157 of the segments being co-planar about the circumference of the heating element at the top of the heating element and lower ends 159 of the segments being staggered vertically with respect to each other because of the varying lengths of the segments. The lower ends 159 of the longest segments 165 define the bottom of the heating element 151. Varying the length of the heating segments in this manner provides a profiled heating power output along the height of the heating element 151; the heating power output increasing from the bottom to the top of the heating element for better profiling the cooling rate of the growing ingot I.

In a preferred method of construction of the heating element 151, vertically extending slots are cut into a tube (not shown) constructed of the resistive heating material to define the serpentine configuration. More particularly, downward extending slots 169 extend down from the top of the heating element 151 and terminate

short of the lower ends 159 of the segments 155, leaving adjacent segments connected to each other at the lower ends. Upward extending slots 171 extend up from the lower ends 159 of the segments 155 and terminate short of the top of the heating element 151, leaving adjacent segments connected to each other at the upper ends 157 of these segments. Alternating the downward and upward extending slots 169, 171 about the circumference of the heating element 151 creates the serpentine configuration of the heating element. Where the lengths of the heating segments 155 are non-uniform, such as in the embodiments of Figs. 34 and 35, portions of the tube (not shown) are cut away to generally define the stepped configuration of the lower ends 159 of the heating segments 155 prior to cutting the vertically extending slots 169, 171 in the tube.

In operation, polycrystalline silicon ("polysilicon") is deposited in the crucible 131 and melted by heat radiated from the crucible heater 137. The seed crystal 149 is brought into contact with the molten silicon M and a single crystal ingot I is grown by slow extraction via the pulling mechanism. The growing ingot I begins cooling immediately as it is pulled upward from the melt and continues to cool as it is pulled upward through the lower crystal growth chamber 127. As portions of the ingot I come into radial registration with the bottom of the heating element 151, heat is radiated by the heating element to these portions of the ingot to reduce the rate of further cooling.

By radiating heat to the ingot I at a temperature of at least 1000°C - 1100°C, the rate of cooling of the ingot between the solidification temperature (e.g., above 1400°C) and 1050°C is substantially reduced, thereby increasing the time during which the ingot resides at a temperature exceeding 1050°C. As portions of the ingot remain at temperatures above 1050°C for relatively long

time durations, radial diffusion of self-interstitials occurs to suppress the concentration below the critical concentration required for agglomeration of interstitial defects. As such, an ingot is produced in which a substantial radial portion of the ingot is self-interstitial dominated and devoid of agglomerated intrinsic point defects. As discussed above, the longer the ingot temperature resides above 1050°C, the radial portion of the ingot devoid of agglomerated intrinsic point defects increases.

As an example, a finite element model analysis was conducted to simulate the growth of three monocrystalline silicon ingots I, each having a diameter of 200mm, according to the Czochralski method in a crystal puller 121 of the type described above. Each of the ingots was grown at a pull rate of 0.3 mm/minute. Growth of the first ingot I was simulated without the heater 123 in the upper pull chamber 129 of the puller housing 125. An electrical resistance heater 123 such as that described above was modeled to simulate the growth of the second ingot I. The heater 123 had a length of about 350mm, extending down into the growth chamber 127 to a height of 493mm above the melt surface. The third ingot I was grown in a crystal puller 121 including a substantially longer heater 123; having a length of about 500mm and extending down into the growth chamber 127 to a height of 493mm above the melt surface.

With reference to Figs. 36, 37 and 38, the temperature of the ingot and various structure in the housing was recorded and isotherms were plotted to indicate the cooling pattern of the ingots. In each of the Figures, the temperatures given are in °K. None of the isotherms translate directly to 1050°C. However, for

comparison purposes, the approximate position of the 1050°C isotherm would be located between the isotherms indicated as legend numbers 10 and 11 as indicated by the dashed line in each of the Figures.

In Fig. 36 (corresponding to the ingot grown without the additional heater in the upper pull chamber) the isotherm representing 1050°C is spaced about 250 mm above the melt surface, indicating rapid cooling of the ingot. For the pull rate of 0.3 mm/min, this represents a residence time above 1050°C of approximately 14 hours.

When the heater 121 is used in the second growth simulation, as shown in Fig. 37, the isotherm representing 1050°C is spaced above the melt surface more than 600 mm. At a pull rate of 0.3 mm/min., the temperature of the growing ingot would reside above 1050° for a time period of more than 33 hours. As discussed above with respect to Example 7, this time period is within the range desired for producing an ingot in which the ingot is devoid of agglomerated intrinsic point defects substantially along the entire radius of the ingot. As seen in Fig. 38, increasing the length of the heater further increases the height of the 1050°C isotherm above the melt surface to about 900 mm, resulting in an ingot residence time above 1050°C of about 50 hours. Fig. 39 is a plot comparing the axial temperature profile of the three ingots produced in the finite element analyses.

It will be observed from the foregoing that the crystal puller described herein satisfies the various objectives of the present invention and attains other advantageous results. The heater 123 having a heating element 151 mounted and extending within the upper pull chamber is adequately sized to radiate heat along a sufficient axial portion of the growing ingot to substantially reduce the cooling rate of the ingot and increase the time during which the ingot temperature

resides above 1050°C. More particularly, the heating element 151 may be sized such that the time during which the ingot I resides above 1050°C is sufficiently long whereby the ingot is devoid of agglomerated intrinsic point defects along substantially the entire radius of the ingot. Increasing the length of the heating element 151 may also allow for the pull rate of the crystal to be increased (but remain within the range of rates in which interstitial dominated silicon is grown) to improve production capacity.

Importantly, by mounting and extending the heater 123 within the upper pull chamber 129 of the housing 125, the heating element 151 can be sized to its desired length without taking up substantial space in the lower growth chamber 127. This allows the heater 123 to be mounted in conventional crystal pullers without requiring additional space within the growth chamber 127 and without obstructing the line of sight from the view port 148 to the liquid/solid interface. The size limitations associated with the lack of space in the growth chamber of the housing are thus overcome.

As various changes could be made in the above constructions without departing from the scope of the invention, it is intended that all matter contained in the above description or shown in the accompanying drawings shall be interpreted as illustrative and not in a limiting sense.

WHAT IS CLAIMED IS:

1. A crystal puller for growing monocrystalline silicon ingots according to the Czochralski method which are devoid of agglomerated intrinsic point defects over a substantial portion of the radius of the ingot, the crystal puller comprising:

a housing defining an interior having a lower growth chamber and an upper pull chamber, the pull chamber having a smaller transverse dimension than the growth chamber;

a crucible in the growth chamber of the housing for containing molten silicon;

a pulling mechanism for pulling a growing ingot upward from the molten silicon through the growth chamber and pull chamber; and

an electrical resistance heater comprising a heating element sized and shaped for being disposed at least partially within the upper pull chamber of the housing in radially spaced relationship with the outer surface of the growing ingot for radiating heat to the ingot as it is pulled upward in the pull chamber relative to the molten silicon, the heating element having an upper end and a lower end, the lower end of the heating element being disposed substantially closer to the molten silicon than the upper end when the heating element is placed in the housing.

2. A crystal puller as set forth in claim 1 wherein the heating element extends down into the lower growth chamber of the housing.

3. A crystal puller as set forth in claim 2 further comprising a port in the housing for viewing the growing ingot from outside the housing while the ingot is being pulled upward from the molten silicon, the lower end of the heating element being at a height above the molten silicon such that viewing of the growing ingot in the interior of the growth chamber via the port in the housing is substantially unobstructed by the heating element.

4. A crystal puller as set forth in claim 1 wherein the housing comprises a pull chamber side wall defining the upper pull chamber, the heating element being mounted on the upper pull chamber wall within the upper pull chamber of the housing.

5. A crystal puller as set forth in claim 4 wherein the heating element includes first and second vertically oriented heating segments arranged in a generally side-by-side relationship and being electrically connected together, and first and second mounting brackets electrically connected to the respective heating segments, said mounting brackets being adapted for mounting the heating element on the housing within the upper pull chamber of the housing in electrical connection with a source of electrical current.

6. A crystal puller as set forth in claim 5 wherein the heating element is constructed such that the heating power output generated by the heating element gradually increases from the lower end to the upper end of the heating element.

7. A crystal puller as set forth in claim 6 wherein the first and second segments each have an upper end and a lower end, the second segment having a length substantially greater than the first segment and being arranged relative to the first segment so that when the heating element is placed in the housing the lower end of the second segment is disposed closer to the molten silicon in the crucible than the lower end of the first segment.

8. A crystal puller as set forth in claim 1 adapted for growing silicon ingots having a diameter of about 200mm, the heating element being sized to radiate sufficient heat to the growing ingot whereby the temperature of the ingot resides above 1050°C for a time period exceeding 25 hours.

9. A crystal puller as set forth in claim 8 in which the heating element is sized to radiate sufficient heat to the growing ingot whereby the temperature of the ingot resides above 1050°C for a time period exceeding 35 hours.

10. A crystal puller as set forth in claim 9 in which the heating element is sized to radiate sufficient heat to the growing ingot whereby the temperature of the ingot resides above 1050°C for a time period equal to or greater than about 50 hours.

FIG. 1

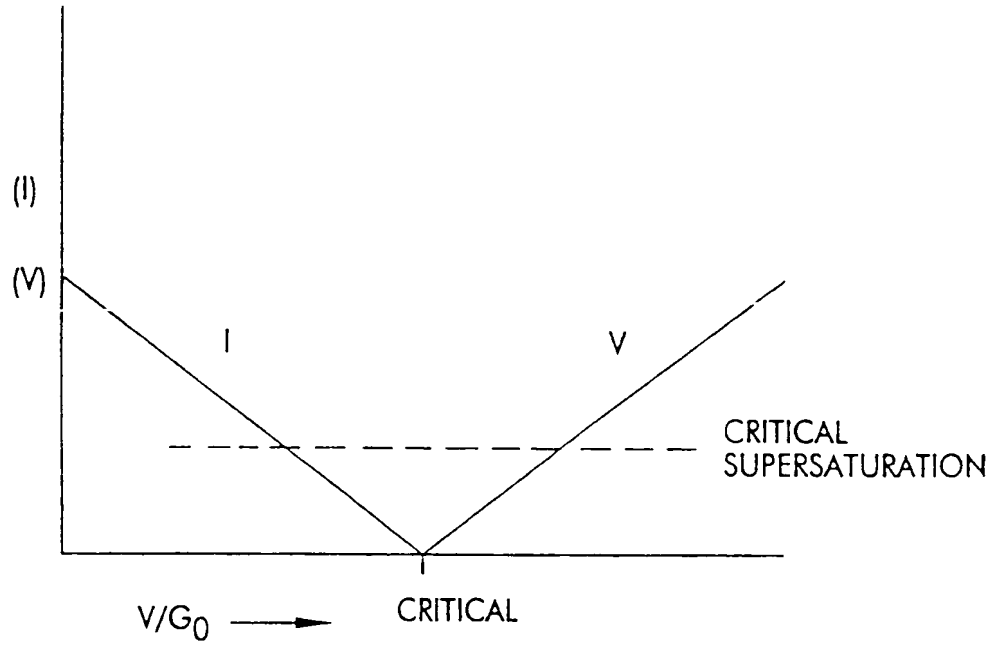

FIG. 2

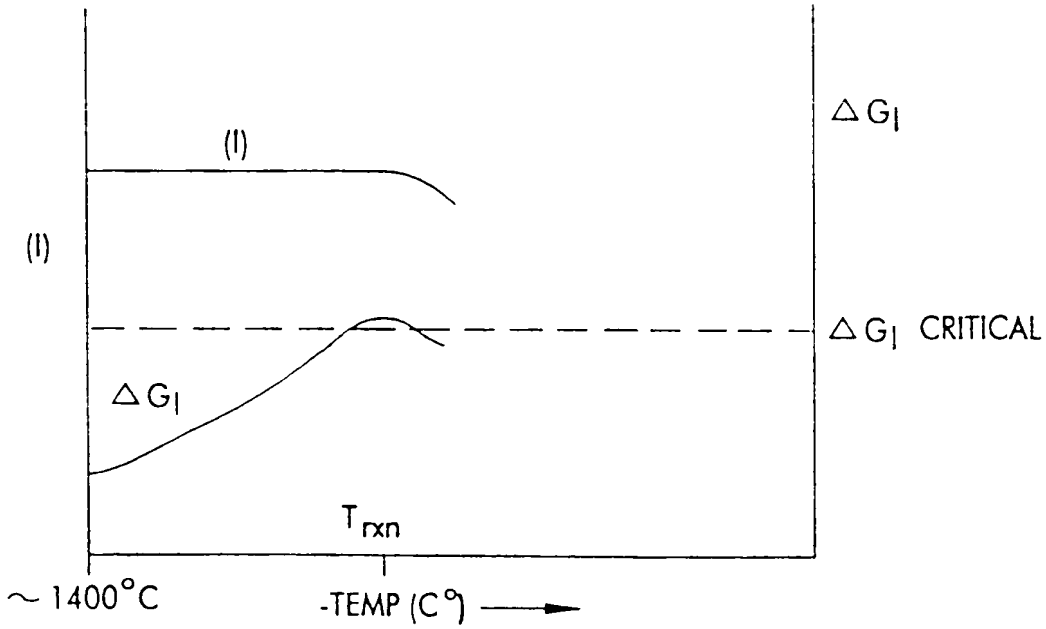

FIG. 3

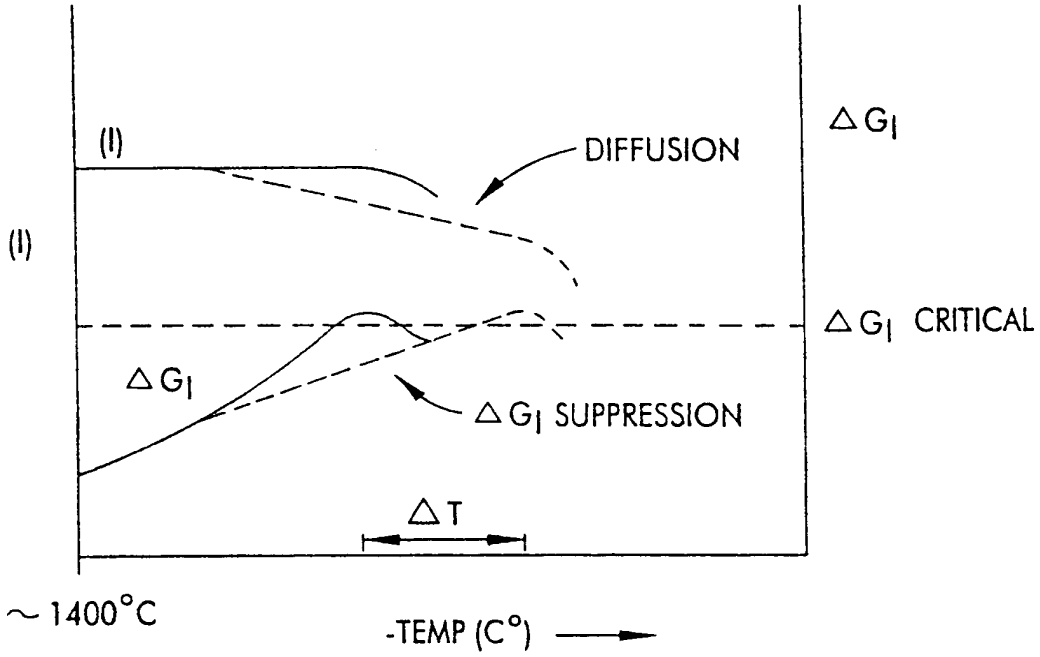

FIG. 4

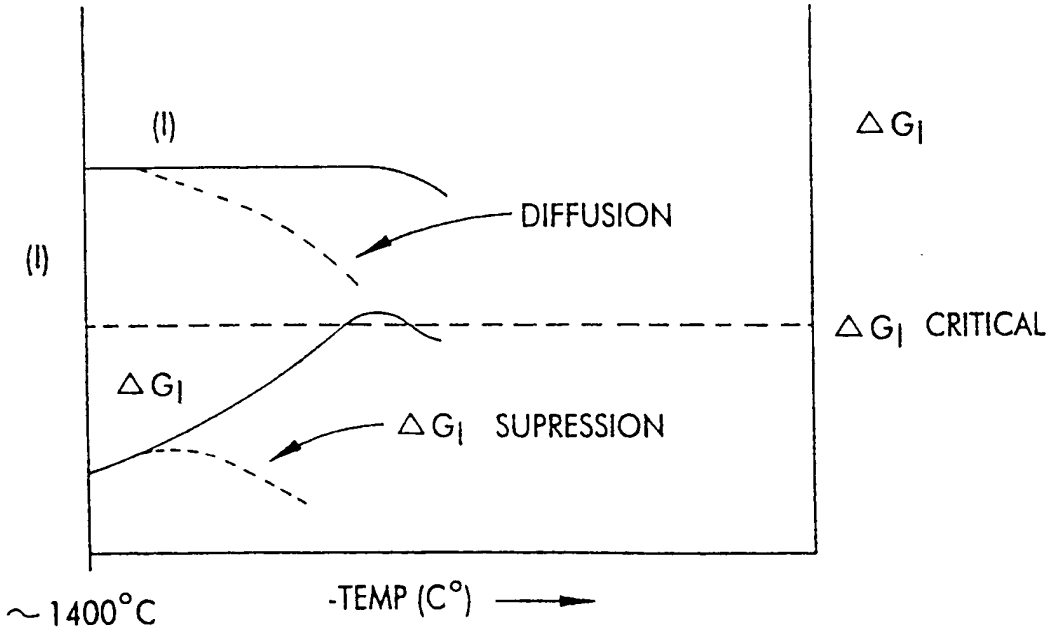

FIG. 5

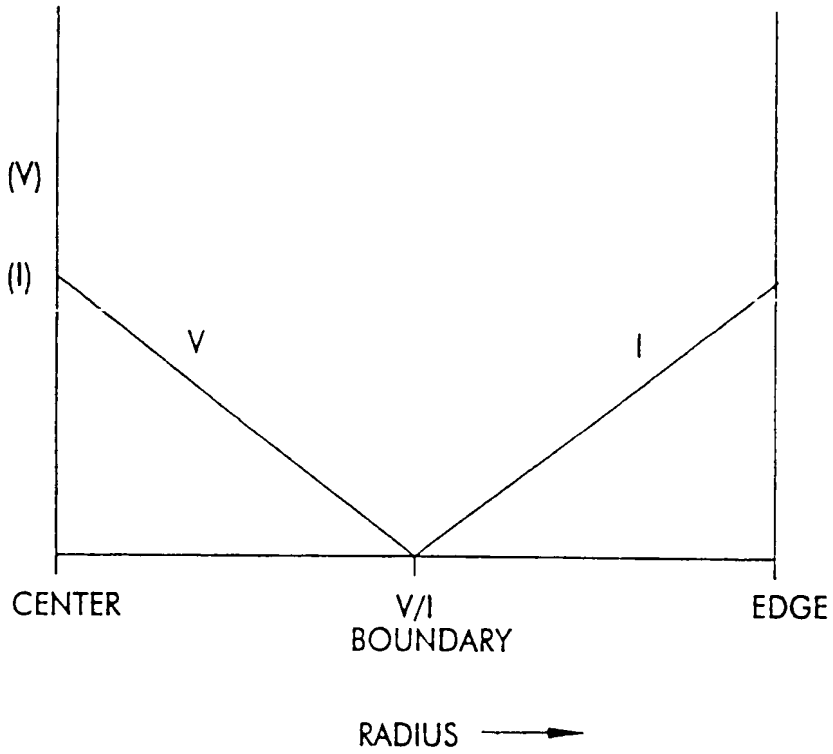

FIG. 6

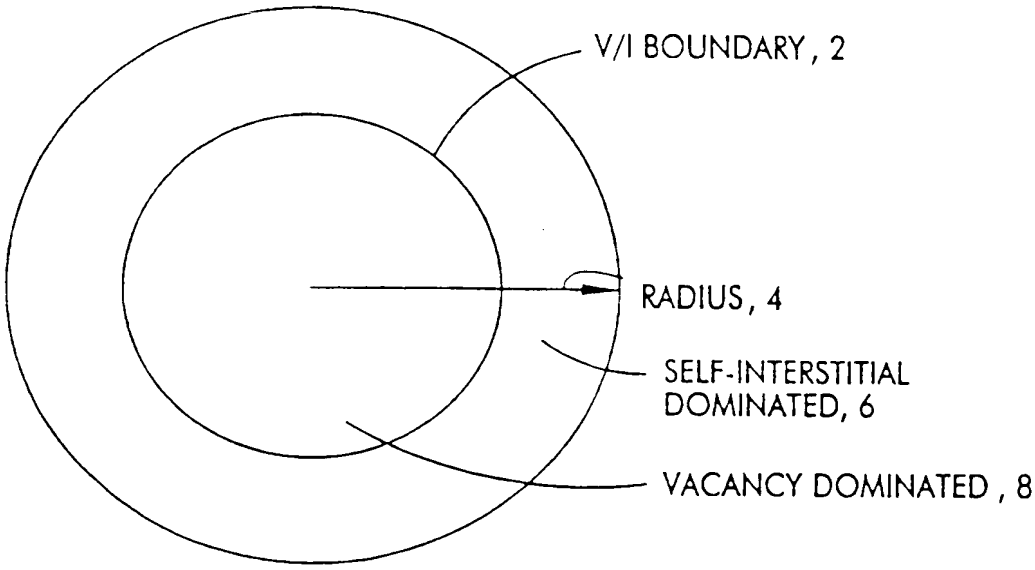

FIG. 7A

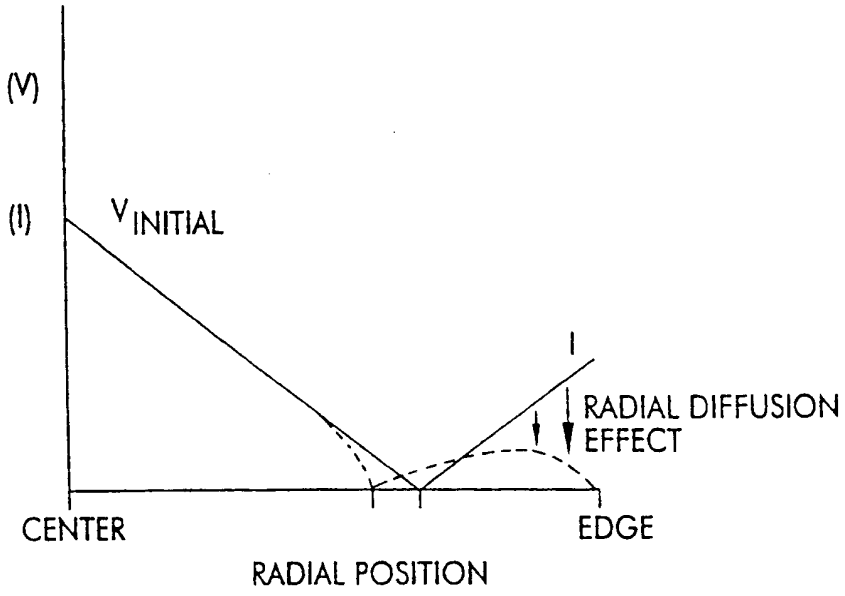

FIG. 7B

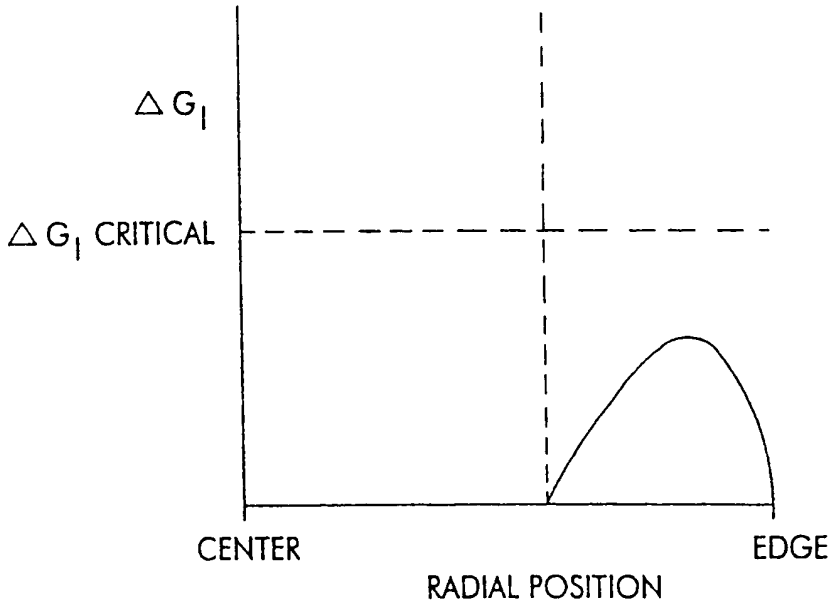

FIG. 7C

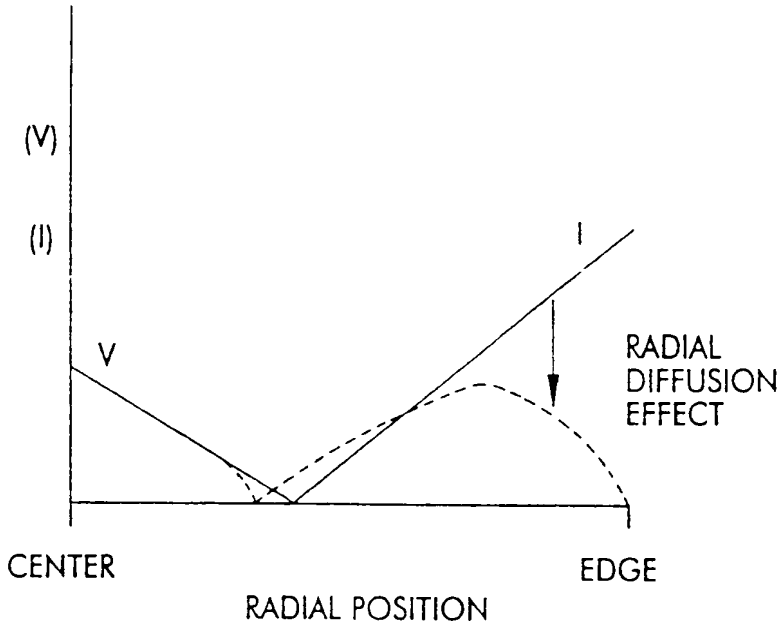

FIG. 7D

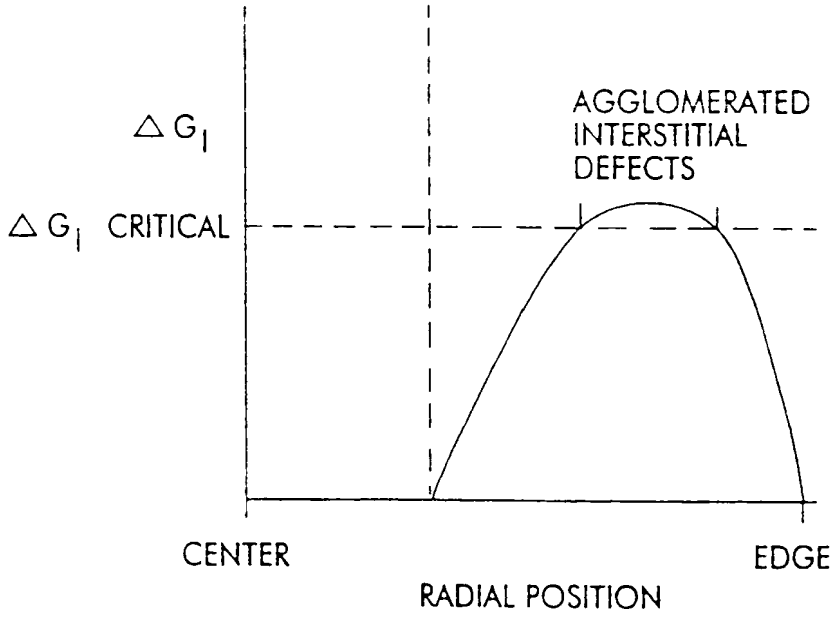

FIG. 7E

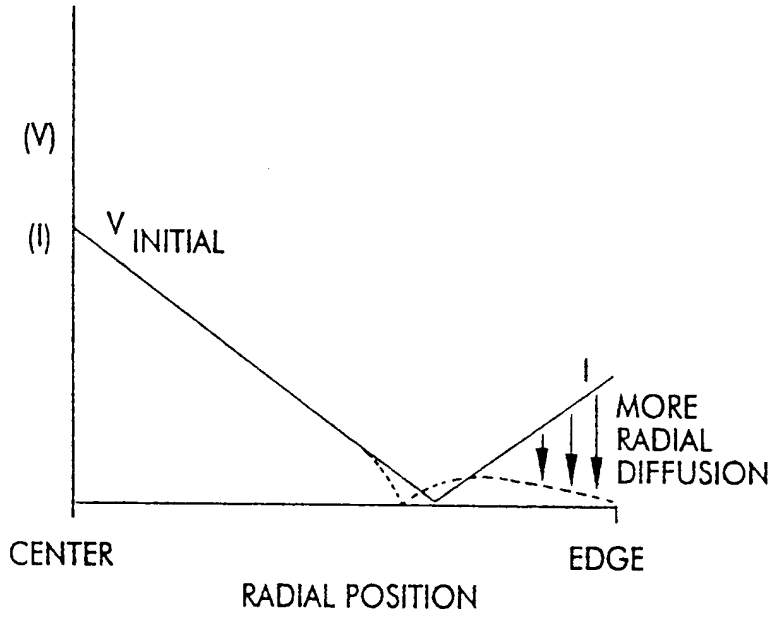

FIG. 7F

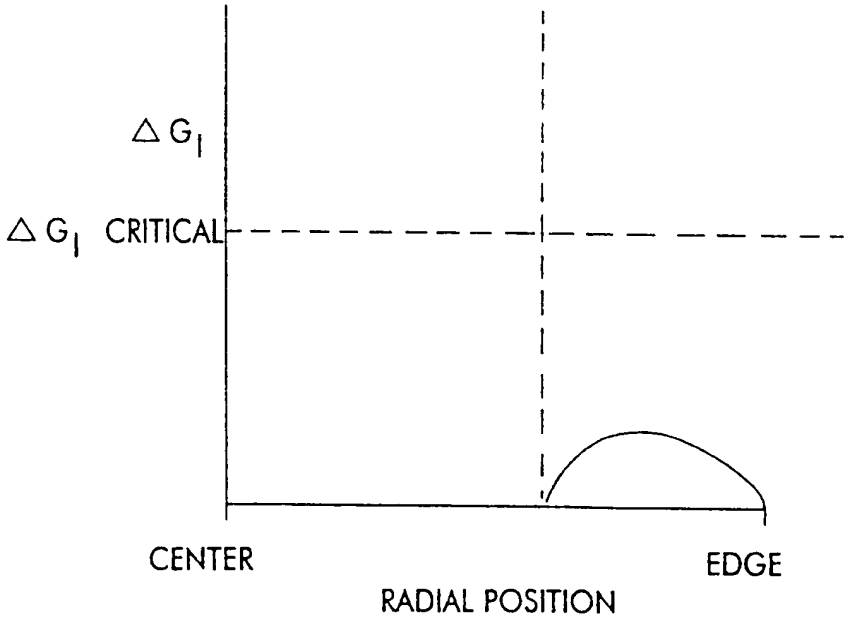

FIG. 7G

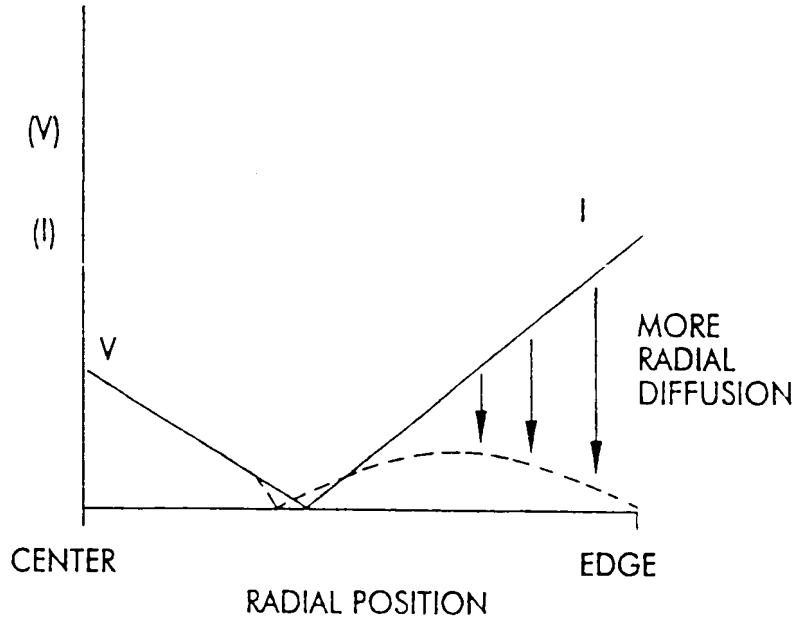

FIG. 7H

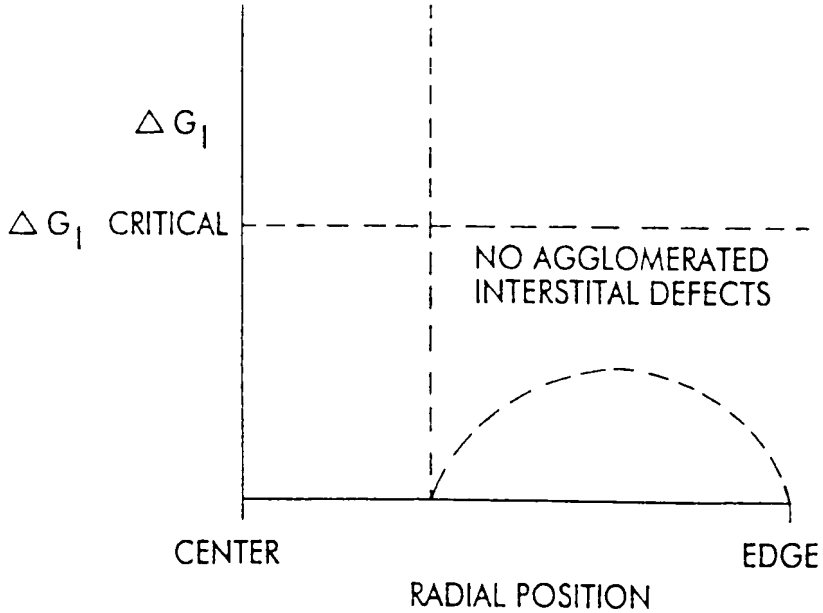

FIG. 7I

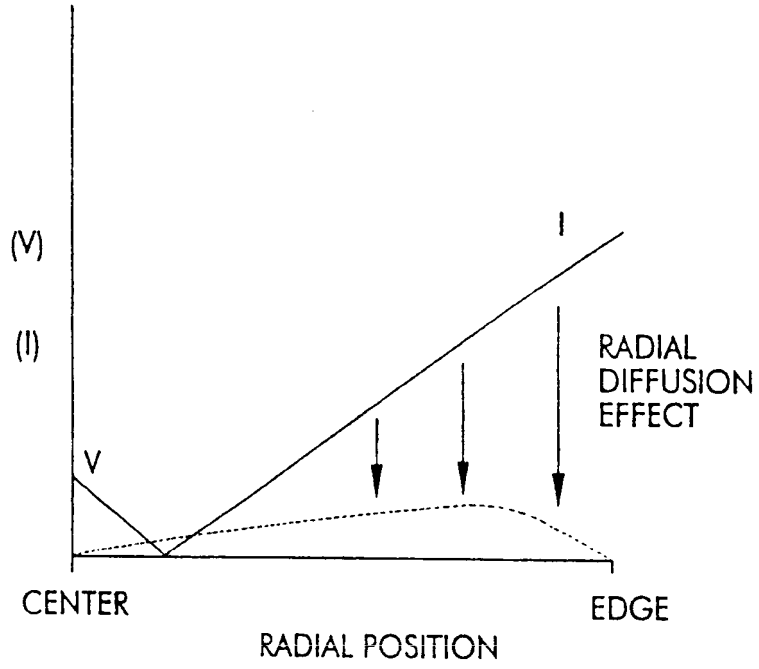

FIG. 7J

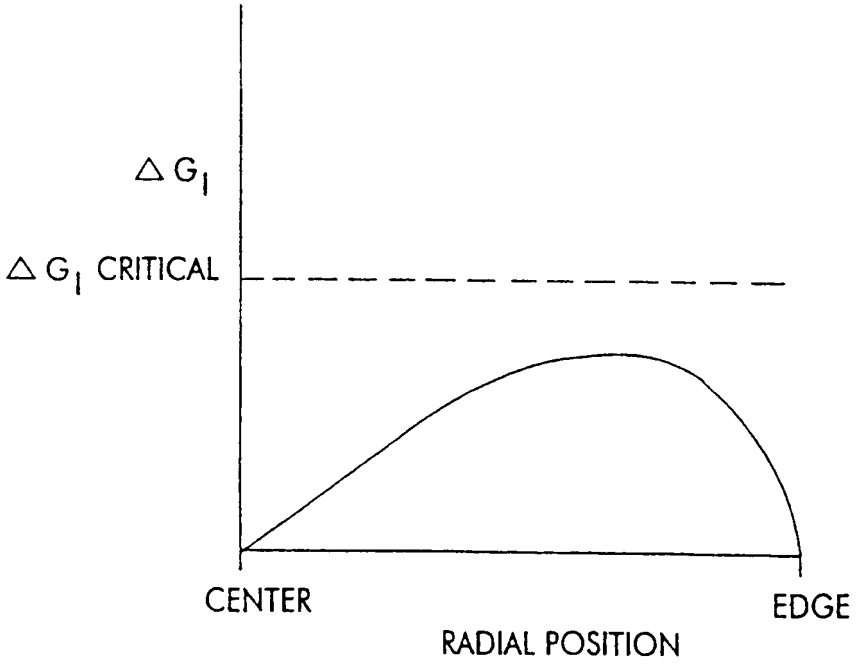

FIG. 8

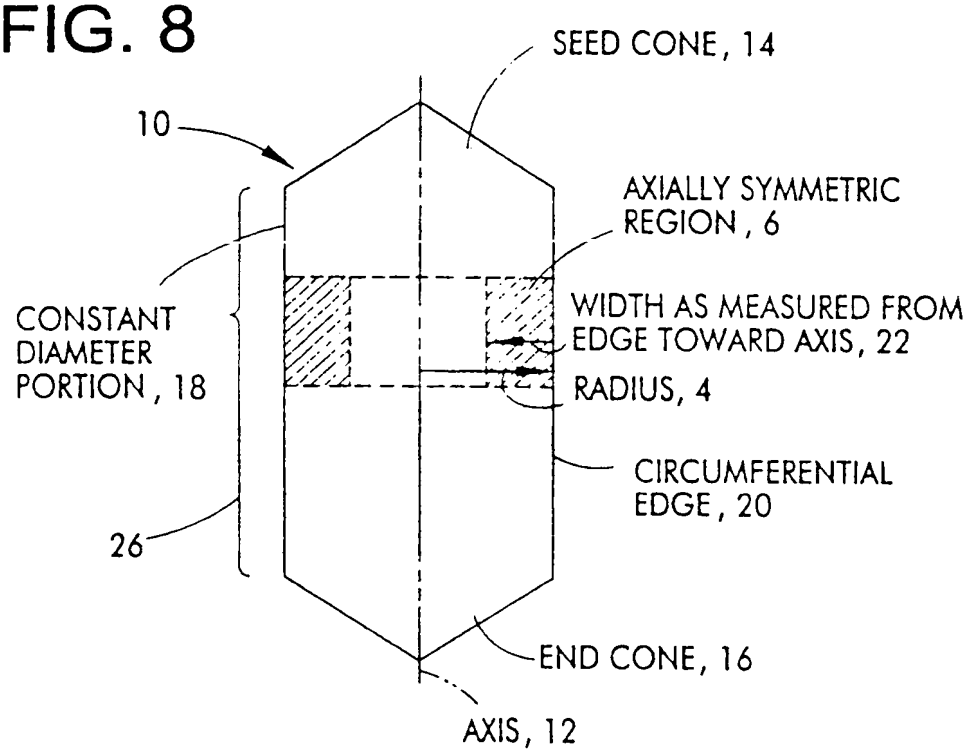

FIG. 9

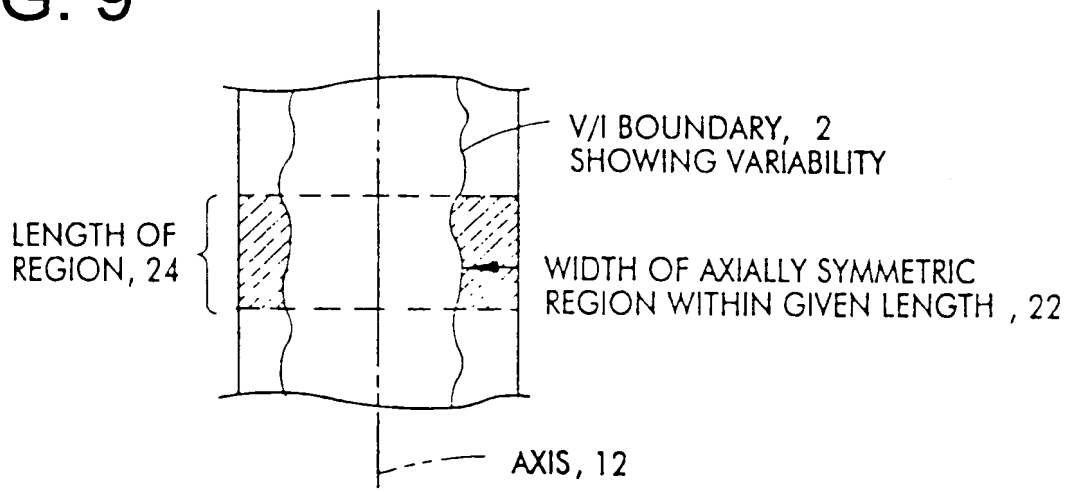

FIG. 10

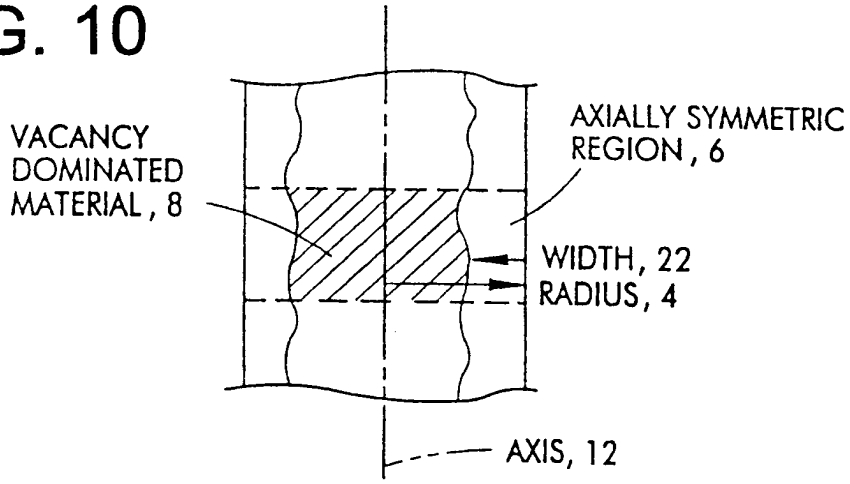

FIG. 11

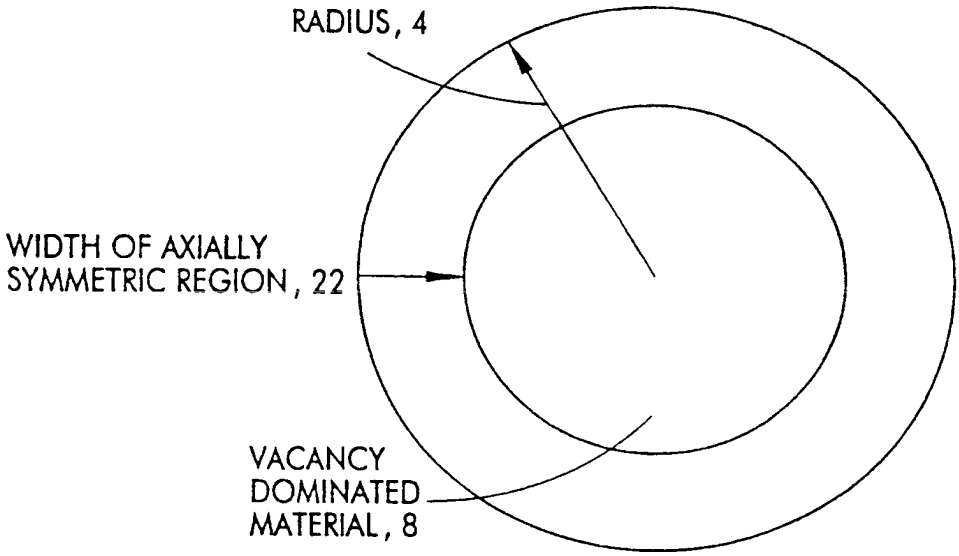

FIG. 12

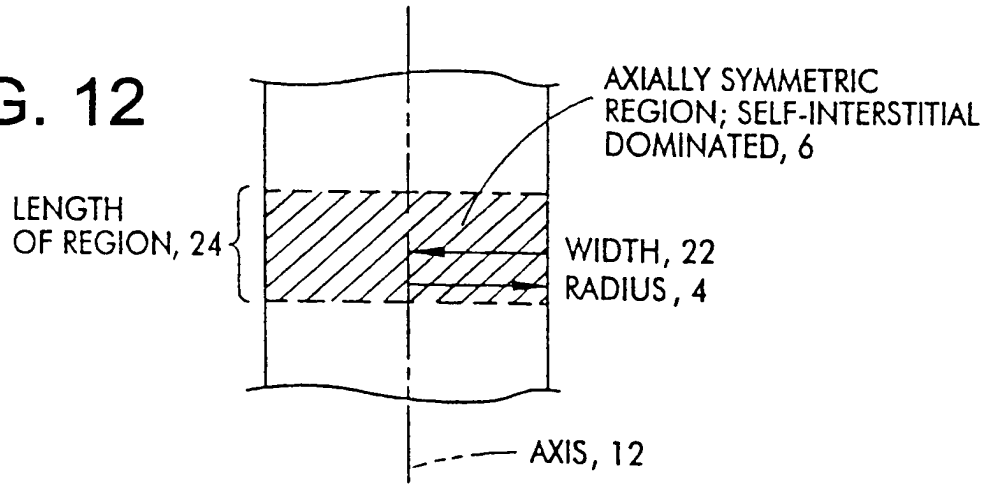

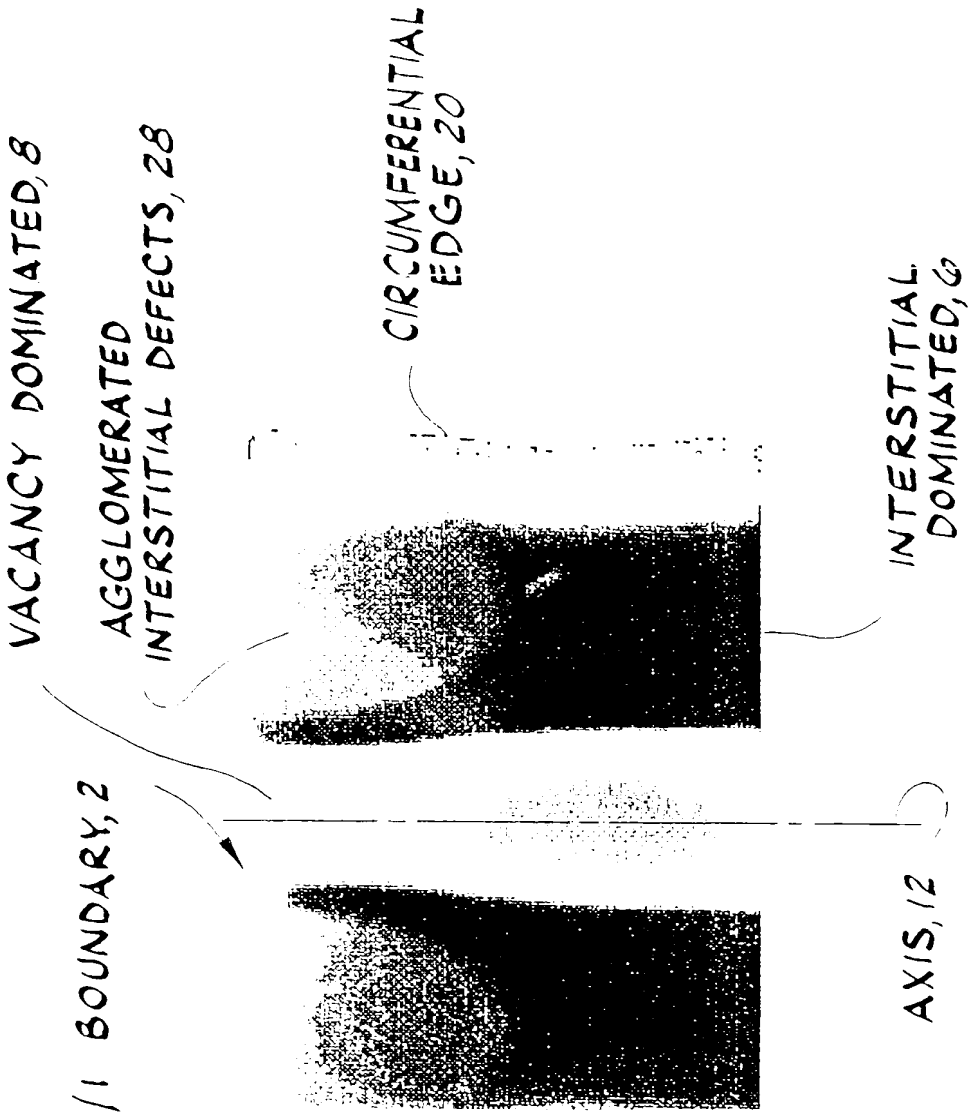

FIG.13

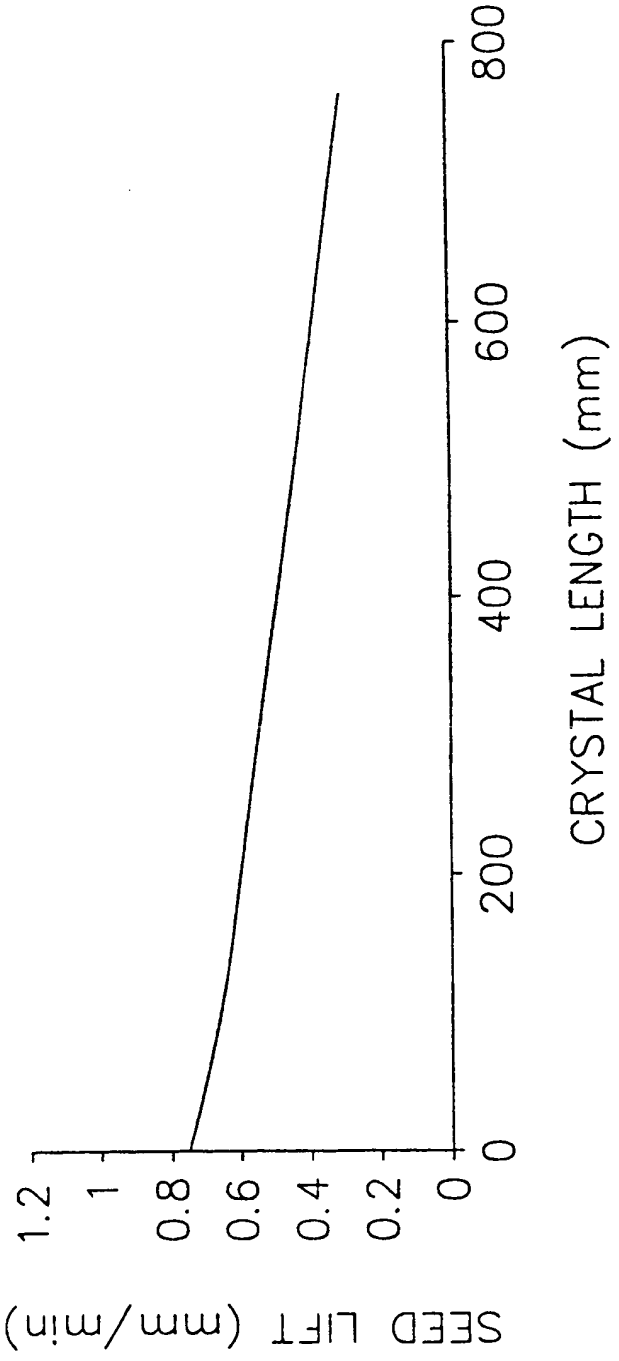

FIG. 14

FIG.15

FIG. 16

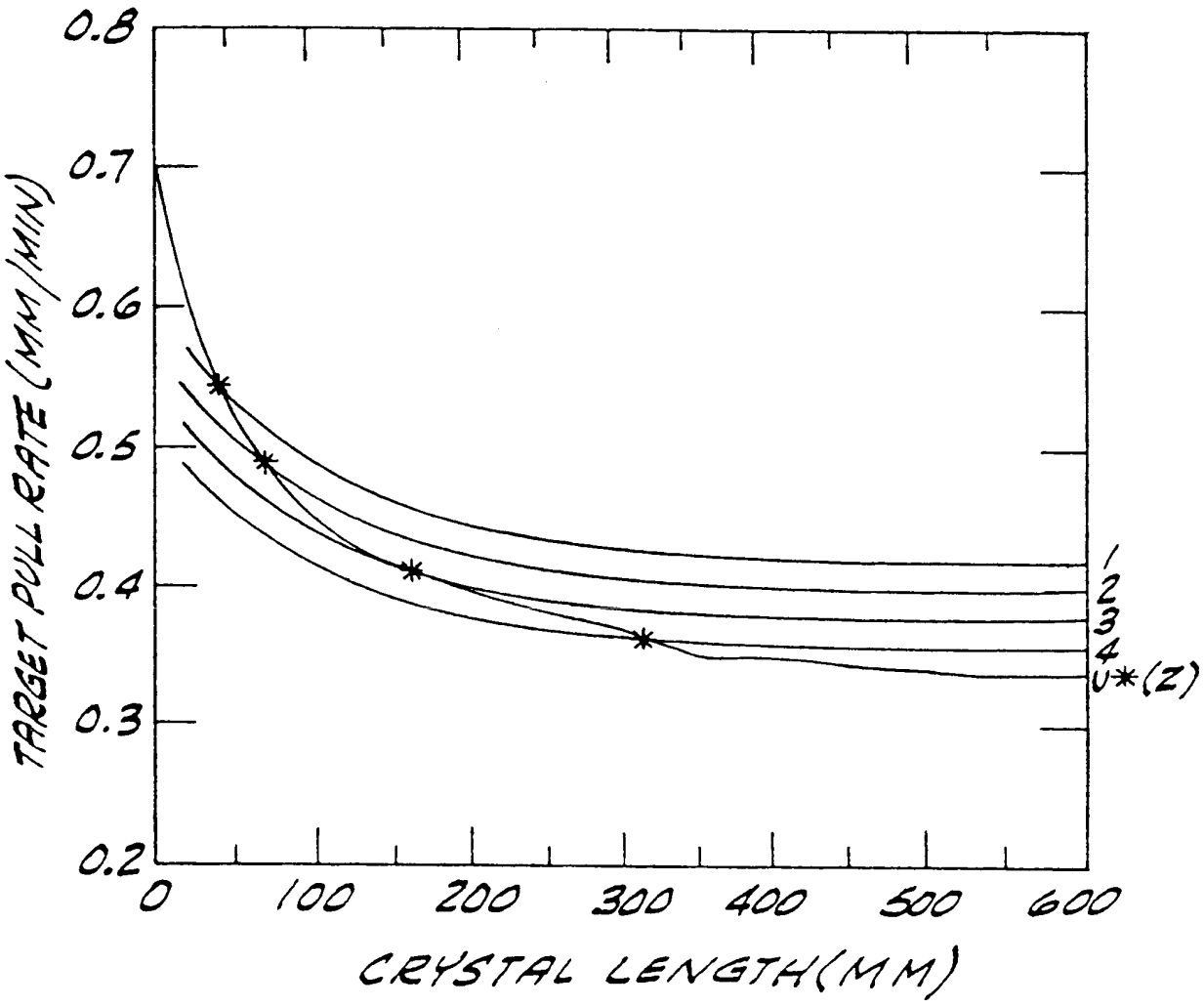

FIG. 17

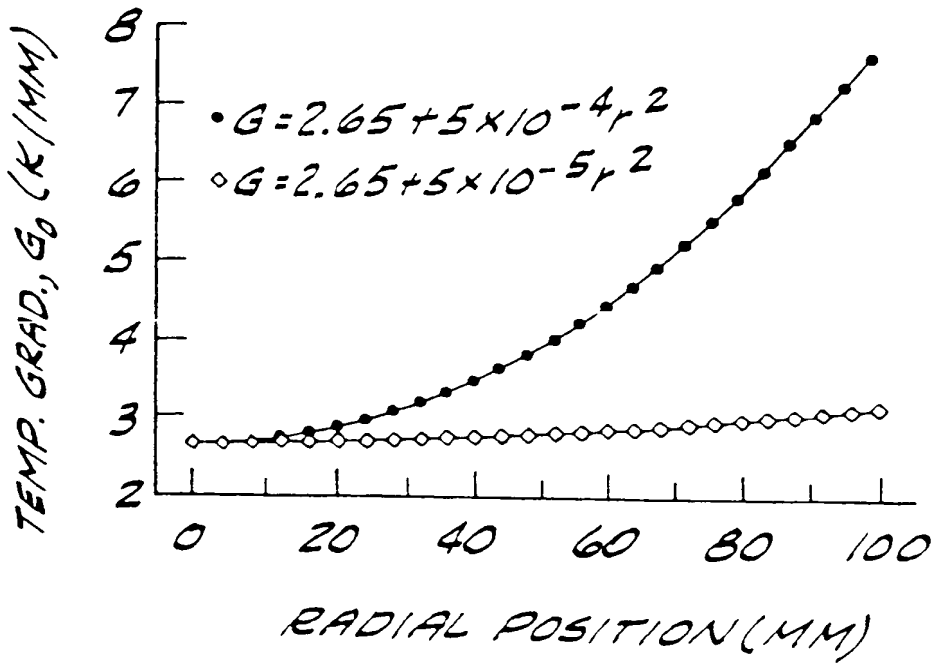

FIG. 18

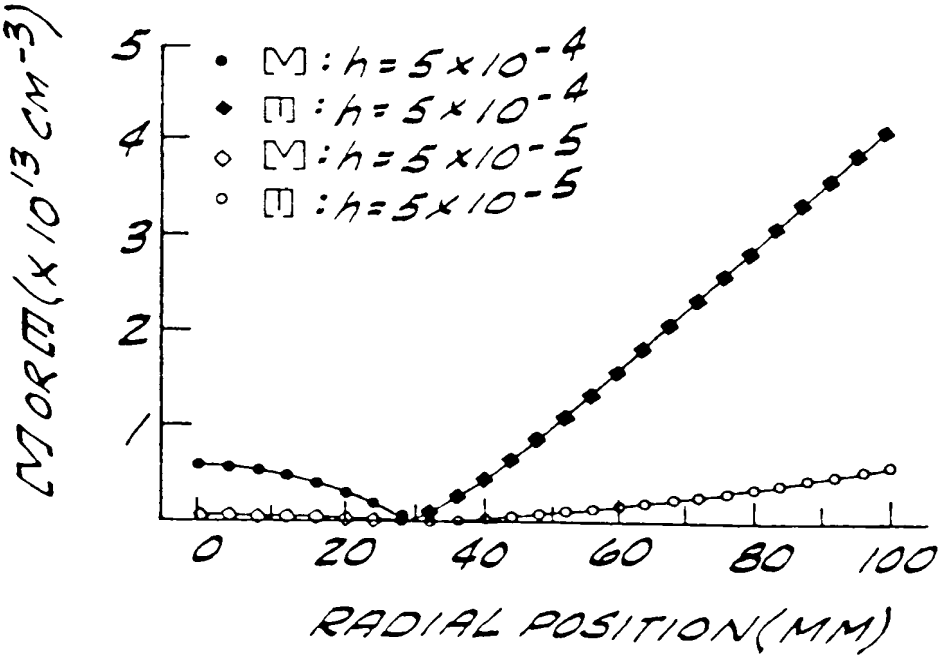

FIG. 19

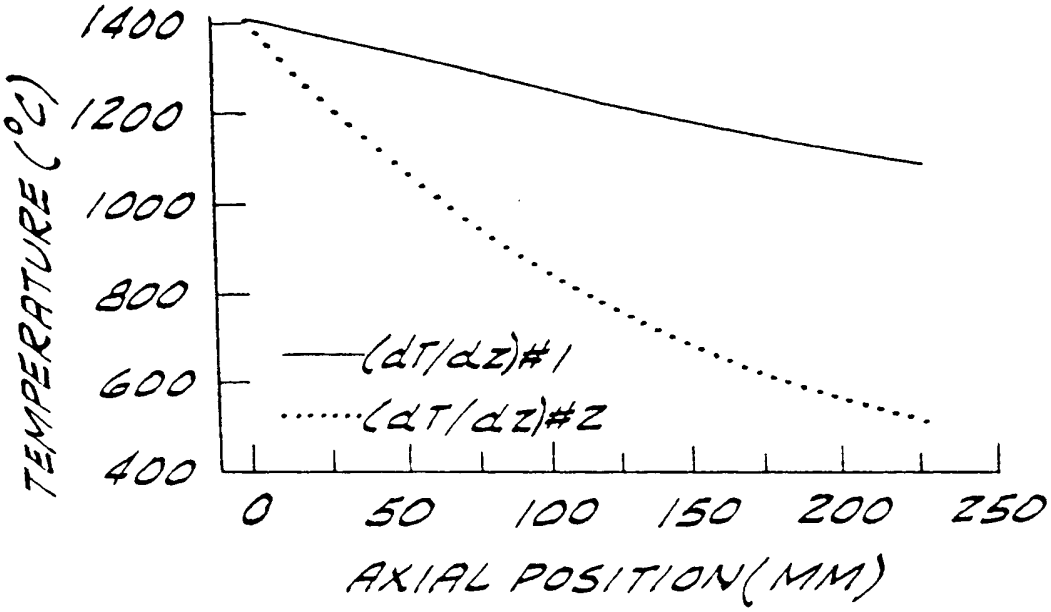

FIG. 20

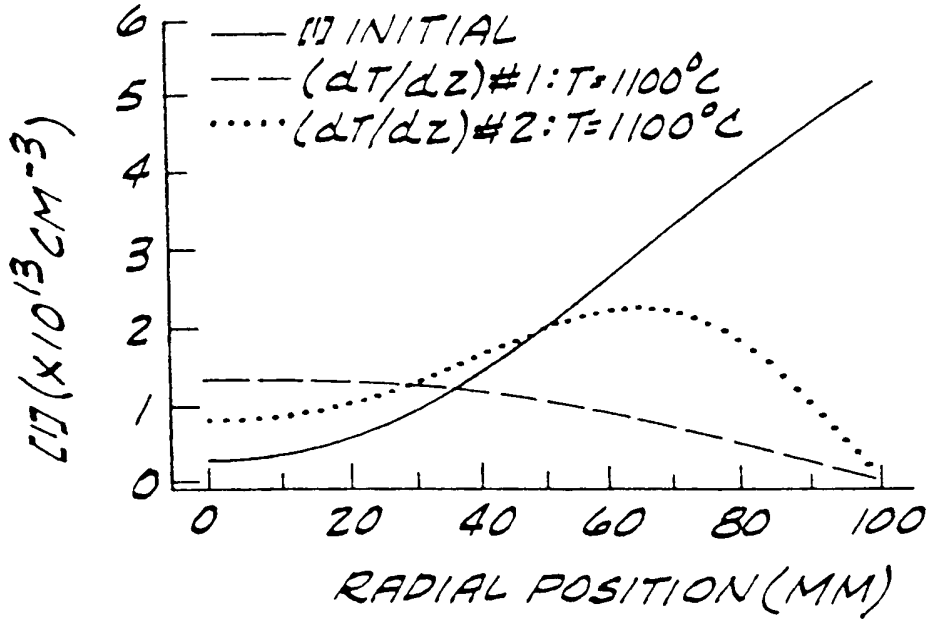

FIG. 21

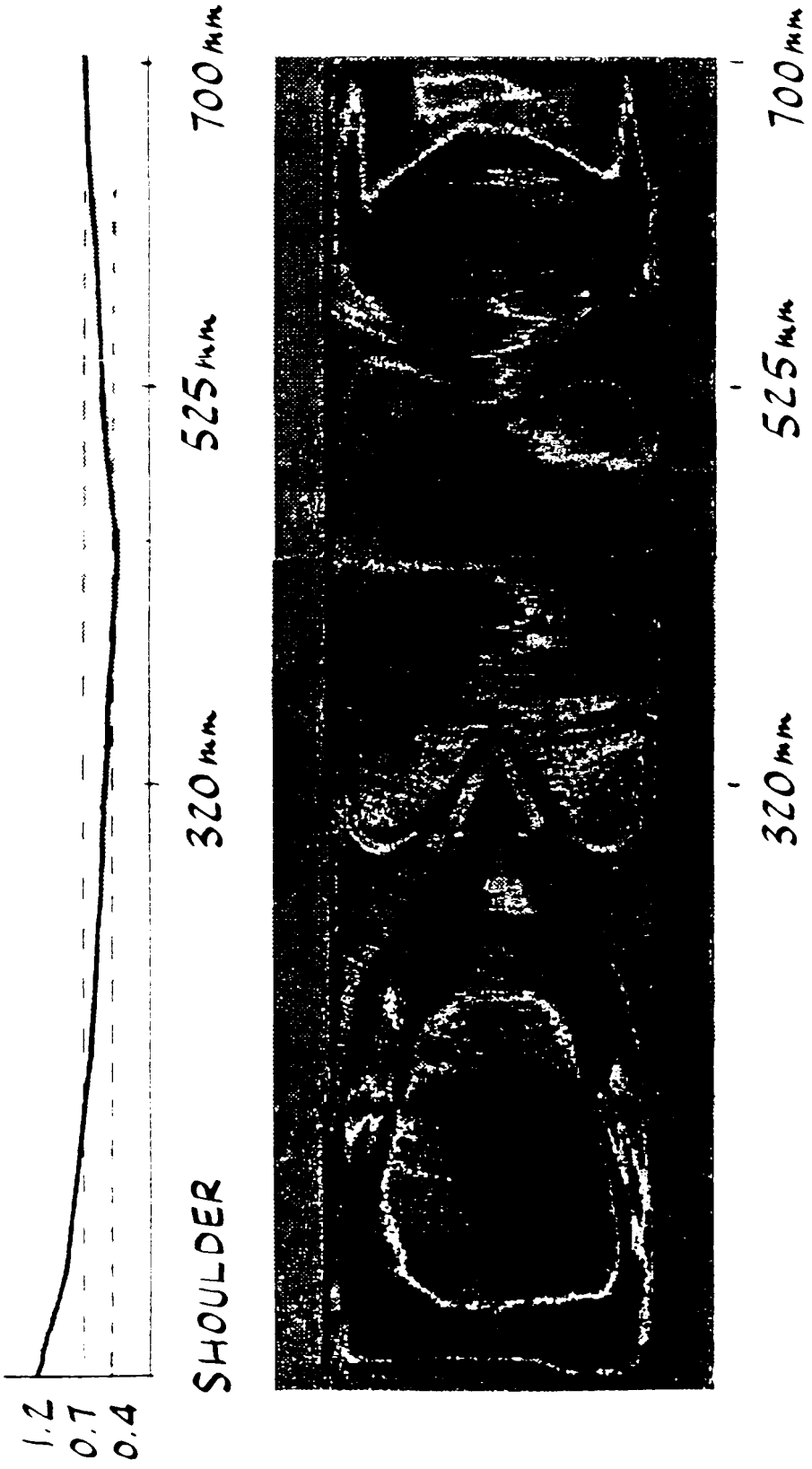

FIG. 22

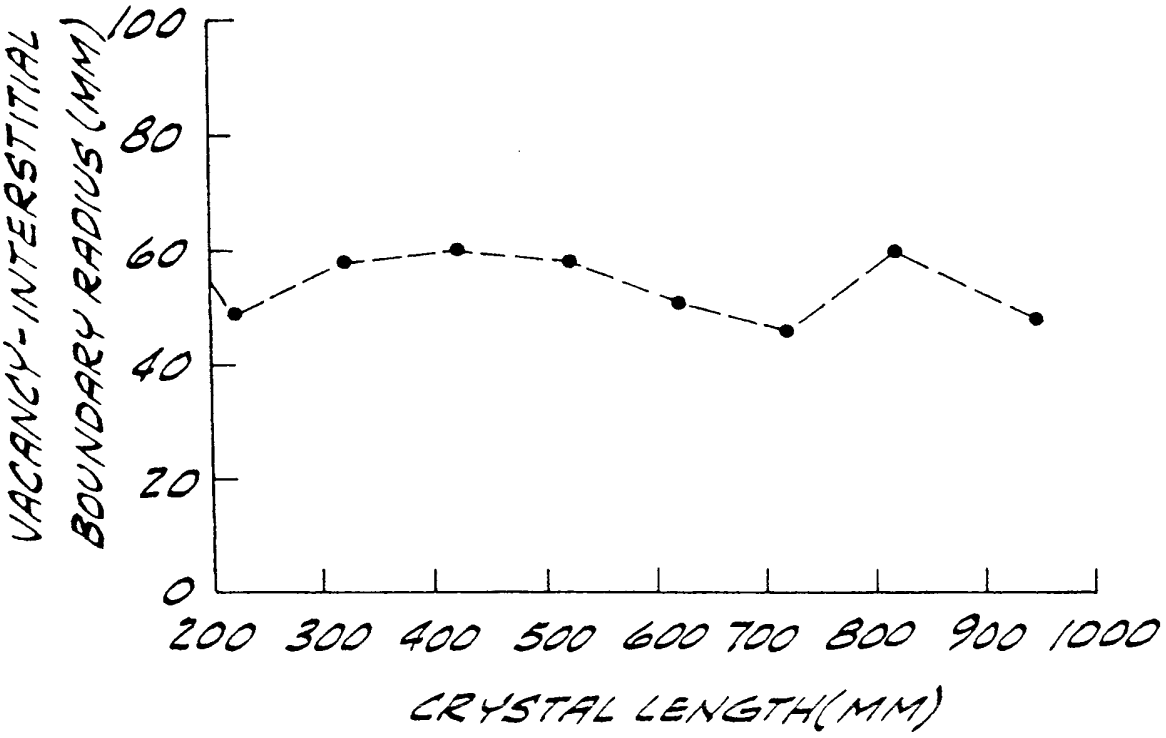

FIG. 23A

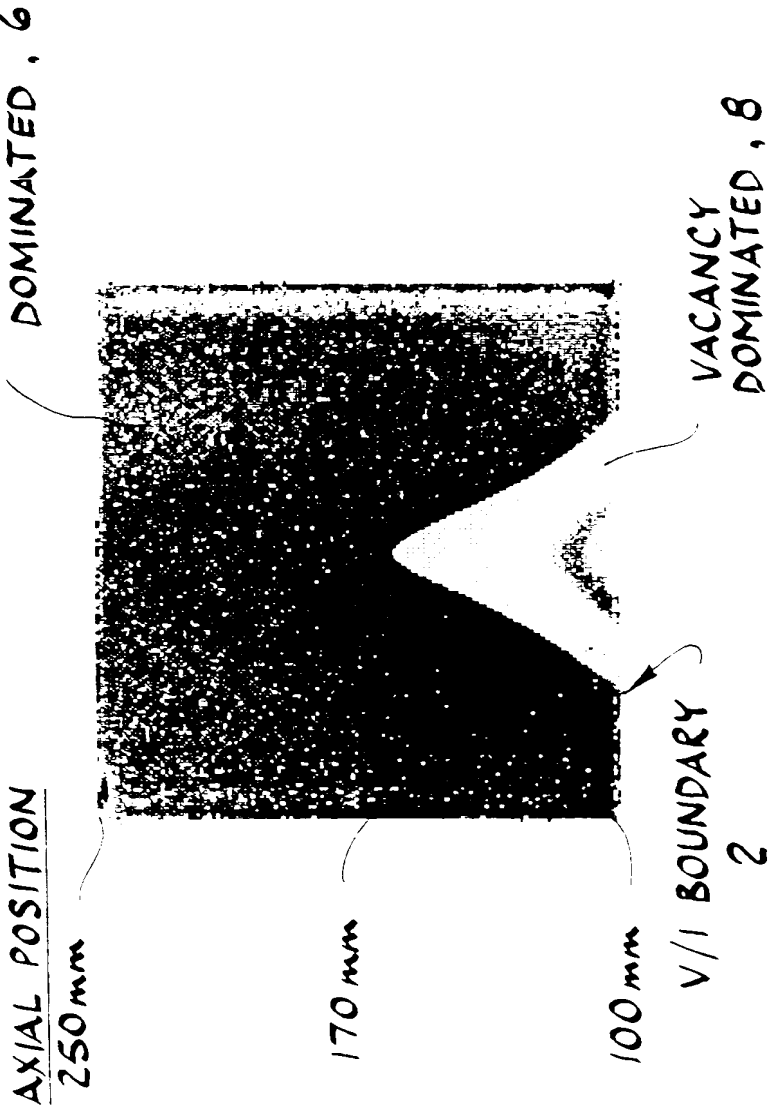

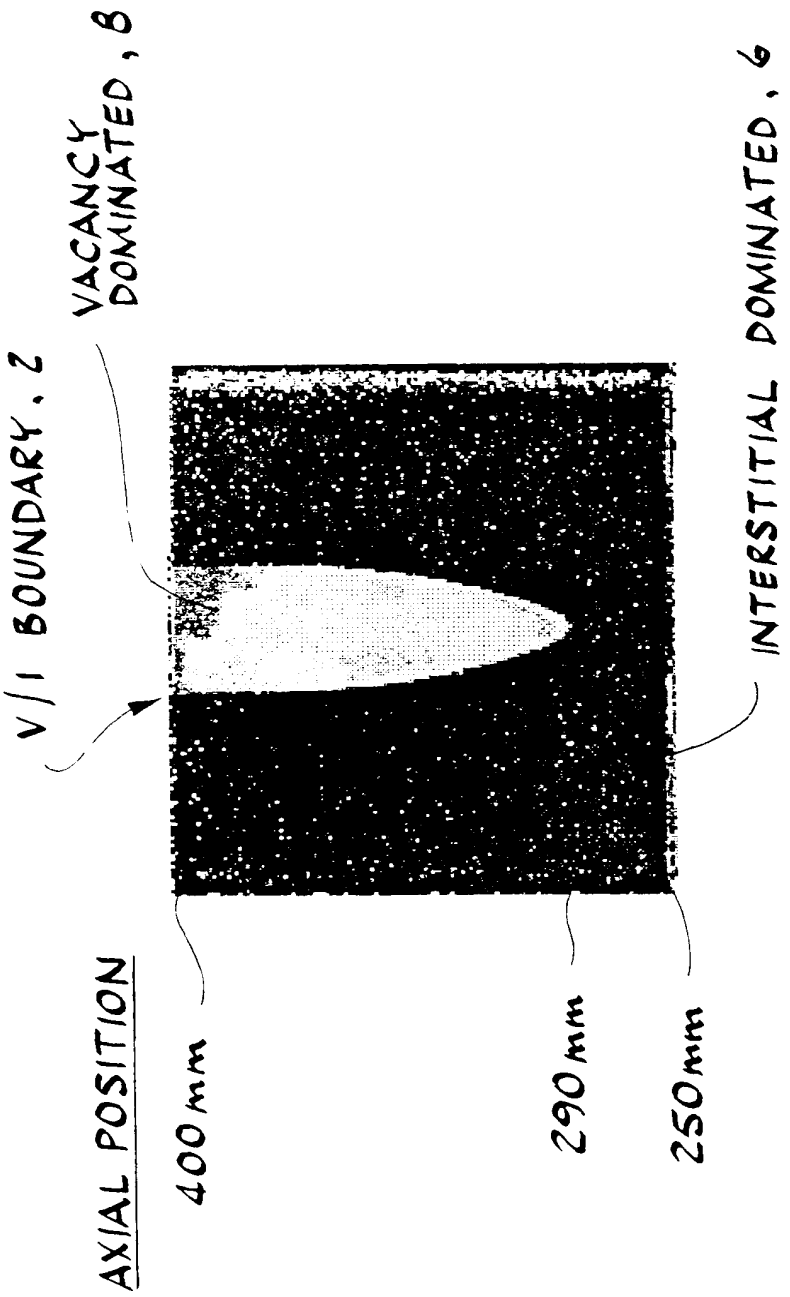

FIG. 23B

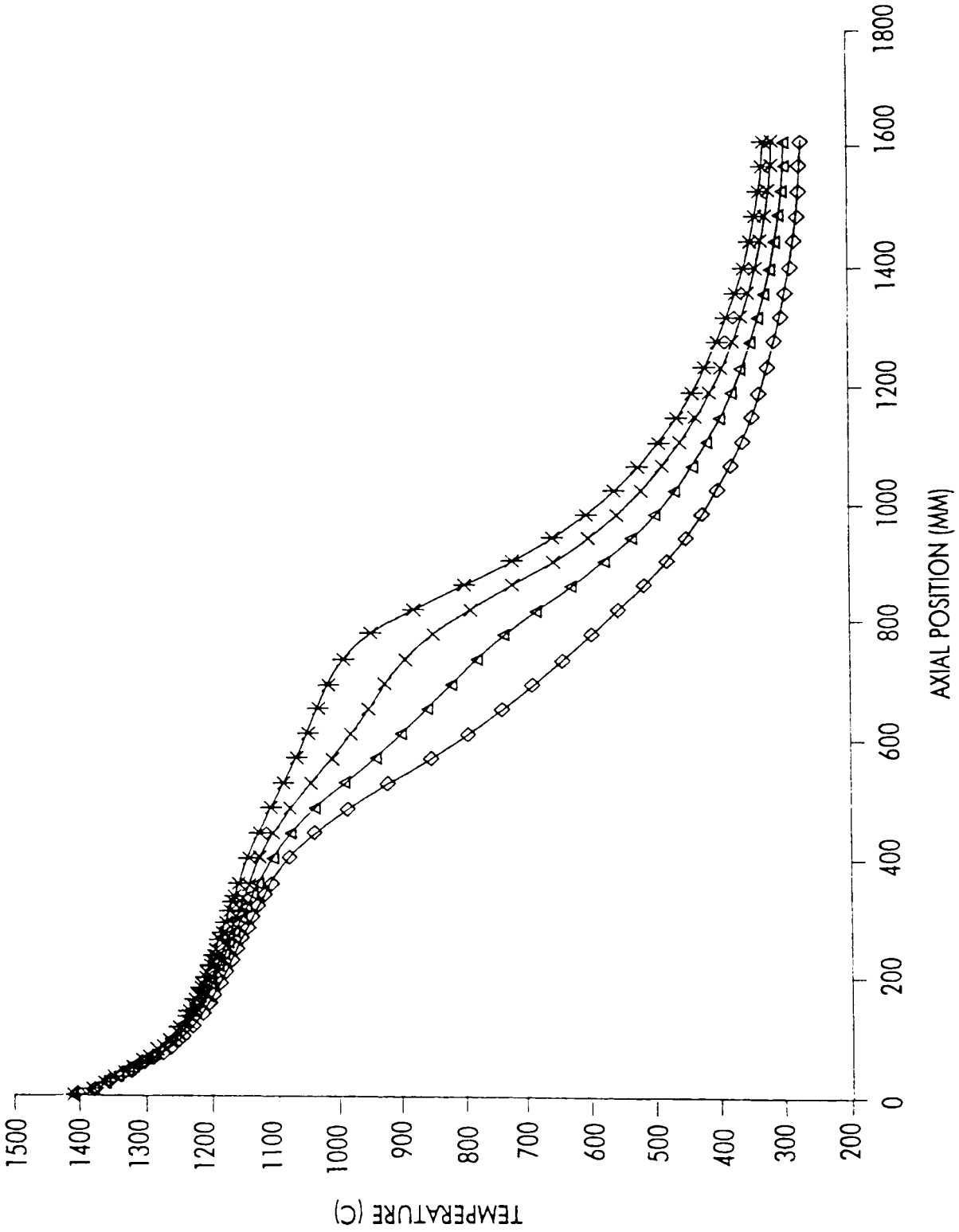

FIG. 24

FIG. 25

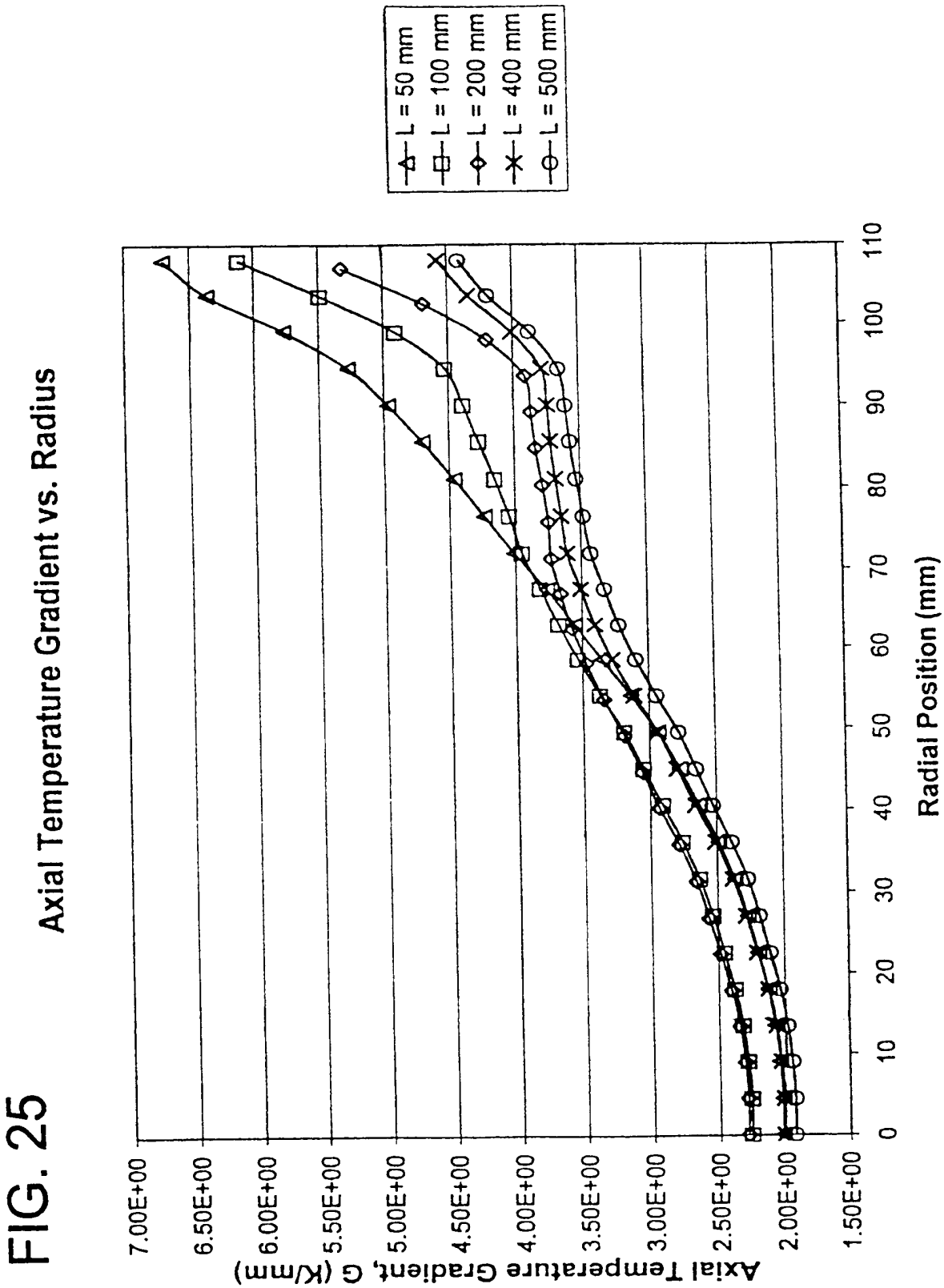

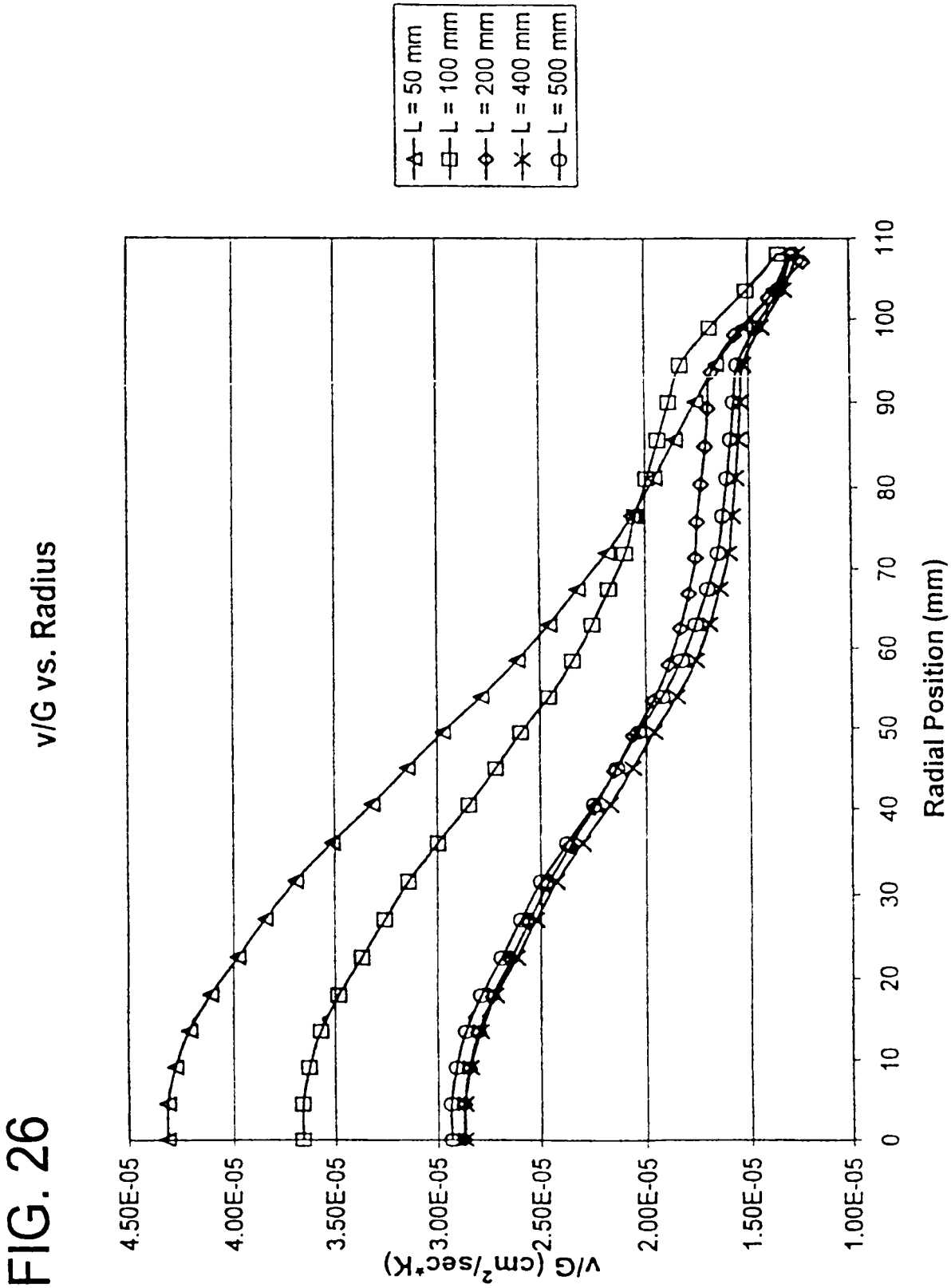

FIG. 26

FIG. 27

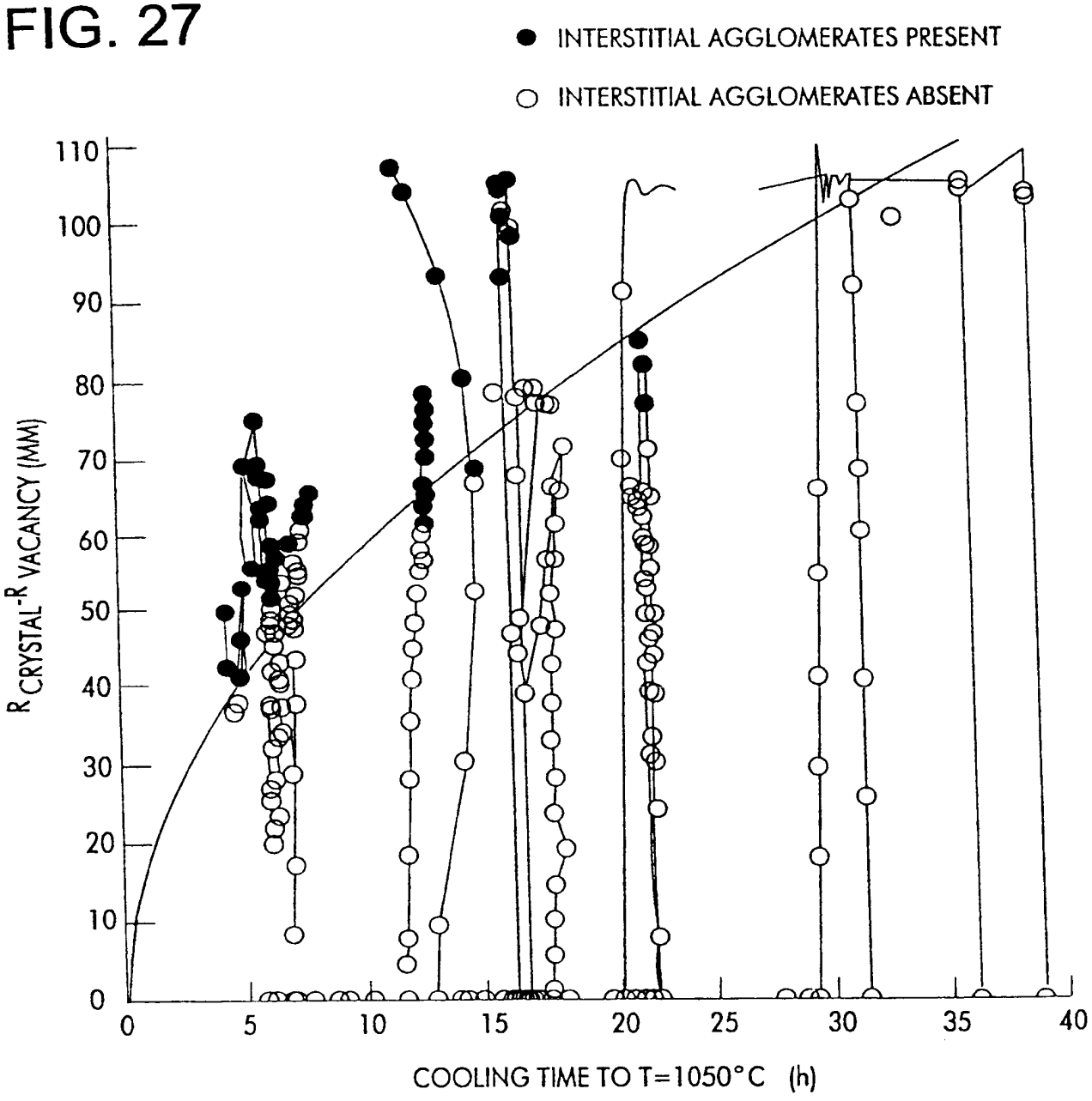

FIG. 28

FIG. 29

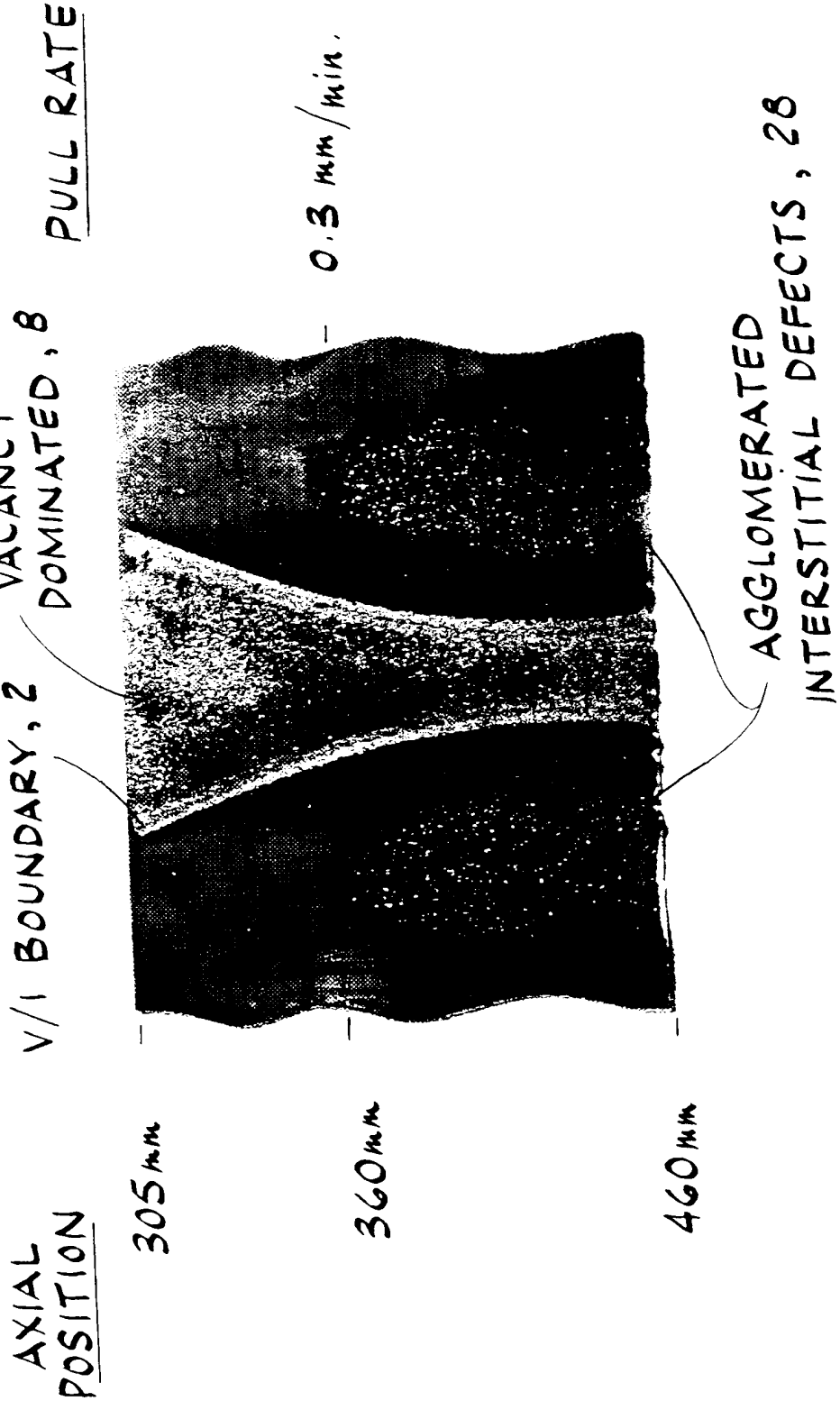

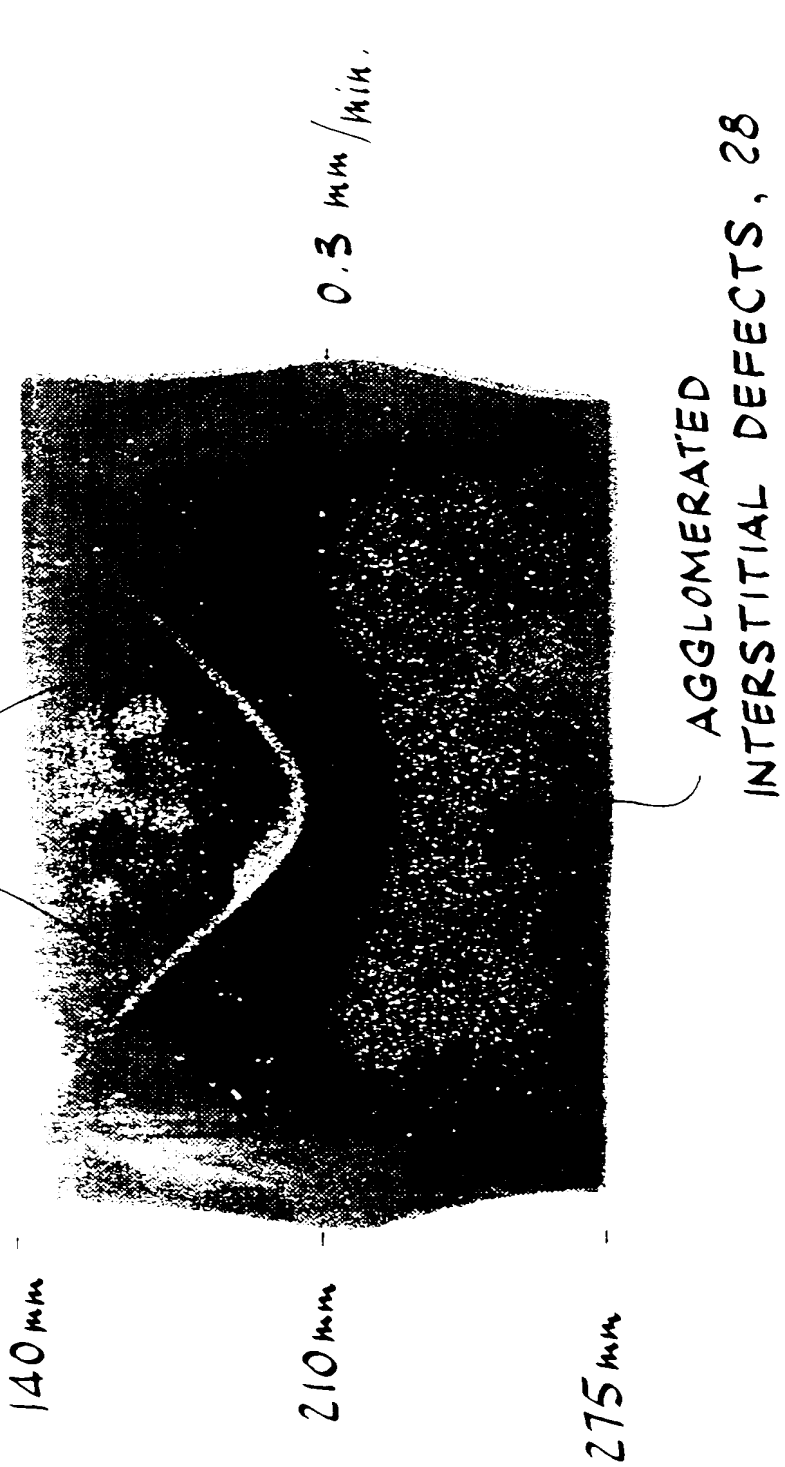

FIG. 30

FIG. 31

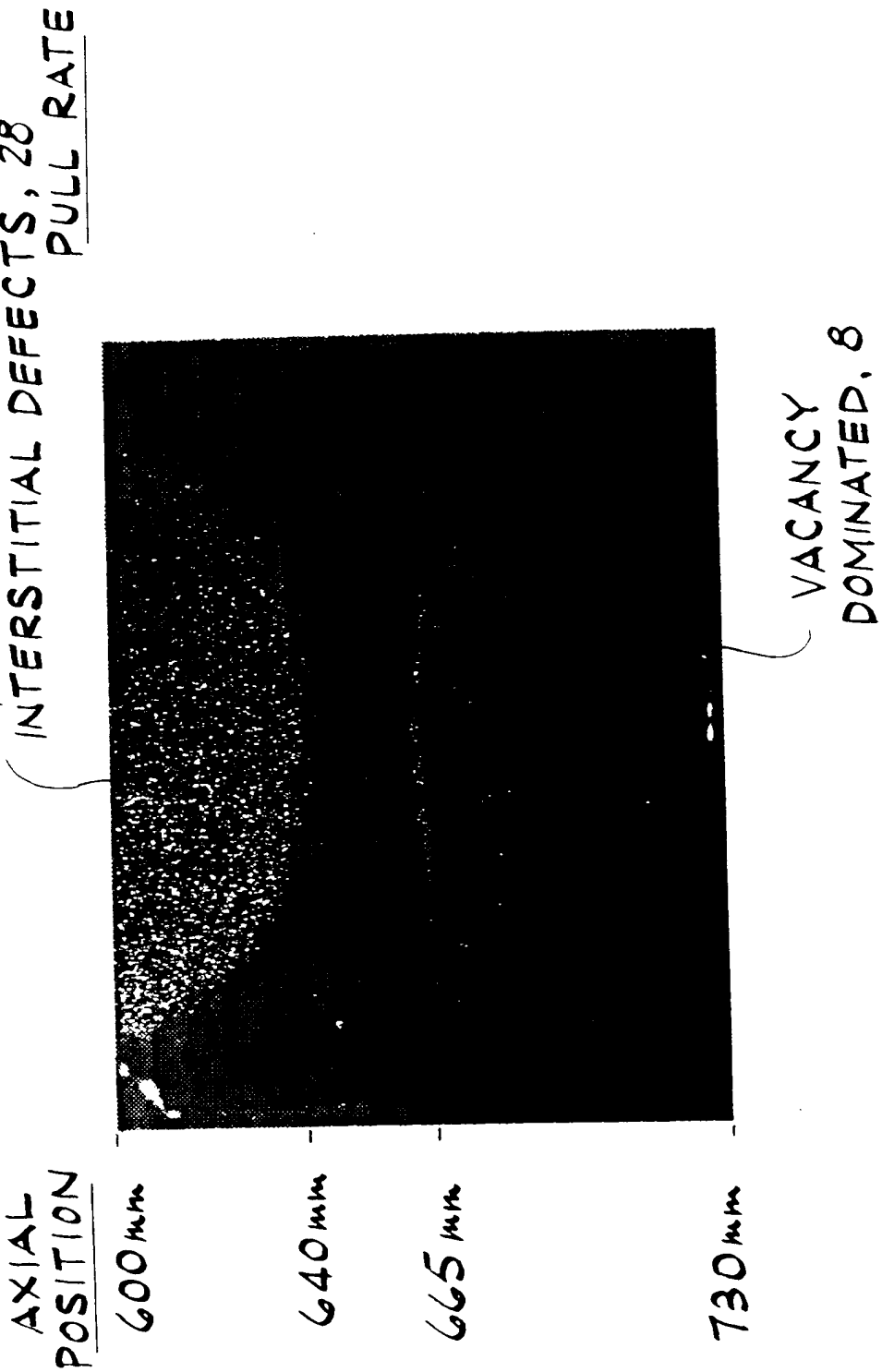

FIG. 32

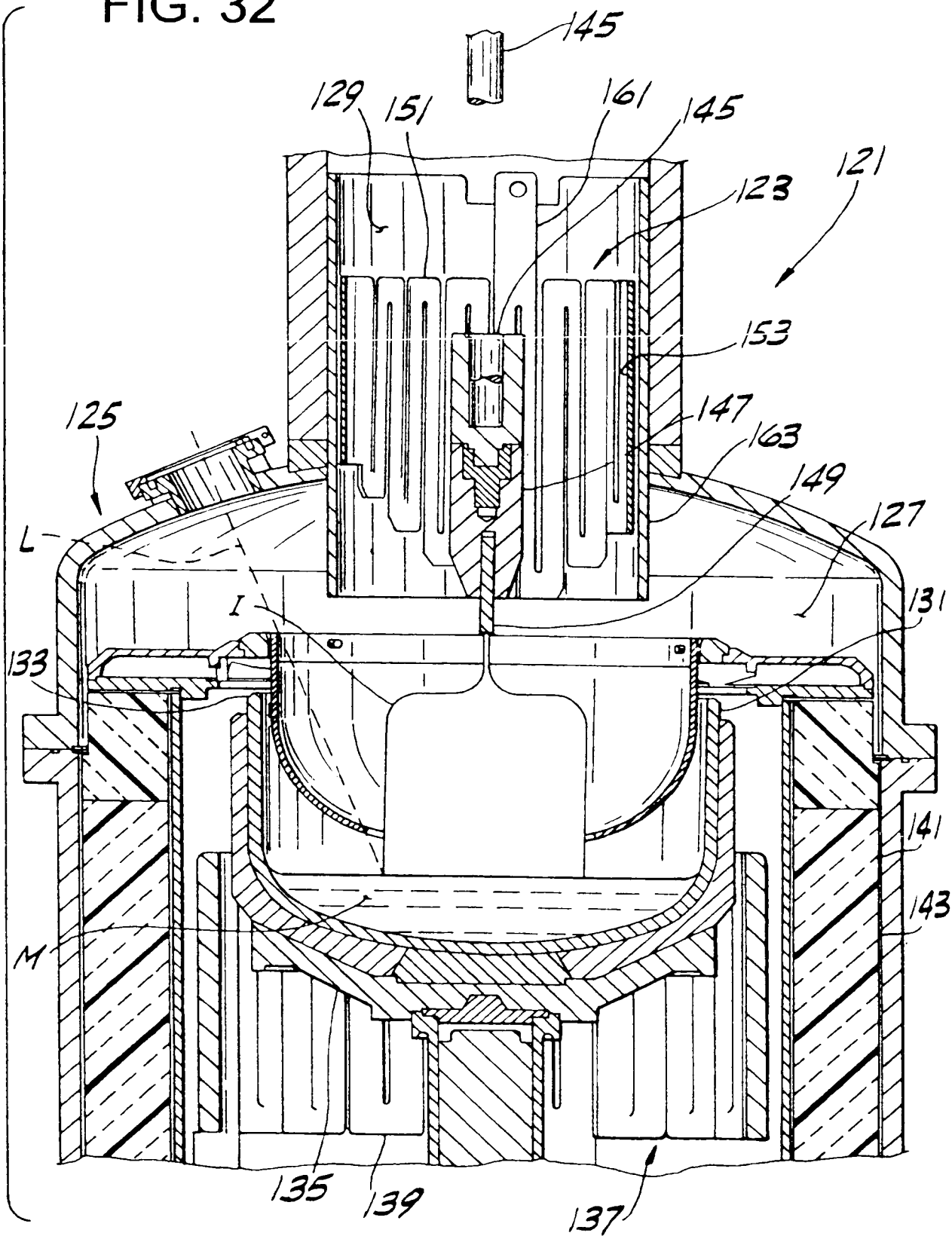

FIG.33

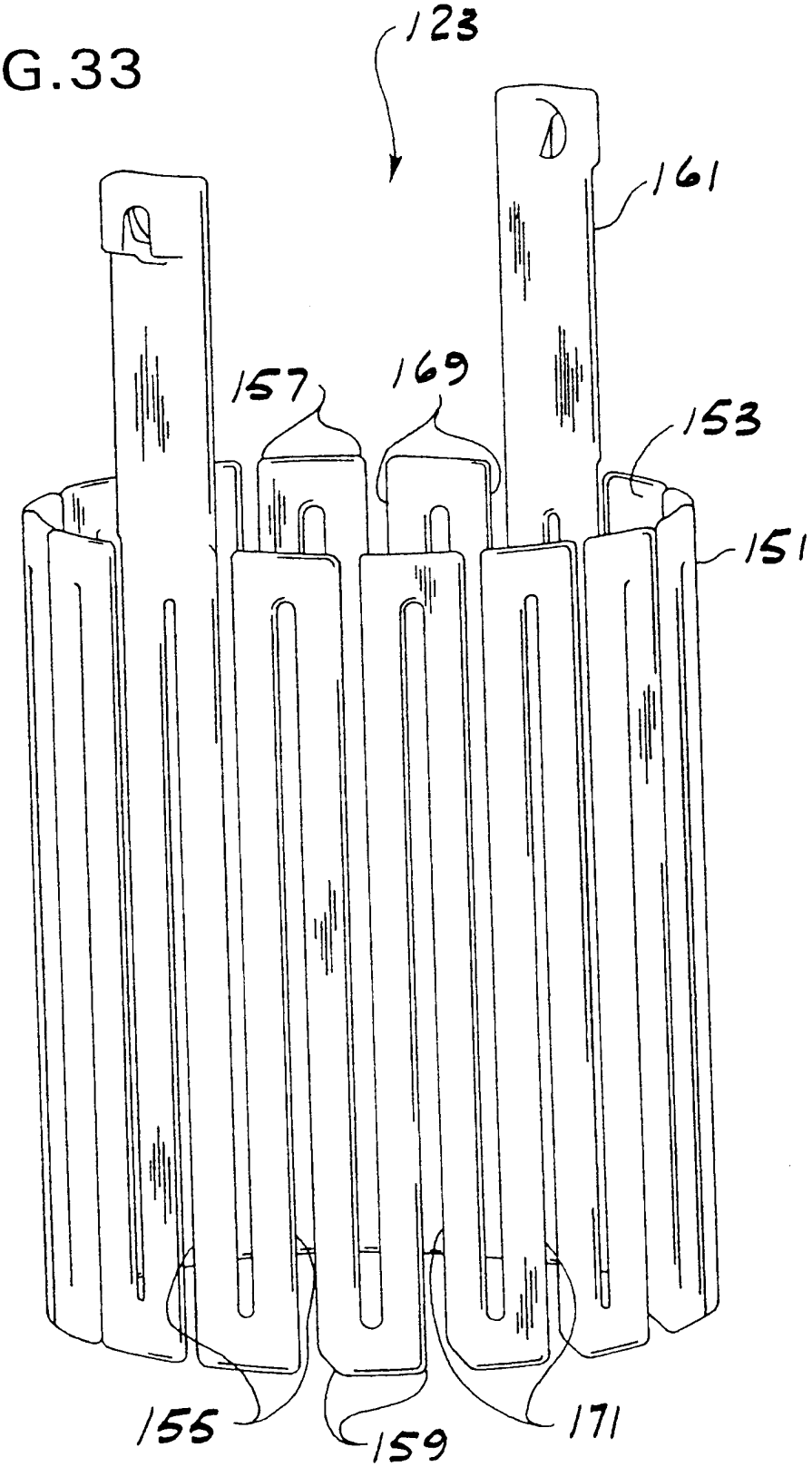

FIG.34

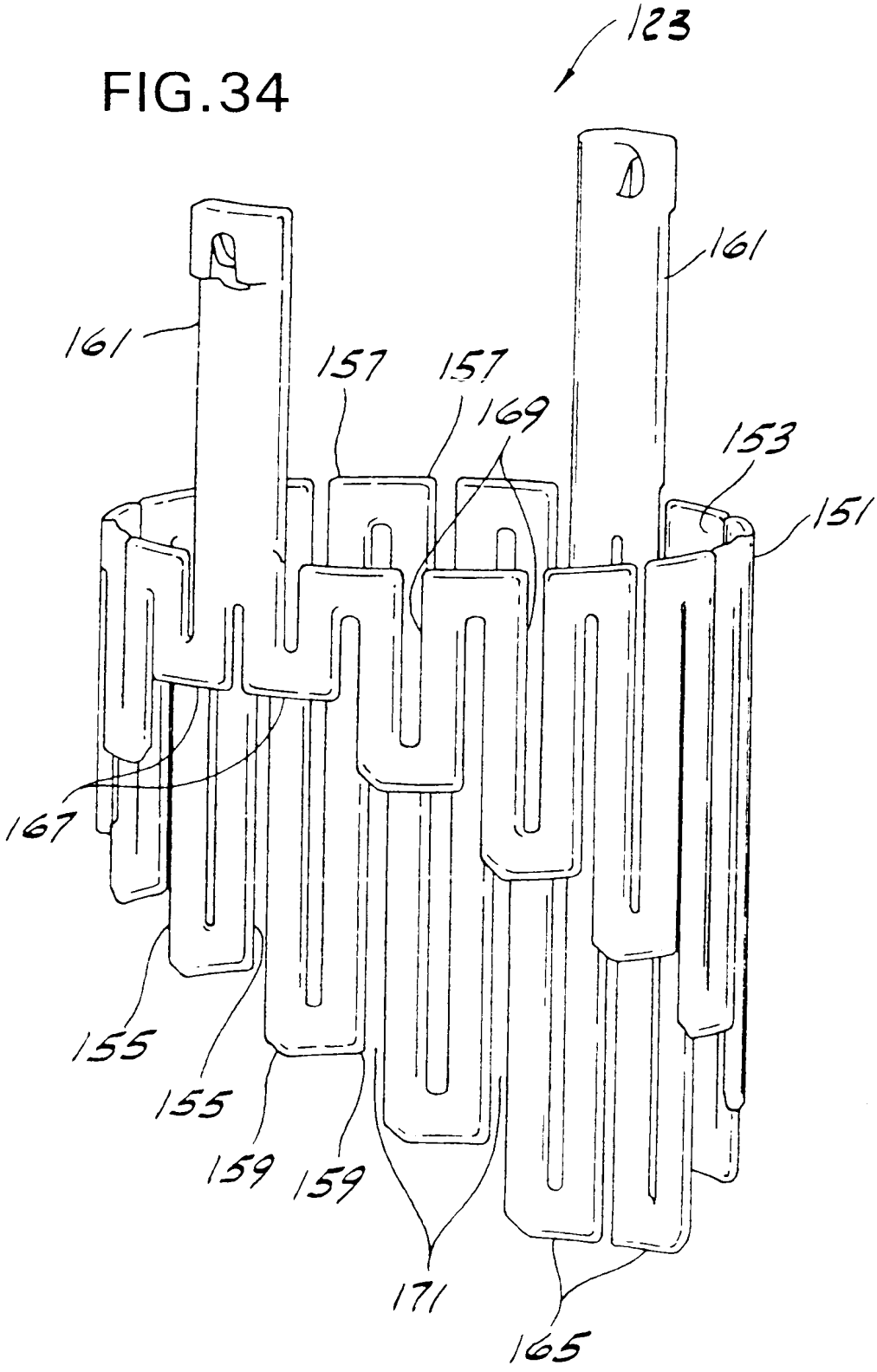

FIG.35

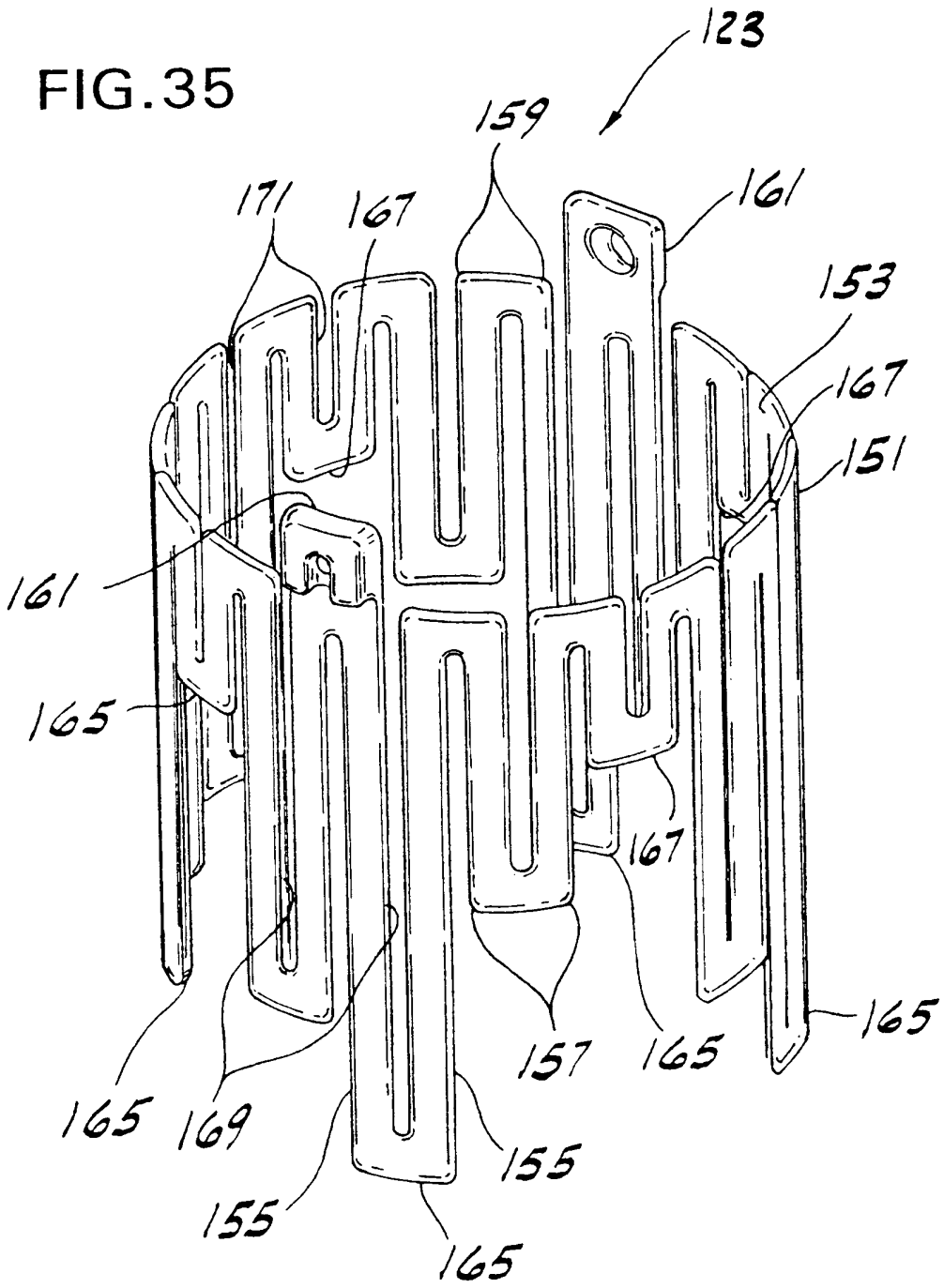

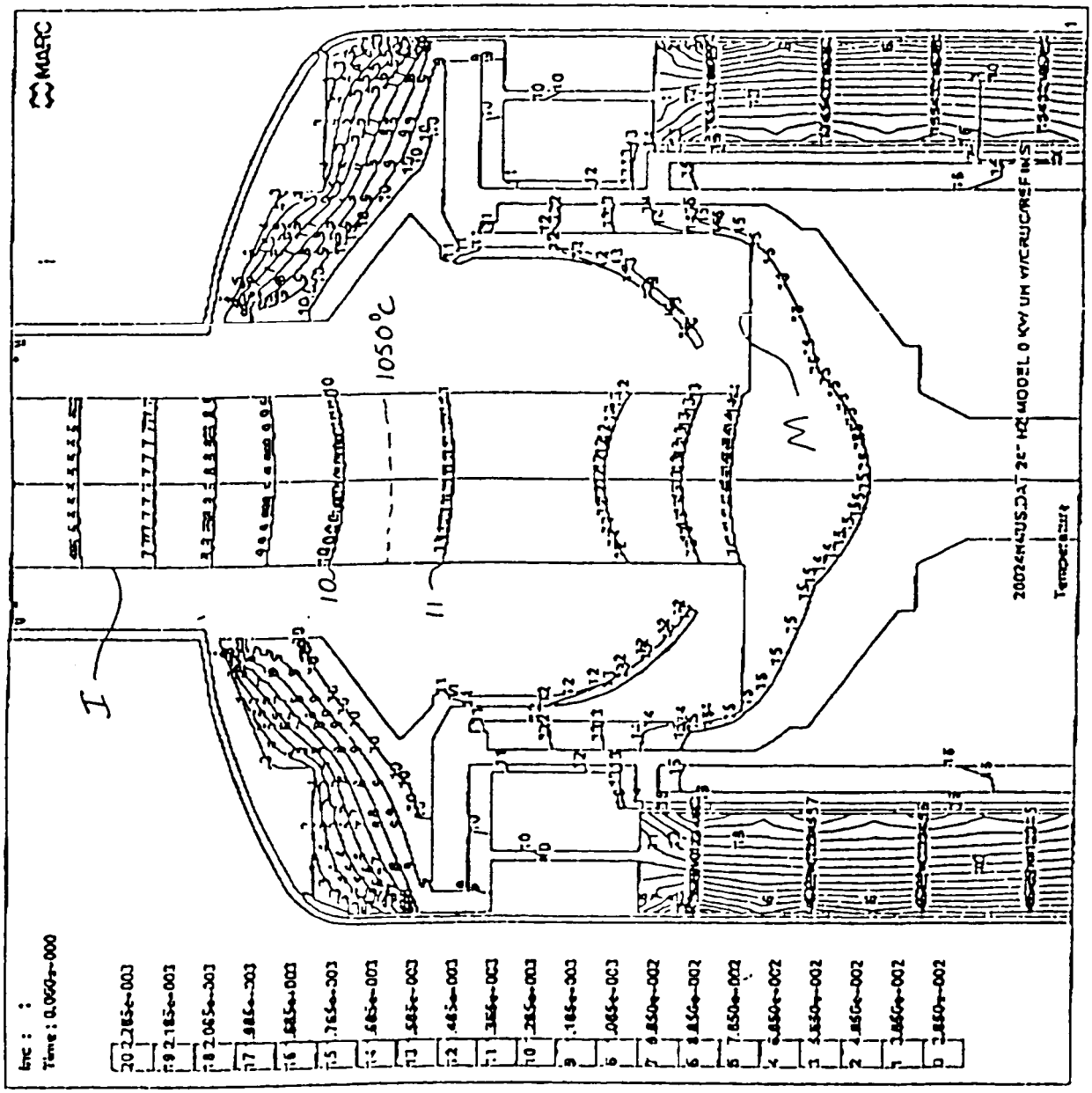

FIG. 36

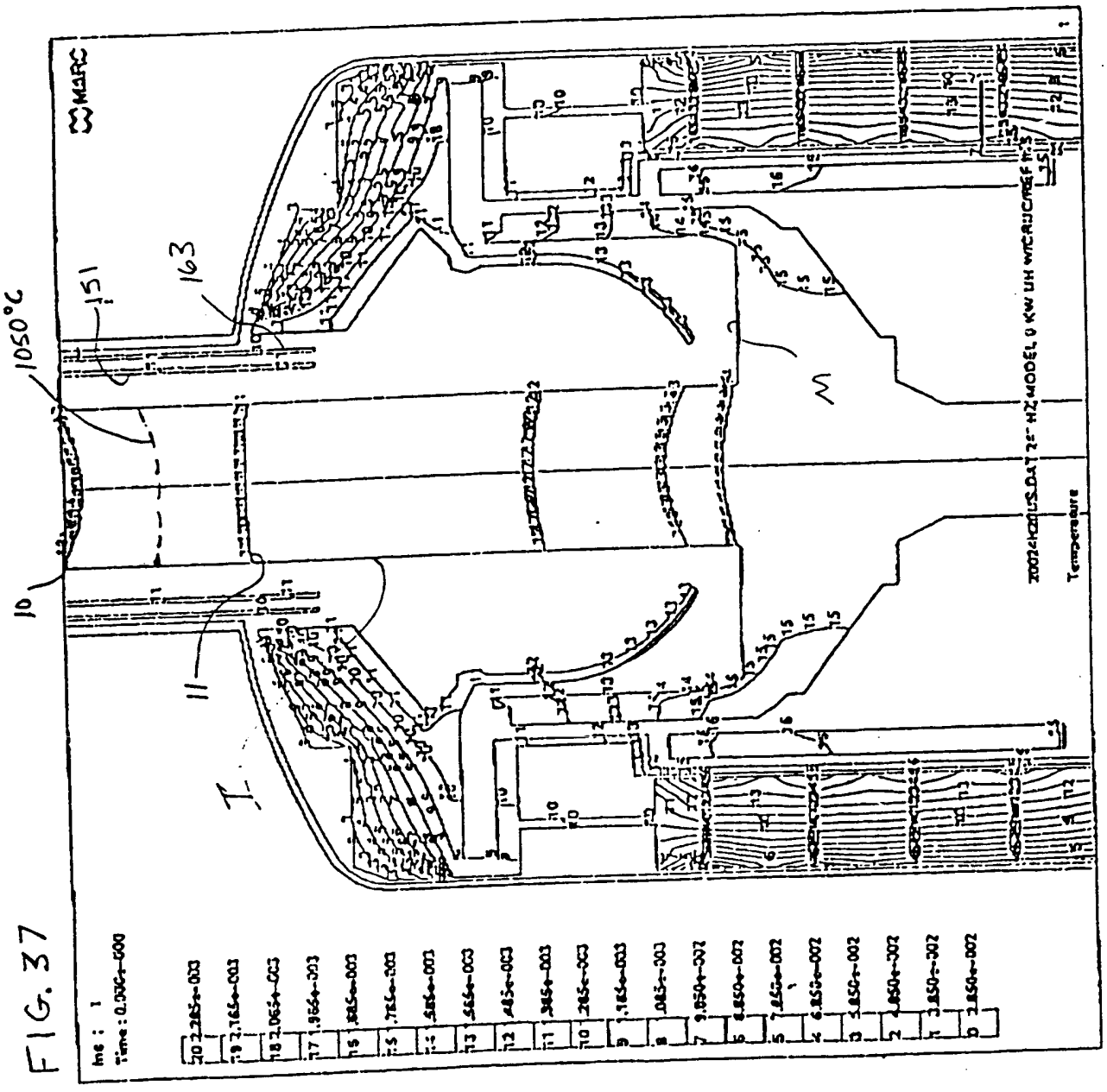

FIG. 37

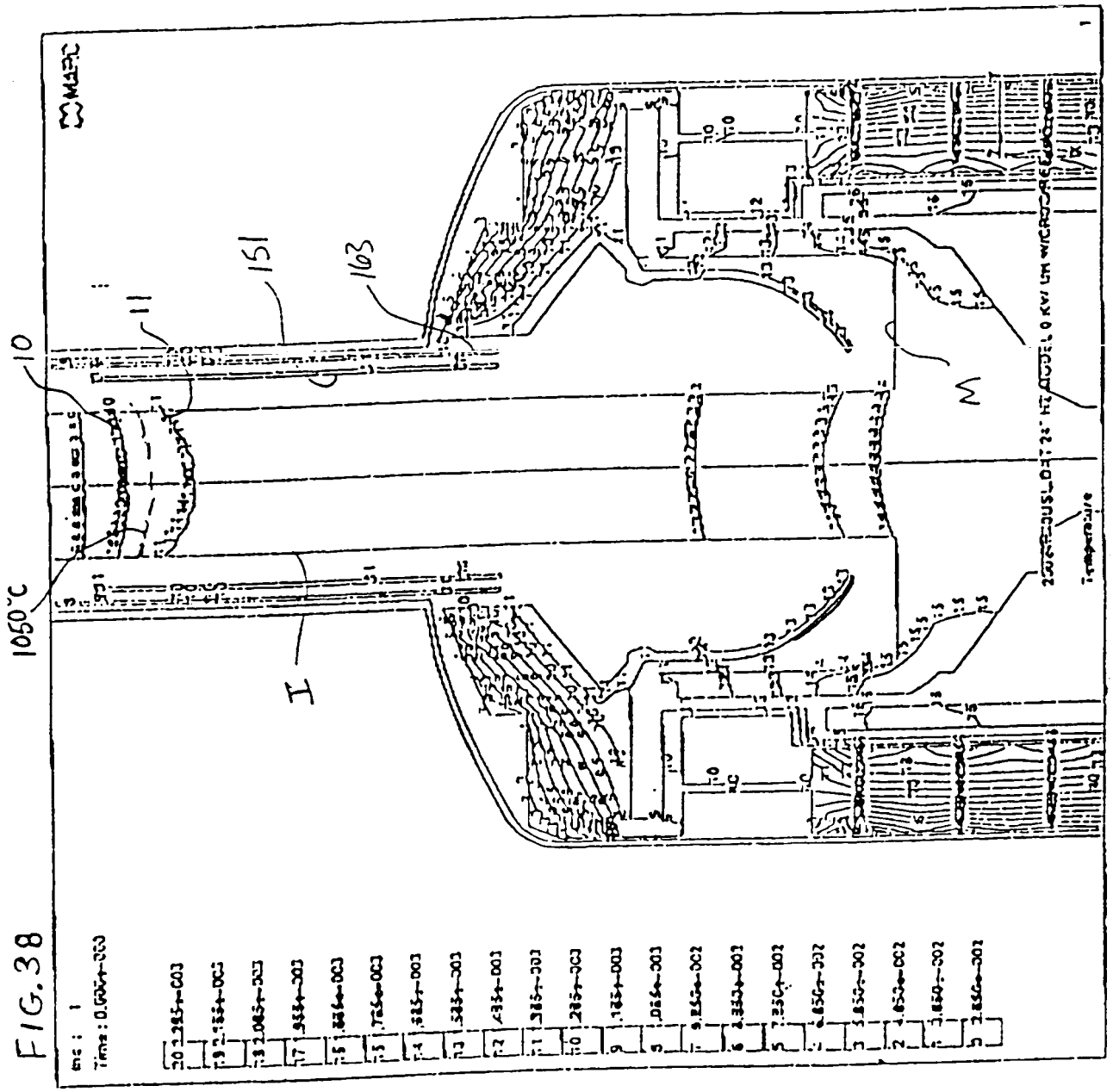

FIG. 38

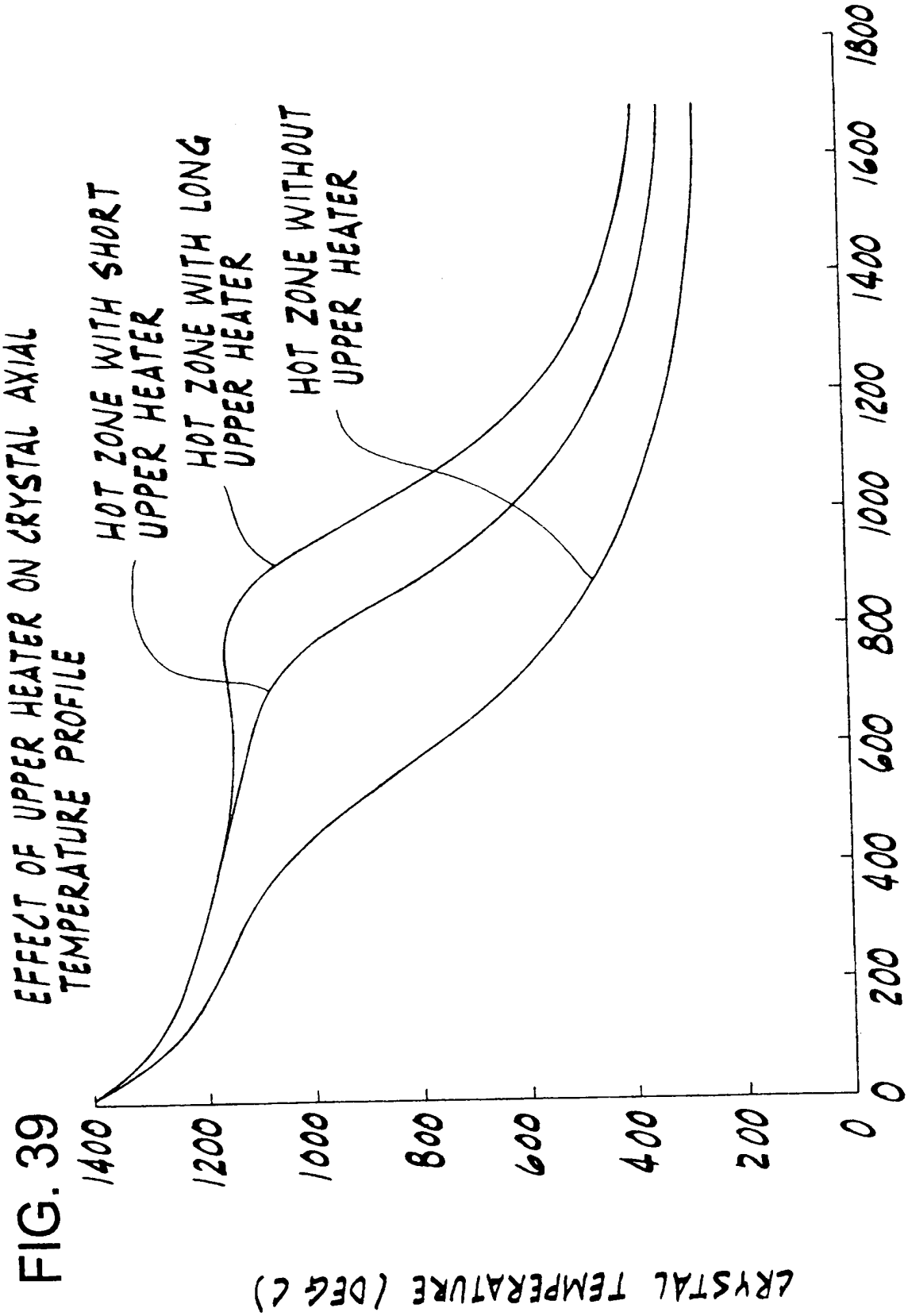

FIG. 39

INTERNATIONAL SEARCH REPORT

Inte onal Application No
PC1/US 99/13643

A. CLASSIFICATION OF SUBJECT MATTER
IPC 6 C30B15/14 C30B29/06

According to International Patent Classification (IPC) or to both national classification and IPC

B. FIELDS SEARCHED

Minimum documentation searched (classification system followed by classification symbols)
IPC 6 C30B

Documentation searched other than minimum documentation to the extent that such documents are included in the fields searched

Electronic data base consulted during the international search (name of data base and, where practical, search terms used)

C. DOCUMENTS CONSIDERED TO BE RELEVANT

Category *	Citation of document, with indication, where appropriate, of the relevant passages	Relevant to claim No.
P,X	US 5 840 120 A (MEMC ELECTRONIC MATERIALS INC) 24 November 1998 (1998-11-24) column 5, line 54 - column 6, line 3; figure 3	1
X	PATENT ABSTRACTS OF JAPAN vol. 18, no. 357 (C-1221), 6 July 1994 (1994-07-06) & JP 06 092780 A (TOSHIBA CORP.), 5 April 1994 (1994-04-05) abstract	1
X	PATENT ABSTRACTS OF JAPAN vol. 98, no. 10, 31 August 1998 (1998-08-31) & JP 10 139600 A (SUMITOMO SITIX CORP), 26 May 1998 (1998-05-26)	1,4
Y	abstract	2

-/--

[X] Further documents are listed in the continuation of box C.

[X] Patent family members are listed in annex.

* Special categories of cited documents :

"A" document defining the general state of the art which is not considered to be of particular relevance

"E" earlier document but published on or after the international filing date

"L" document which may throw doubts on priority claim(s) or which is cited to establish the publication date of another citation or other special reason (as specified)

"O" document referring to an oral disclosure, use, exhibition or other means

"P" document published prior to the international filing date but later than the priority date claimed

"T" later document published after the international filing date or priority date and not in conflict with the application but cited to understand the principle or theory underlying the invention

"X" document of particular relevance; the claimed invention cannot be considered novel or cannot be considered to involve an inventive step when the document is taken alone

"Y" document of particular relevance; the claimed invention cannot be considered to involve an inventive step when the document is combined with one or more other such documents, such combination being obvious to a person skilled in the art.

"&" document member of the same patent family

Date of the actual completion of the international search	Date of mailing of the international search report
9 September 1999	17/09/1999

Name and mailing address of the ISA	Authorized officer
European Patent Office, P.B. 5818 Patentlaan 2 NL - 2280 HV Rijswijk Tel. (+31-70) 340-2040, Tx. 31 651 epo nl, Fax: (+31-70) 340-3016	Cook, S

1

Form PCT/ISA/210 (second sheet) (July 1992)

INTERNATIONAL SEARCH REPORT

Inte onal Application No
PC1/US 99/13643

C.(Continuation) DOCUMENTS CONSIDERED TO BE RELEVANT

Category °	Citation of document, with indication,where appropriate, of the relevant passages	Relevant to claim No
Y	PATENT ABSTRACTS OF JAPAN vol. 18, no. 347 (C-1219), 30 June 1994 (1994-06-30) & JP 06 087686 A (MITSUBISHI MATERIALS CORP.), 29 March 1994 (1994-03-29) abstract	2
A	PATENT ABSTRACTS OF JAPAN vol. 11, no. 30 (C-400), 29 January 1987 (1987-01-29) & JP 61 201692 A (MITSUBISHI METAL CORP) abstract	1,8-10
X	PATENT ABSTRACTS OF JAPAN vol. 7, no. 225 (C-189) '1370!, 6 October 1983 (1983-10-06) & JP 58 120591 A (OKI DENKI KOGYO KK), 18 July 1983 (1983-07-18) abstract	1-3
A	EP 0 823 497 A (MEMC ELECTRONIC MATERIALS INC) 11 February 1998 (1998-02-11) example 3	1,8-10
A	EP 0 504 837 A (SHIN ETSU LTD) 23 September 1992 (1992-09-23)	

1

Form PCT/ISA/210 (continuation of second sheet) (July 1992)

INTERNATIONAL SEARCH REPORT

Information on patent family members

Inte ional Application No
PC /US 99/13643

Patent document cited in search report		Publication date	Patent family member(s)		Publication date
US 5840120	A	24-11-1998	NONE		
JP 06092780	A	05-04-1994	NONE		
JP 10139600	A	26-05-1998	NONE		
JP 06087686	A	29-03-1994	NONE		
JP 61201692	A	06-09-1986	JP	1742752 C	15-03-1993
			JP	3067994 B	24-10-1991
JP 58120591	A	18-07-1983	NONE		
EP 823497	A	11-02-1998	US	5779791 A	14-07-1998
			JP	10095698 A	14-04-1998
			SG	54540 A	16-11-1998
EP 504837	A	23-09-1992	JP	5070283 A	23-03-1993
			DE	69207454 D	22-02-1996
			DE	69207454 T	23-05-1996
			US	5248378 A	28-09-1993